RWE Renewables UK Dogger Bank South (West) Limited

RWE Renewables UK Dogger Bank South (East) Limited

Dogger Bank South Offshore Wind Farms

Environmental Statement

Volume 7

Appendix 8-3 – Marine Physical Processes Modelling Technical Report (Revision 2) (Tracked)

January 2025

Application Reference: 7.8.8.3

APFP Regulation: 5(2)(a)

Revision: 02

Company:	**RWE Renewables UK Dogger Bank South (West) Limited and RWE Renewables UK Dogger Bank South (East) Limited**	Asset:	**Development**
Project:	**Dogger Bank South Offshore Wind Farms**	Sub Project/Package:	**Consents**
Document Title or Description:	Appendix 8-3–Marine Physical Processes Modelling Technical Report (Revision 2) (Tracked)		
Document Number:	004300148-02	Contractor Reference Number:	PC2340-RHD-OF-ZZ-AX-Z-0085

Rev No.	Date	Status/Reason for Issue	Author	Checked by	Approved by
01	June 2024	Final for DCO Application	RHDHV	RWE	RWE
02	January 2025	Submission to accompany Project Change Request 1.	RHDHV	RWE	RWE

Revision Change Log			
Rev	**Page**	**Section**	**Description**
01	N/A	N/A	Final for DCO Application
02	30-31	8.3.2.4	Text amendments reflecting proposed reduction in Offshore Platforms and removal of GBS foundations.
02	33-35	8.3.2.5	Text amendments reflecting proposed reduction in Offshore Platforms and removal of GBS foundations
02	46	8.3.3.4	Text amendments reflecting proposed reduction in Offshore Platforms and removal of GBS foundations.
02	49-50	8.3.4.2	Amendments to Figure 8-3-31, Figure 8-3-32 and Figure 8-3-33 reflecting updated cable routes.
02	124 - 133	Annex C	Modelling updates reflecting updated Project Design Envelope.
02	149 - 158	Annex C	Modelling updates reflecting updated Project Design Envelope.
02	178 - 195	Annex D	Modelling updates reflecting updated Project Design Envelope.
02	202 -207	Annex D	Modelling updates reflecting updated Project Design Envelope.

Contents

Tables

Figures

Glossary

Term	Definition
Array Areas	The DBS East and DBS West offshore Array Areas, where the wind turbines, offshore platforms and array cables would be located. The Array Areas do not include the Offshore Export Cable Corridor or the Inter-Platform Cable Corridor within which no wind turbines are proposed. Each area is referred to separately as an Array Area.
Array Cables	Offshore cables which link the wind turbines to the Offshore Converter Platform(s).
Astronomical Tide	The predicted tide levels and character that would result from the gravitational effects of the earth, sun, and moon without any atmospheric influences.
Bathymetry	Topography of the seabed.
Beach	A deposit of non-cohesive sediment (e.g. sand, gravel) situated on the interface between dry land and the sea (or other large expanse of water) and actively 'worked' by present-day hydrodynamic processes (i.e. waves, tides and currents) and sometimes by winds.
Clay	Fine-grained sediment with a typical particle size of less than 0.002mm.
Cumulative Effects Assessment (CEA)	The assessment of the combined effect of the Projects in combination with the effects of a number of different (defined cumulative) schemes, on the same single receptor/resource.
Current	Flow of water generated by a variety of forcing mechanisms (e.g. waves, tides, wind).
Dogger Bank South (DBS) Offshore Wind Farms	The collective name for the two Projects, DBS East and DBS West.
Effect	Term used to express the consequence of an impact. The significance of an effect is determined by correlating the magnitude of the impact with the value, or sensitivity, of the receptor or resource in accordance with defined significance criteria.
Expert Topic Group (ETG)	A forum for targeted engagement with regulators and interested stakeholders through the EPP.

Term	Definition
Gravel	Loose, rounded fragments of rock larger than sand but smaller than cobbles. Sediment larger than 2mm (as classified by the Wentworth scale used in sedimentology).
High Water	Maximum level reached by the rising tide.
Hydrodynamic	The process and science associated with the flow and motion in water produced by applied forces.
Inter-Platform Cable Corridor	The area where Inter-Platform Cables would route between platforms within the DBS East and DBS West Array Areas, should both Projects be constructed.
Inter-Platform Cables	Buried offshore cables which link offshore platforms.
Intertidal	Area on a shore that lies between Mean High Water Springs (MHWS) and Mean Low Water Springs (MLWS).
Landfall	The point on the coastline at which the Offshore Export Cables are brought onshore, connecting to the onshore cables at the Transition Joint Bay (TJB) above mean high water.
Long-Term	Refers to a time period of decades to centuries.
Low Water	The minimum height reached by the falling tide.
Mean High Water Springs	MHWS is the average of the heights of two successive high waters during a 24 hour period.
Mean Low Water Springs	MLWS is the average of the heights of two successive low waters during a 24 hour period.
Mean Sea Level	The average level of the sea surface over a defined period (usually a year or longer), taking account of all tidal effects and surge events.
Neap Tide	A tide that occurs when the tide-generating forces of the sun and moon are acting at right angles to each other, so the tidal range is lower than average.
Nearshore	The zone which extends from the swash zone to the position marking the start of the offshore zone (~20m).
Numerical Modelling	Refers to the analysis of coastal processes using computational models.

Term	Definition
Offshore	Area seaward of nearshore in which the transport of sediment is not caused by wave activity.
Offshore Development Area	The Offshore Development Area for ES encompasses both the DBS East and West Array Areas, the Inter-Platform Cable Corridor, the Offshore Export Cable Corridor, plus the associated Construction Buffer Zones.
Offshore Export Cable Corridor	This is the area which will contain the offshore export cables ~~(and potentially the ESP)~~ between the Offshore Converter Platforms and Transition Joint Bays at the landfall.
Offshore Export Cables	The cables which would bring electricity from the offshore platforms to the Transition Joint Bays (TJBs).
Sand	Sediment particles, mainly of quartz with a diameter of between 0.063mm and 2mm. Sand is generally classified as fine, medium or coarse.
Sand Wave	Bedforms with wavelengths of 10 to 100m, with amplitudes of 1 to 10m.
Sediment	Particulate matter derived from rock, minerals or bioclastic matter.
Sediment Transport	The movement of a mass of sediment by the forces of currents and waves.
Shore Platform	A platform of exposed rock or cohesive sediment exposed within the intertidal and subtidal zones.
Short-Term	Refers to a time period of months to years.
Significant Wave Height	The average height of the highest of one third of the waves in a given sea state.
Silt	Sediment particles with a grain size between 0.002mm and 0.063mm, i.e. coarser than clay but finer than sand.
Spring Tide	A tide that occurs when the tide-generating forces of the sun and moon are acting in the same directions, so the tidal range is higher than average.
Suspended Sediment	The sediment moving in suspension in a fluid kept up by the upward components of the turbulent currents or by the colloidal suspension.

Term	Definition
The Applicants	The Applicants for the Projects are RWE Renewables UK Dogger Bank South (East) Limited and RWE Renewables UK Dogger Bank South (West) Limited. The Applicants are themselves jointly owned by the RWE Group of companies (51% stake) and Masdar (49% stake).
The Projects	DBS East and DBS West (collectively referred to as the Dogger Bank South Offshore Wind Farms).
Tidal Current	The alternating horizontal movement of water associated with the rise and fall of the tide.
Tidal Range	Difference in height between high and low water levels at a point.
Wave Height	The vertical distance between the crest and the trough.
Wavelength	The horizontal distance between consecutive wave crests (or alternative troughs).
Wind Turbine	Power generating device that is driven by the kinetic energy of the wind.

Acronyms

Term	Definition
BODC	British Oceanographic Data Centre
DBS	Dogger Bank South
DHI	Danish Hydraulic Institute
ECMWF	The European Centre for Medium-Range Weather Forecasts. It is an independent intergovernmental organisation supported by most of the nations of Europe.
ERA5	ECMWF Reanalysis v5 (ERA5). ERA5 is the fifth generation ECMWF reanalysis for the global climate and weather for the past 8 decades, and for the global wave for the past 4 decades.
ES	Environmental Statement
ETG	Expert Topic Group
Hs	Significant wave height
JONSWAP	JONSWAP (Joint North Sea Wave Project) spectra is an empirical relationship that defines the distribution of energy with frequency within the ocean. It is effectively a fetch-limited version of the Pierson-Moskowitz spectrum.
km	kilometre
Lidar	Light Detection and Ranging
MHWS	Mean High Water Spring
MIKE21-SW MIKE3-HD MIKE3-MT	They are modules of MIKE modelling suite developed by DHI. MIKE21-SW is a 2D Spectral Wave model; MIKE 3-HD is a 3D Hydrodynamic model; and MIKE3-MT is a 3D sediment transport model.
RP	Return Period (RP1 – 1 in 1 year; RP100 – 1 in 100 year)
Tm	Mean wave period
TSHD	Trailing suction hopper dredger
UKHO	UK Hydrographic Office

8.3 Introduction

1. This document presents the methodology and results of the Project-specific marine physical processes modelling work undertaken to inform the Dogger Bank South (DBS) Offshore Wind Farms (hereafter referred to as 'the Projects') Environmental Statement (ES).

2. Through the Evidence Plan Process for the Marine Physical Environment Expert Topic Group (ETG), RWE Renewables UK Dogger Bank South (West) Limited and RWE Renewables UK Dogger Bank South (East) Limited (hereafter referred to as 'the Applicants') previously issued a Marine Physical Processes Method Statement on the 7th April 2022, which presented the case for the use of a conceptual modelling approach for the marine physical environment assessment within the Preliminary Environmental Statement (PEIR) and ES. This approach would not have included any Project-specific modelling, instead utilising the existing modelling conducted for the Dogger Bank A, B, C, and Sofia offshore wind farms to determine the potential effects of the Projects on the marine environment.

3. The physical and sedimentary conditions of the Projects and Dogger Bank A and B were predicted to be similar given their proximity and the comparability of physical environmental conditions between locations. The results of modelling with respect to construction effects on suspended sediment concentration were considered to provide suitable evidence (and were suitable analogues) to support the assessment of effects caused by installation of monopiles within the Offshore Development Area. The previous modelling undertaken for Dogger Bank A, B and C and Sofia for operational effects was undertaken at geographical and geometrical worst case scales far in excess of the likely Rochdale Envelope for the Projects and therefore was considered to be appropriate to support assessment the Projects. This process was developed further through further rounds of consultation with the ETG, with a technical note issued in December 2022 expanding on the information included within the initial method statement and responses issued to queries raised during the 20th January 2023 Marine Physical Environment ETG.

4. Following receipt of comments on the PEIR from stakeholders confirming their preference for Project-specific modelling to be undertaken for final application, the Applicants decided to undertake Project-specific modelling to inform the ES.

5. This report details the methodology, inputs into the model and final results of the modelling work in relation to the following modelling campaigns:

    - Wave modelling;

- Hydrodynamic modelling; and
- Sediment dispersion modelling.

8.3.1 Data Collection

8.3.1.1 Bathymetry

6. Detailed bathymetry data has been provided by RWE Renewables covering the Agreement for Lease Areas which include the Array Areas, namely DBS West and DBS East (**Figure 8-3-1**) as well as the Offshore Export Cable Corridor (**Figure 8-3-2**). This was obtained from site specific survey undertaken for the Project (Fugro, 2023a; 2023b).

7. Bathymetry in nearshore areas was obtained from the UK Hydrographic Office (UKHO) Data Portal[1], including 2011 data covering 2km to 5km offshore from Flamborough Head to Spurn Point, and 2020 data covering up to 15km offshore between Flamborough Head and Withernsea (see **Figure 8-3-2**).

8. For any beach areas not covered by nearshore bathymetry data, the latest available Light Detection and Ranging (Lidar) from Department of Environment, Food and Rural Affairs (Defra) Data Service Platform[2] was used (see **Figure 8-3-2**).

9. For offshore areas where there was no detailed bathymetry available from RWE Renewables, bathymetry data was obtained from the European Marine Observation and Data Network Bathymetry Portal[3] for the wave model (see **Figure 8-3-2**) and the local hydrodynamic model.

[1] https://datahub.admiralty.co.uk/portal/apps/sites/#/marine-data-portal
[2] https://environment.data.gov.uk/survey
[3] https://emodnet.ec.europa.eu/geoviewer/

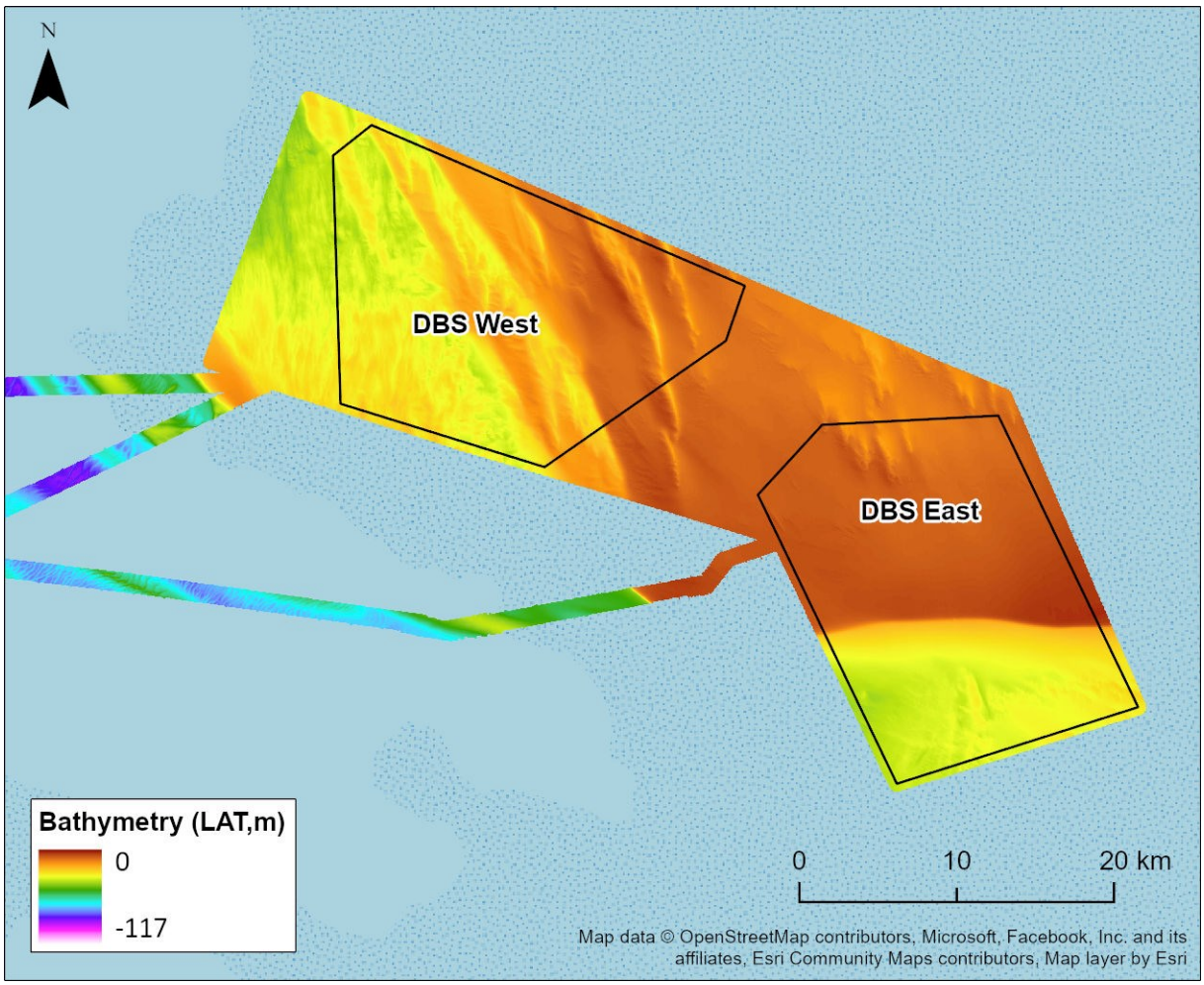

Figure 8-3-1: Detailed bathymetry of the Array Areas DBS West and DBS East

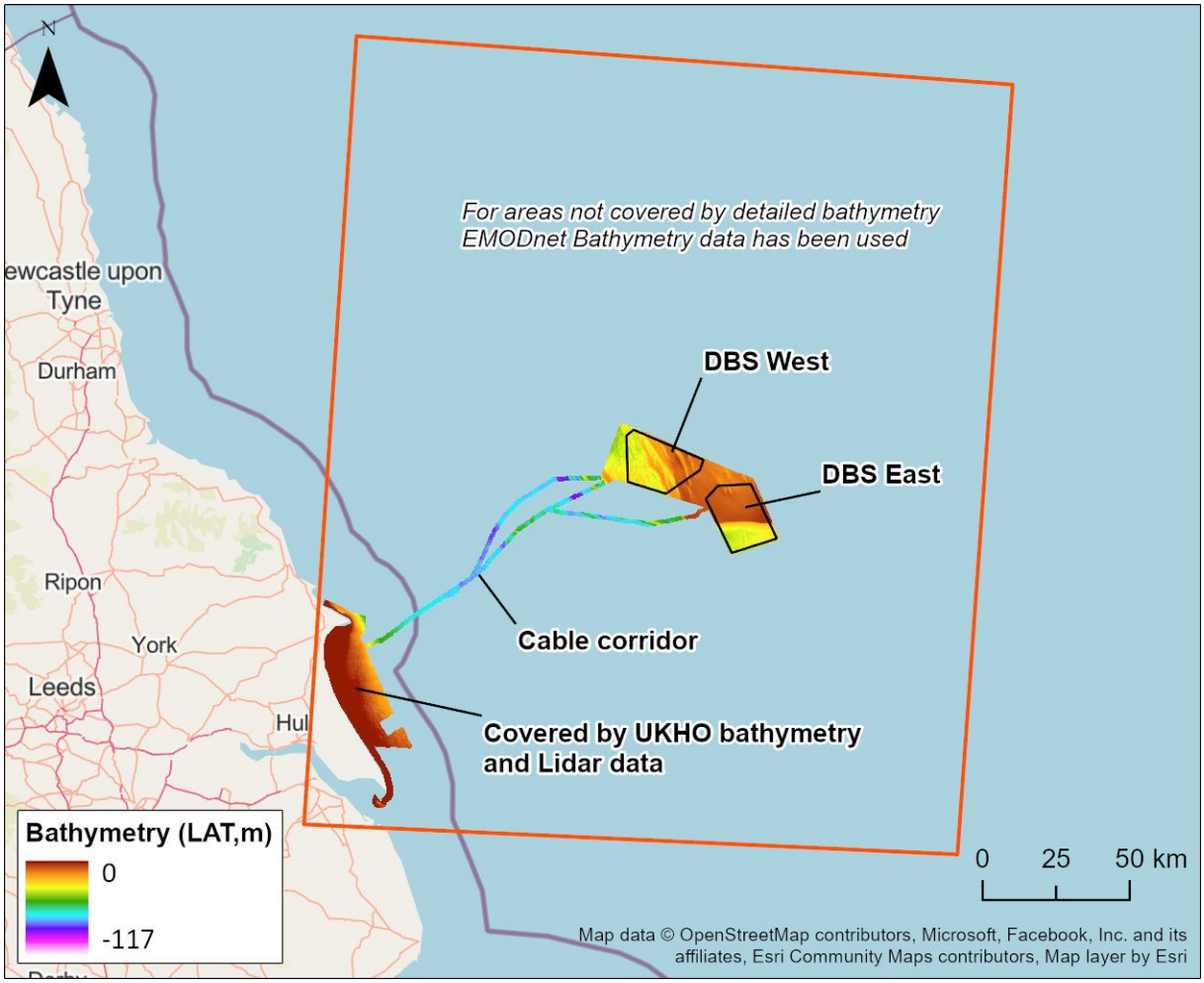

Figure 8-3-2: Coverage of Bathymetry Data Used in the Wave Model

8.3.1.2 Wind and Wave Data

8.3.1.2.1 Measured Wave Data

10. Measured wave buoy data has been provided by RWE Renewables at two locations, one for each Array Area for the period between 15th March 2022 and 11th May 2023. The wave buoy data was collected by Partrac, hereafter referred to as 'Partrac wave buoy' data.

11. Measured wave buoy data was also downloaded from the Channel Coastal Observatory[4] near Hornsea, hereafter referred to as 'Hornsea wave buoy' data.

12. The locations of the Partrac wave buoys offshore and the nearshore Hornsea wave buoy are shown in **Figure 8-3-3**.

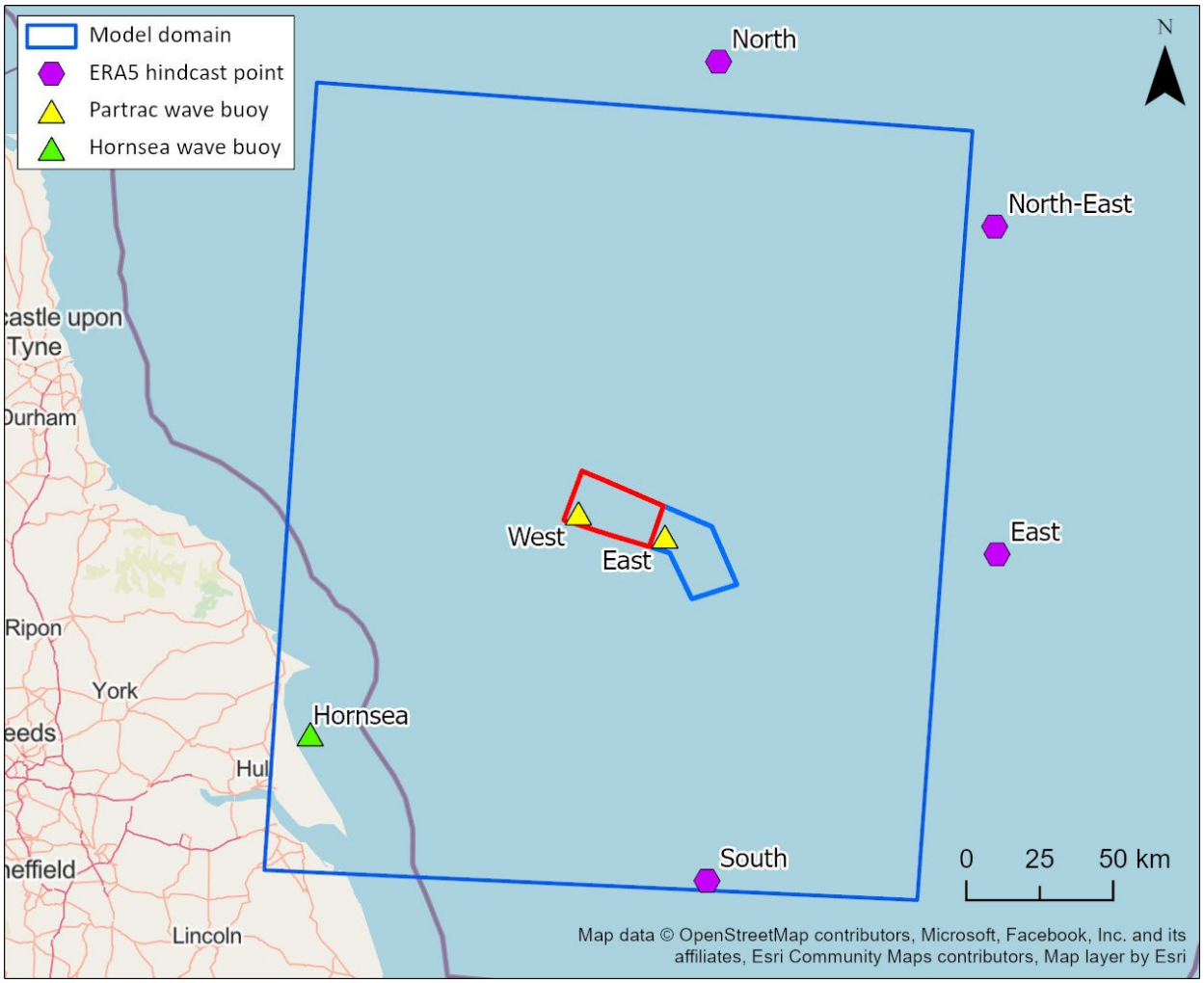

Figure 8-3-3: Wave Buoy Locations and ERA5 Hindcast Model Points Used for Wave Model Calibration and Verification (yellow triangles are Partrac wave buoy offshore and green triangle is Hornsea wave buoy nearshore)

[4] https://coastalmonitoring.org/realtimedata/

8.3.1.2.2 Hindcasted Wind and Wave Data

13. Atmospheric hindcast wind and wave data close to the wave model boundary has been downloaded from European Centre for Medium-Range Weather Forecasts (ECMWF)[5] covering the period between January 1979 and May 2023. This data is often called 'ERA5 hindcast data' and hereafter referred to as this in this report.

8.3.1.3 Water Level Data

14. Measured water levels from 1st March 2022 to 31st May 2023 were downloaded from British Oceanographic Data Centre (BODC)[6] at three locations; North Shields, Whitby and Cromer. The locations (1,2, and 3) are shown in **Figure 8-3-4** and the coordinates in **Table 8-3-1**. These measured water levels were used to calibrate the regional and local hydrodynamic models.

Table 8-3-1 Locations of the Measured Water Levels

ID	Station name	Longitude (degrees)	Latitude (degrees)	Time interval (minutes)	Duration
1	North Shields	-1.40	55.01	60	3/2022 – 5/2023
2	Whitby	-0.61	54.49	60	3/2022 – 5/2023
3	Cromer	1.30	52.93	60	3/2022 – 5/2023

[5] https://www.ecmwf.int/en/forecasts/dataset/ecmwf-reanalysis-v5
[6] https://www.bodc.ac.uk/

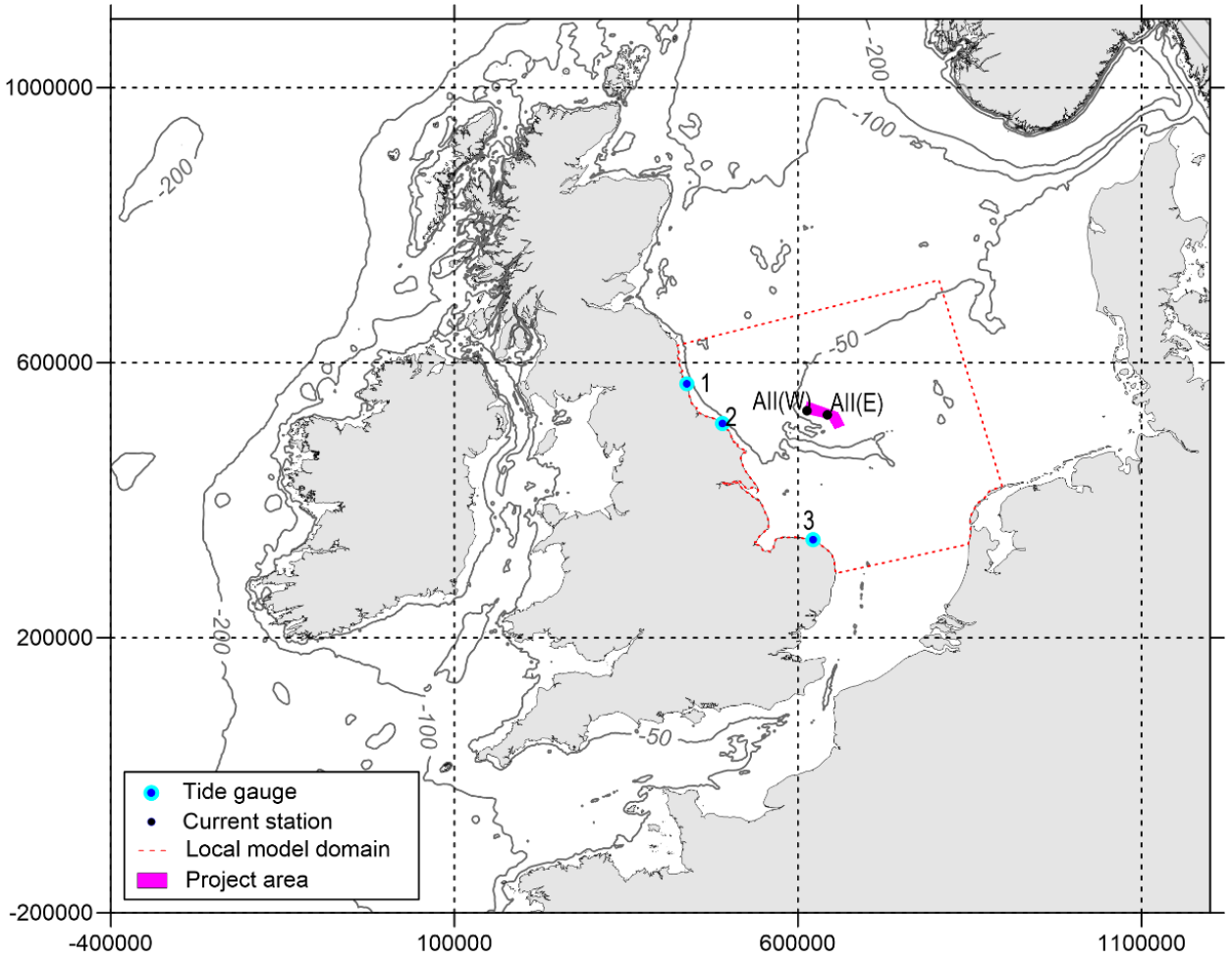

Figure 8-3-4 Locations of Tidal Gauges and Current Stations

8.3.1.4 Tidal Current Data

15. Measured current data was collected by Partrac at the same locations as the two wave buoys shown in **Figure 8-3-3** (**Table 8-3-2**). This data was used in the calibration of the local hydrodynamic model. A description of the measured data including locations is provided in **Table 8-3-2**.

Table 8-3-2 Locations of the Measured Current Speeds

Station name	Longitude (degrees)	Latitude (degrees)	Time interval (minutes)	Duration
DBS West	001°17.734'E	54°37.147'N	20	3/2022 – 5/2023
DBS East	001°45.188'E	54°33.196'N	20	3/2022 – 5/2023

8.3.2 Wave Modelling

8.3.2.1 Model Configuration

16. The MIKE21-SW model was set up with the bathymetry data described in section 8.3.1.1. The south-west corner of the model is located near the Humber Estuary and extends approximately 268km northwards and 224km eastwards. The wave model extent is shown in **Figure 8-3-5**.

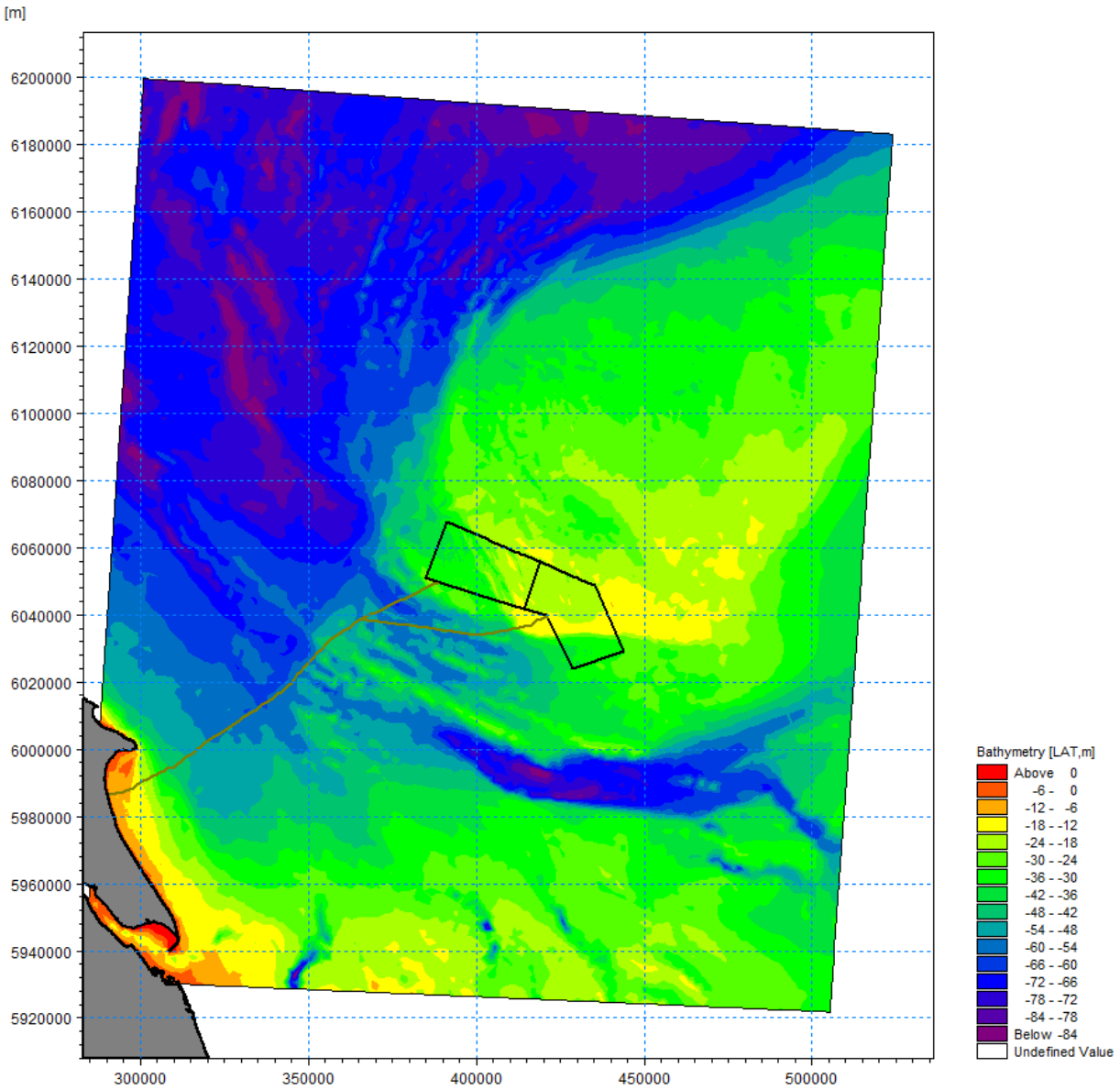

Figure 8-3-5: Extent of the MIKE21-SW-FM Model Domain and Bathymetry

17. The MIKE21-SW modelling software allows unstructured triangular meshes which enables the model to use a coarser grid (2,000m) across areas further away from the proposed development site and a finer mesh in the areas of greatest interest (200m). This approach enables higher computational efficiency whilst still maintaining sufficient accuracy of mesh coverage in areas of greatest interest. **Figure 8-3-6** shows the mesh resolutions in the vicinity of the Array Areas.

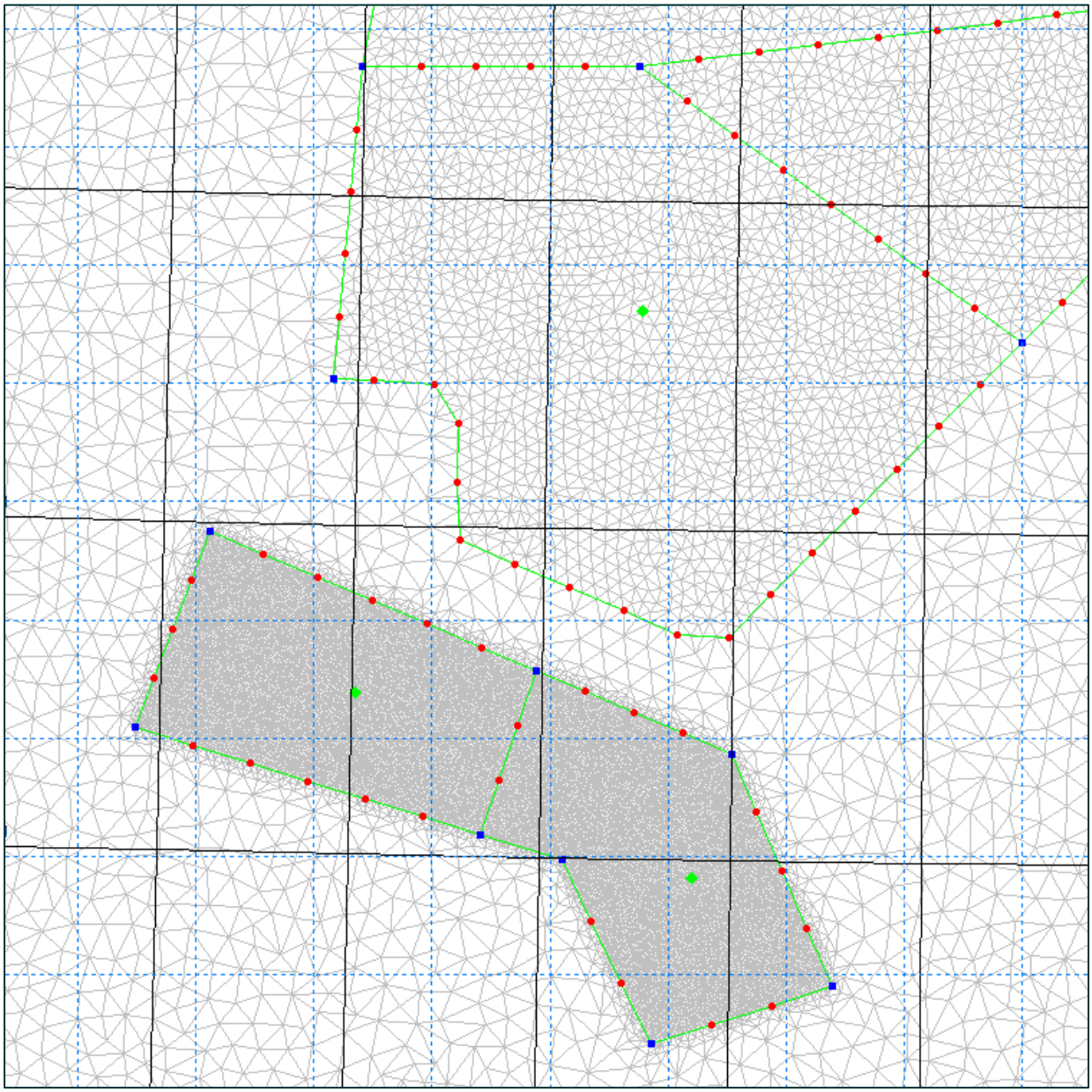

Figure 8-3-6: Wave Model Mesh Resolution (close-up view)

18. The wave model has been run with mean high water spring (MHWS) at 6.1mCD based on the Admiralty Tide Table at Bridlington. Given the relatively deep water at the site, the model results are not sensitive to water level (between high and low tides).

19. ERA5 hindcast data has been applied to the model boundary. **Table 8-3-3** shows the key wave model settings that have been chosen. The Joint North Sea Wave Project (JONSWAP) spectrum and the standard shape parameters were adopted for model simulation.

Table 8-3-3: MIKE21-SW Model Settings

MIKE21 Parameter	Chosen Parameter
Basic Equations	Spectral Formulation: Directionally Decoupled Time Formulation: Quasi Stationary
Spectral Discretization	360 degrees rose: 36 directions
Solution Technique	Low order, fast algorithm Iterations: 50
Diffraction	None
Wave Breaking	Gamma data: Constant value of 0.8 Alpha: 1 Gamma (wave steepness): 1
Bottom Friction (roughness height)	0.001m
Wave growth by wind	SPM73

8.3.2.2 Model Calibration and Verification

8.3.2.2.1 Model Calibration

20. A model calibration exercise was completed to ensure that the wave model produces similar wave heights (both in magnitude and pattern) when comparing the measured wave buoy data for storm events. For the calibration process, ERA5 hindcast wind and wave data was downloaded for the same period as the measured 'Partrac wave buoy' data. The hindcast data was downloaded at four locations around the model boundary (**Figure 8-3-3**).

21. The largest storm events recorded during the wave buoy deployment between March 2022 to May 2023 were chosen, and the ERA5 offshore wave and wind conditions for these events applied to the model domain boundary. In this exercise, waves from north, north-east, east and south were chosen for their frequency and magnitude as well as their travelling directions relative to the UK coastline. For a storm event with waves approaching from the north, the ERA5 hindcast point 'North' was applied for the boundary condition; for a storm event with waves approaching from the east, the ERA5 hindcast point 'East' was used. The same approach was used for waves from other directions. The model results for these storm events have been extracted from the same location as the Partrac wave buoys East and West for comparison.

22. The figures in Annex A present comparisons between the measured and modelled wave height data at the locations of the Partrac wave buoys located inside the Array Areas. The measured data are presented as small crosses, and the modelled data is drawn as solid lines. For both sets of data, the DBS West buoy is shown in blue and the DBS East buoy in red. The figures also show the ERA5 hindcast wave height (dashed orange), wind speed (dashed pink) and wind direction (dotted green) that has been applied to the model boundary.

23. Overall, there is a good agreement between the measured wave height and modelled wave height for storm events. It should be noted that ERA5 hindcast wind and wave data were produced by numerical models and were not measured data. Therefore, when the ERA5 hindcast wave height data at the offshore boundary was lower than the measured wave height inside the model domain, it was not possible to match the measured data if hindcast wind was not sufficiently strong to grow waves. Another factor that could have an impact on the measured data is localised weather conditions around the wave buoys which are not captured in the ERA5 hindcast data and therefore can lead to discrepancies in the comparison.

24. A summary of the 12 calibration storm events is presented in **Table 8-3-4**.

Table 8-3-4: Summary of the Wave Model Calibration for Storm Events

Calibration Storm Event	Wave Direction	Comments
Event 1	North	Good agreement; modelled data matches the ERA5 curve well.
Event 2	North	Good agreement; similar to Event 1.
Event 3	North	Reasonable agreement; modelled wave heights are slightly underestimated. This might be due to the fact that the ERA5 wind data is not approaching from the north for the whole event duration, and localised weather conditions could also have an impact on the measured data.
Event 4	North	Good agreement.
Event 5	North	Good agreement; modelled data matches the ERA5 curve well, but when measured data is higher than the ERA5 boundary data, the model can't achieve a good match.
Event 6	North-East	Reasonable agreement; modelled data matches the ERA5 curve well, the higher wave height of the measured data could be due to localised weather conditions.
Event 7	North-East	Reasonable agreement; modelled data matches the ERA5 curve well, but overestimates the wave height. The higher wave height during the night of 1st April 2023 couldn't be achieved by the model because the ERA5 boundary conditions were nowhere near as high.
Event 8	East	Good agreement.
Event 9	East	Good agreement.
Event 10	South (South-West)	Good agreement; modelled data matches the ERA5 curve well especially for the first peak on 30th December 2022 with waves and wind from south, where the wind direction differs from that of the wave direction on 1st January 2023 the agreement is still reasonable but modelled wave height are slightly overestimated.

Calibration Storm Event	Wave Direction	Comments
Event 11	South	Good agreement; modelled data matches the ERA5 curve and the measured data well. The wave height peak on 2nd November 2022 could not be achieved due to the much lower ERA5 boundary condition. The reason might be localised weather conditions when the measurements were taken.
Event 12	South	Good agreement.

8.3.2.2.2 Model Verification

25. The wave model with the same settings (**Table 8-3-3**) from the calibration process was run to compare the measured wave data near Hornsea (see **Figure 8-3-3**). **Figure 8-3-7**, **Figure 8-3-8** and **Figure 8-3-9** show a comparison between the measured and modelled wave height at the locations of Hornsea wave buoy for storm waves from the north, east and north-east, respectively. The measured data are presented as small crosses, the modelled data are drawn as solid lines. The figures also show the ERA5 hindcast wave height (dashed orange), wind speed (dashed pink) and wind direction (dotted green) that has been applied to the model boundary. Overall, there is a reasonably good agreement (both in magnitude and pattern) between the measured and the modelled wave heights for three storm events, considering that the model was driven by hindcasted data.

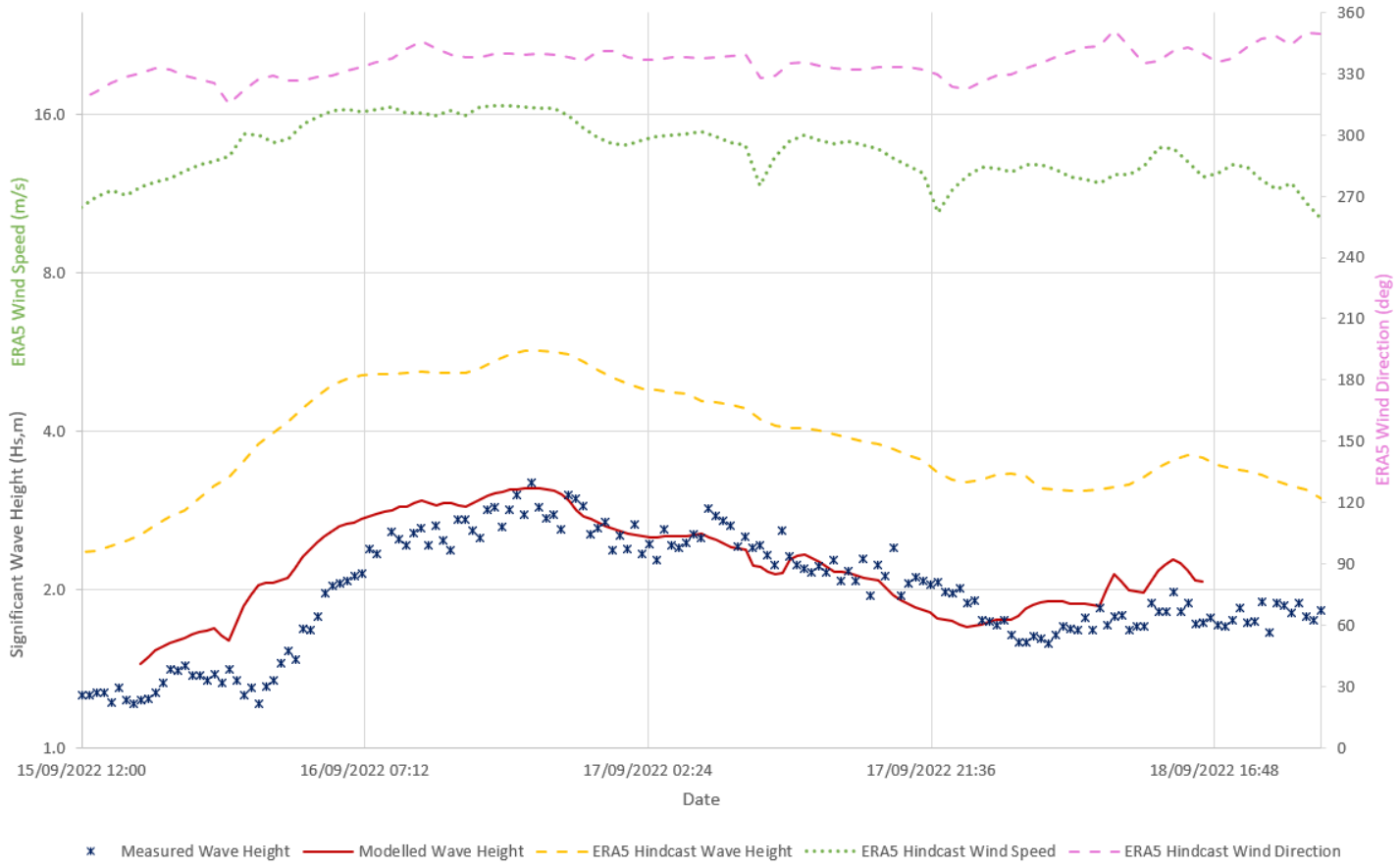

Figure 8-3-7: Comparison of Measured and Modelled Wave Height at Hornsea Wave Buoy for Waves Approaching from the North

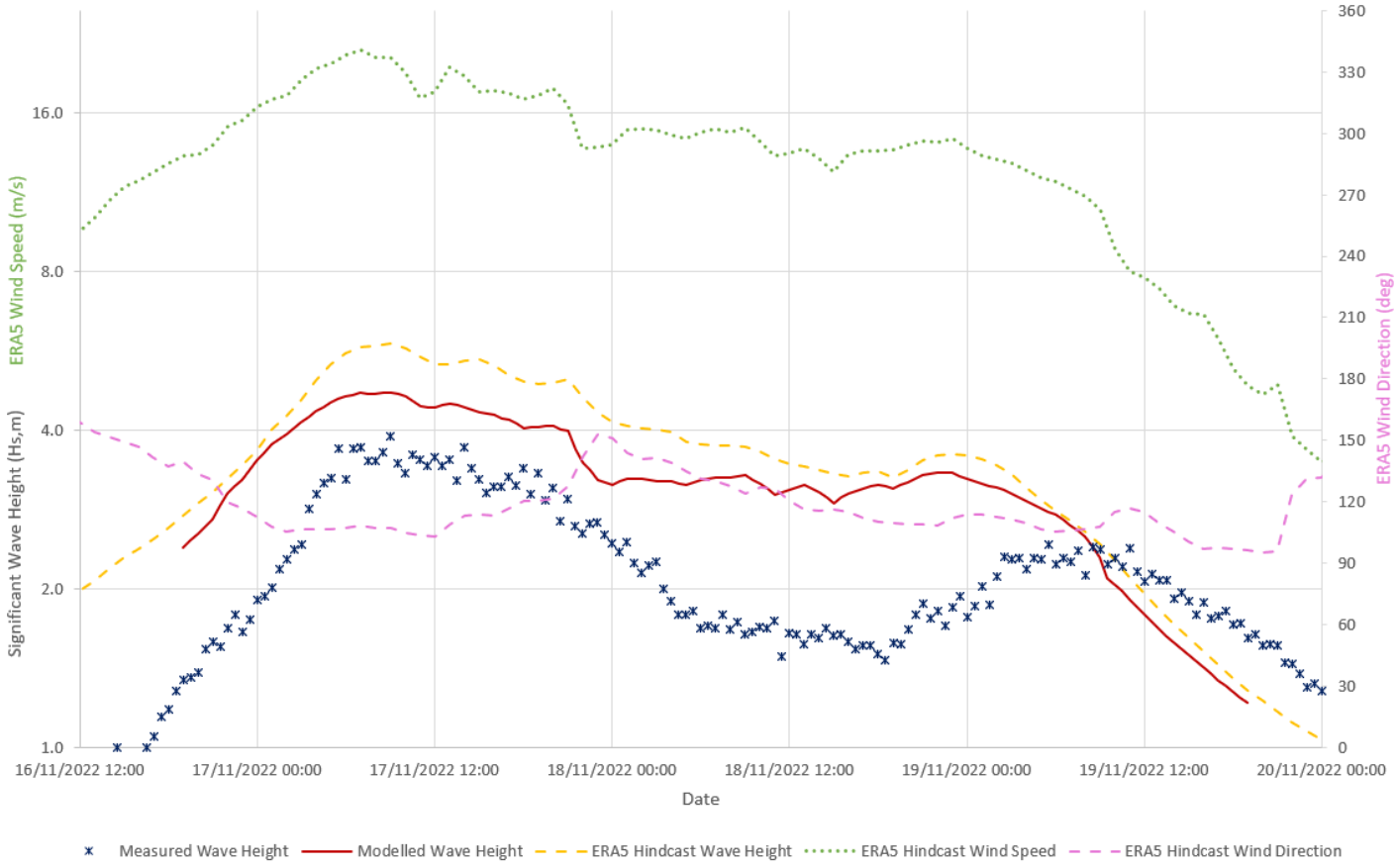

Figure 8-3-8: Comparison of Measured and Modelled Wave Height at Hornsea Wave Buoy for Waves Approaching from the East.

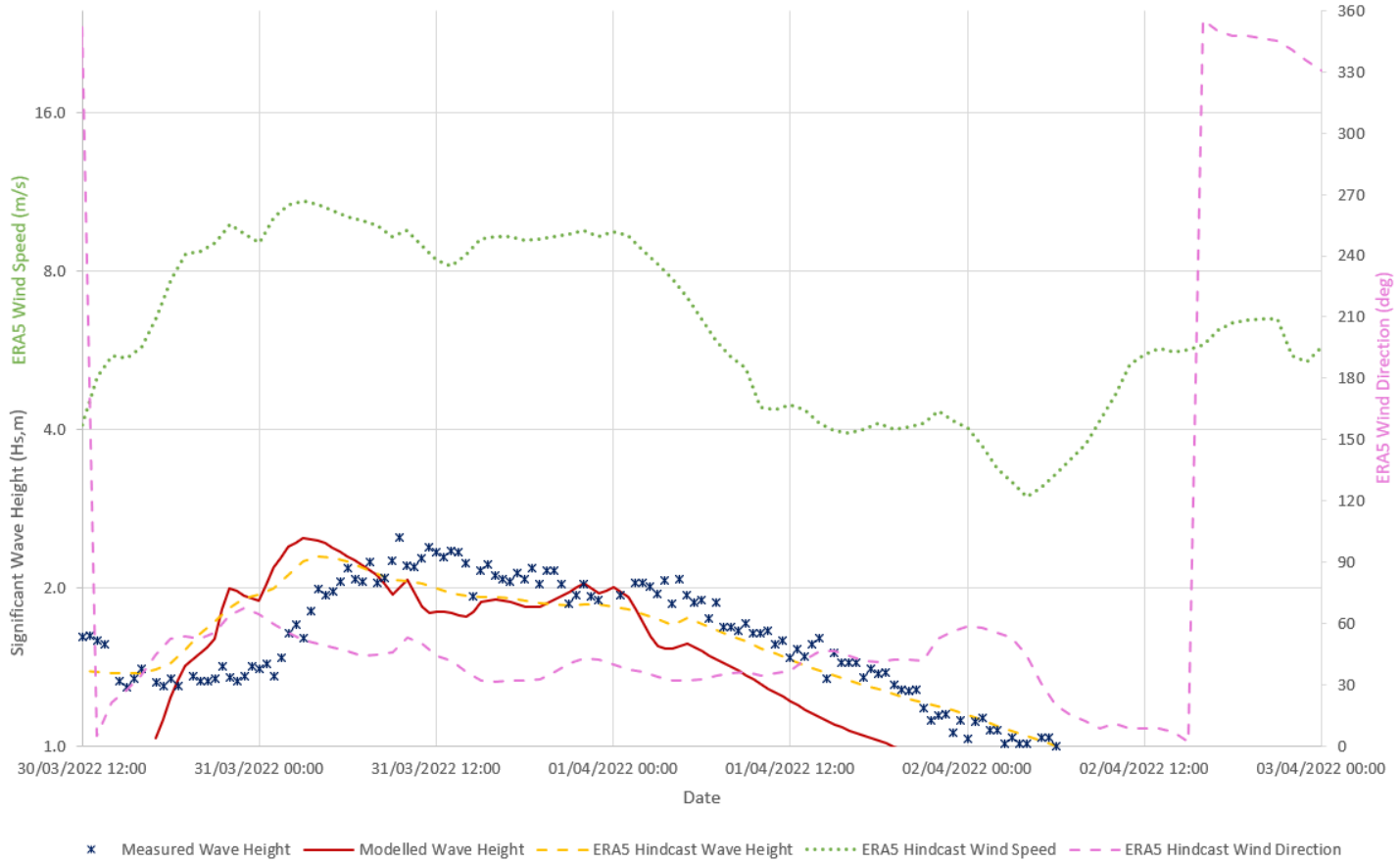

Figure 8-3-9: Comparison of Measured and Modelled Wave Height at Hornsea Wave Buoy for Waves Approaching from the North-east

8.3.2.3 Offshore Extreme Wave and Wind Analysis

26. ERA5 hindcast wave and wind time series data close to the wave model boundary has been downloaded from the European Centre for Medium-Range Weather Forecasts (ECMWF)[5] covering the period between January 1979 and May 2023.

27. The time series data has been used in the extreme wave analysis and the results for the considered wave directions are presented in **Table 8-3-5**. Based on these results, it was decided that the model representing waves approaching from the north should be run with the higher wave height of directional sector north to north-west for conservativeness. The wave direction of east was also chosen as this directional sector has the second largest waves and a relatively shorter distance to the UK mainland.

28. The significant wave heights for the 1 in 1 year and 1 in 50 year return periods from two chosen wave directions have been highlighted in red (**Table 8-3-5**).

Table 8-3-5: Extreme Offshore Wave Height at ERA5 Hindcast Point (for relevant wave directions)

Return Period	Significant Wave Height (Hs, m) per Wave Direction Sector					
	N-NW (315-345° N)	N (345-15°N)	N-NE (15-45°N)	E-NE (45-75°N)	E (75-105°N)	E-ES (105-135°N)
1	6.40	5.53	3.44	3.83	4.54	4.33
5	8.24	7.11	4.62	5.37	6.01	5.7
10	9.02	7.95	5.13	6.04	6.58	6.21
25	10.05	9.27	5.8	6.95	7.31	6.82
50	10.82	10.47	6.3	7.63	7.84	7.24
100	11.6	11.86	6.81	8.33	8.35	7.62
250	12.61	14.08	7.47	9.25	9.02	8.08
500	13.38	16.08	7.97	9.95	9.51	8.4
1000	14.14	18.42	8.48	10.65	9.99	8.69

Note: highlighted wave conditions were chosen for assessing potential effects from the Projects in this study

8.3.2.4 Model Simulations for Assessing Potential Impact

29. The wave model was run for the following three scenarios:

- 'Baseline' – without the Projects;
- 'Option 1' – with wind farm layout Option 1 with turbines spaced at approximately 1,000m around the perimeter and at approximately 3,000m spacing inside the Array Areas as shown in **Figure 8-3-10**.
- 'Option 2' – with wind farm layout Option 2 with turbines placed at approximately 830m spacing covering an indicatively smaller part of Array Areas as shown in **Figure 8-3-11**.

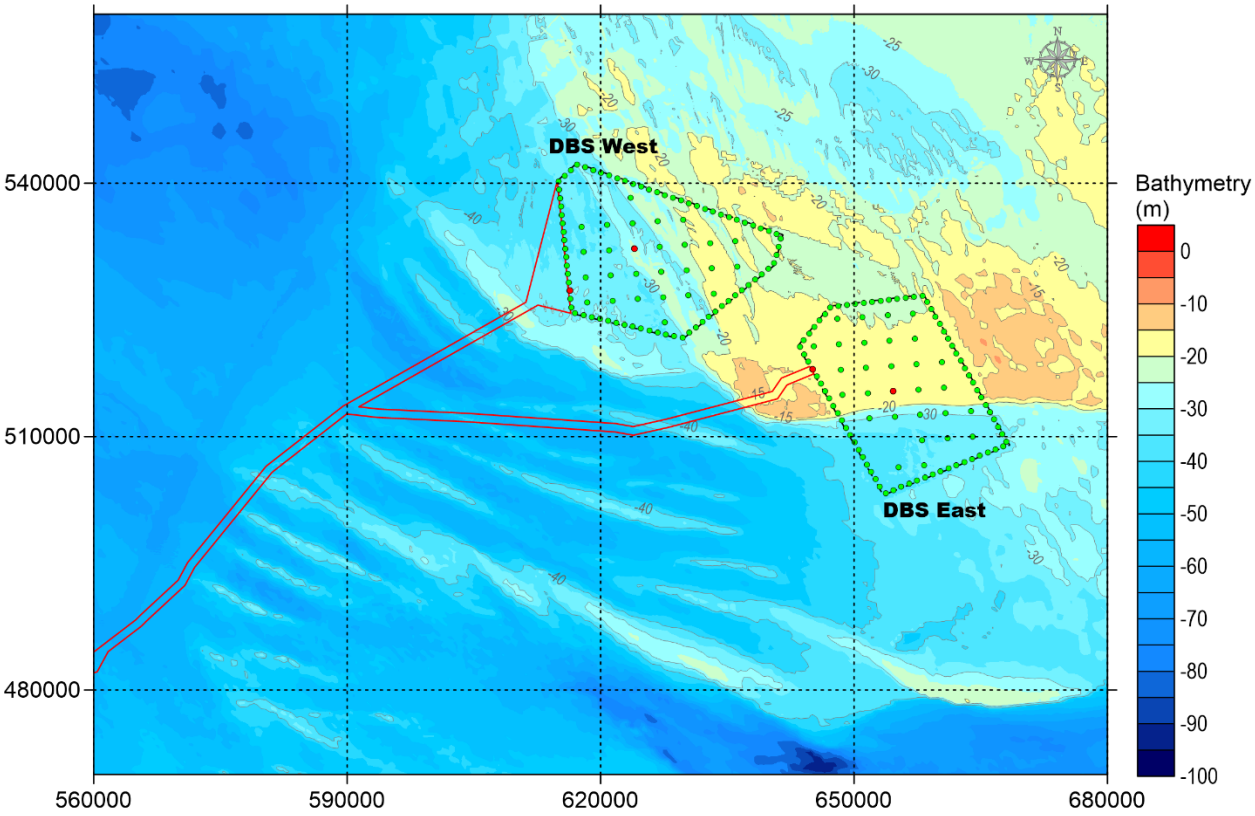

Figure 8-3-10: Windfarm Layout for Option 1 (perimeter alignment of turbines) (red dots: platform foundations ~~65m diameter; purple dot: two platform foundations positioned next to each other, and each foundation has a diameter of 65m; green dots: turbine foundations 15m diameter;~~)15m diameter)

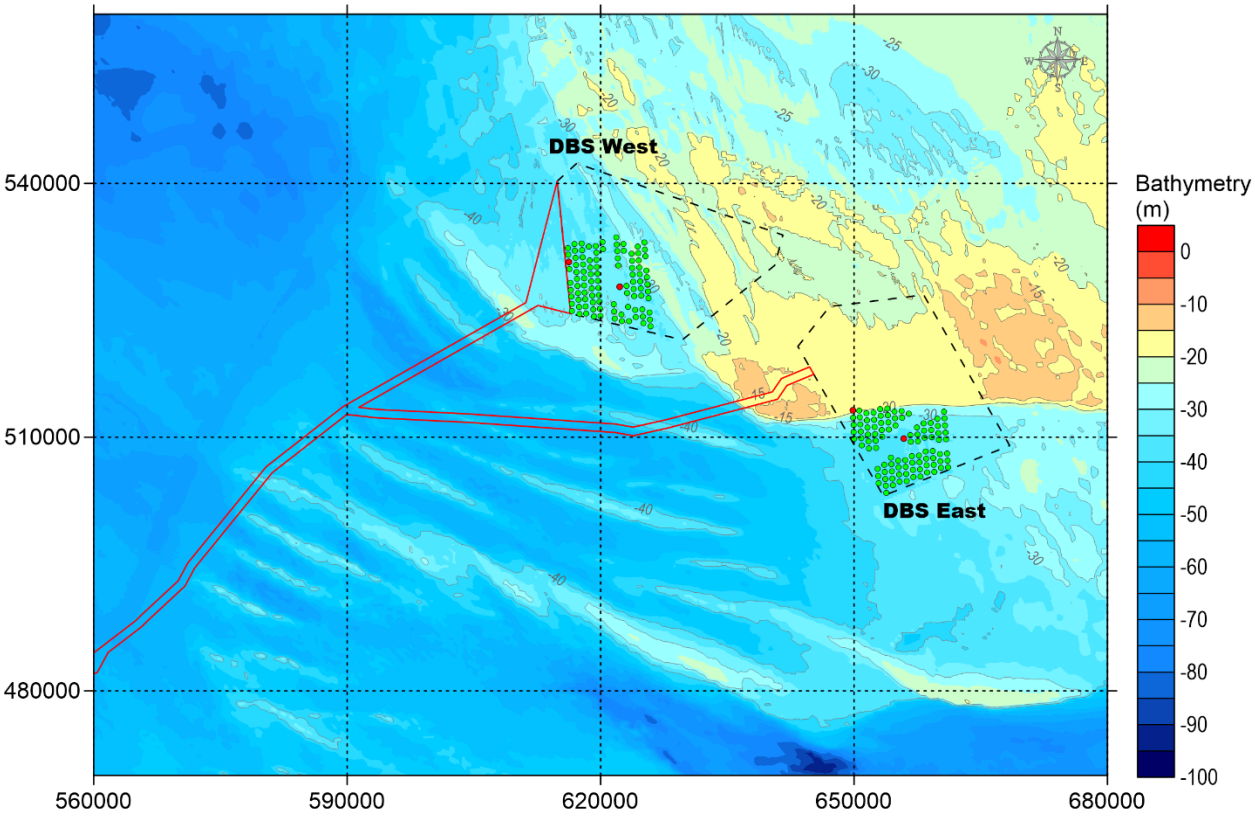

Figure 8-3-11: Windfarm Layout for Option 2 (indicative alignment of turbines spaced closer together) (red dots: platform foundations ~~65m diameter; purple dot: two platform foundations positioned next to each other, and each foundation has a diameter of 65m; green dots: turbine foundations 15m diameter;~~15m diameter)

30. It should be noted that the ~~nine~~four offshore platform locations ~~(one located along the Offshore Export Cable Corridor)~~ for both options have been chosen to represent realistic positions within the Array Areas.

31. Both layout options have been modelled with 200 turbines and ~~nine~~four offshore platform foundations (100 turbines~~, four~~ and two platform foundations for each wind farm Project's Array Area ~~and one offshore platform foundation along the Offshore Export Cable Corridor~~).

32. Each turbine foundation has been defined as a monopile with a diameter of 15m. This is based on the monopile foundation parameter for 'Large Turbines' specified in **Volume 7, Chapter 5 Project Description (application ref: 7.5)**. Each platform foundation has been defined as monopile with a diameter of ~~65m, as a worst-case proxy for a GBS foundation~~15m.

33. The wave model has been run for:

- Two return periods; 1 in 1 year and 1 in 100 years, plus 50th percentile value representing average wave condition.
- Two wave directions; waves approaching from the 'north' and 'east'. These directions have been selected due to their potential impact on environmental receptors along the UK coast. Also, these two directions have larger wave heights than other directions with respect to extreme wave conditions.

34. **Table 8-3-6** summarises all the wave model input parameters, including wave height, wave period, wave direction, wind speed and wind direction. For each wave condition, the wave model was run for three scenarios, including 'Baseline' and the two wind farm layouts; 'Option 1' and 'Option 2'.

Table 8-3-6: Wave Model Input Parameters

Return Period	Direction Sector	Wave Height (Hs, m)	Wave Period (Tp, s)	Wave Direc-tion (°N)	Wind Speed (m/s)	Wind Direc-tion (°N)
50th per-centile	North (345°N – 15°N)	1.75	8.72	345	8.0	345
50th per-centile	East (75°N – 105°N)	1.52	6.84	90	7.5	90
RP1	North (345°N – 15°N)	6.40	11.13	345	17.8	345
RP1	East (75°N – 105°N)	4.54	8.69	90	15.7	90
RP100	North (345°N – 15°N)	11.60	14.98	345	23.0	345
RP100	East (75°N – 105°N)	8.35	11.80	90	19.8	90

35. The model results are presented in **Annex B** and include:

- Modelled significant wave height for the 'Baseline' condition for the chosen test wave conditions;
- Difference in modelled significant wave height in metres between 'Baseline' and wind farm 'Option 1' for the chosen test wave conditions;

- Difference in modelled significant wave height in metres between 'Baseline' and wind farm 'Option 2' for the chosen test wave conditions;
- Difference in modelled significant wave height in percentage between 'Baseline' and wind farm 'Option 1' for the chosen test wave conditions; and
- Difference in modelled significant wave height in percentage between 'Baseline' and wind farm 'Option 2' for the chosen test wave conditions.

8.3.2.5 Discussion of Wave Model Results

36. For both wind farm layout options, the modelled significant wave heights near the wind farm Projects' Array Areas are reduced by the turbine foundations and offshore platforms. For 'Option 1', significant wave heights are reduced by a maximum of 0.1 to 0.7m. For 'Option 2', significant wave heights are reduced by a maximum of 0.2 to 0.7m. The largest reduction in significant wave height occurs local to the offshore platforms.

37. Whilst 'Option 2' has a slightly greater effect of reducing wave height than 'Option 1', the area affected by 'Option 2' is still quite small and local to the Array Areas, if a reduction of 4 to 6cm in wave height is considered as a criterion.

38. The affected area is smallest under the 50th percentile wave condition, whilst the affected area is largest under the 1 in 1 year wave conditions compared to the 1 in 100 year wave conditions. This is likely due to the wave conditions for the 1 in 100 year return period having longer wave periods. Waves with longer wave periods lose less energy by wave diffraction process in passing around obstacles.

39. The affected area for waves approaching from the 'north' extends southwards, and for waves coming from the 'east' extend westwards.

40. The extent of affected areas for the 50th percentile is similar between the two layout options. Areas with a 1 to 2cm reduction in wave height extend on average about 13km to the south for waves approaching from the 'north', and about ~~30km~~39km west for waves approaching from the 'east'. The affected areas with a 4 to 6cm reduction in wave height are much smaller and are located inside the wind farm Array Areas for waves approaching from both the 'north'~~, whilst reductions for waves approaching from~~ and the 'east' ~~are between 3 to 7km to the west~~.

41. The extent of the affected areas for the 1 in 1 year return period are similar between the two layout options. Areas of 1 to 2cm reduction in wave height extend on average about ~~56km to the south~~ 60km for waves approaching ~~from~~from both the '~~North~~'north' and ~~west for waves approaching from~~ the 'east', rippling out to the south and west respectively. The affected areas with a 4 to 6cm reduction in wave height are much smaller and are on average about ~~15km~~8km to the south ~~or~~for waves approaching from the 'north', and about 13km west~~, depending on wave direction~~ for waves approaching from the 'east'.

42. The extent of affected areas for the 1 in 100 year return period are smaller for both layout options compared to 1 in 1 year return period. Areas of 1 to 2cm reduction in wave height extend on average about ~~30km~~40km to the south for waves approaching from the 'north', and about 20km west for waves approaching from the 'east'. The affected areas for 4 to 6cm reduction in wave height are much smaller, and on average extend ~~7km~~4km to the south or west, depending on wave direction.

43. It should be noted that all these changes are relatively small when expressed as percentages; less than 5% for the maximum affected areas.

8.3.3 Hydrodynamic Modelling

8.3.3.1 Model Descriptions

44. Royal HaskoningDHV's established regional hydrodynamic model was used to provide boundary conditions for a local hydrodynamic model which was set up for investigating potential impact on hydrodynamics by the proposed wind farm. The local hydrodynamic model was also used to drive a suspended sediment dispersion model which is presented in section 8.3.4.

8.3.3.1.1 Regional Model

45. The regional model was built in MIKE21-HD modelling software developed by DHI. The computational mesh of the established regional model consists of 292,000 elements and 143,000 nodes. As the regional model was developed for simulation of the large-scale circulation patterns, the mesh resolution is relatively coarse, ranging from 1 - 5km. In general, the grid resolution increases towards the coast to capture more detail in the nearshore shallow water (**Figure 8-3-12**).

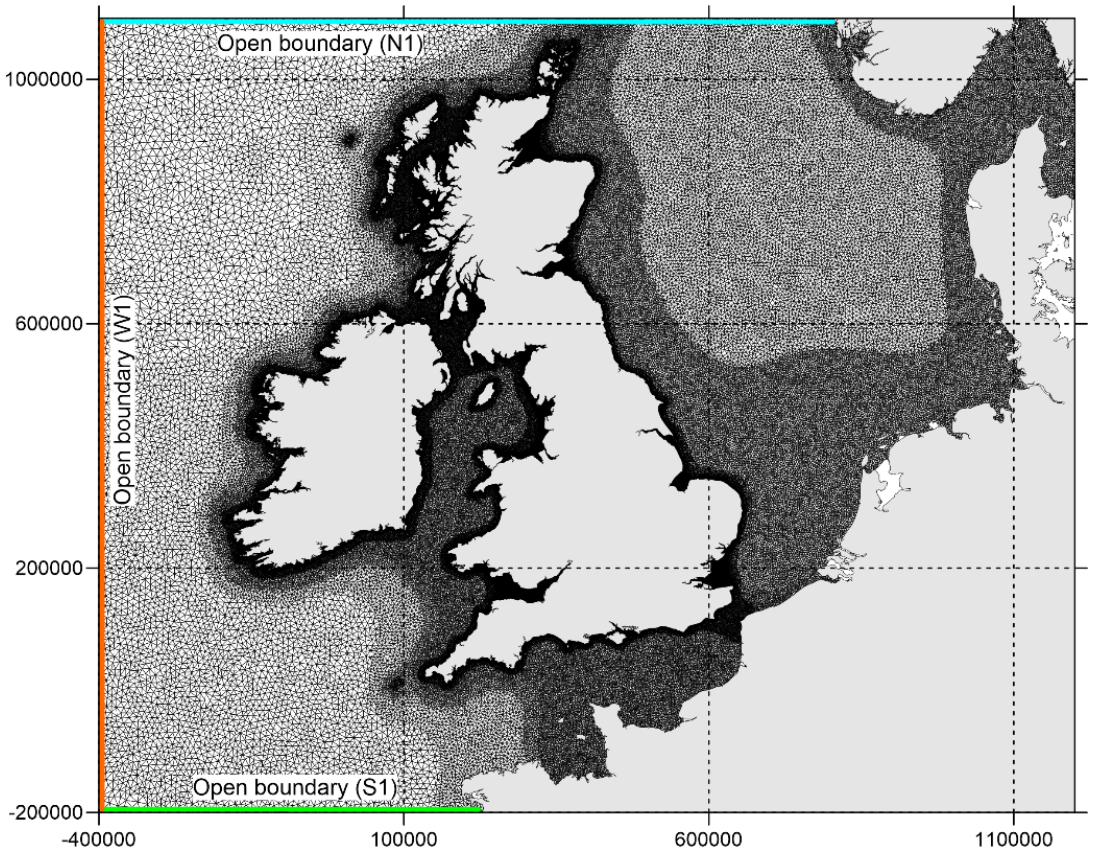

Figure 8-3-12 Computational Mesh of the Regional Hydrodynamic Model

46. The model bathymetry and grid were constructed based on C-Map[7] data (global digital navigation charts) and UKHO Portal1 data with coastline positions digitised from Google Earth[8]. The model bathymetry, shown in **Figure 8-3-13** has then been generated by the combined bathymetric data (of C-Map and UKHO Portal data).

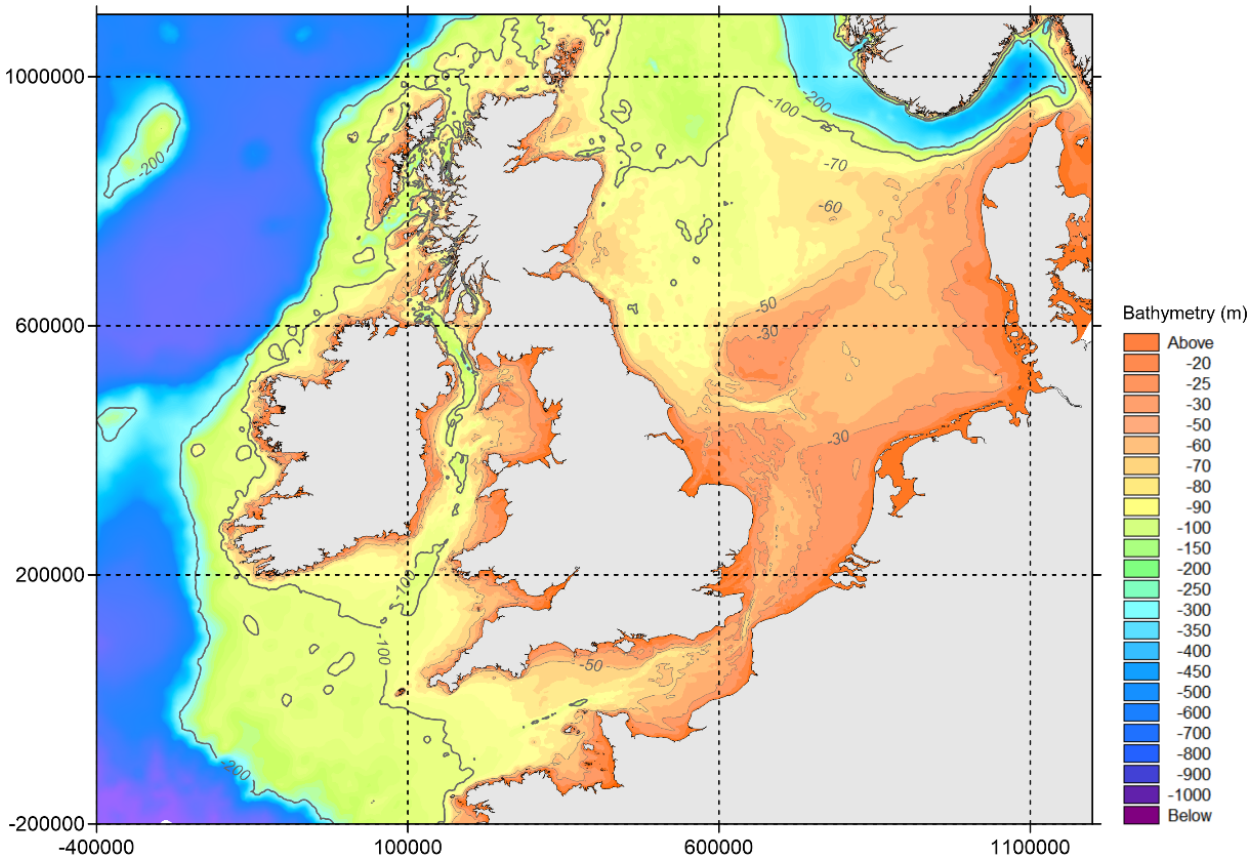

Figure 8-3-13 Bathymetry of the Regional Hydrodynamic Model

8.3.3.1.2 Local Model

47. A local hydrodynamic model was developed using MIKE3-HD software. Like the regional model, the flexible mesh was adopted in the local model. A coarser grid (1,000 - 2,000m) was used in remote areas and a finer grid (200 - 300m) in the areas of interest. For later model application runs for assessing the potential impact, the mesh was further refined around the project site.

[7] https://www.c-map.com/en-gb/home/
[8] https://earth.google.com/

48. The computational mesh of the local model consists of 52,516 elements and 26,799 nodes (see **Figure 8-3-14**). The local model bathymetry is shown in **Figure 8-3-15**.

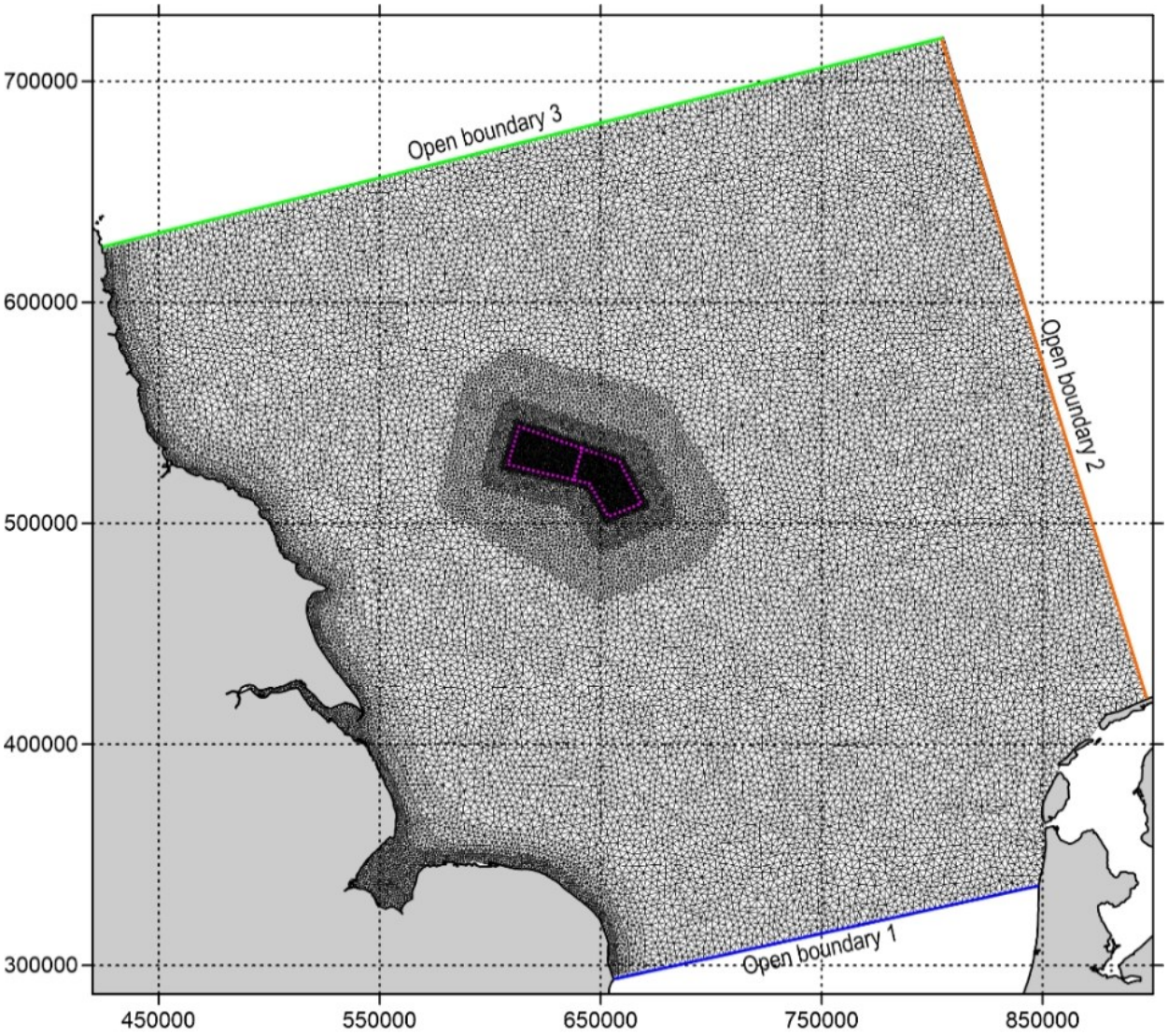

Figure 8-3-14 Computational Mesh of the Local Hydrodynamic Model

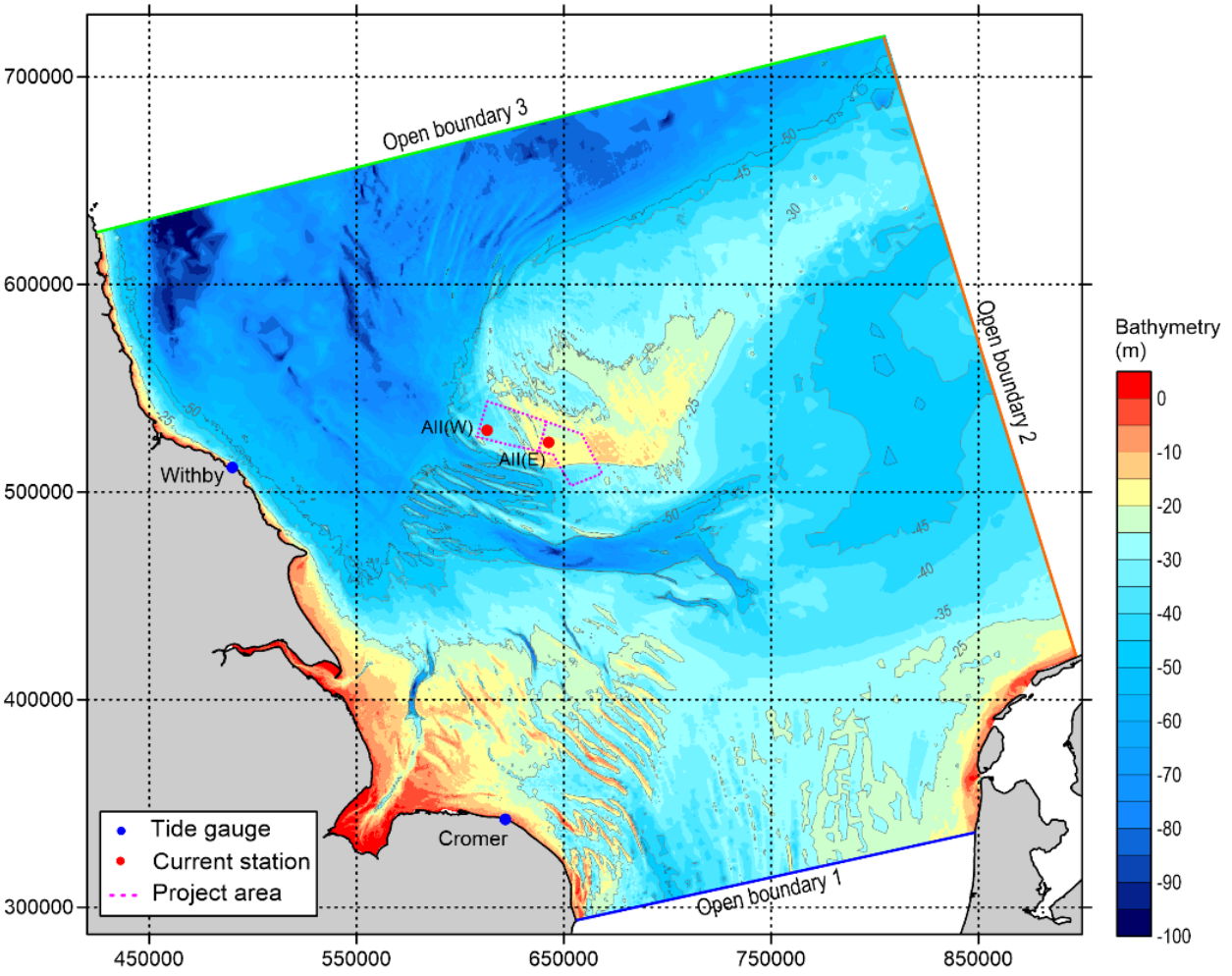

Figure 8-3-15 Bathymetry of the Local Model Domain (with tidal gauges and current stations marked)

8.3.3.2 Model Boundary Conditions

49. At the open boundaries of the regional model, water levels were used, which vary in time and along the boundaries. The input data for these boundaries were extracted (at locations N1, S1 and W1 as in **Figure 8-3-12**) from the Global Tidal Model of DHI with a spatial resolution of 0.25° × 0.25°. The data represents the major diurnal (K1, O1, P1 and Q1) and semidiurnal tidal constituents (M2, S2, N2 and K2) based on OPEX/POSEIDON altimetry data.

50. **Figure 8-3-14** shows the boundaries of the local model. The open boundaries 1 and 3 are set as velocity boundaries varying in time, and open boundary 2 is set to water level boundary varying in time along the boundary. The velocity and water level along these boundaries were provided from the regional model.

8.3.3.3 Model Calibration

8.3.3.3.1 Regional Model Re-Calibration (water levels)

51. For this study, the regional model has been re-calibrated using measured water levels recorded at North Shields, Whitby and Cromer. Re-calibration performance is assessed by both visual comparison and quantifying errors using statistical parameters including Correlation Coefficient and Mean Absolute Error. **Figure 8-3-16**, **Figure 8-3-17** and **Figure 8-3-18** show the modelled and measured water levels, and **Table 8-3-7** presents quantified errors. Both visual comparison and error statistics show reasonably good agreement between the measured and modelled water levels.

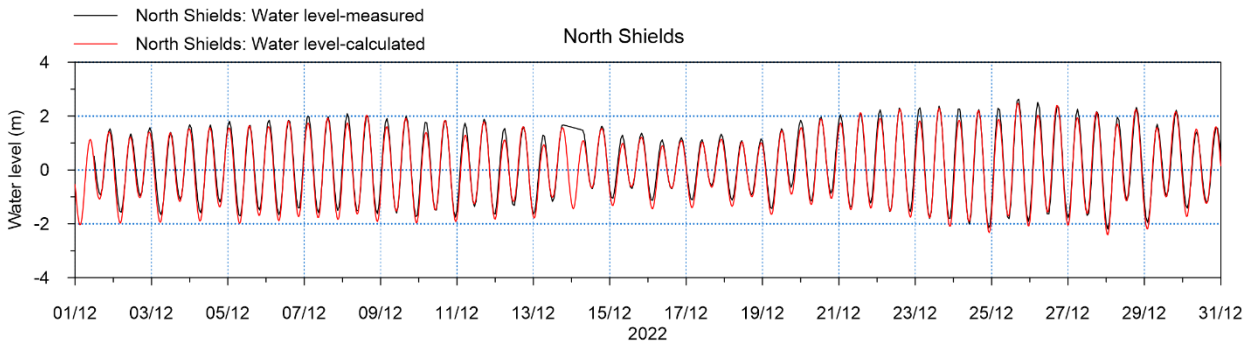

Figure 8-3-16 Time Series Comparison Between Simulated vs Observed Water Levels at North Shields in December 2022 (Regional model)

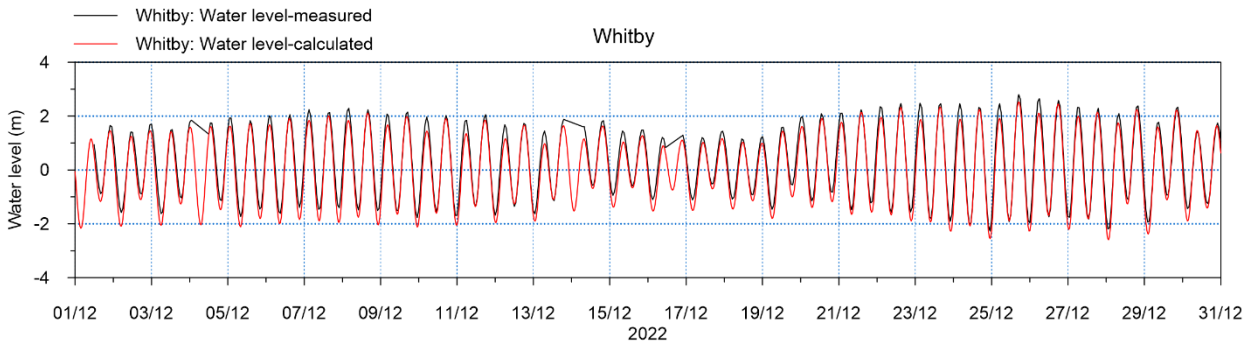

Figure 8-3-17 Time Series Comparison Between Simulated vs Observed Water Levels at Whitby in December 2022 (Regional model)

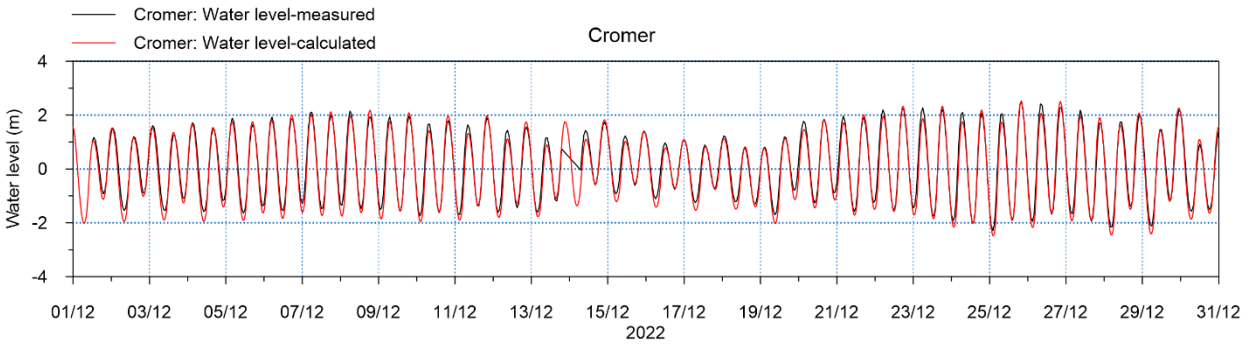

Figure 8-3-18 Time Series Comparison Between Simulated vs Observed Water Levels at Cromer in December 2022 (Regional model)

Table 8-3-7 Water Level Time Series Statistics for Regional Model

Name of station	Mean Error (m/s)	Mean Absolute Error (m/s)	Standard Deviation (m)	Correlation Coefficient (R)
North Shields	0.12	0.17	0.17	0.98
Whitby	0.24	0.26	0.18	0.98
Cromer	0.13	0.18	0.20	0.98

8.3.3.3.2 Local Model Calibration (water level)

52. The local model has been calibrated using measured water levels recorded at Whitby and Cromer for two periods (June 2022 and December 2022). Model calibration performance is assessed by both visual comparison and quantifying errors using statistical parameters including Correlation Coefficient and Mean Absolute Error. **Figure 8-3-19** to **Figure 8-3-22** show the modelled and measured water levels, and **Table 8-3-8** presents quantified errors. Both visual comparison and error statistics show reasonably good agreement between measured and modelled water levels.

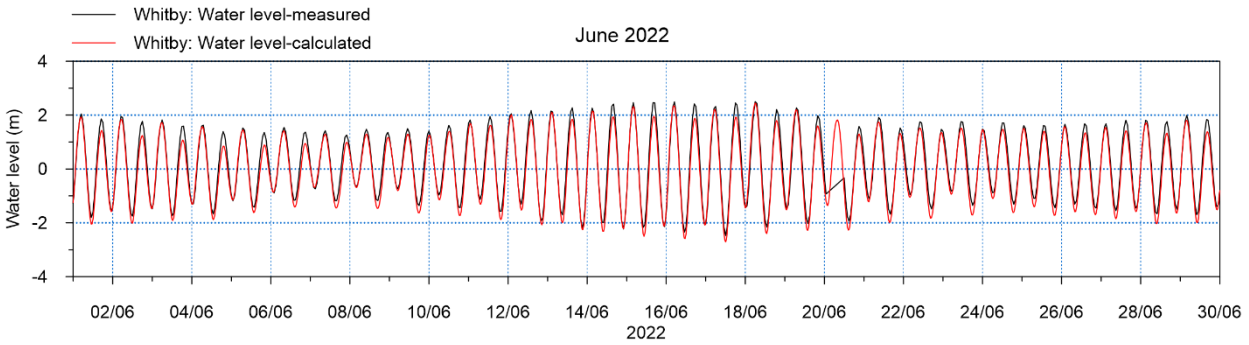

Figure 8-3-19 Time Series Comparison Between Simulated vs Observed Water Levels at Whitby in June 2022 (Local model)

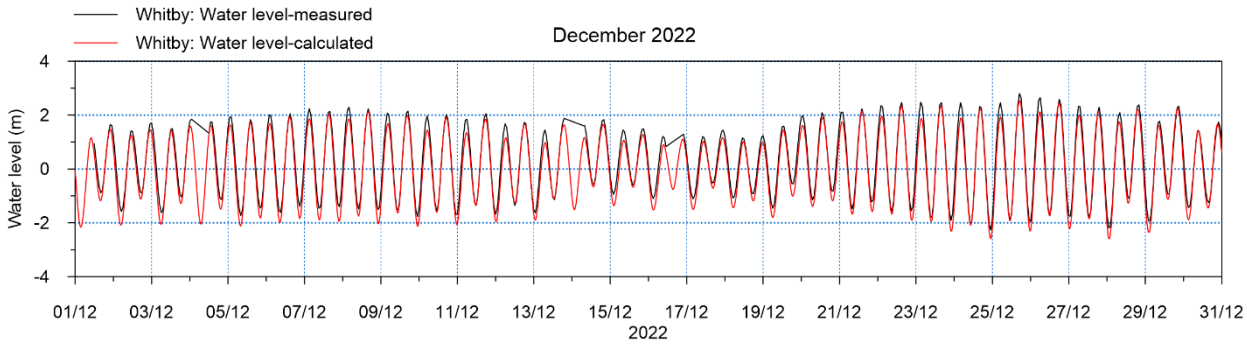

Figure 8-3-20 Time Series Comparison Between Simulated vs Observed Water Levels at Whitby in December 2022 (Local model)

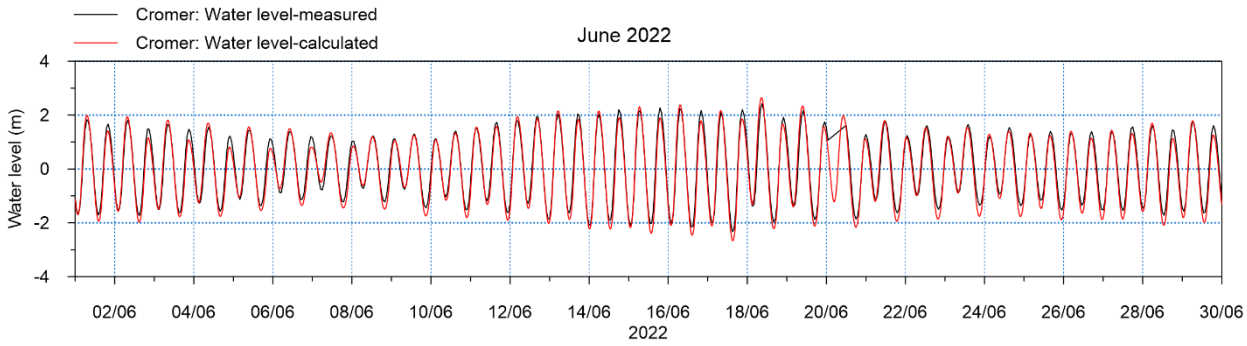

Figure 8-3-21 Time Series Comparison Between Simulated vs Observed Water Levels at Cromer in June 2022 (Local model)

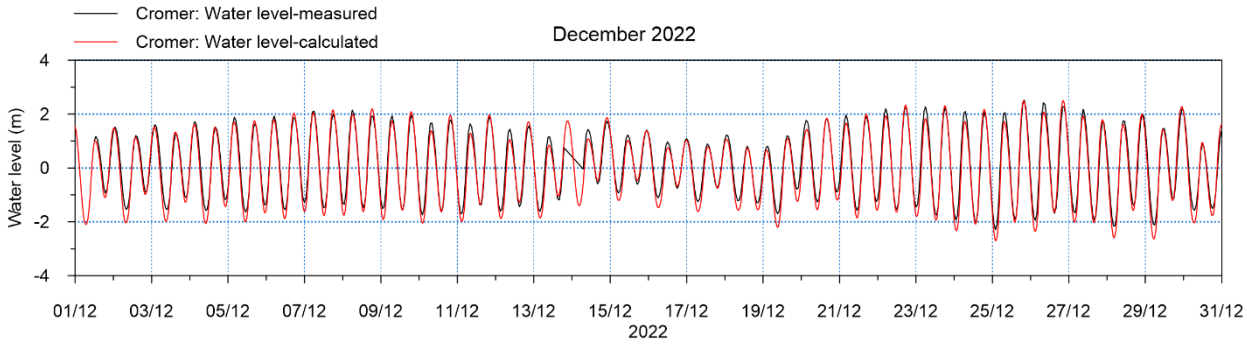

Figure 8-3-22 Time Series Comparison Between Simulated vs Observed Water Levels at Cromer in December 2022 (Local model)

Table 8-3-8 Water Level Time Series Statistics for Local Model

Name of station	Mean Error (m/s)	Mean Absolute Error (m/s)	Standard Deviation (m)	Correlation Coefficient (R)
Whitby	0.24	0.26	0.18	0.98
Cromer	0.17	0.23	0.22	0.98

8.3.3.3.3 Local Model Calibration (currents)

53. The local model has been also calibrated using measured current data recorded at 'Partrac wave buoys" (DBS West and DBS East, see section 8.3.1.2) for two periods (June 2022 and December 2022). Model calibration performance is assessed by both visual comparison and quantifying errors using statistical parameters including Correlation Coefficient and Mean Absolute Error. **Figure 8-3-23** to **Figure 8-3-30** show the modelled and measured current speed and direction, and **Table 8-3-9** and **Table 8-3-10** present quantified errors at DBS West and DBS East, respectively. The model errors in predicted current speed are low, below 0.06m/s for Mean Absolute Error, which provides confidence in using the model to assess potential impact on tidal currents and associated bed shear stress.

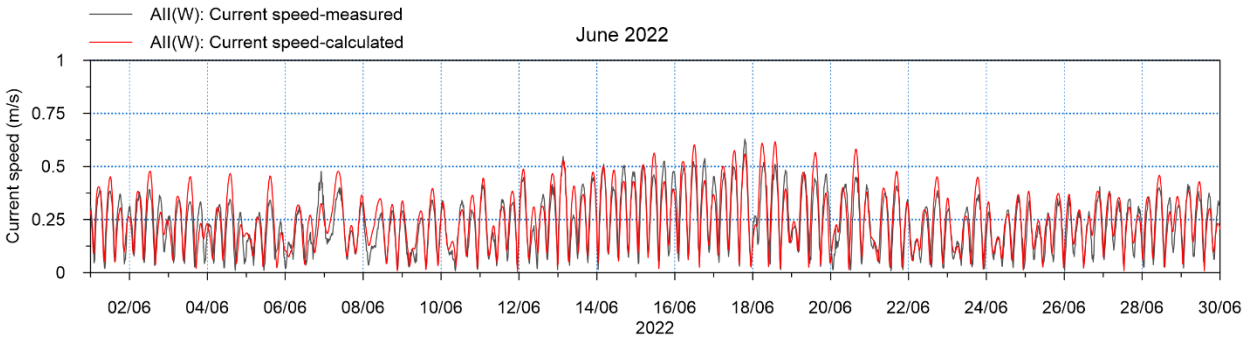

Figure 8-3-23 Time Series Comparison Between Simulated vs Observed Current Speeds at DBS West in June 2022 (Local model)

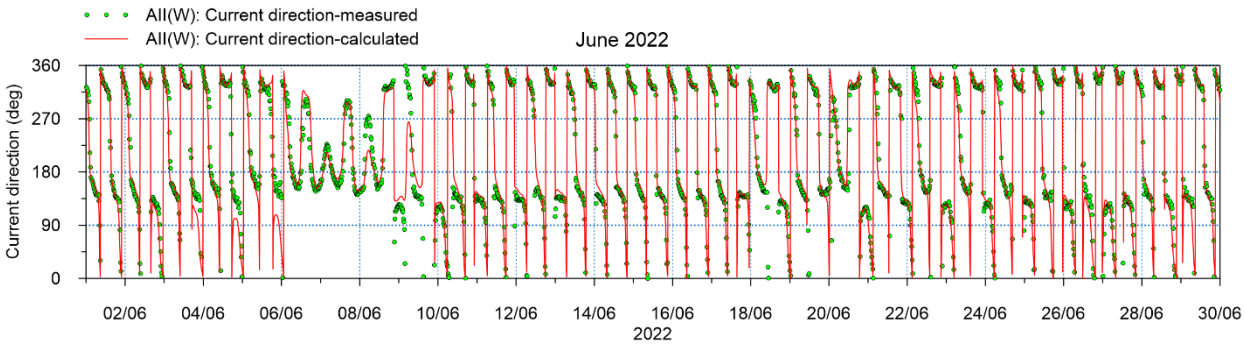

Figure 8-3-24 Time Series Comparison Between Simulated vs Observed Current Directions at DBS West in June 2022 (Local model)

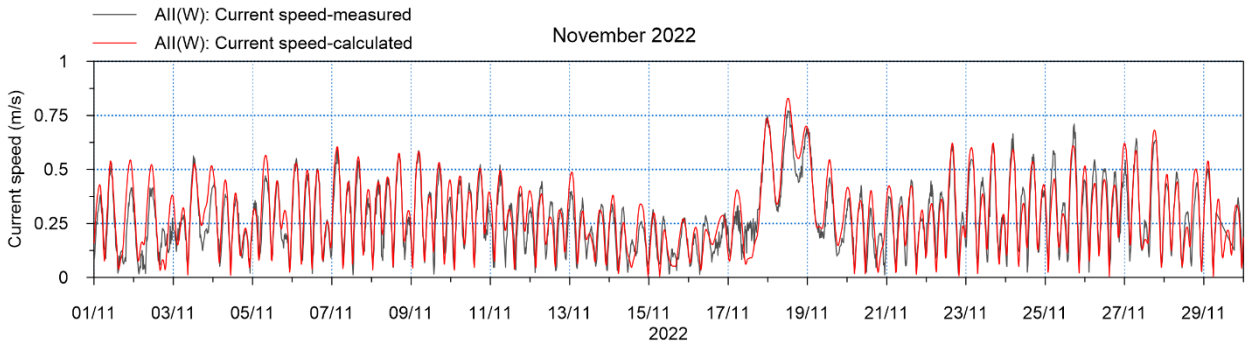

Figure 8-3-25 Time Series Comparison Between Simulated vs Observed Current Speeds at DBS West in November 2022 (Local model)

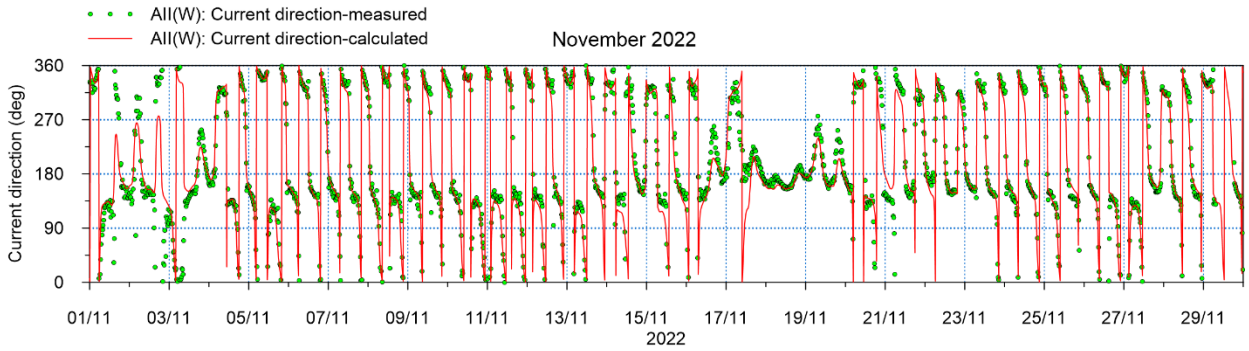

Figure 8-3-26 Time Series Comparison Between Simulated vs Observed Current Directions at DBS West in November 2022 (Local model)

Table 8-3-9 Current Speed Time Series Statistics at DBS West

Time	Mean Error (m/s)	Mean Absolute Error (m/s)	Standard Deviation (m)	Correlation Coefficient (R)
June	-0.019	0.053	0.062	0.73
November	-0.019	0.054	0.064	0.83

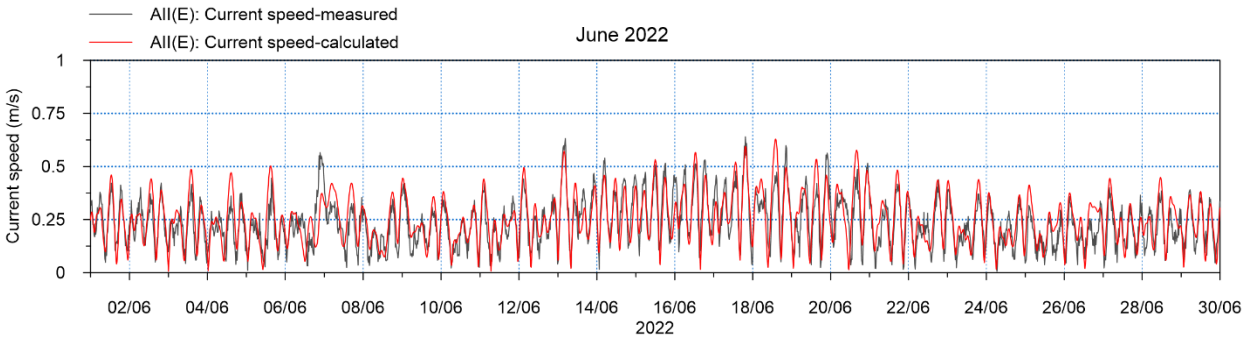

Figure 8-3-27 Time Series Comparison Between Simulated vs Observed Current Speeds at DBS East in June 2022 (Local model)

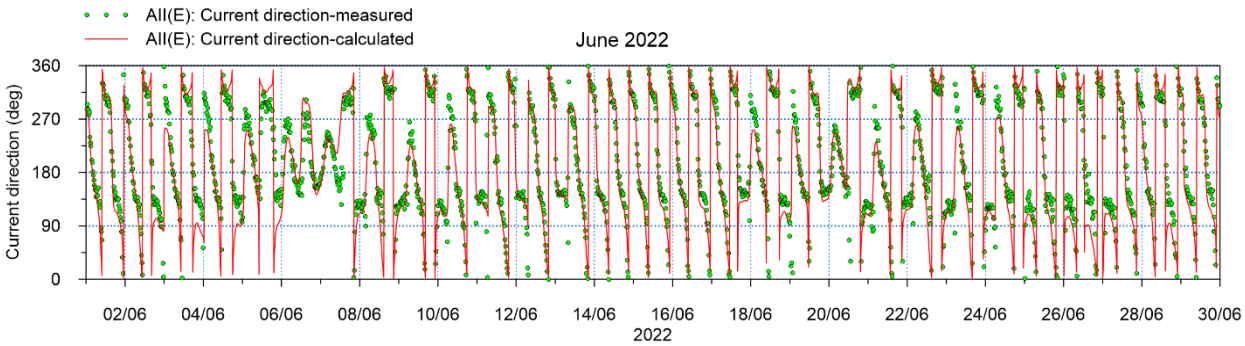

Figure 8-3-28 Time Series Comparison Between Simulated vs Observed Current Directions at DBS East in June 2022 (Local model)

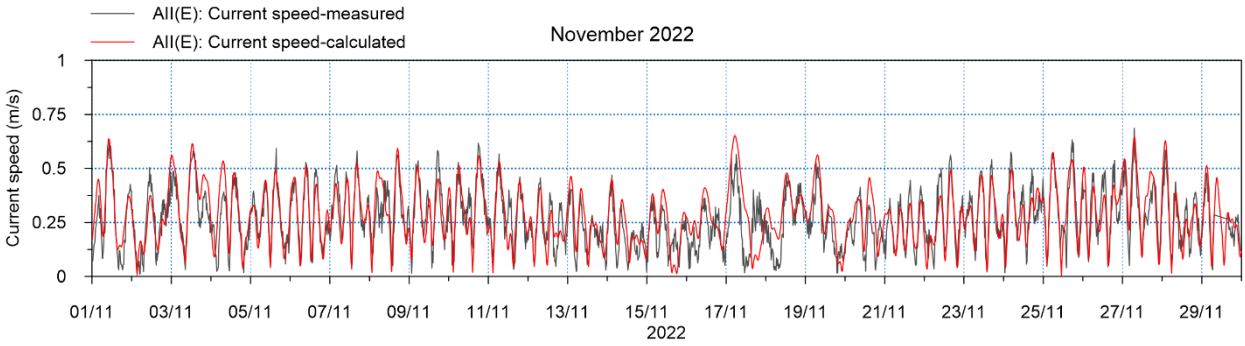

Figure 8-3-29 Time Series Comparison Between Simulated vs Observed Current Speeds at DBS East in November 2022 (Local model)

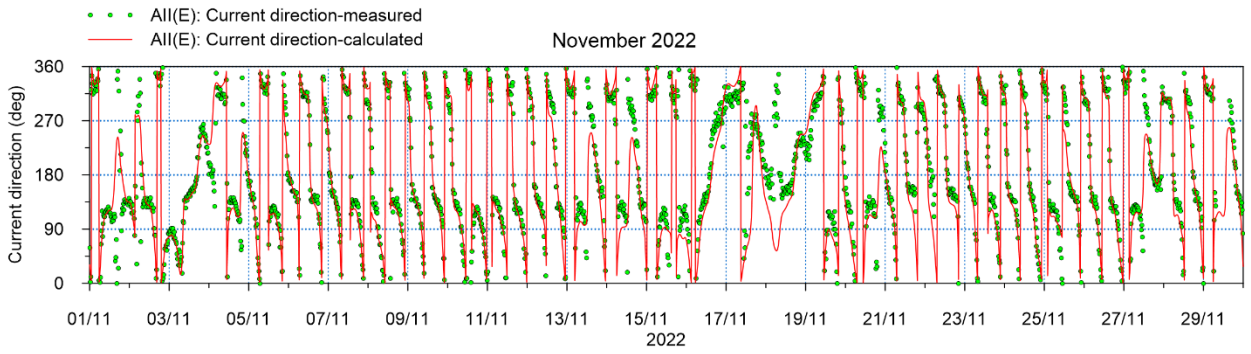

Figure 8-3-30 Time Series Comparison Between Simulated vs Observed Current Directions at DBS East in November 2022 (Local model)

Table 8-3-10 Current Speed Time Series Statistics at DBS East

Time	Mean Error (m/s)	Mean Absolute Error (m/s)	Standard Deviation (m)	Correlation Coefficient (R)
June	-0.017	0.058	0.07	0.65
November	-0.015	0.063	0.08	0.65

8.3.3.4 Hydrodynamic Model Results and Discussions

54. The hydrodynamic model was run for the three layouts described in section 8.3.2.4; "Baseline", Option 1 and Option 2. For each layout, the calibrated model has been run for a period of 30 days. The model results are presented as contour plots in **Annex C**, and include:

- Spatial variation of modelled peak speeds of southeast and northwest flowing tidal currents during a spring and neap tide for Baseline, Option 1 and Option 2;
- Spatial variation of the maximum modelled tidal current speed over the 30-day simulation for Baseline, Option 1 and Option 2;
- Spatial variation of modelled bed shear stress at peak southeast and northwest flowing currents during a spring and neap tide;
- Spatial variation of maximum modelled bed shear stress over a 30-day simulation for Baseline, Option 1 and Option 2;
- Difference in modelled peak current speeds of southeast and northwest flowing tidal currents during a spring and neap tide between Baseline, Option 1 and Option 2;

- Difference in maximum modelled tidal current speed over the 30-day simulation between Baseline, Option 1 and Option 2;
- Difference in modelled bed shear stress at peak southeast and northwest flowing currents during a spring and neap tide between Baseline, Option 1 and Option 2; and
- Difference in maximum modelled bed shear stress over a 30-day simulation between Baseline, Option 1 and Option 2.

55. The model predicted a maximum tidal current speed of 0.6 to 0.7m/s around the Array Areas over a 30 day period. The northwest-flowing currents are slightly stronger than the southeast-flowing currents.

56. For Option 1, the model predicts a small decrease in current speed at the lee side of each foundation and a small increase on two sides of each foundation. ~~This is particularly clear around the platform foundations because their diameters are 4.3 times larger than the turbine foundations.~~ There is also a predicted overlap of the "shadow" areas of foundations along the perimeter due to the shorter distance between turbines. Because of the overlaps, the difference plots show a "shadow area" of current speed decrease in the west of DBS West when currents are going northwest, and a "shadow area" of current speed increase in the west of DBS East. The width of these "shadow" areas outside of the Array Areas is no more than 3km, and the predicted change of current speed (decrease or increase) is no more than 0.01m/s during a spring tide, and smaller during a neap tide.

57. For Option 2, the model results show that the "shadow" area of each foundation overlaps with the neighbouring foundation's "shadow" area due to the shorter distance between turbines compared to Option 1. During spring fide, under southeast-flowing currents, the current speed decreases in the southwest part of both DBS West and DBS East Array Areas and increases in the northeast part. The prediction is opposite under northwest-flowing currents. The width of the affected area outside the Array Areas is no more than 3.5km during a spring tide. The affected area outside the Array Areas is smaller during a neap tide.

58. The difference plots of bed shear stress describe similar patterns of change to the tidal currents described above. However, the model predicts stronger bed shear stress by peak northwest-flowing currents than southeast-flowing currents and marked variations of maximum bed shear stress within the Array Areas. This could manifest as northwest movement of sandbanks and spatially varied seabed mobility within the Array Areas under the force of tidal currents.

8.3.4 Suspended Sediment Dispersion Modelling

8.3.4.1 Model Configuration

59. Over the construction period, there is potential that the seabed and coast will be disturbed. Installation of foundations and cables will generate additional suspended sediment into the water column, which may result in the formation of sediment plumes. The mobilised sediment may then be transported away from the disturbance by waves and tidal currents. The magnitude of the plume will be a function of seabed type, the installation method and the hydrodynamic conditions in which dispersion takes place.

60. The simulation of the release and spreading of fine sediments due to foundation and cable installation activities have been modelled using the 3D model MIKE3-MT. The MIKE3-MT model is coupled with the 3D MIKE3-HD hydrodynamic model described in section 8.3.3 and uses the same mesh. The number of vertical mesh was set to five in the suspended sediment dispersion simulations.

61. This dispersion model considers:

- The release of sediments as a function of time, location and sediment characteristics;
- Advection and dispersion of the suspended sediment in the water column as a function of the 3D hydrodynamics predicted by MIKE3-HD;
- Settling and deposition of the dispersed sediment; and
- The effect of waves in keeping sediment in suspension for a longer period.

62. In the suspended sediment dispersion modelling, it is assumed that the initial suspended concentration in the model domain is zero and flow entering the model domain at the open boundaries contains no sediments. The suspended sediment dispersion model predicts excess suspended sediments induced by the proposed construction activities only.

63. In this modelling exercise, sediment re-suspension is not considered. Therefore, the predicted sediment deposition is a result of the proposed construction.

64. For the entire simulation periods, a wave condition of H_s=1m and T_s=6s were applied throughout the entire simulation period.

8.3.4.2 Construction Activities and Sediment Release

65. The proposed construction involves the following activities which will cause suspended sediment release into the water column:

- Export cables
  - Levelling through sand waves.
  - Trenching.
- Array cables (see **Figure 8-3-31**)
  - Levelling through sand waves.
  - Trenching.
- Inter-platform cables (**Figure 8-3-32** and **Figure 8-3-33**)
  - Levelling through sand waves.
  - Trenching.
- Installing turbines and platforms (locations shown in **Figure 8-3-10**)
  - Seabed preparation.
  - Drilling.

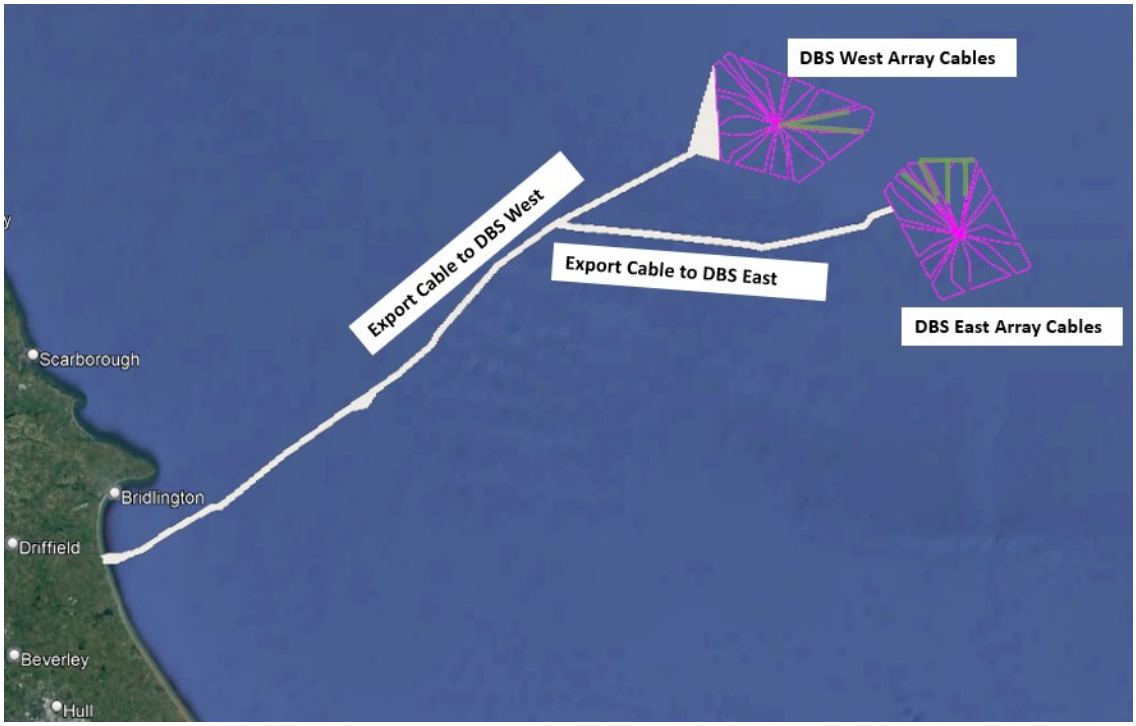

Figure 8-3-31 Offshore Export Cable Routes and Array Cable Routes (green lines indicate areas requiring seabed levelling

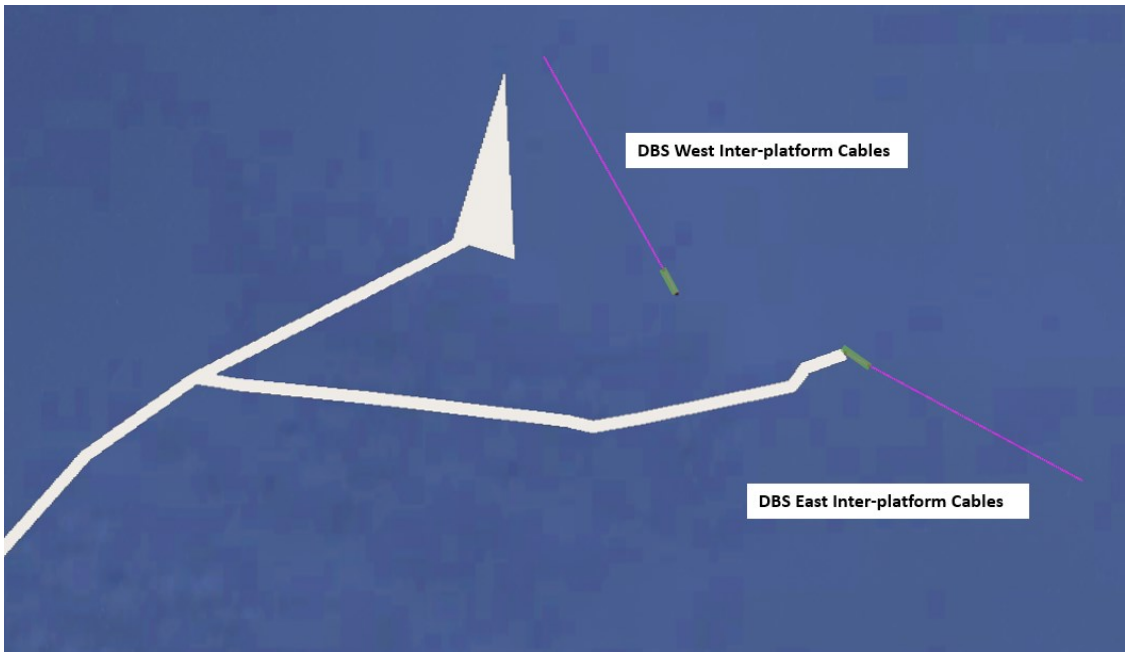

Figure 8-3-32 Inter-Platform Cable Routes for DBS West and DBS East Routes (green lines indicate areas requiring seabed levelling)

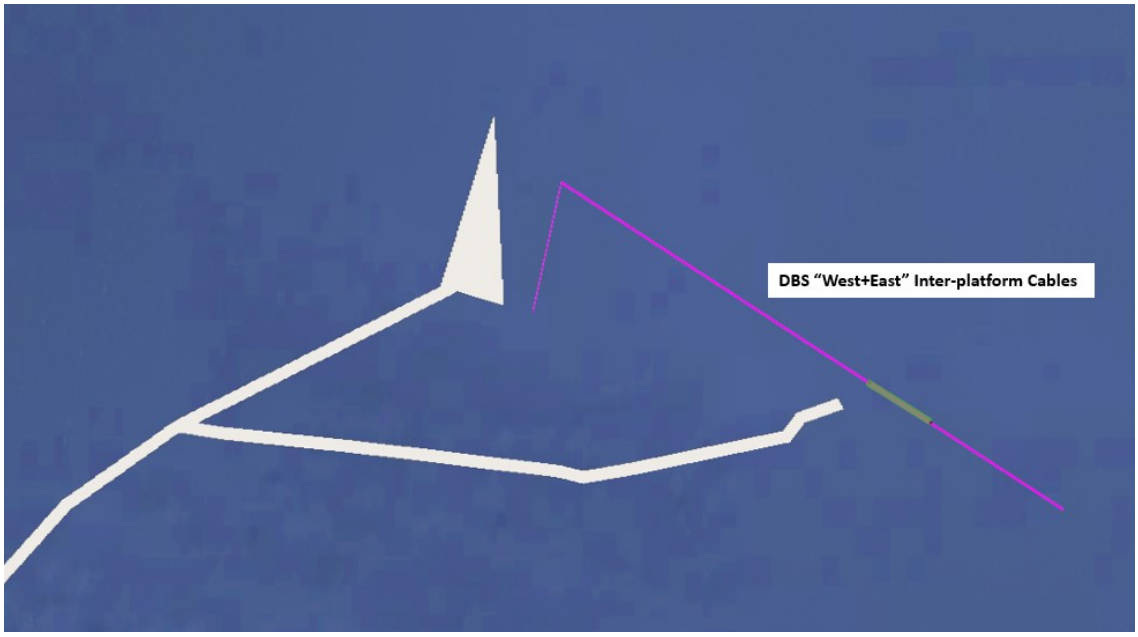

Figure 8-3-33 Inter-Platform Cable Routes for DBS "West and East" Routes (green lines indicate areas requiring seabed levelling)[9]

66. For the above construction activities, the sediment plumes from the construction of the Projects have been simulated. **Table 8-3-11** to **Table 8-3-14** list the relevant construction activities including construction method, duration and sediment release rates. The sediment release rate of 15kg/s for levelling cable routes through sand waves is estimated by using an 'S-Factor' of 15kg/m^3 for trailing suction hopper dredger (TSHD) and a production rate of 1m^3/s. The sediment release rate of 6kg/s for seabed preparation and drilling is based on an 'S-Factor' of 6kg/m^3 for CSD and a production rate of 1m^3/s. These 'S-Factor' values are taken from CIRIA guidance (CIRIA, 1999).

[9] For modelling purposes, the inter-platform cable route for DBS East and DBS West combined consists of three separate inter-platform cables running in parallel, with a minimum separation distance of 50m.

Table 8-3-11 Construction Activities for Export Cables

Activities	Length (km)	Volume (million m^3)	Method	Production Rate (m^3/s)	Duration (days)	Sediment Release rate (kg/s)
Export Cable to DBS West - levelling	87.6	16.3	TSHD	1	188	15
Export Cable to DBS East – levelling	100.0	18.4	TSHD	1	212	15
Export Cable to DBS West - trenching	153.0	0.9	Cable Plough	0.67	16	1,100*
Export Cable to DBS East - trenching	188.9	1.1	Cable Plough	0.67	20	1,100*

Note *: 100% sediment is released in the bottom layer during trenching by cable plough

Table 8-3-12 Construction Activities for Array Cables

Activity	Length (km)	Volume (million m^3)	Method	Production Rate (m^3/s)	Duration (days)	Sediment Release Rate (kg/s)
Array Cables in DBS West - levelling	32.5	0.37	TSHD	1	4.2	15
Array Cables in DBS East – levelling	32.5	0.37	TSHD	1	4.2	15
Array Cables in DBS West - trenching	325	1.95	Cable Plough	0.67	33.9	1,100*
Array Cables in DBS East - trenching	325	1.95	Cable Plough	0.67	33.9	1,100*

Note *: 100% sediment is released in the bottom layer during trenching by cable plough

Table 8-3-13 Construction Activities for Inter-Platform Cables

Activity	Length (km)	Volume (million m^3)	Method	Production Rate (m^3/s)	Duration (days)	Sediment Release Rate (kg/s)
Inter-platform cable for DBS West - levelling	12.9	0.14	TSHD	1	1.7	15
Inter-platform cable for DBS East – levelling	11.5	0.13	TSHD	1	1.5	15
Inter-platform cable for DBS "West+East" – levelling	34.2	0.38	TSHD	1	4.5	15
Inter-platform cable for DBS West – trenching	128.8	0.77	Cable Plough	0.67	8.9	1,100*
Inter-platform cable for DBS East - trenching	115	0.69	Cable Plough	0.67	8.0	1,100*
Inter-platform cable for DBS "West+East" - trenching	341.6	2.0	Cable Plough	0.67	23.7	1,100*

Note *: 100% sediment is released in the bottom layer during trenching by cable plough

Table 8-3-14 Construction Activities for Turbine and Platform Foundations

Activity	Volume (m^3 per)	Production Rate (m^3/s)	Duration (hours per)	Sediment Release Rate (kg/s)
Drill Turbine Foundation	12,064	1	3.35	6
Drill Platform Foundation	14,074	1	3.9	6
Bed preparation for Turbine Foundation	3,111	1	0.9	6
Bed preparation for Platform Foundation	32,436	1	9	6

8.3.4.3 Seabed Sediment Properties

67. **Table 8-3-15** presents the sediment composition in percentages within the DBS East Array Area, DBS West Array Area and each Projects respective Offshore Export Cable Corridor. These values were taken from the site-specific geophysical survey reports competed for the Projects Array Areas and Offshore Export Cable Corridor (Fugro 2023a, 2023b).

Table 8-3-15 Sediment Composition (in percentages) for Dispersion Simulation

Sediment size	Export Cable to DBS West	Export Cable to DBS East	DBS West	DBS East
Silt/Clay	0%	0%	0%	0%
Fine Sand	21%	22%	13%	30%
Medium Sand	45%	50%	44%	50%
Coarse Sand	18%	17%	33%	15%
Gravel/Cobble	17%	11%	10%	5%

68. **Table 8-3-16** presents sediment settling velocities and critical bed shear stress for different sediment size factions used in the suspended sediment dispersion modelling. These values were calculated using the Soulsby method (Soulsby, 1998).

Table 8-3-16 Sediment Settling Velocities and Critical Bed Shear Stresses

Sediment size	Sediment Size (mm)	Settling Velocity (m/s)	Critical Bed Shear Stress (N/m^2)
Silt/Clay	0.031	0.000554	0.0847
Fine Sand	0.13	0.00935	0.1548
Medium Sand	0.3	0.0372	0.2025
Coarse Sand	1.3	0.135	0.657
Gravel/Cobble	2	0.1734	1.166

8.3.4.4 Model Simulations

69. The coupled 3D MIKE3-MT and MIKE3-HD model has been run for the entire period of each relevant construction activity (described in **Table 8-3-11** to **Table 8-3-14**) in which sediment will be released into water column. The model results are presented as contour plots of maximum suspended sediment concentrations for bottom, middle and surface layers and total sediment deposition thickness as a result of each construction activity. These contour plots are provided in **Annex D** of this report.

70. The model results presented in this report are all excess suspended sediment concentration and excess sediment deposition caused by the proposed construction activities for the Project. The suspended sediment concentration and deposition caused by natural morphological processes are not modelled and included.

71. Time series plots of predicted suspended sediment concentration are presented at selected points (**Figure 8-3-34**) during trenching the offshore export cable route and array cable routes (**Figure 8-3-35** to **Figure 8-3-42**). The plots are presented only for the periods and locations that predicted suspended sediment concentrations are measurable (exceeding 0.5mg/l)

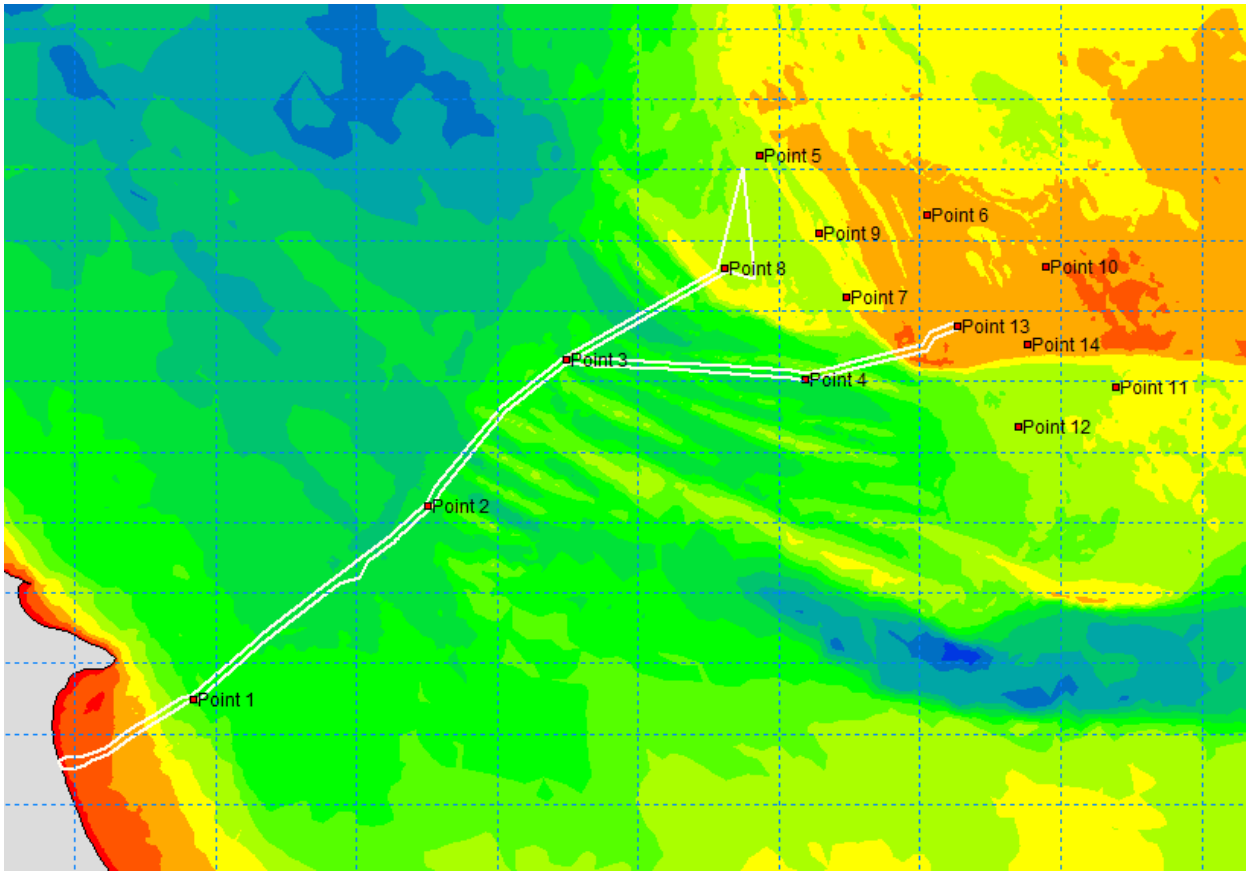

Figure 8-3-34 Locations of Time Series Plots of Predicted Suspended Sediment Concentration

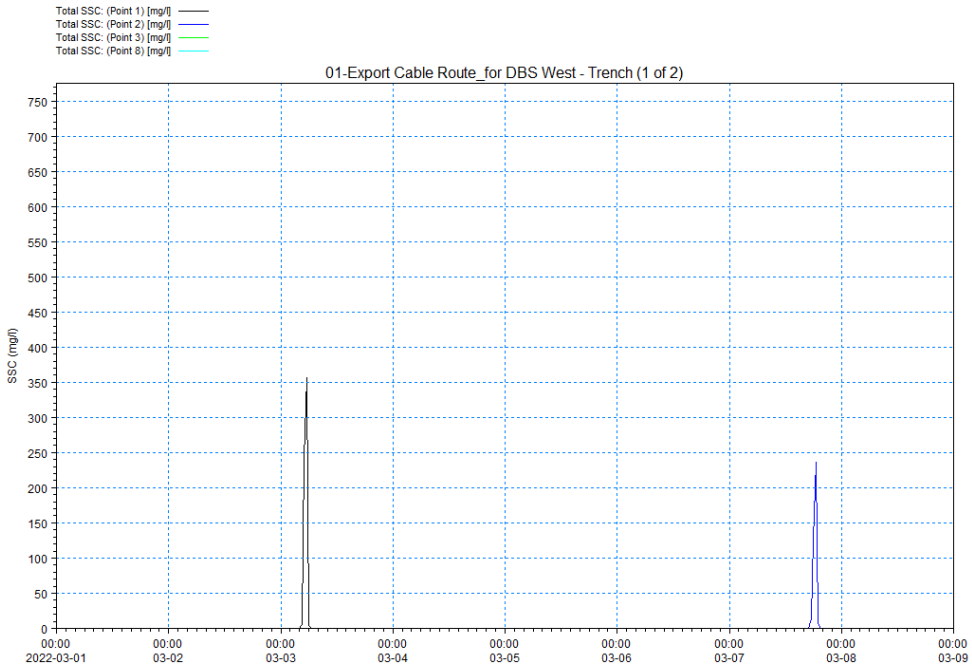

Figure 8-3-35 Predicted Suspended Sediment Concentration at Points 1 & 2 – Offshore Export Cable to DBS West – Trenching

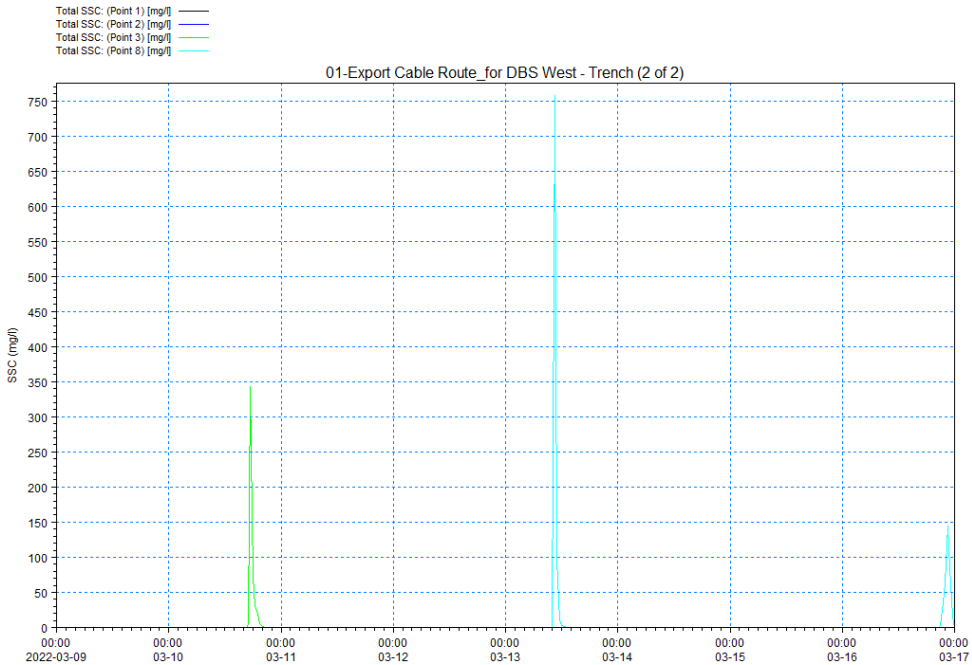

Figure 8-3-36 Predicted Suspended Sediment Concentration at Points 3 & 8 – Offshore Export Cable to DBS West - Trenching

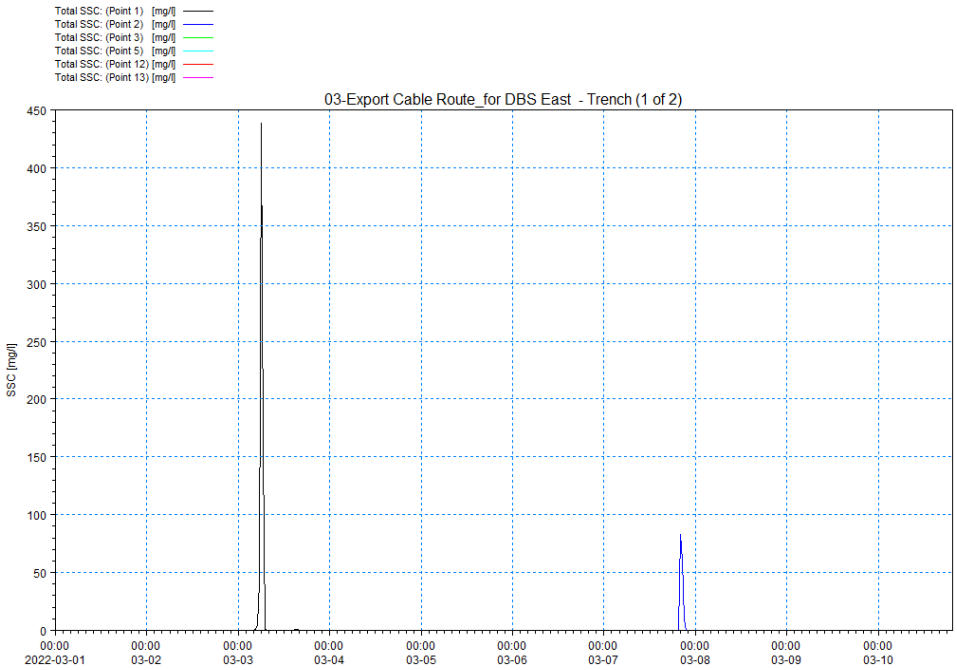

Figure 8-3-37 Predicted Suspended Sediment Concentration at Points 1 & 2 – Offshore Export Cable to DBS East – Trenching

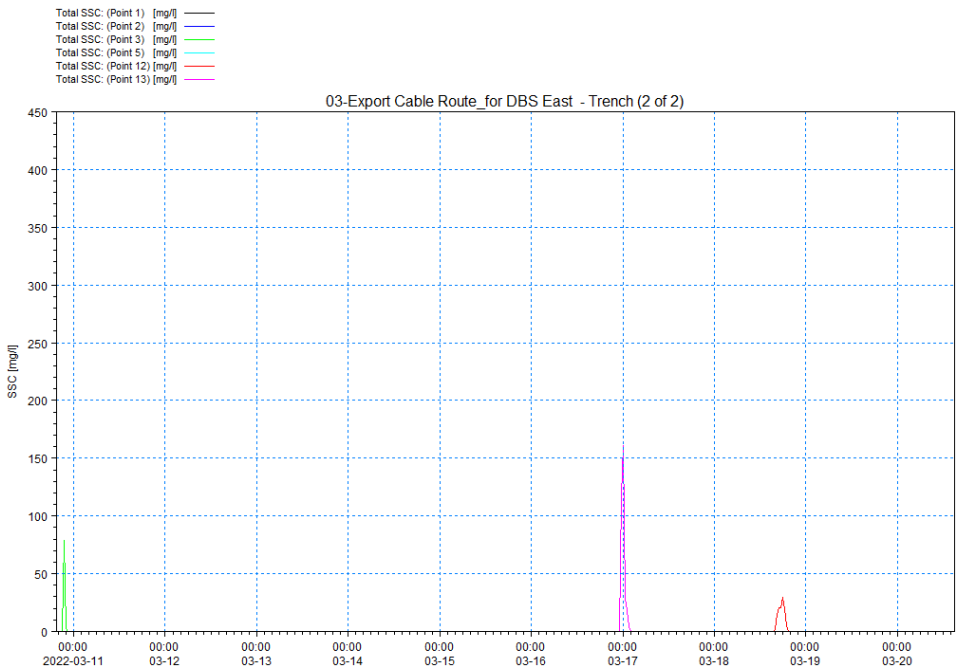

Figure 8-3-38 Predicted Suspended Sediment Concentration at Points 3, 5,12 & 13 – Offshore Export Cable to DBS East - Trenching

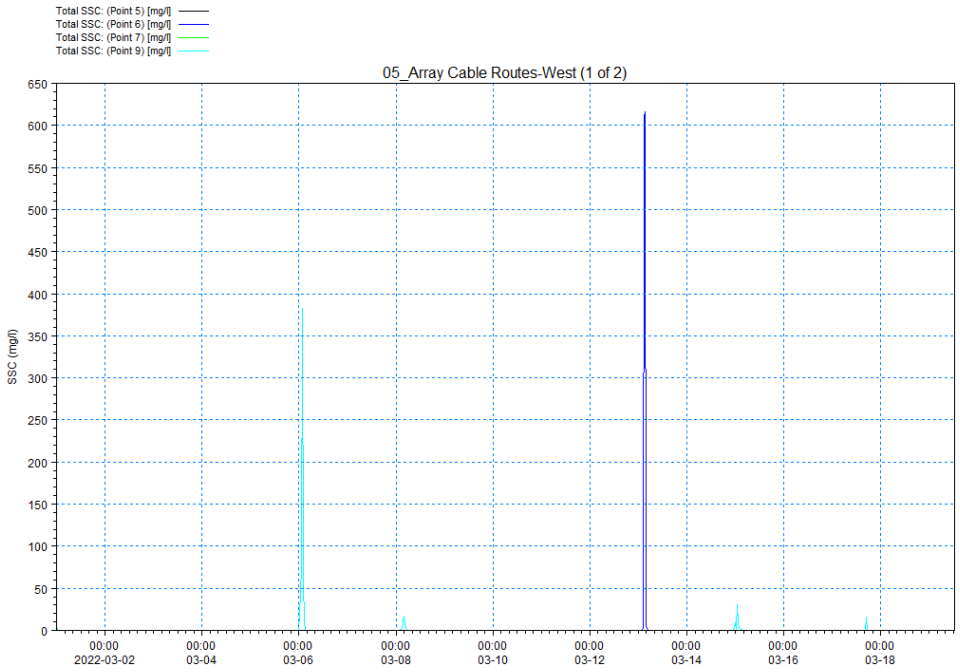

Figure 8-3-39 Predicted Suspended Sediment Concentration at Points 5, 6, 7 & 9 – Array Cables DBS West - Trenching

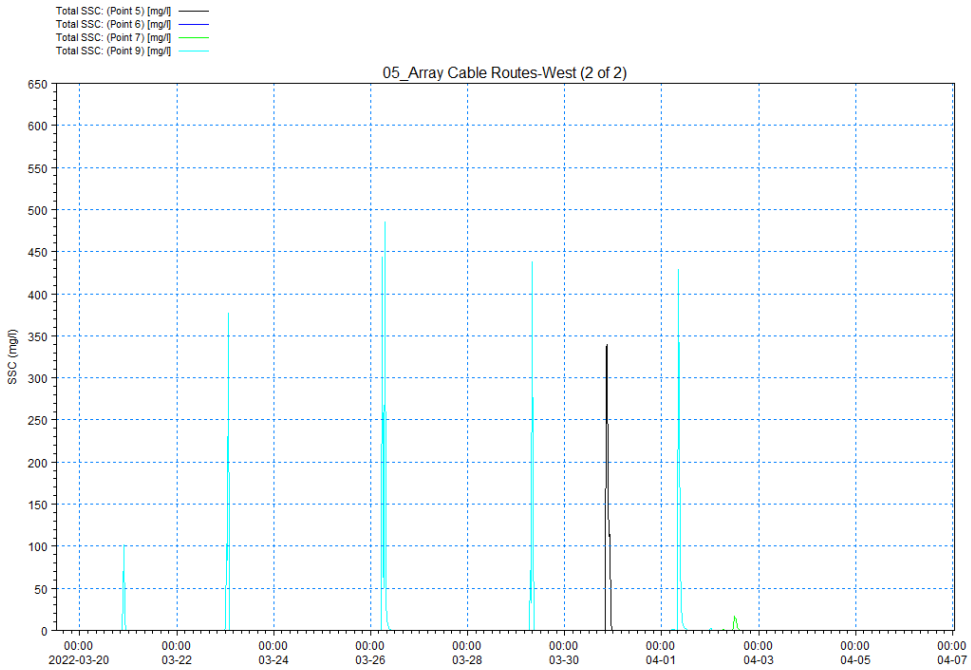

Figure 8-3-40 Predicted Suspended Sediment Concentration at Points 5, 6, 7 & 9 – Array Cables DBS West – Trenching (continued)

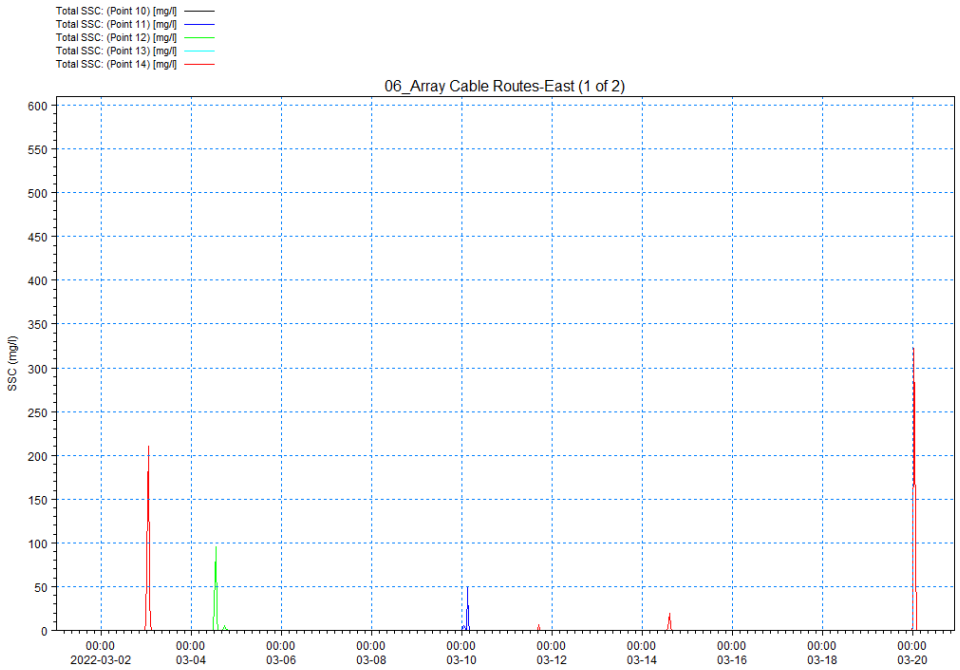

Figure 8-3-41 Predicted Suspended Sediment Concentration at Points 10-14 – Array Cables DBS East - Trenching

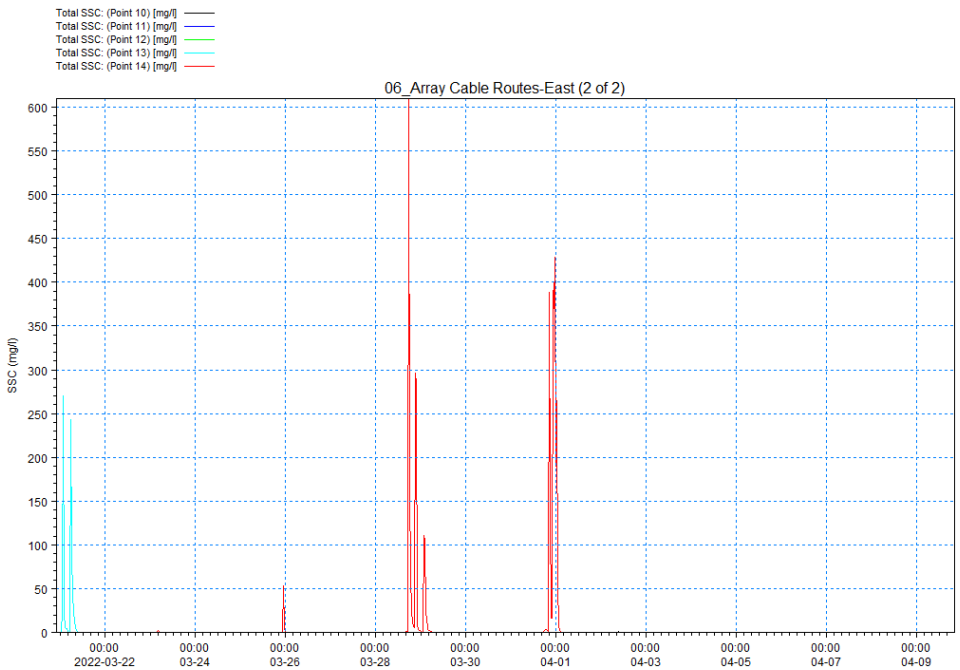

Figure 8-3-42 Predicted Suspended Sediment Concentration at Points 10-14 – Array Cables DBS East – Trenching (continued)

8.3.4.5 Discussion of Suspended Sediment Dispersion Model Results

8.3.4.5.1 Offshore Export Cable Corridor

72. The maximum suspended sediment concentration caused by the levelling processes through sand waves is less than 5mg/l in the bottom layer and less than 2mg/l in the surface layer. This is due to relatively low sediment release rate by TSHD compared to cable ploughing for trenching.

73. The model results predict higher near-bed maximum suspended sediment concentration (up to 750mg/l in the bottom layer) because of trenching along the Offshore Export Cable Corridor. This is because the cable plough method would disturb 100% of the sediments into the bottom layer. The maximum suspended sediment concentration by trenching is much lower in the surface layer (below 5mg/l).

74. Sediment plumes are larger in the nearshore area due to faster tidal currents, and much smaller in offshore areas. **Table 8-3-17** and **Table 8-3-18** present estimated sediment 'plume' size (using the threshold value of 0.5mg/l) in the nearshore, halfway, and offshore along the Offshore Export Cable Corridor by trenching and levelling respectively. The 'plume' size is based on the modelled maximum suspended sediment concentration over the entire simulation. Therefore, the 'plume' size is the maximum extent of modelled maximum suspended sediment concentrations exceeding 0.5mg/l. It should be noted that the maximum suspended sediment concentration may not happen at the same time within a "plume".

Table 8-3-17 Estimated Sediment 'Plume' Size Based on Modelled Maximum Suspended Sediment Concentrations Exceeding 0.5mg/l During Trenching for Offshore Export Cables

Location	Bottom Layer	Middle Layer	Surface Layer
Nearshore	28.5km	26km	9km
Half way between shore and Array Areas	12km	7.5km	<1km
Offshore	2km	<1km	<500m

Table 8-3-18 Estimated Sediment 'Plume' Size Based on Modelled Maximum Suspended Sediment Concentrations Exceeding 0.5mg/l During Levelling for Offshore Export Cables

Location	Bottom Layer	Middle Layer	Surface Layer
Half way between shore and Array Areas	8km	1km	<500m
Offshore	<2km	<500m	<500m

75. The time series plots show that modelled excess suspended sediment concentrations greater than 0.5mg/l at any location only last no more than 1.5 hours.

76. The model results predict local sediment deposition along the Offshore Export Cable Corridor after both levelling and trenching processes.

8.3.4.5.2 Array and Inter-Platform Cable Routes

77. Like the Offshore Export Cable Corridor, the model predicts low suspended sediment concentrations for levelling within the Array Areas and inter-platform cable routes. The maximum suspended sediment concentrations are less than 0.5mg/l and 5mg/l in the surface and bottom layers, respectively. The predicted plume extent in the bottom layer is slightly larger than the surface layer during the levelling process by TSHD.

78. The model results show relatively high suspended sediment concentrations during trenching within the Array Areas and inter-platform cable routes by cable plough. The maximum suspended sediment concentrations are predicted between 1,000 and 1,500mg/l near the centre of DBS East. However, due to weak offshore tidal currents, the plumes generated by cable plough largely remain local and there are no overlaps of suspended sediment plumes between DBS West and DBS East.

79. The plume size of levelling array and inter-platform cables is less than 500m in the bottom layer due to low sediment release rates by TSHD. However, the plumes created by trenching the array cable routes almost completely cover the Array Areas in the middle and surface layers, and the plume generated by trenching inter-platform cable routes is also extensive within the Array Areas. However, these plumes largely stay within the Array Areas apart from isolated locations where the plume spreads out of the Array Areas by up to 5km.

80. The time series plots show that the modelled excess suspended sediment concentrations above 0.5mg/l caused by trenching array cables lasts no more than 2 hours at any location.

81. Like the Offshore Export Cable Corridor, the model predicts local sediment deposition along the cable routes for both levelling and trenching. The maximum sediment deposition would occur at the centres of the array cable routes in DBS West and East due to the radial distribution of array cables.

8.3.4.5.3 Turbine and Platform Foundations

82. The model predicts low suspended sediment concentrations caused by the drilling and seabed preparation for installing turbine and platform foundations. The model results show that the maximum suspended sediment concentrations are less than 0.5mg/l and 2mg/l in the surface and bottom layers, respectively. The predicted sediment deposition from the drilling and seabed preparation is less than 5mm. Hence, the extent of the deposition is undetectable in the contour plots presented in **Annex D**.

References

Fugro (2023a). DBS WPM1 Array Area Seafloor Results. Report 004267910.

Fugro (2023b). DBS WPM2 WPM3 ECR Seafloor and Shallow Geological Results. Report 004267912.

CIRIA (1999). Scoping the assessment of sediment plumes arising from dredging.

Soulsby, R.L. (1998) Dynamics of marine sands. Technical Report. Thomas Telford.

Annex A – Wave Model Calibration Results

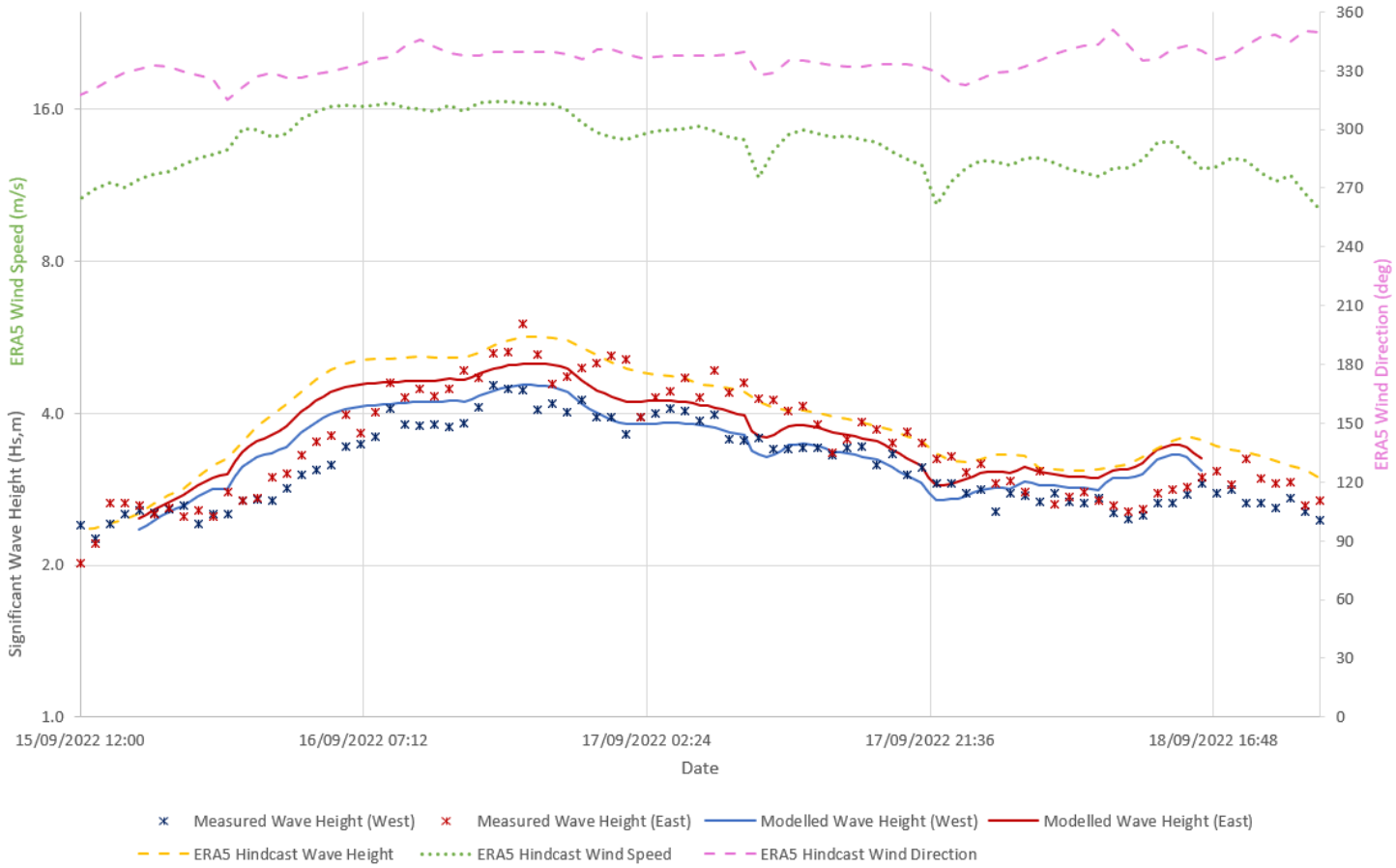

Figure A- 1 Comparison of Measured and Modelled Wave Height for Waves Coming From North – Event 1

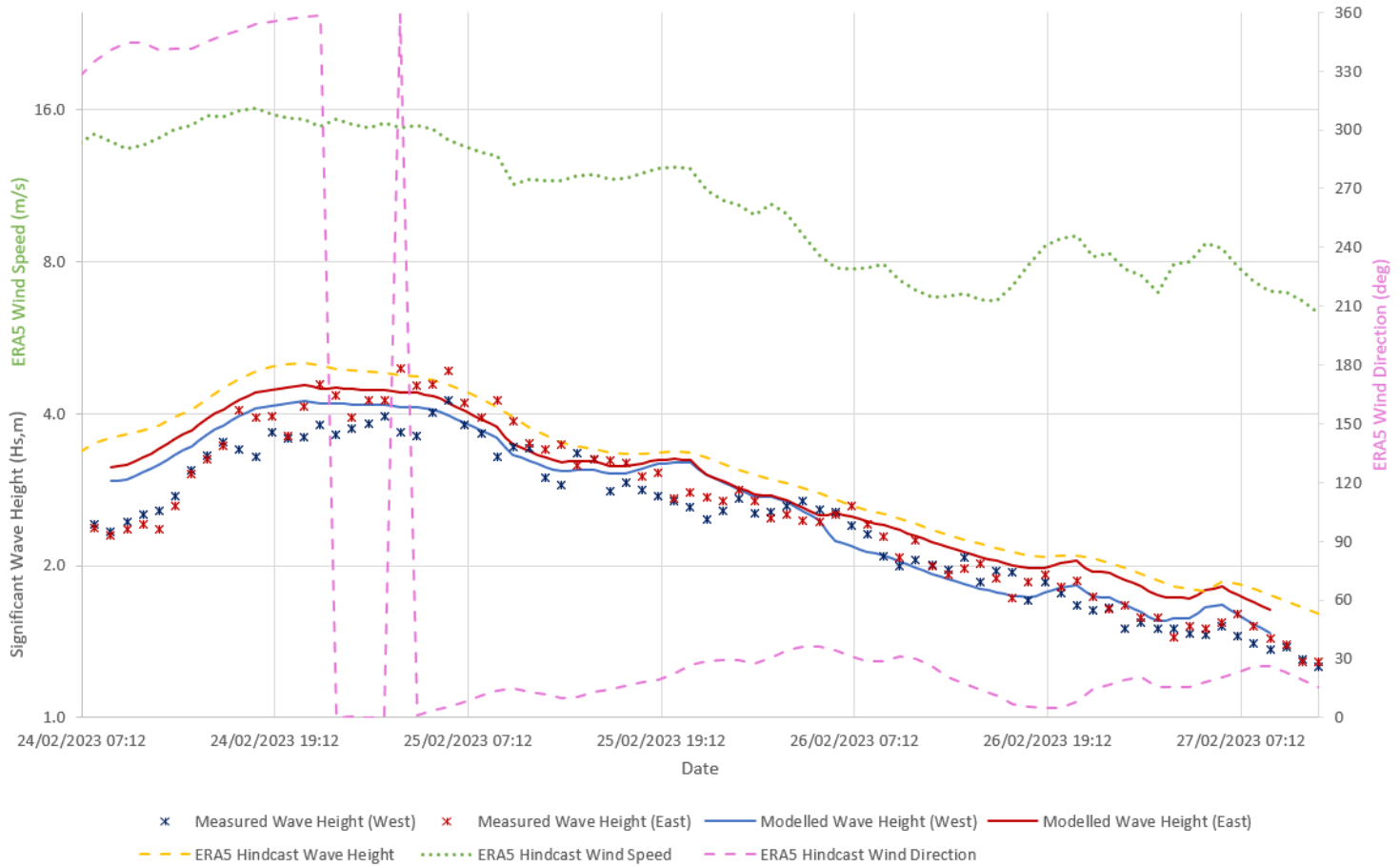

Figure A- 2 Comparison of Measured and Modelled Wave Height for Waves Coming From North – Event 2

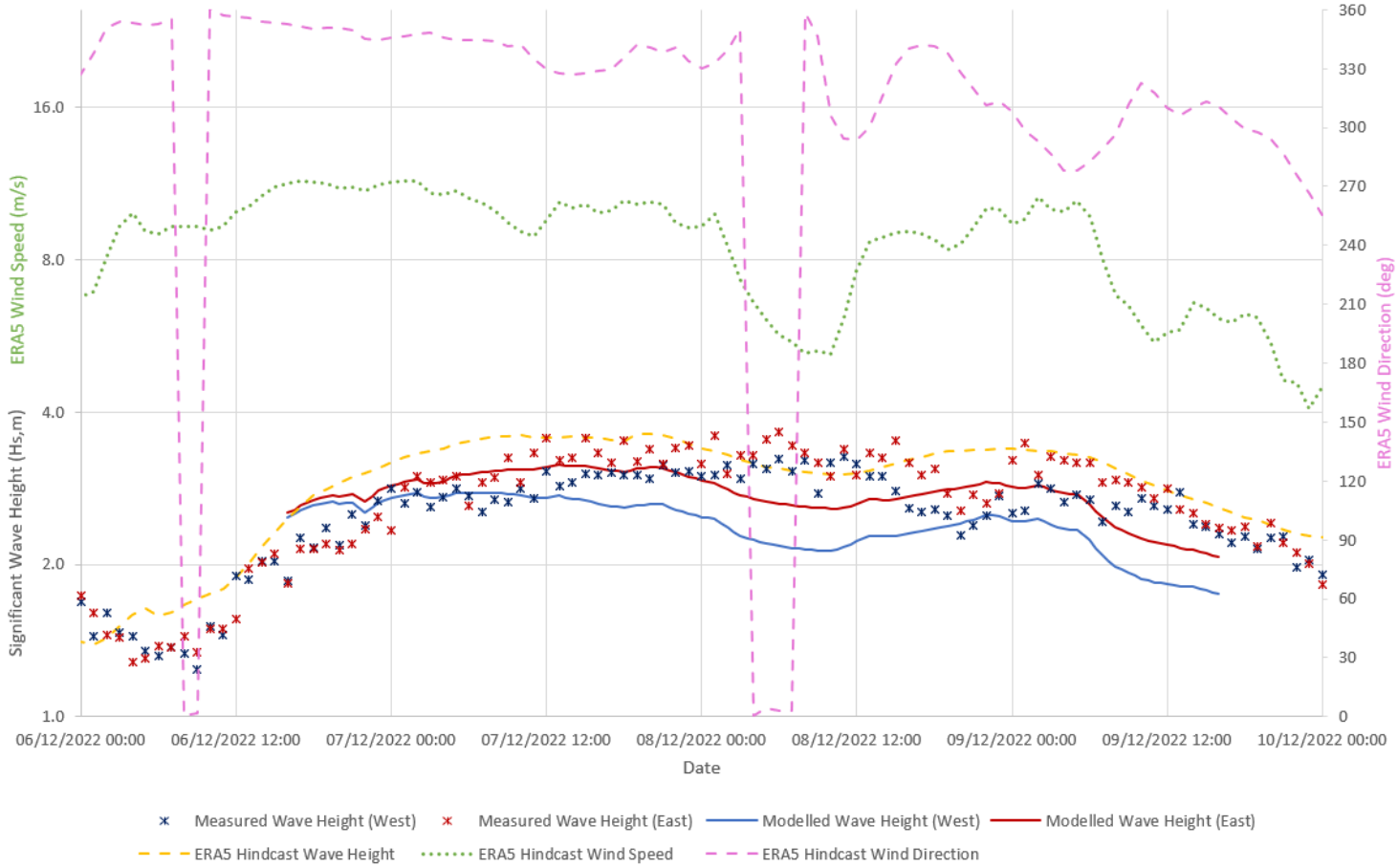

Figure A- 3 Comparison of Measured and Modelled Wave Height for Waves Coming From North – Event 3

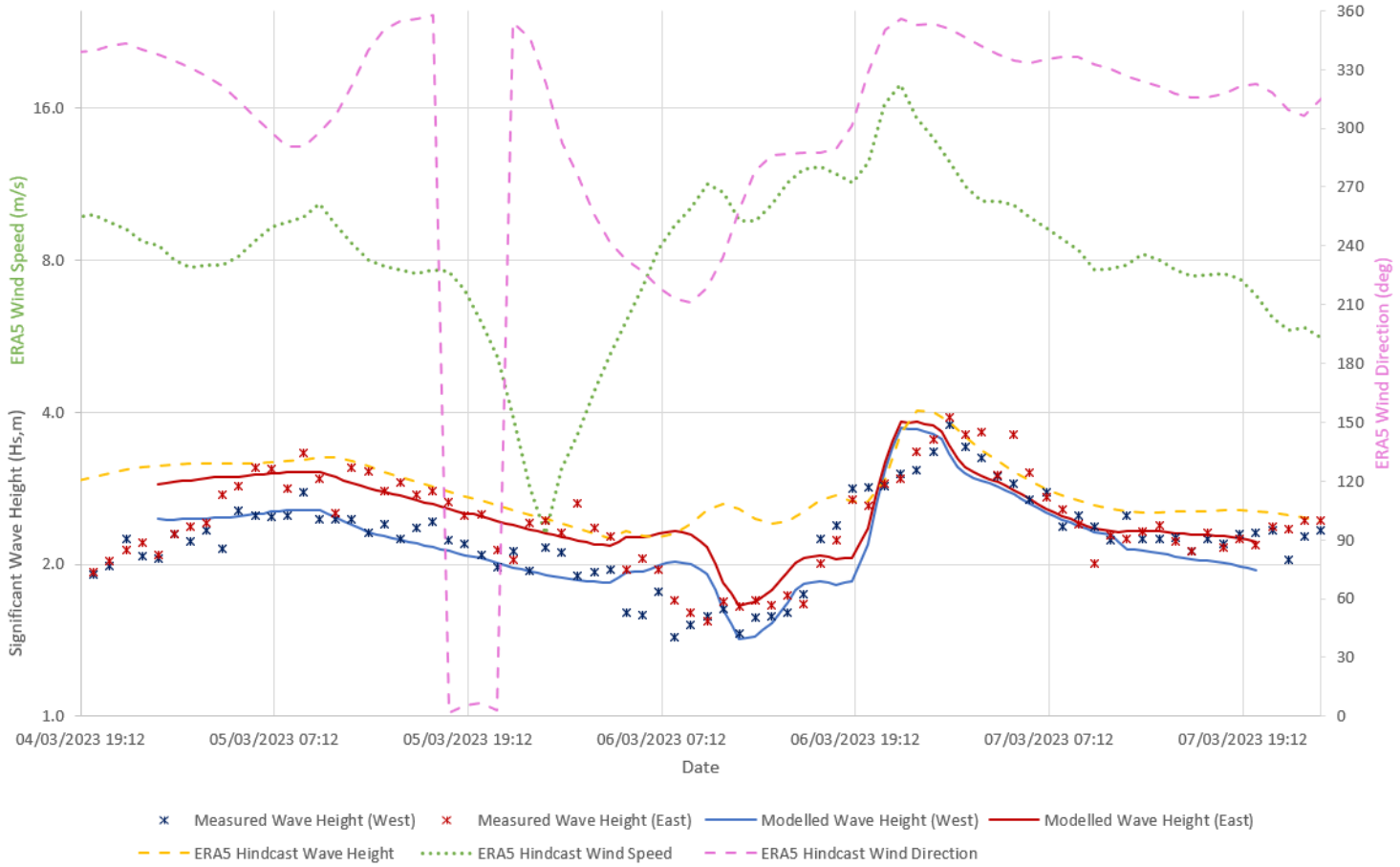

Figure A- 4 Comparison of Measured and Modelled Wave Height for Waves Coming From North – Event 4

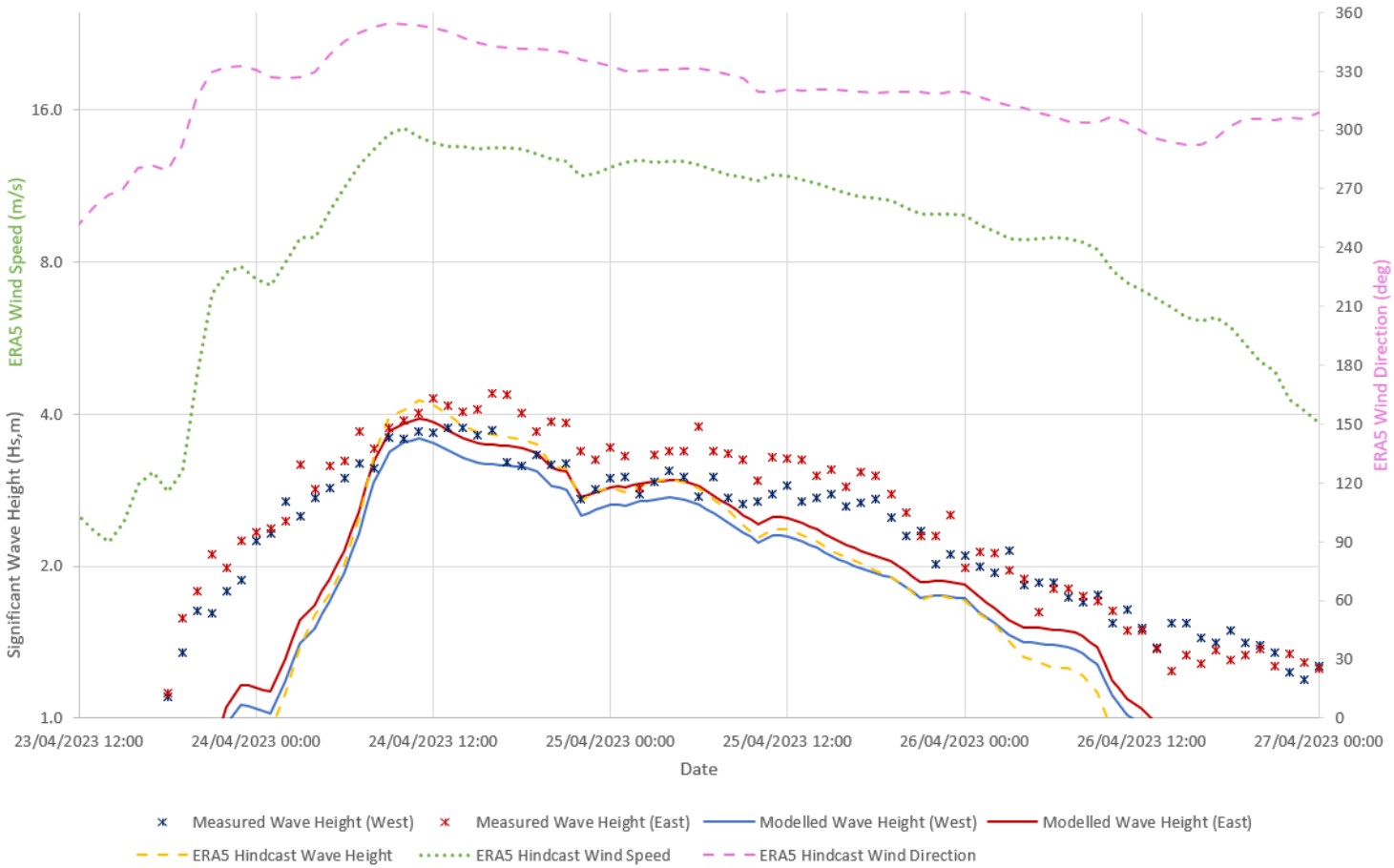

Figure A- 5 Comparison of measured and modelled wave height for waves coming from North – Event 5

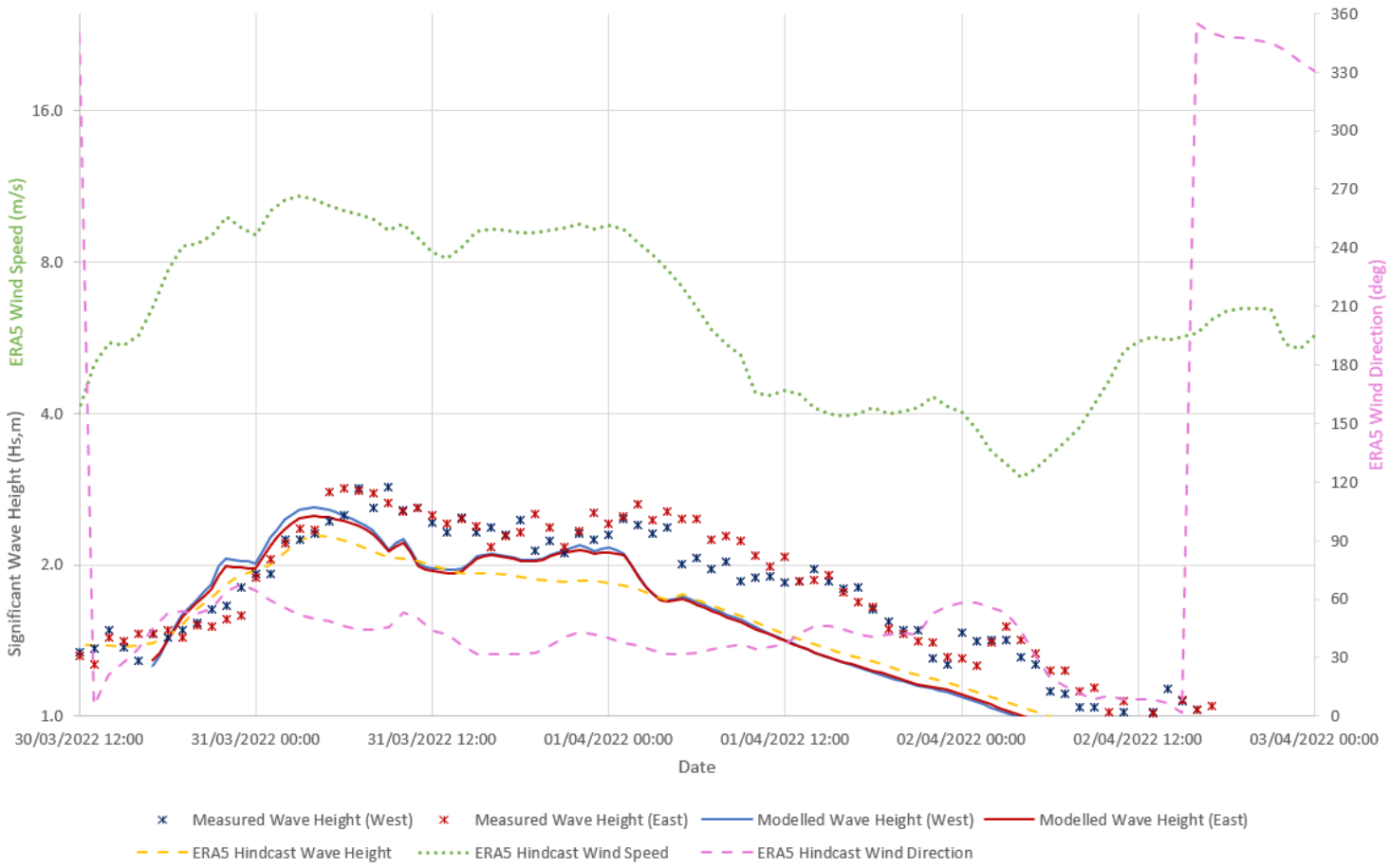

Figure A- 6 Comparison of measured and modelled wave height for waves coming from North-East – Event 6

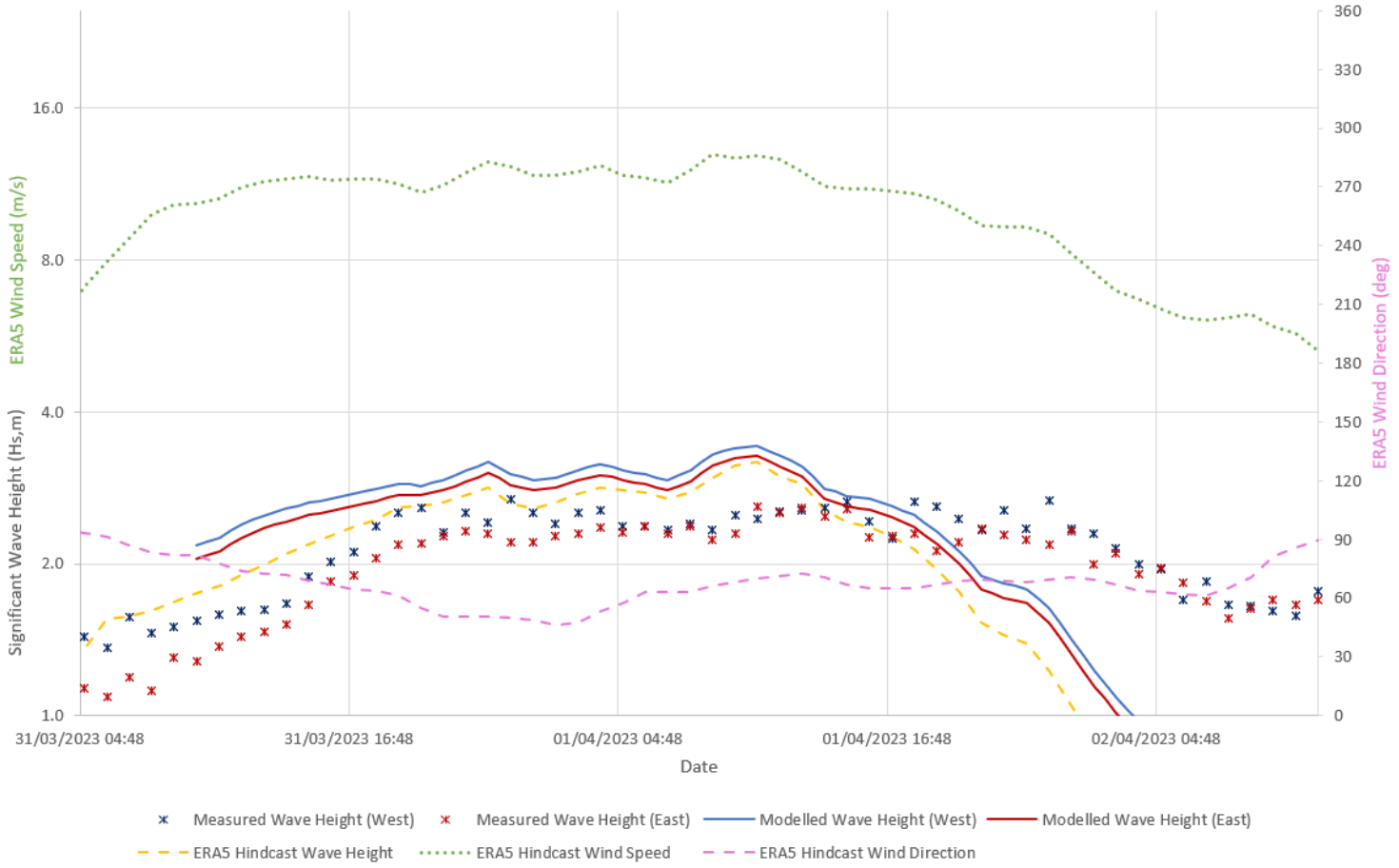

Figure A- 7 Comparison of measured and modelled wave height for waves coming from North-East – Event 7

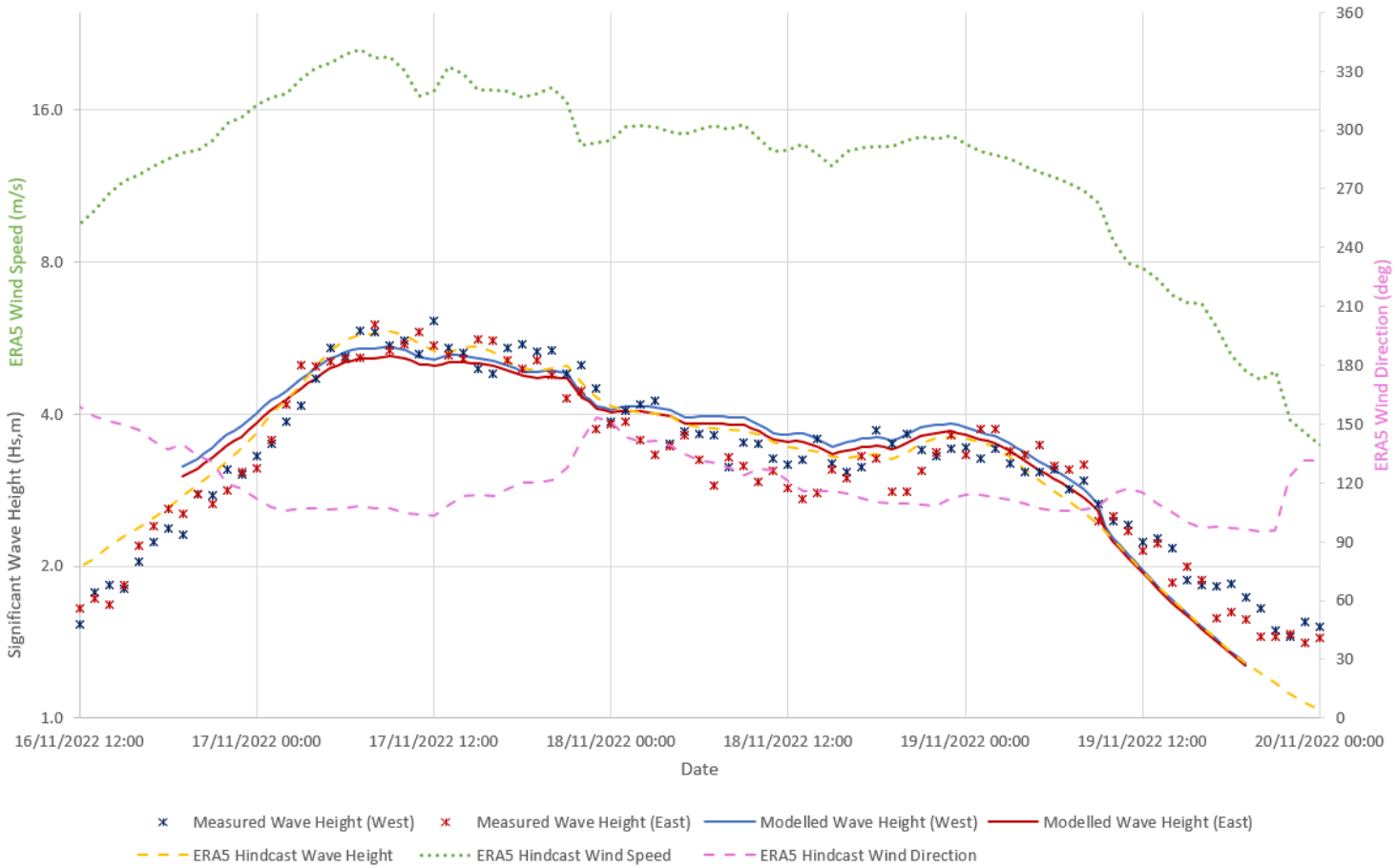

Figure A- 8 Comparison of measured and modelled wave height for waves coming from East – Event 8

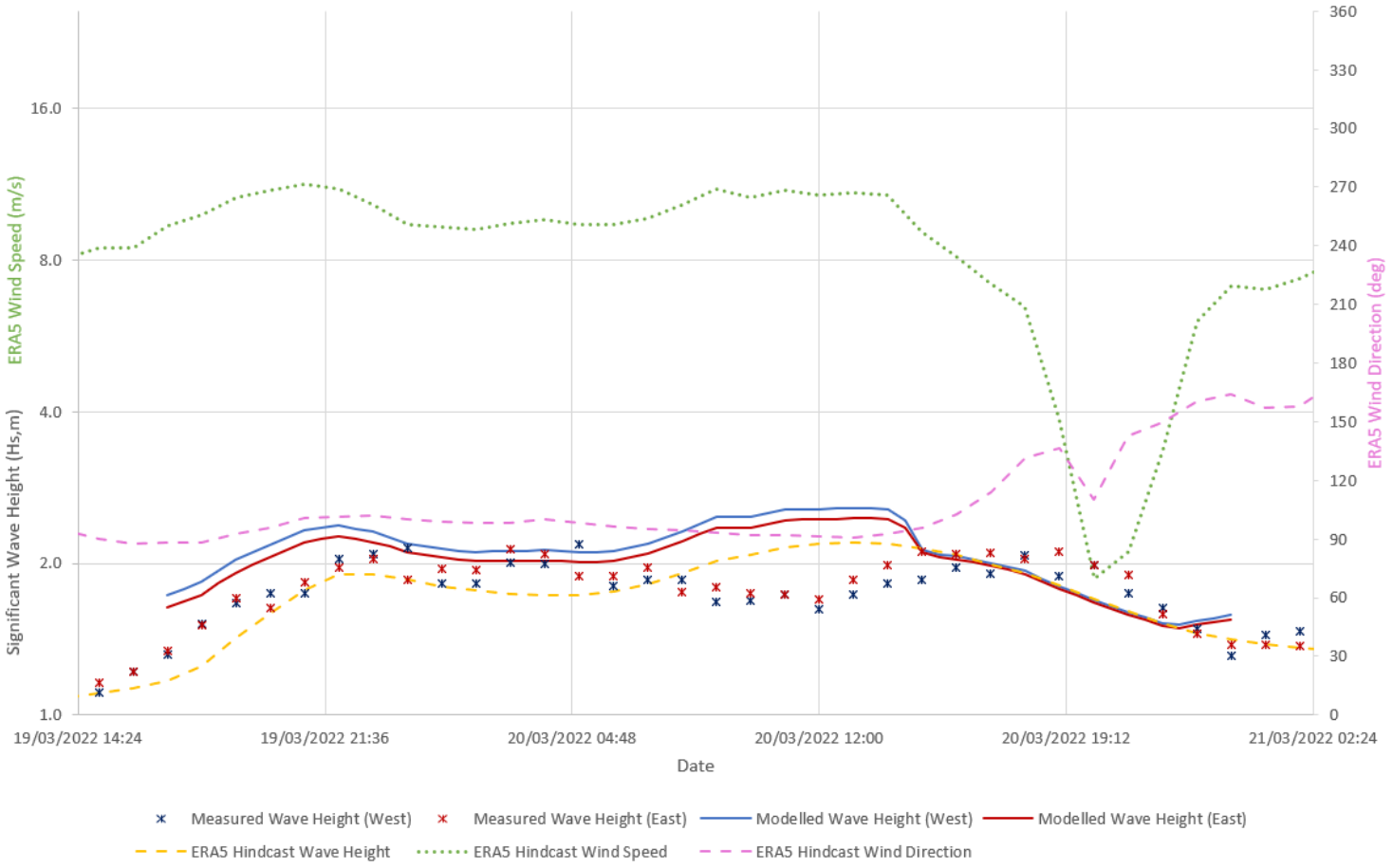

Figure A- 9 Comparison of measured and modelled wave height for waves coming from East – Event 9

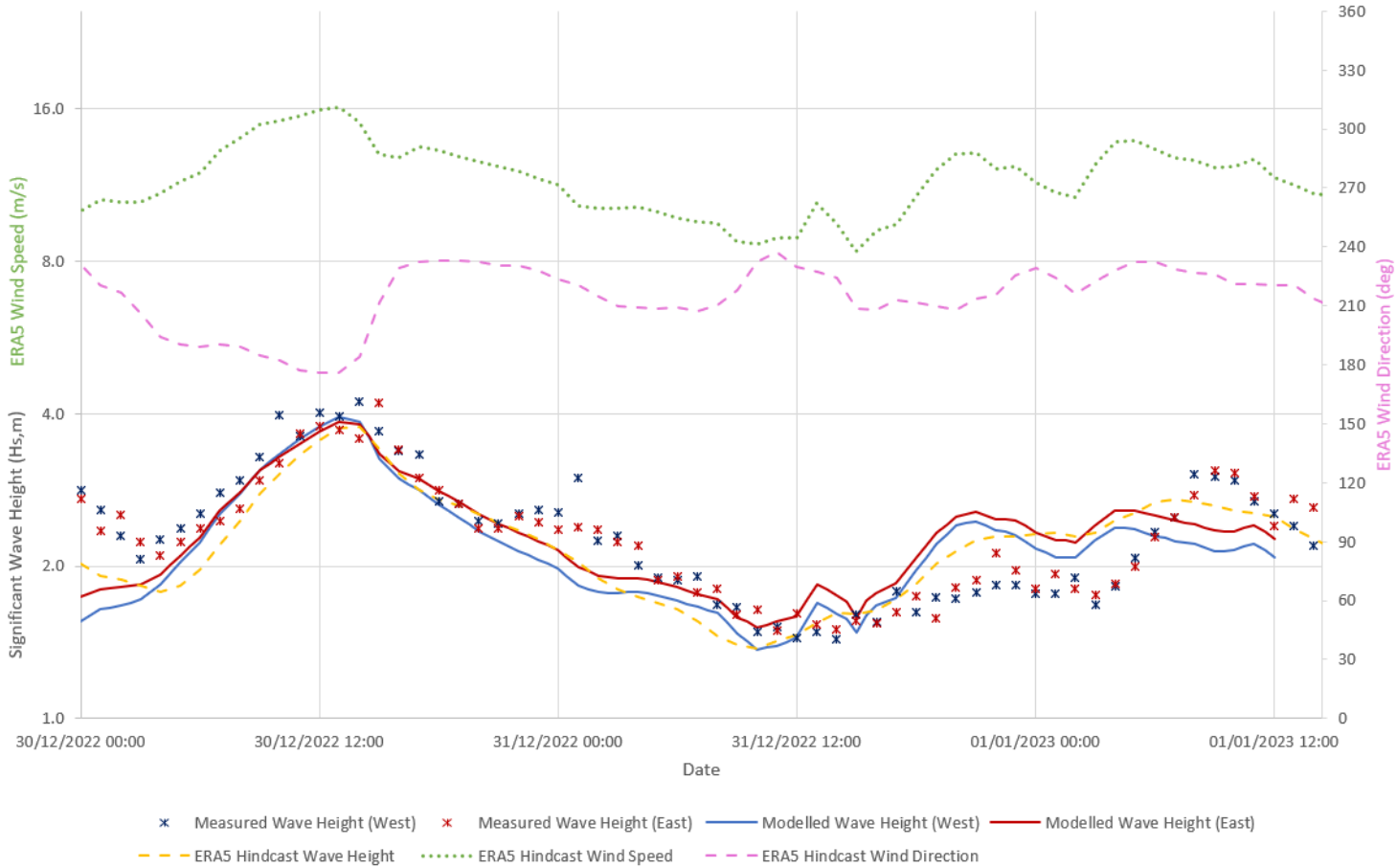

Figure A- 10 Comparison of measured and modelled wave height for waves coming from South – Event 10

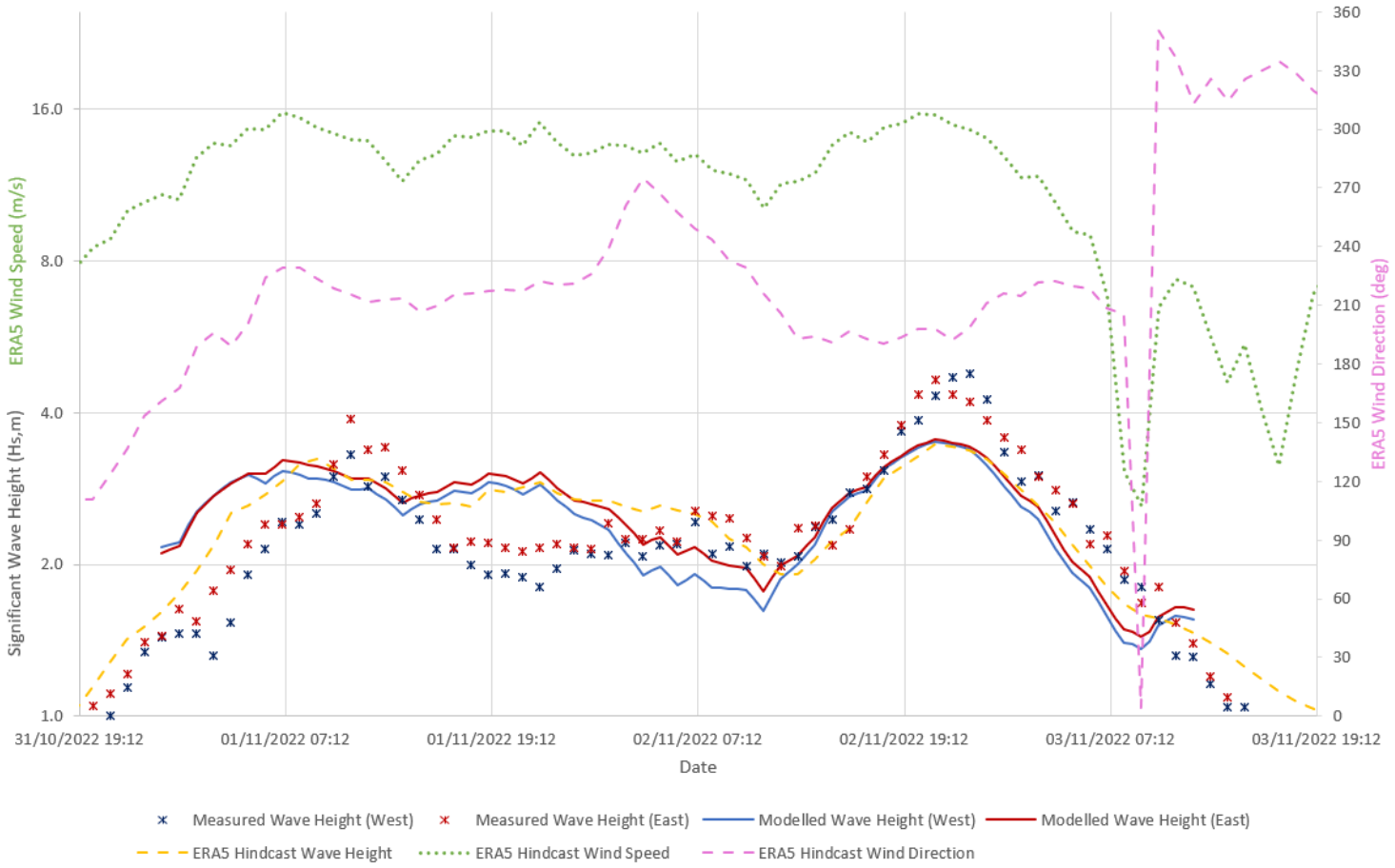

Figure A- 11 Comparison of measured and modelled wave height for waves coming from South – Event 11

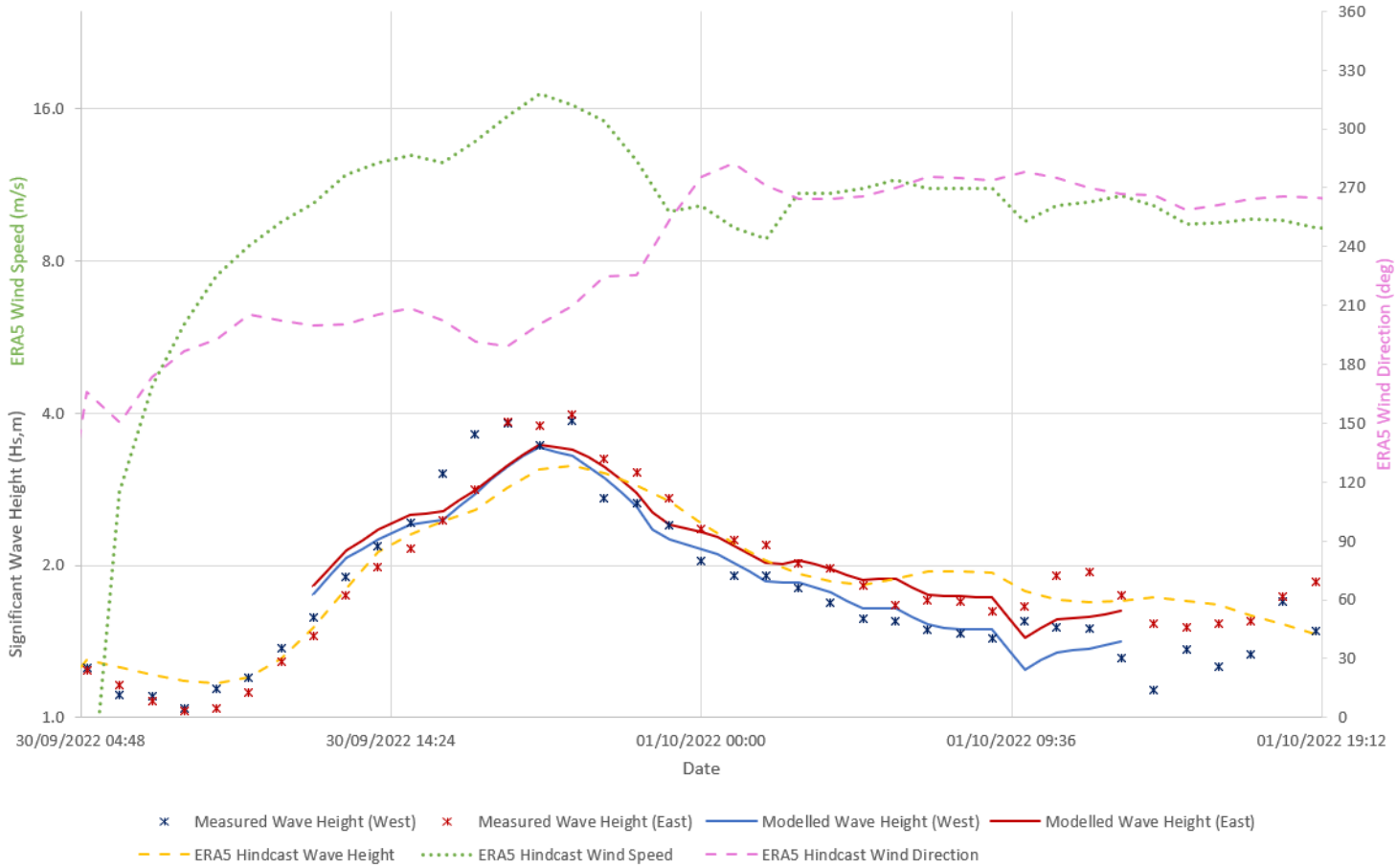

Figure A- 12 Comparison of measured and modelled wave height for waves coming from South – Event 12

Annex B – Results of Wave Model Assessment Runs

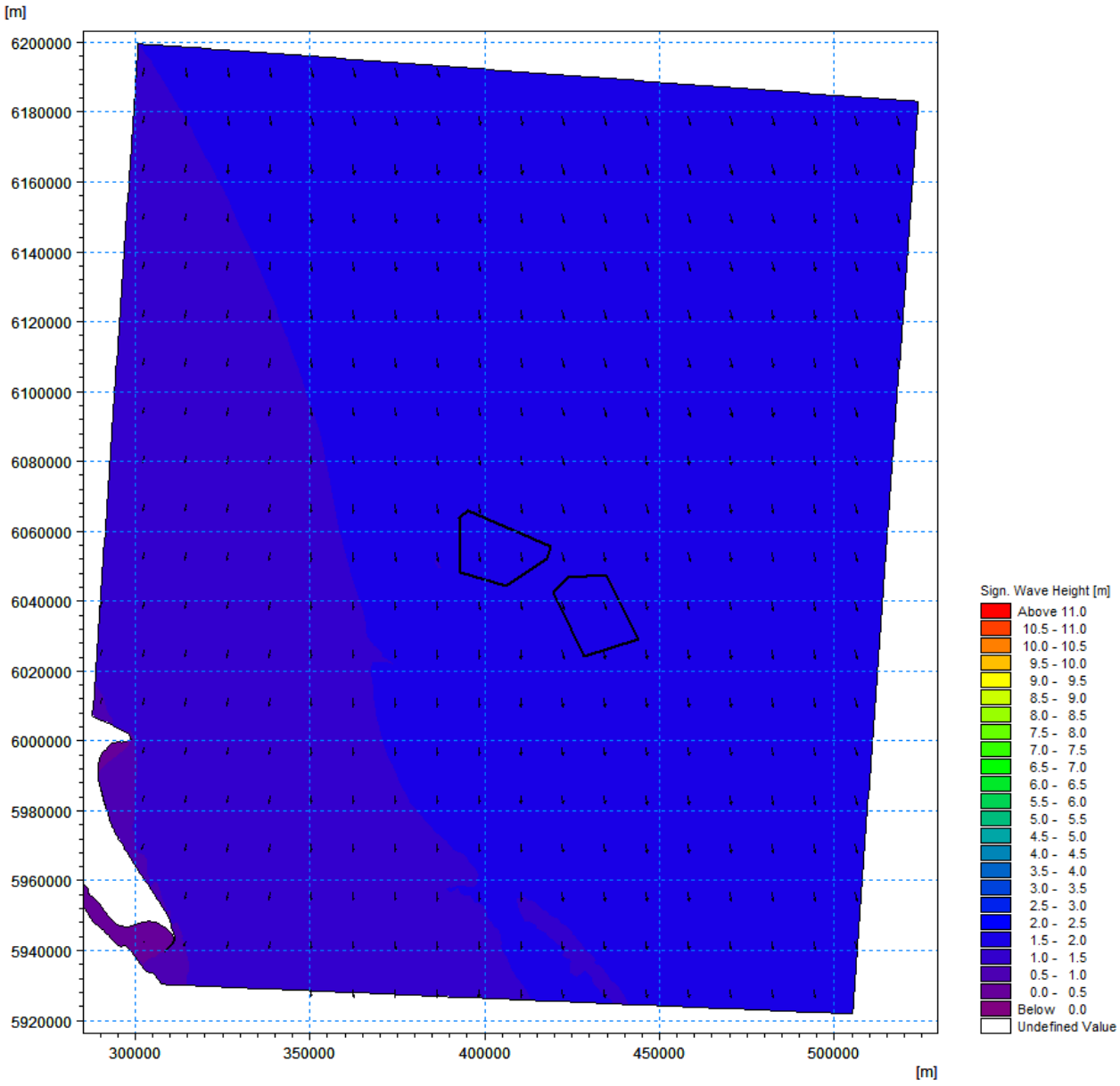

Figure B- 1 Significant Wave Height for Baseline And 50Percentile Waves Coming From North

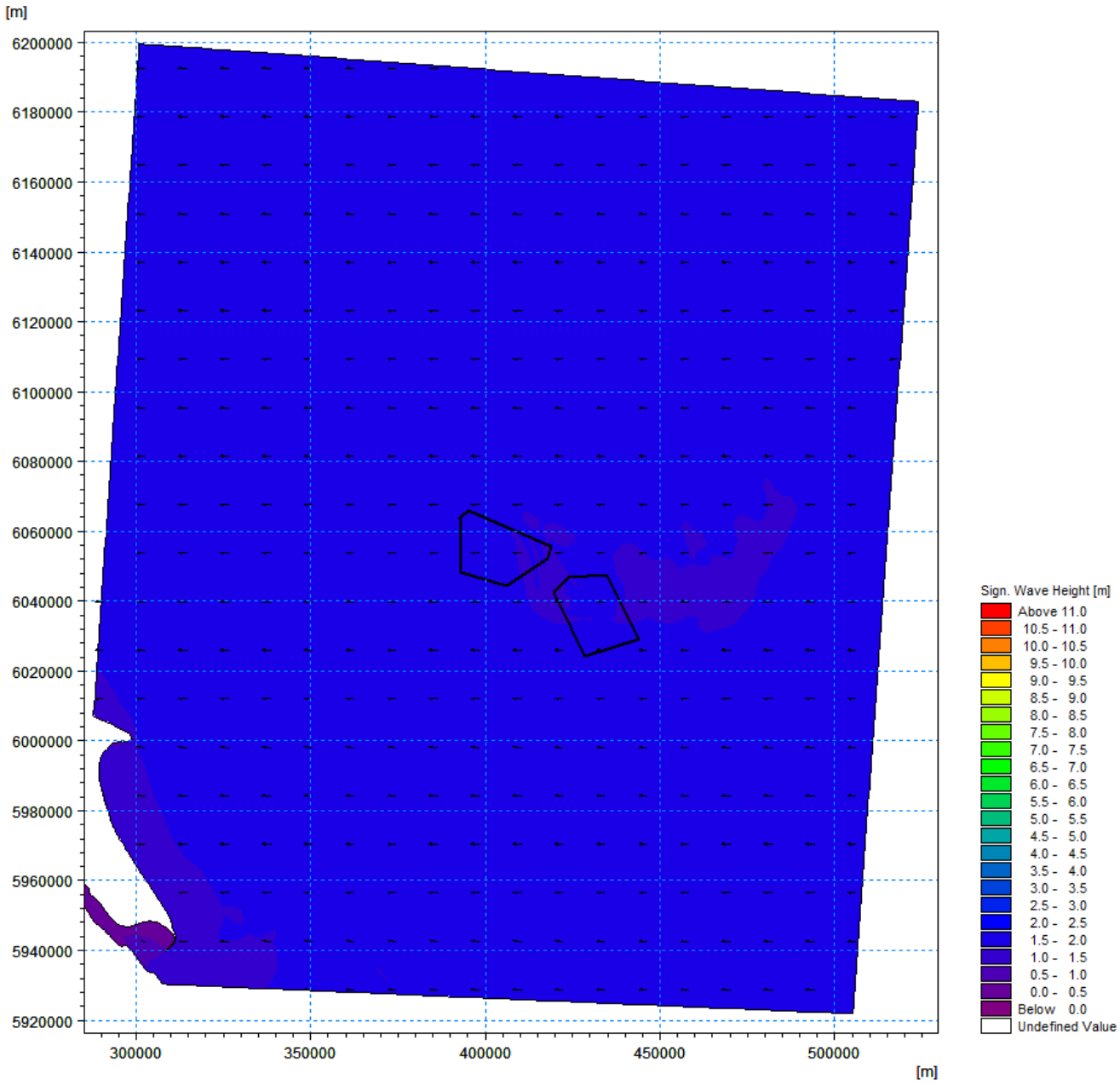

Figure B-2: Significant Wave Height for Baseline and 50 Percentile Waves Coming From East

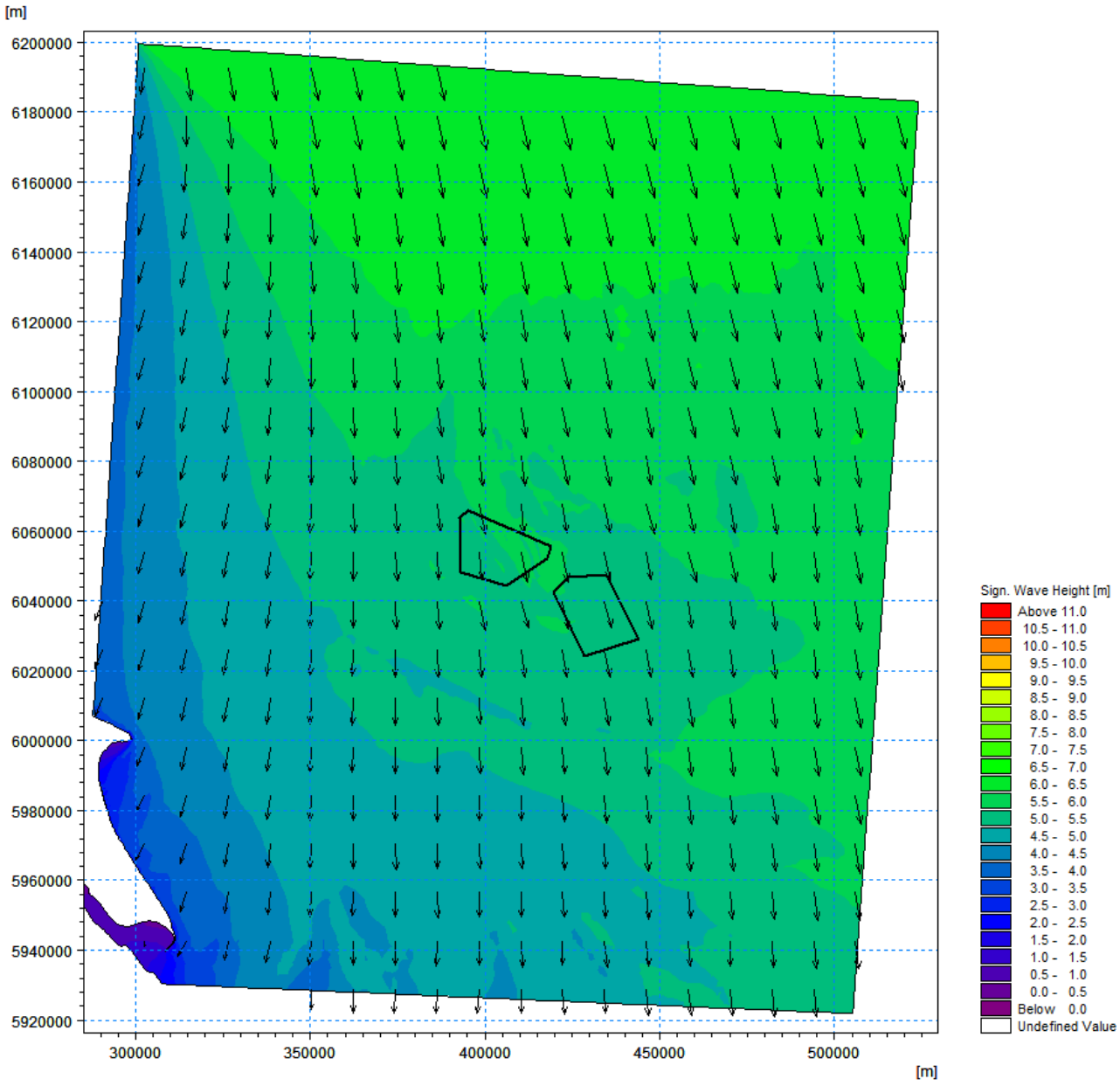

Figure B-3: Significant Wave Height for Baseline and 1 In 1 Year Waves Coming From North

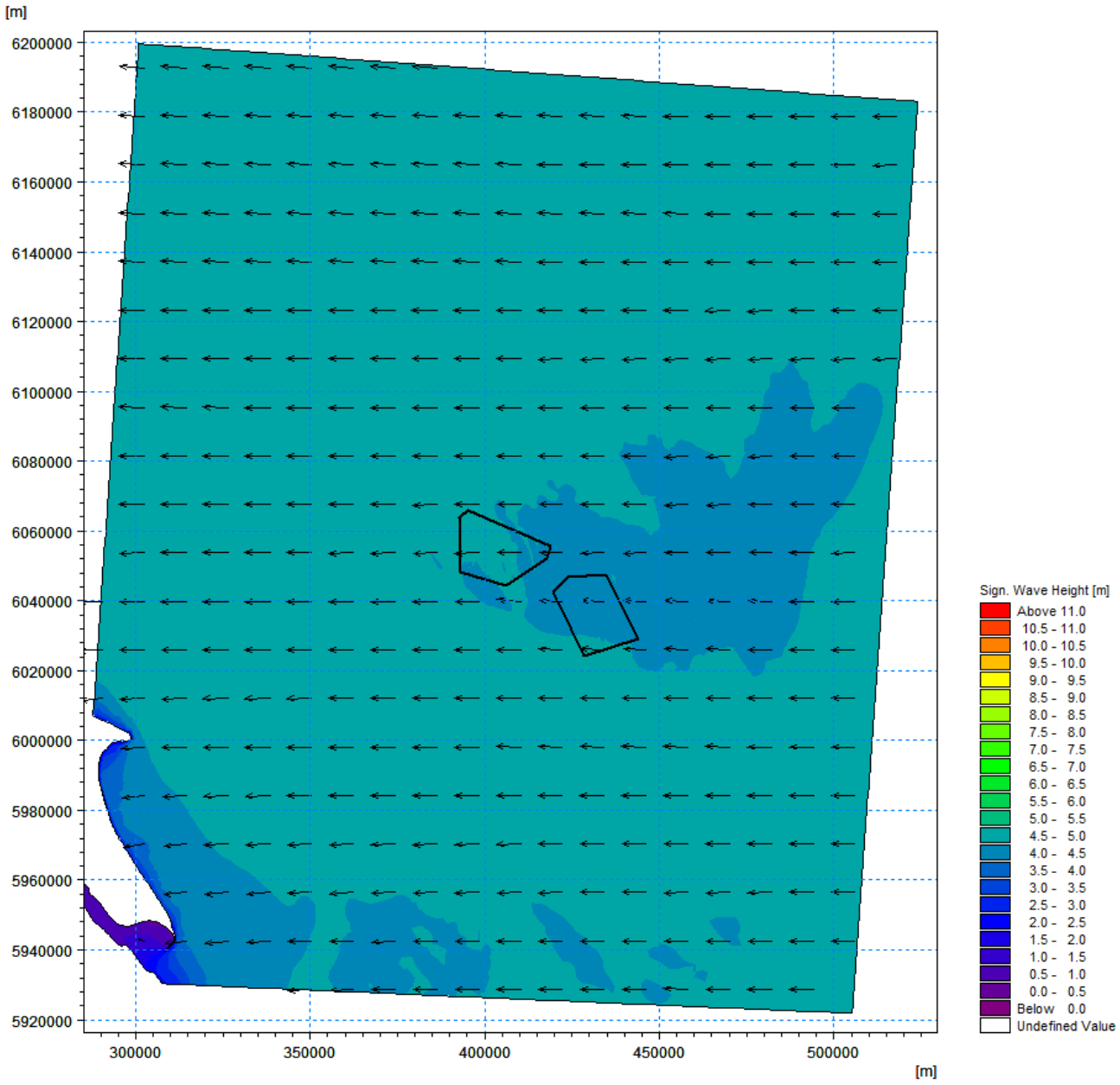

Figure B-4: Significant Wave Height for Baseline and 1 In 1 Year Waves Coming From East

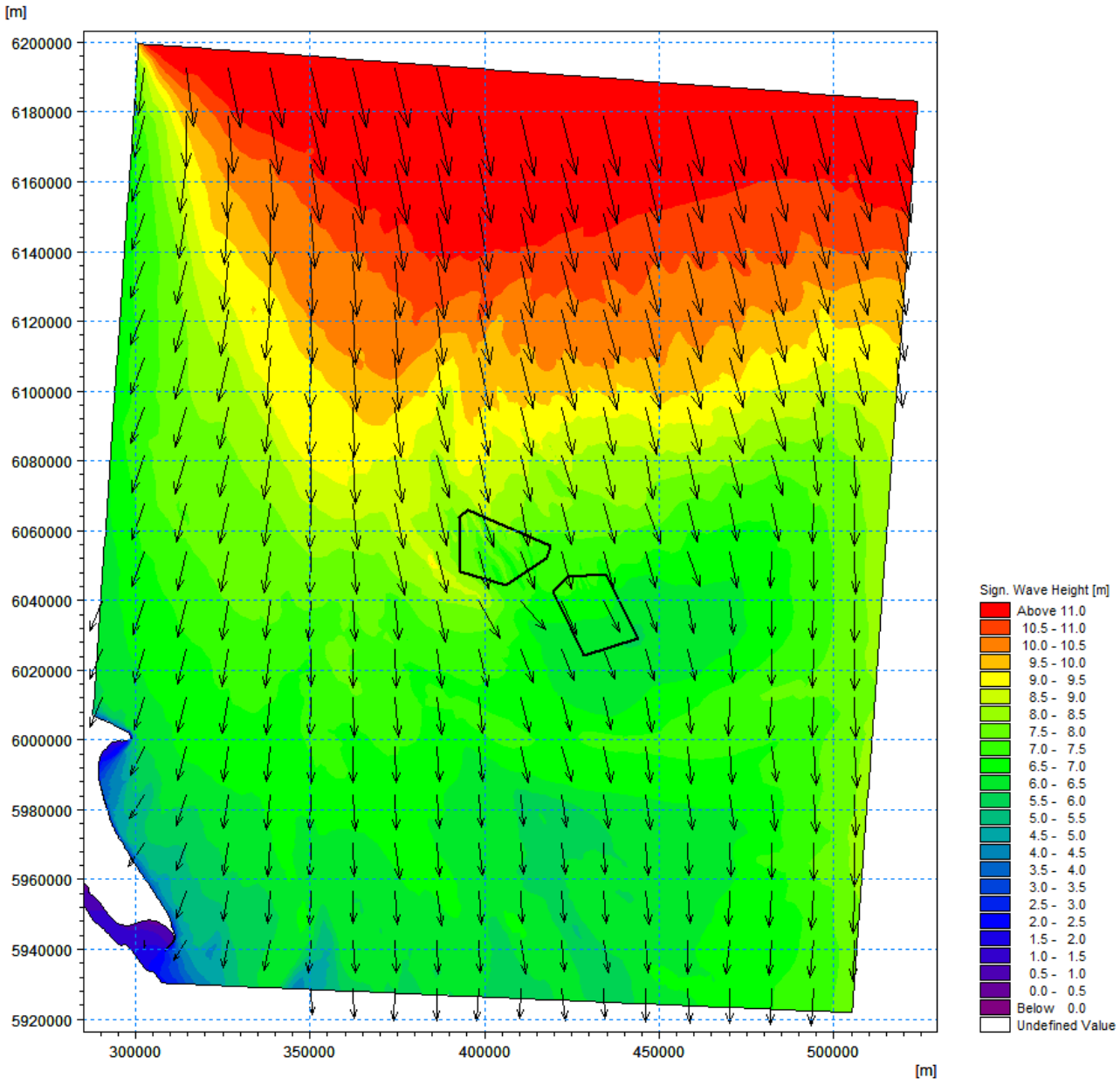

Figure B-5: Significant Wave Height for Baseline and 1 In 100 Years Waves Coming From North

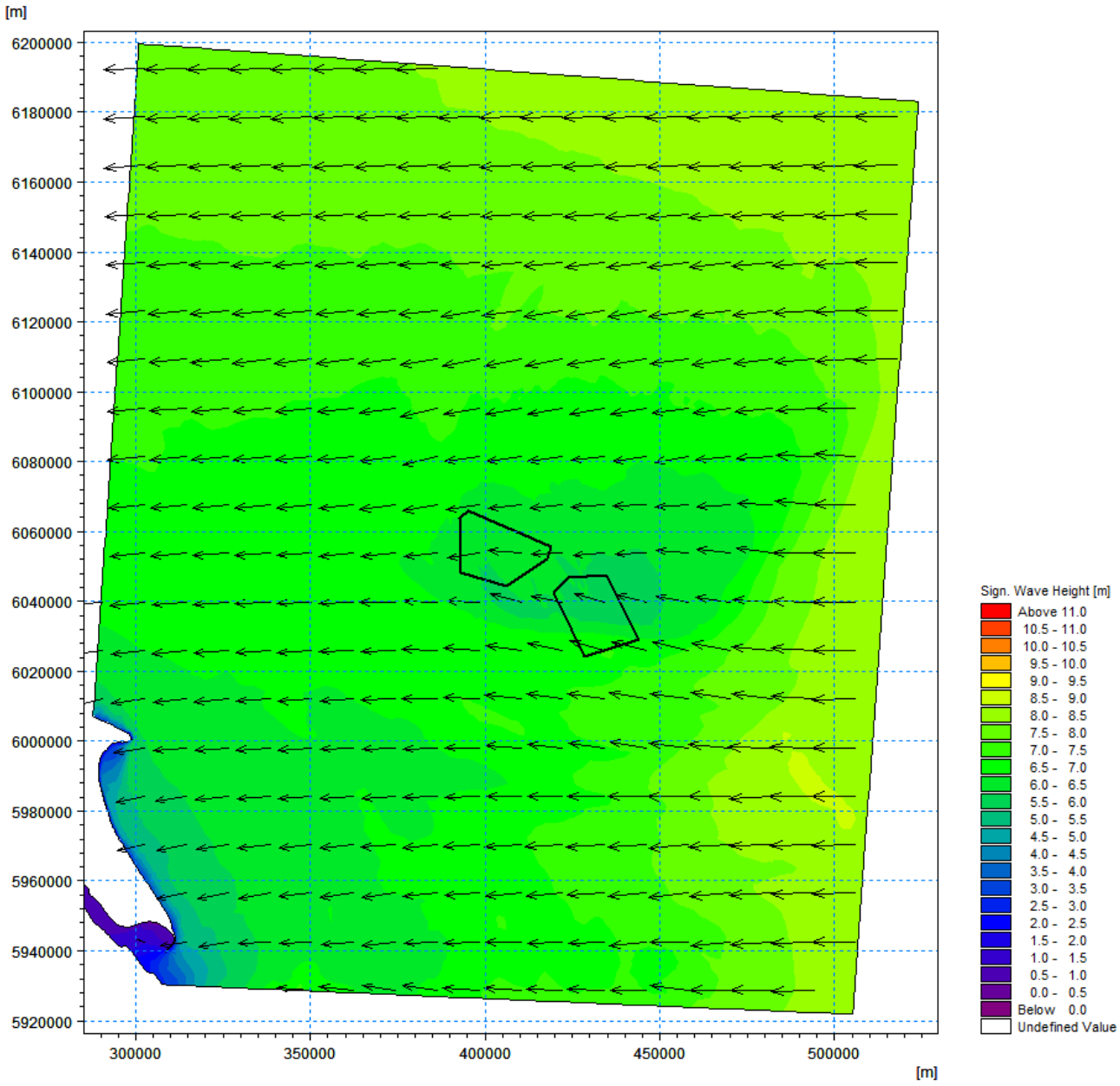

Figure B-6: Significant Wave Height for Baseline and 1 In 100 Year Waves Coming From East

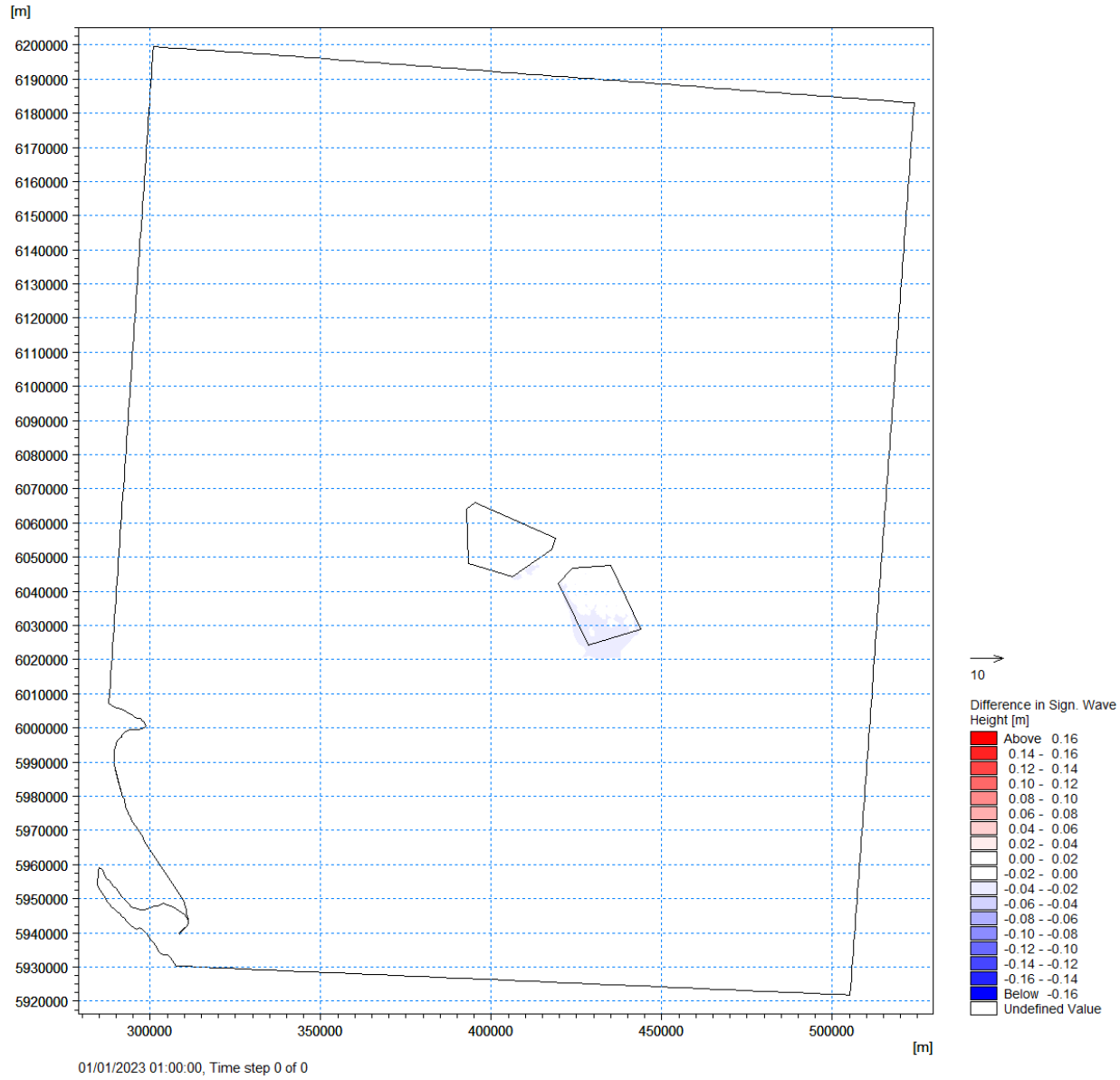

Figure B-7: Difference In Significant Wave Height Between Baseline and Windfarm Option 1 For 50 Percentile Waves Coming from North

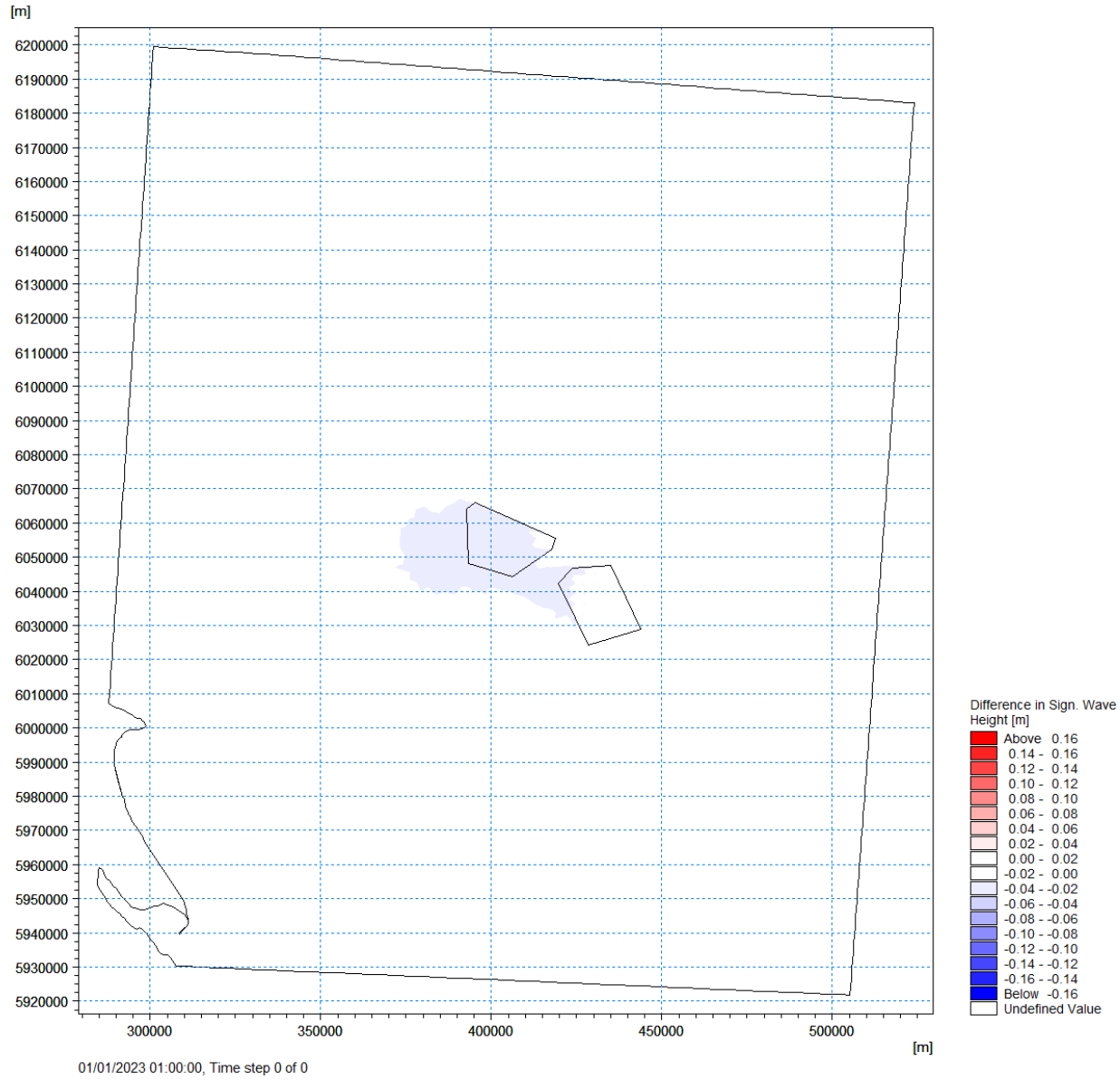

Figure B-8: Difference in Significant Wave Height Between Baseline and Windfarm Option 1 for 50 Percentile Waves Coming From East

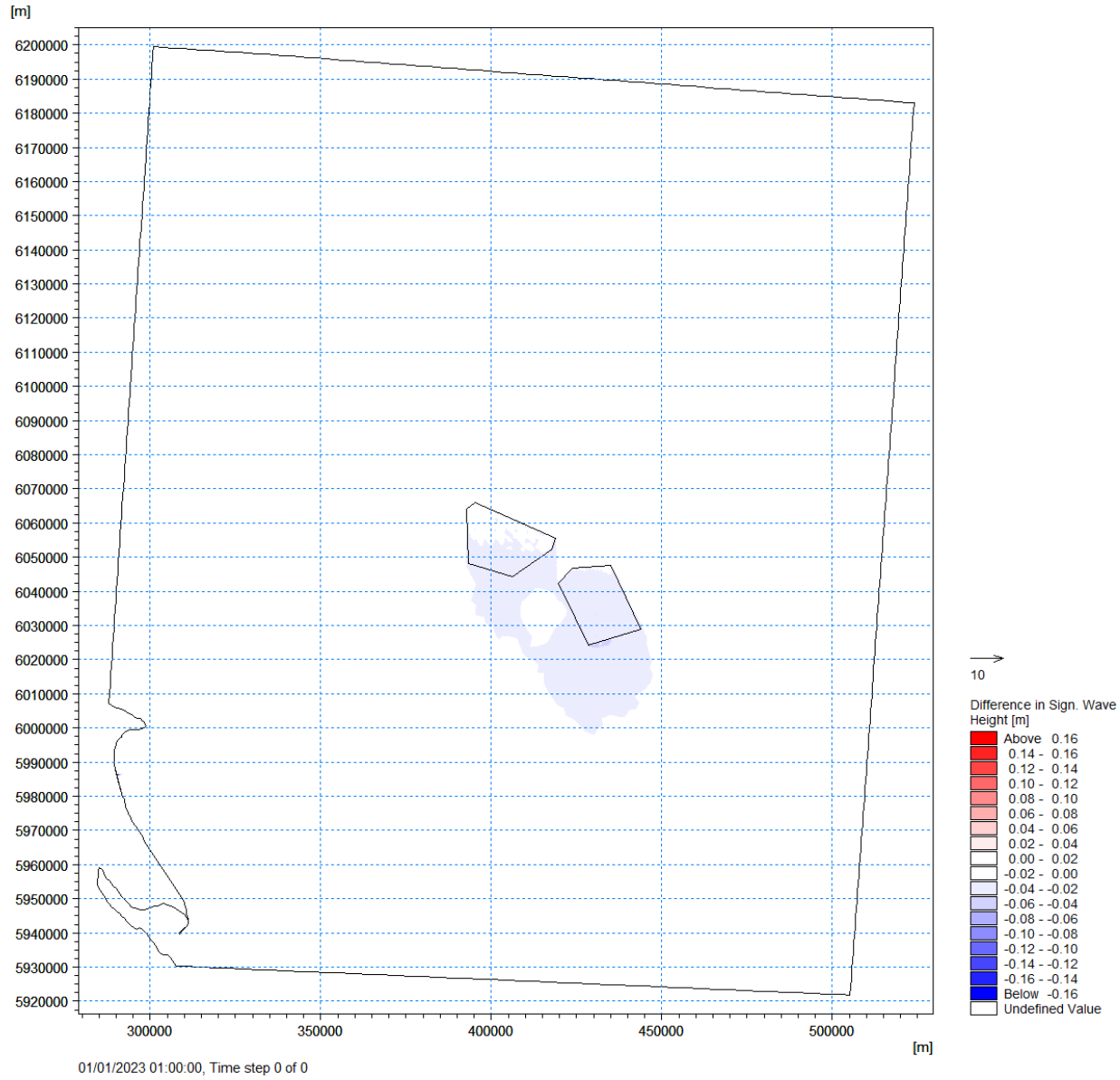

Figure B-9: Difference in Significant Wave Height Between Baseline and Windfarm Option 1 for 1 in 1 Year Waves Coming From North

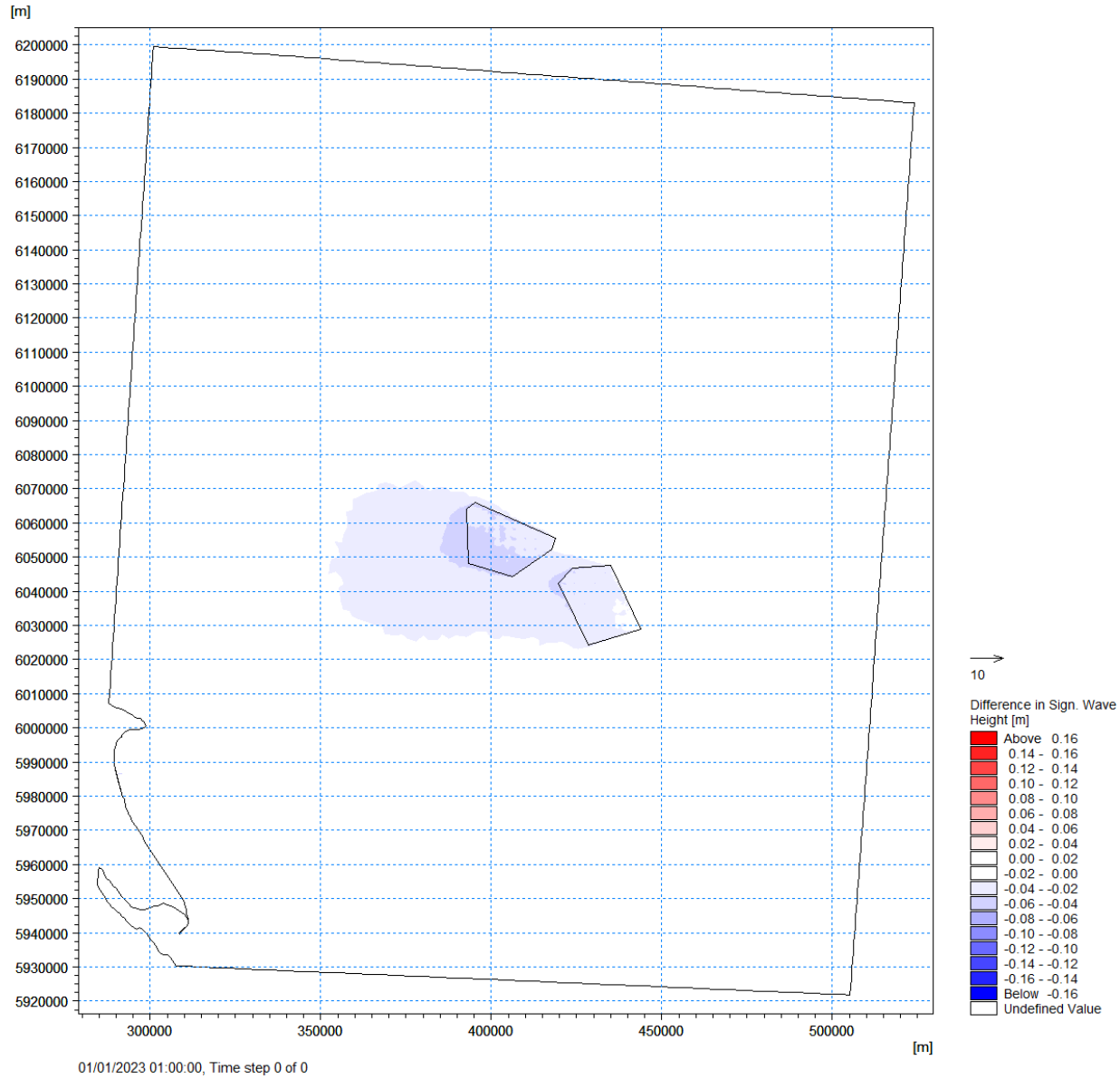

Figure B-10: Difference in Significant Wave Height Between Baseline and Windfarm Option 1 for 1 in 1 Year Waves Coming From East

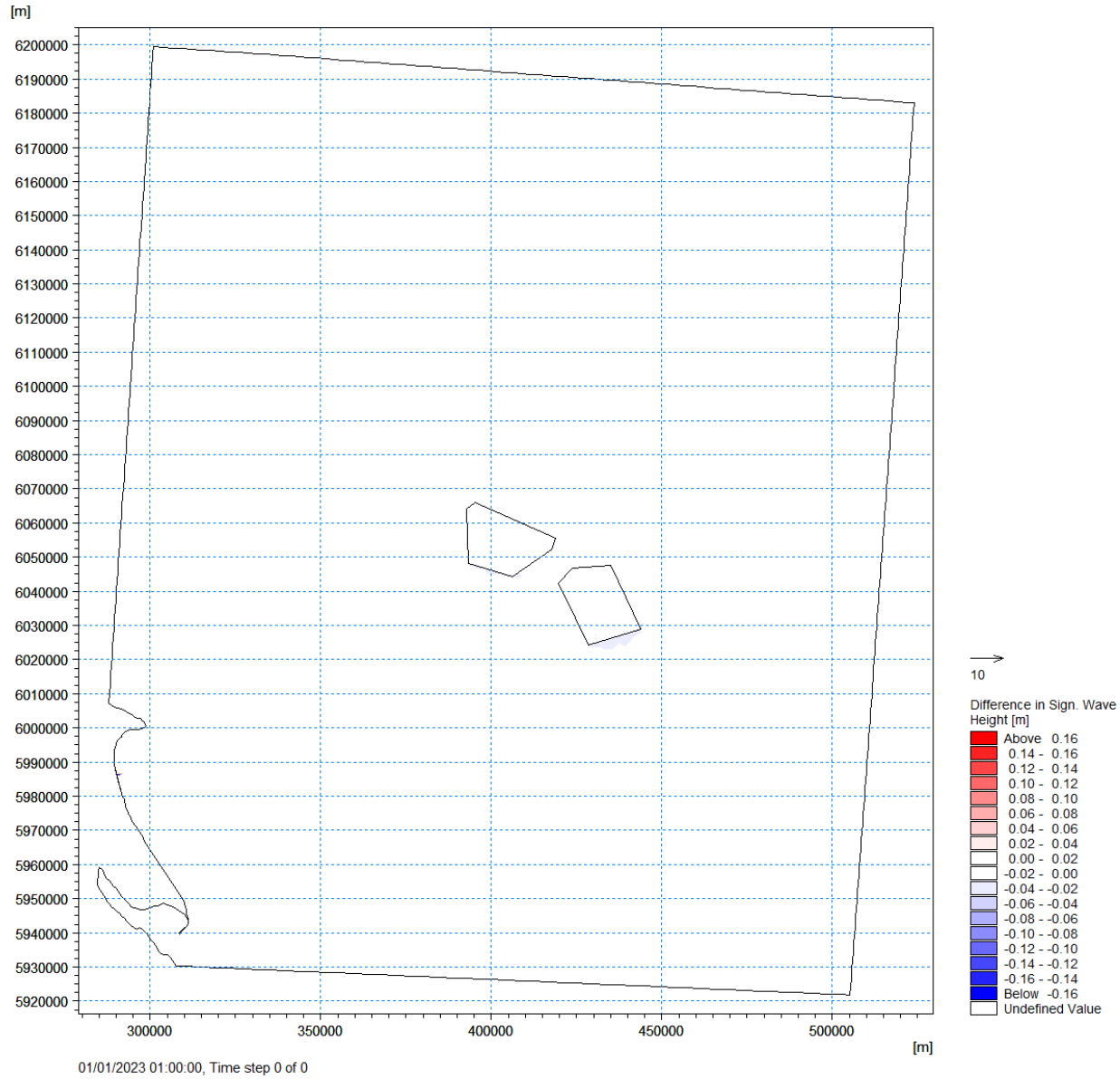

Figure B-11: Difference in Significant Wave Height Between Baseline and Windfarm Option 1 for 1 in 100 Year Waves Coming From North

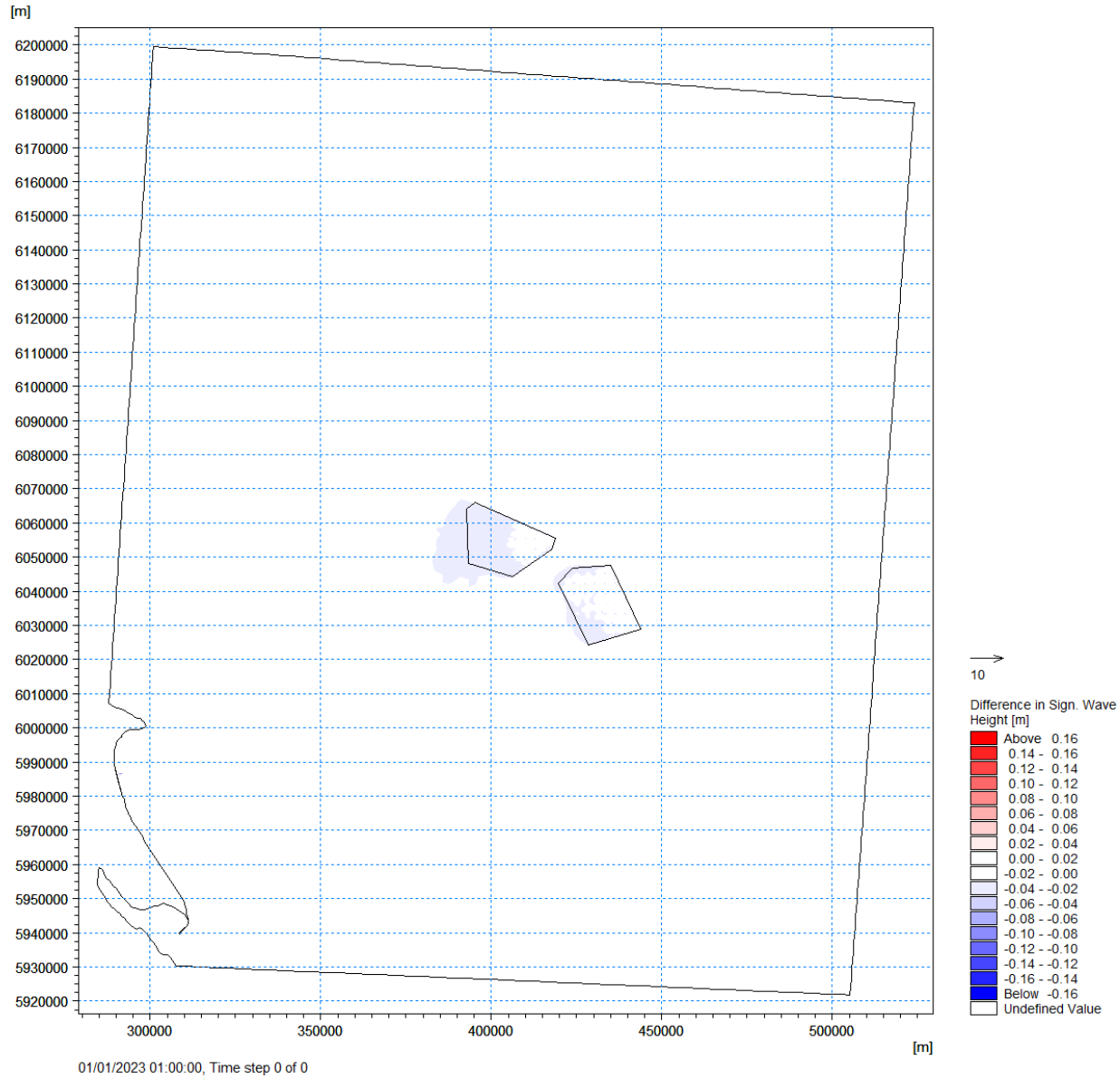

Figure B-12: Difference in Significant Wave Height Between Baseline and Windfarm Option 1 for 1 in 100 Year Waves Coming From East

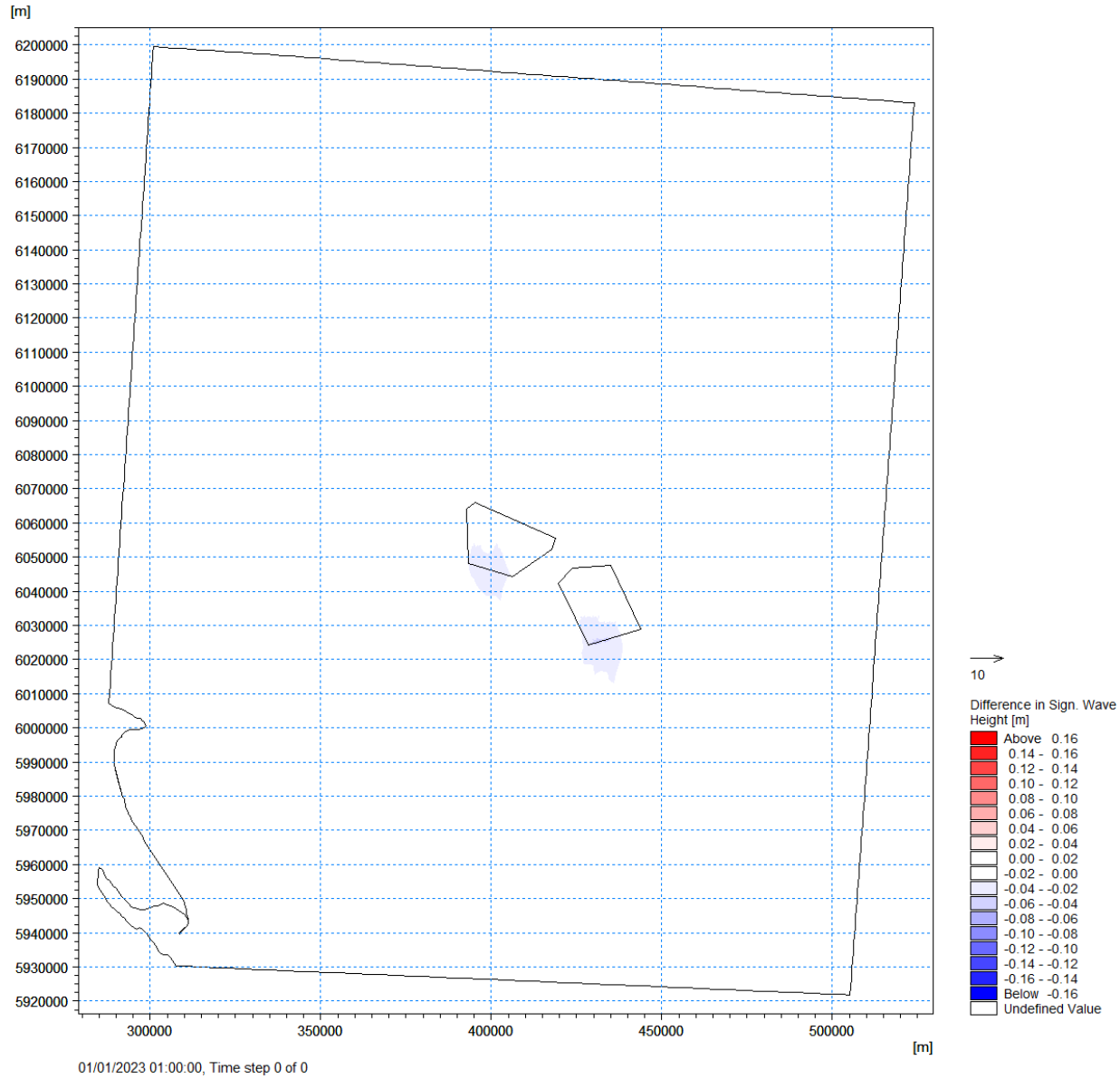

Figure B-13: Difference in Significant Wave Height Between Baseline and Windfarm Option 2 for 50 Percentile Waves Coming From North

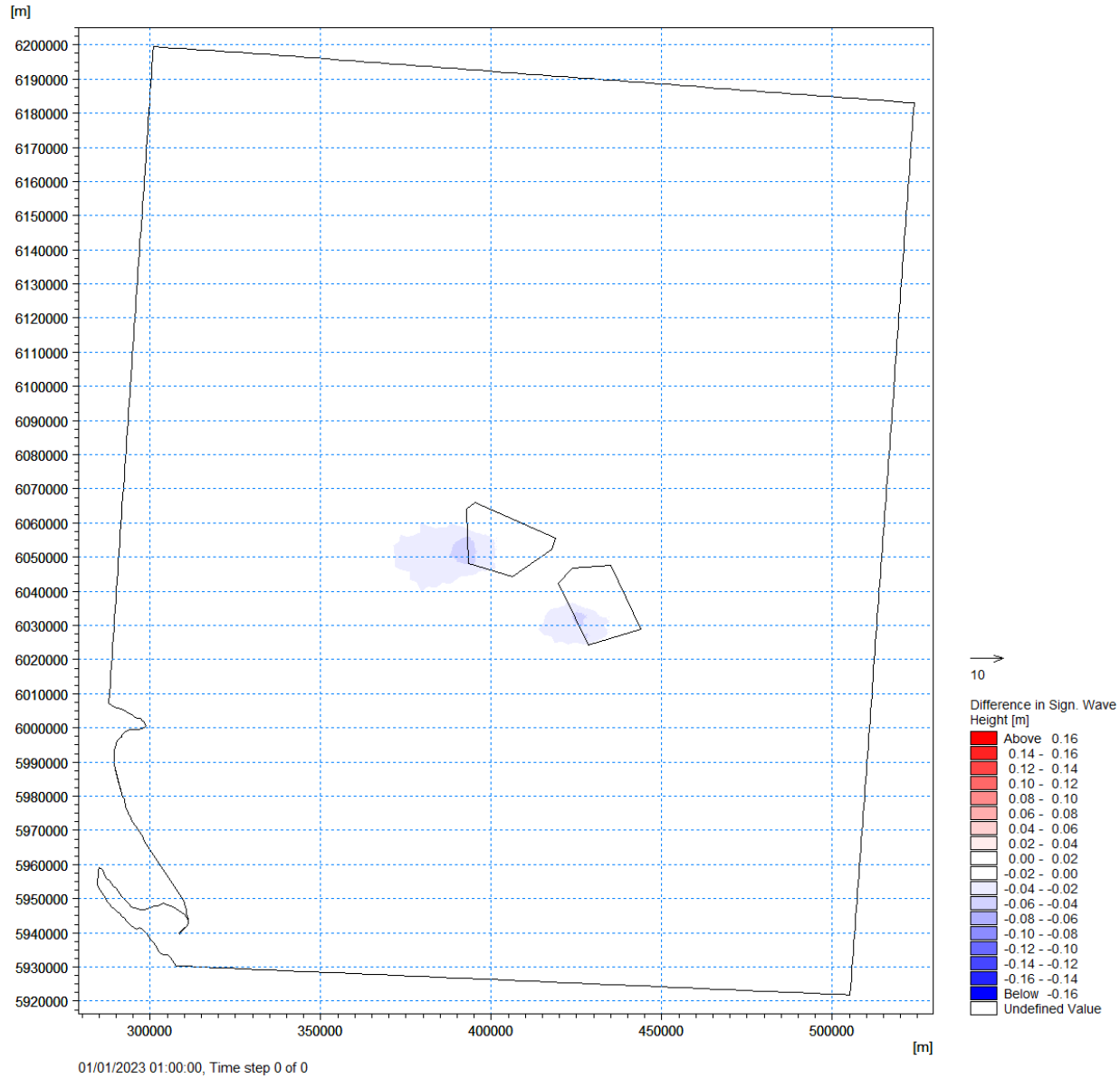

Figure B-14: Difference in Significant Wave Height Between Baseline and Windfarm Option 2 for 50 Percentile Waves Coming From East

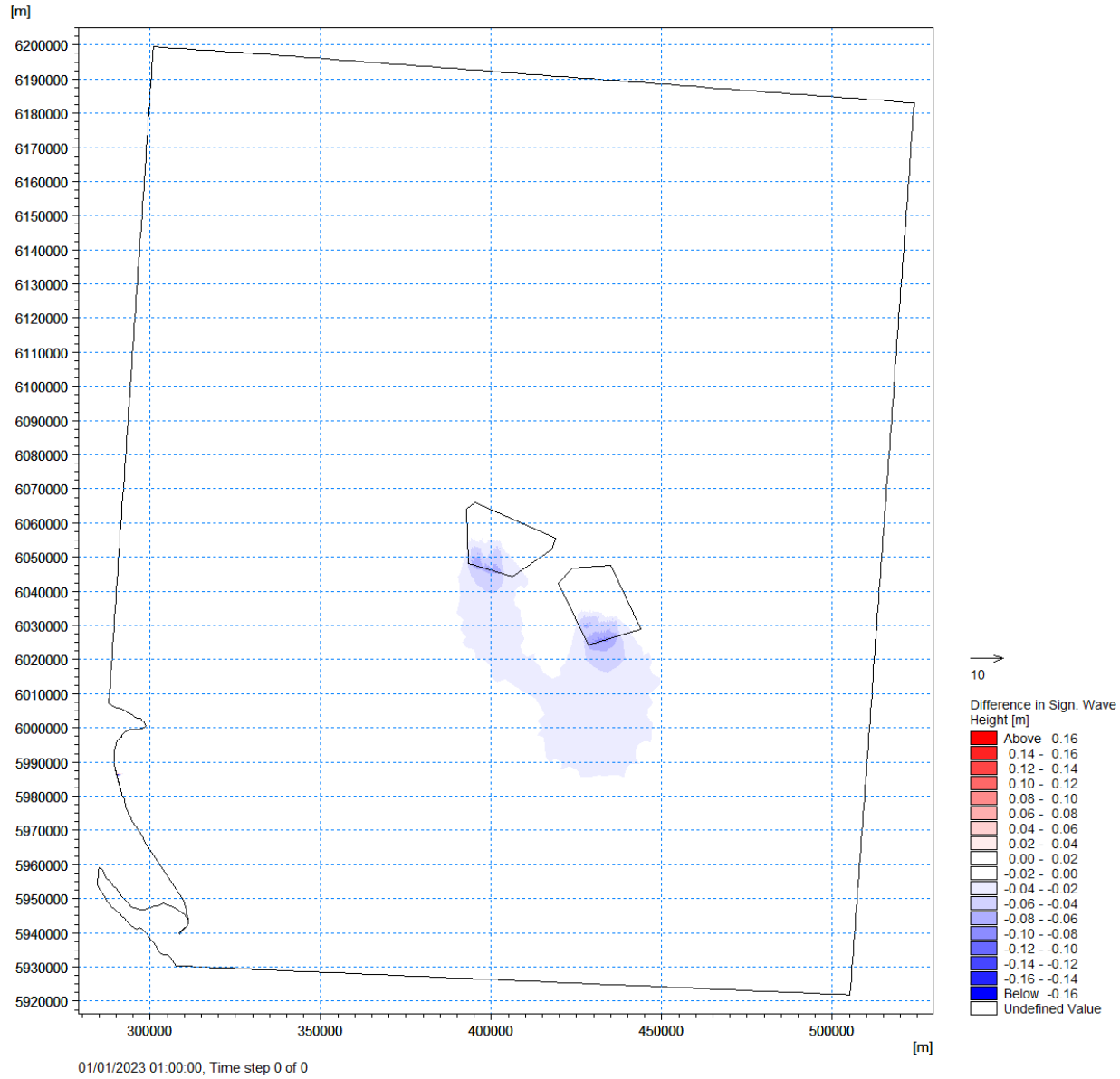

Figure B-15: Difference in Significant Wave Height Between Baseline and Windfarm Option 2 for 1 in 1 Year Waves Coming From North

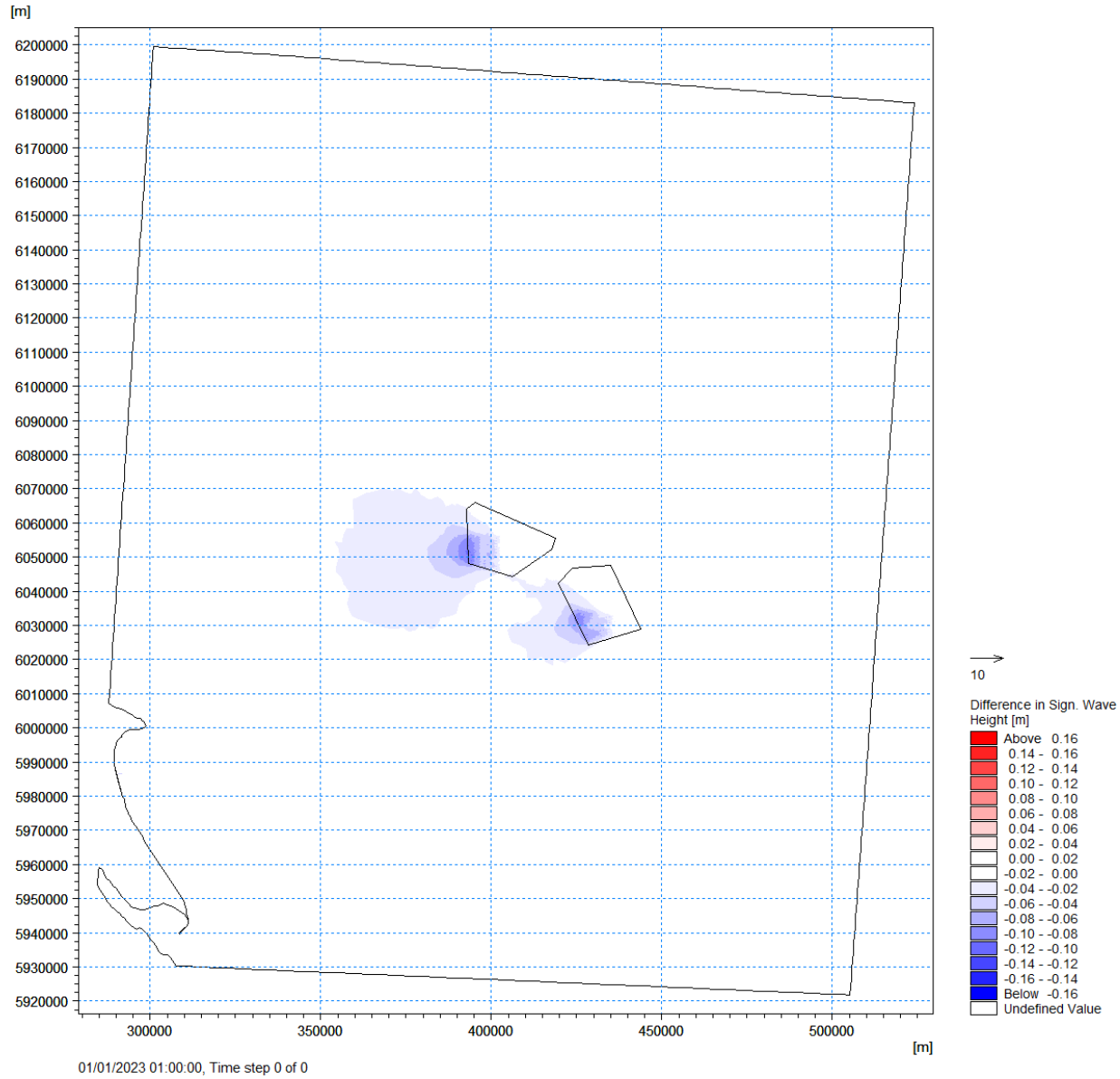

Figure B-16: Difference in Significant Wave Height Between Baseline and Windfarm Option 2 for 1 in 1 Year Waves Coming From East

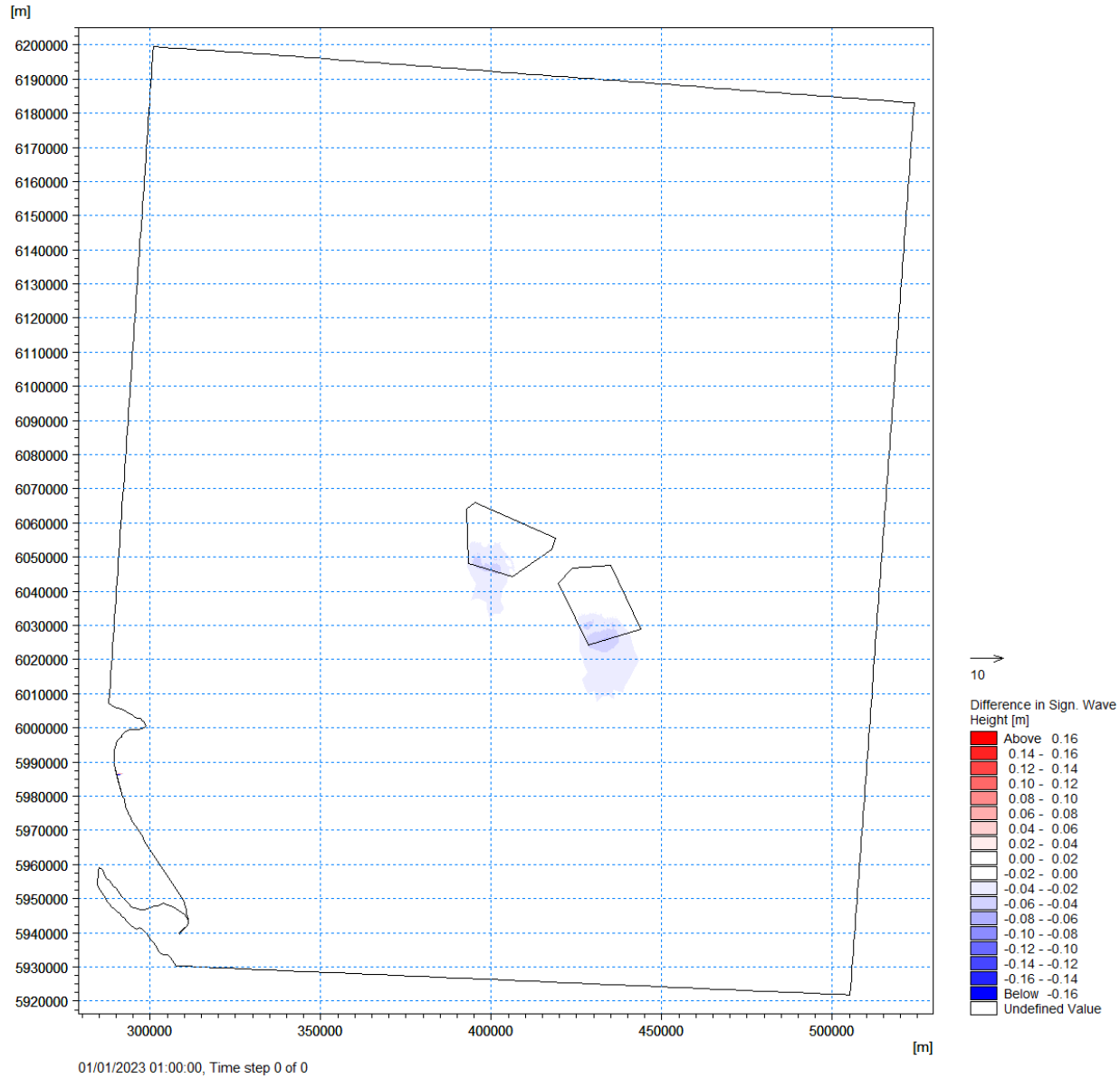

Figure B-17: Difference in Significant Wave Height Between Baseline and Windfarm Option 2 for 1 in 100 Year Waves Coming From North

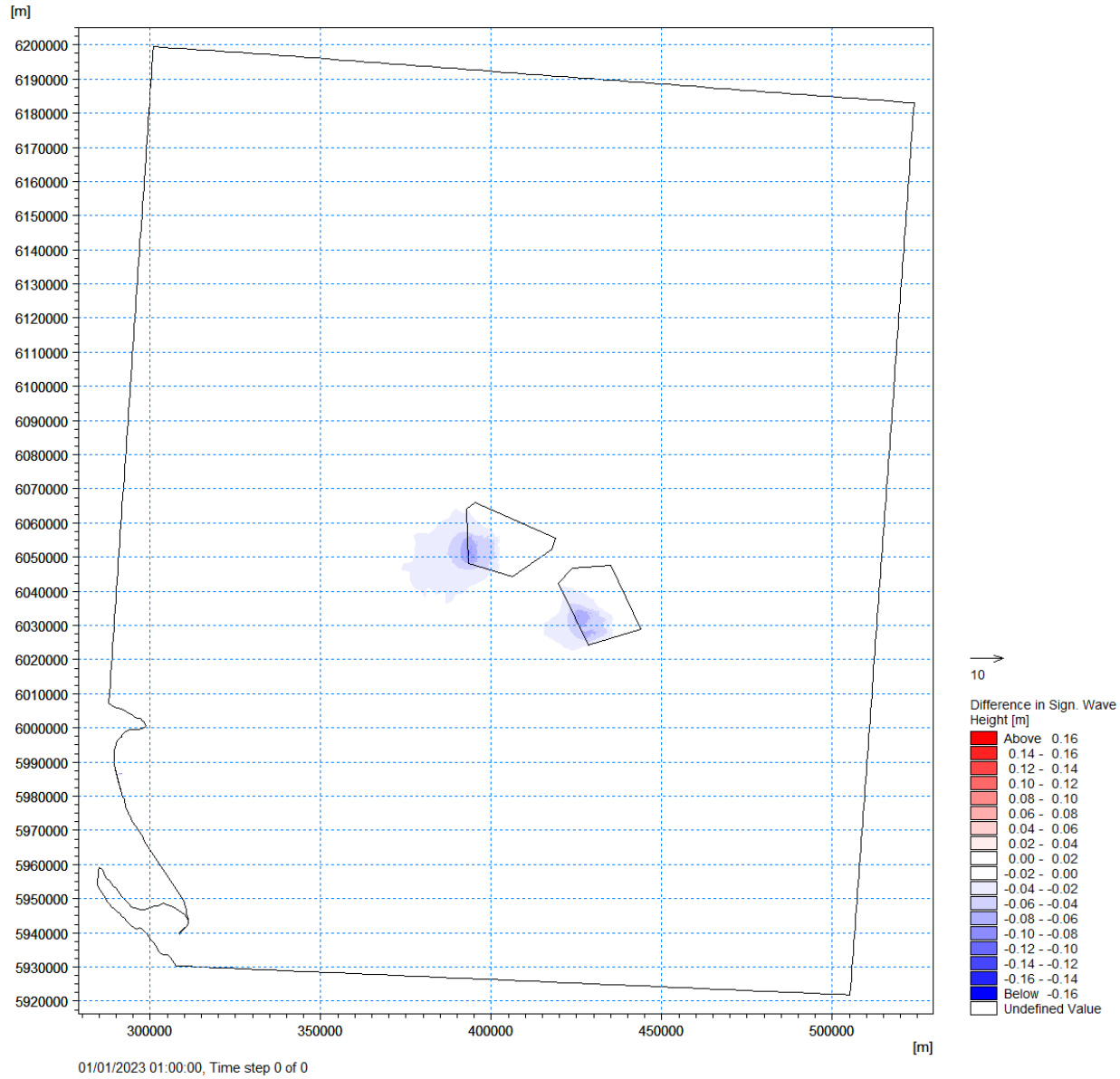

Figure B-18: Difference in Significant Wave Height Between Baseline and Windfarm Option 2 for 1 in 100 Year Waves Coming From East

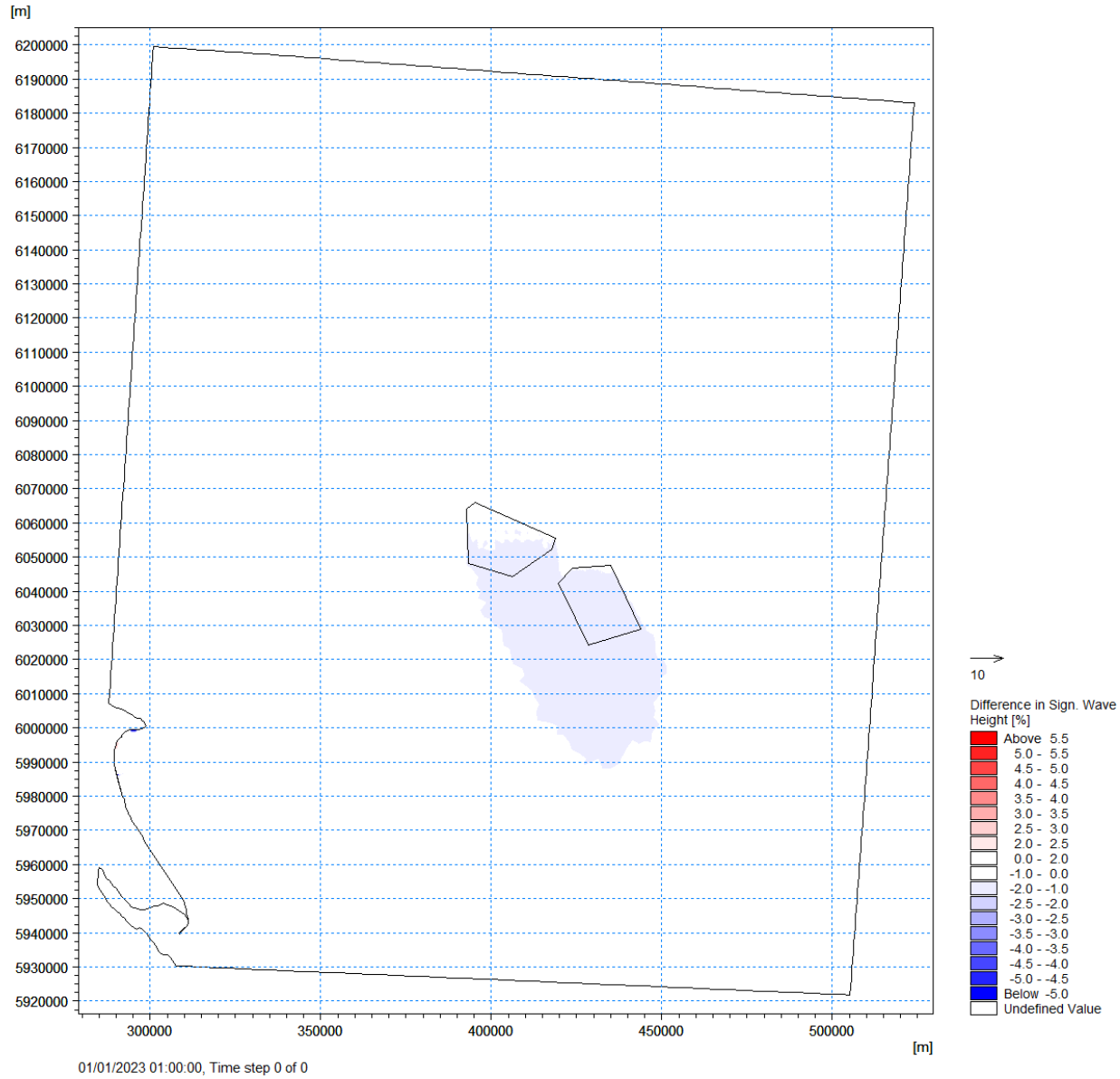

Figure B-19: Difference in Significant Wave Height in Percentage Between Baseline and Windfarm Option 1 for 50 Percentile Waves Coming From North

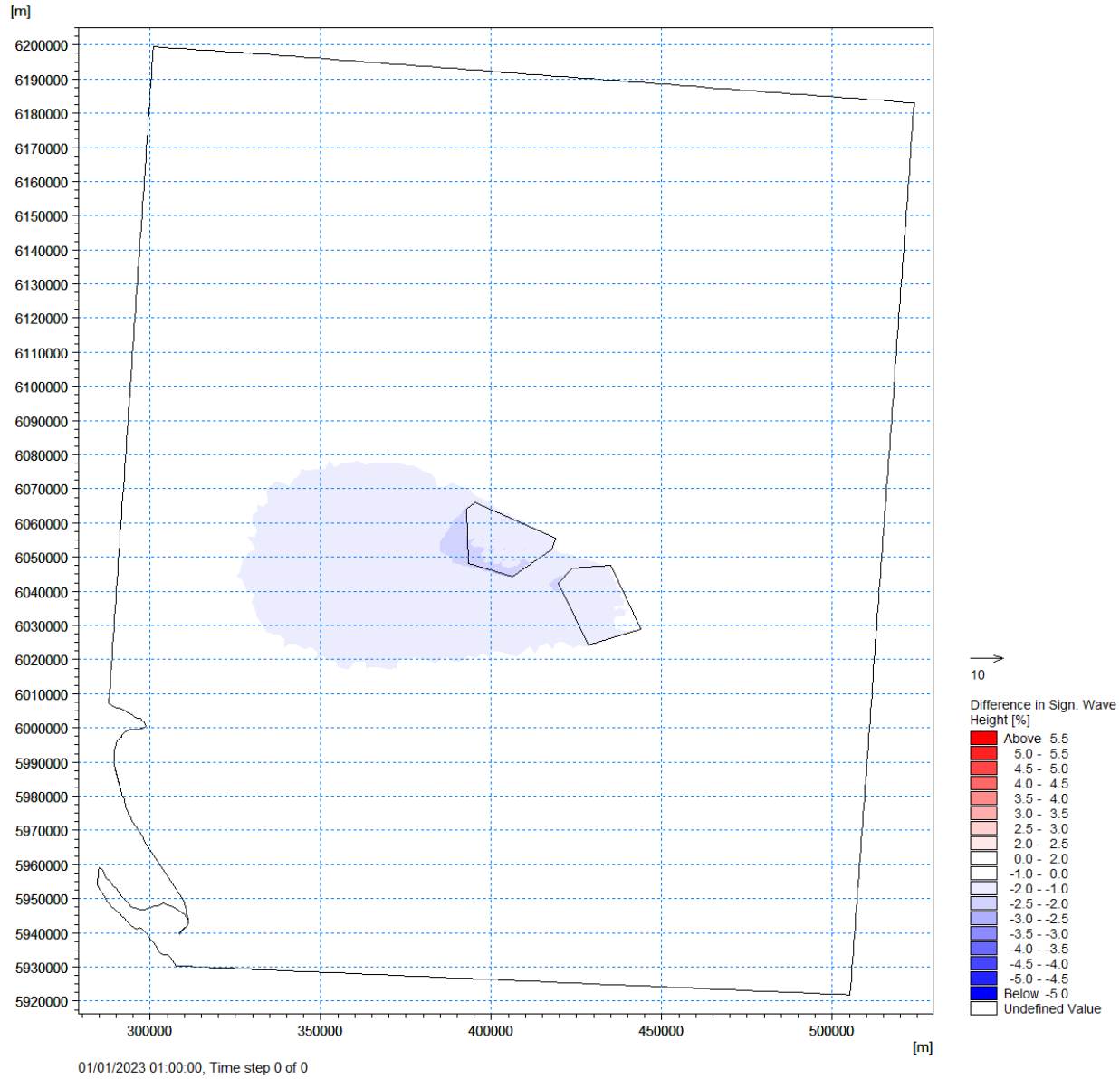

Figure B-20: Difference in Significant Wave Height in Percentage Between Baseline and Windfarm Option 1 for 50 Percentile Waves Coming From East

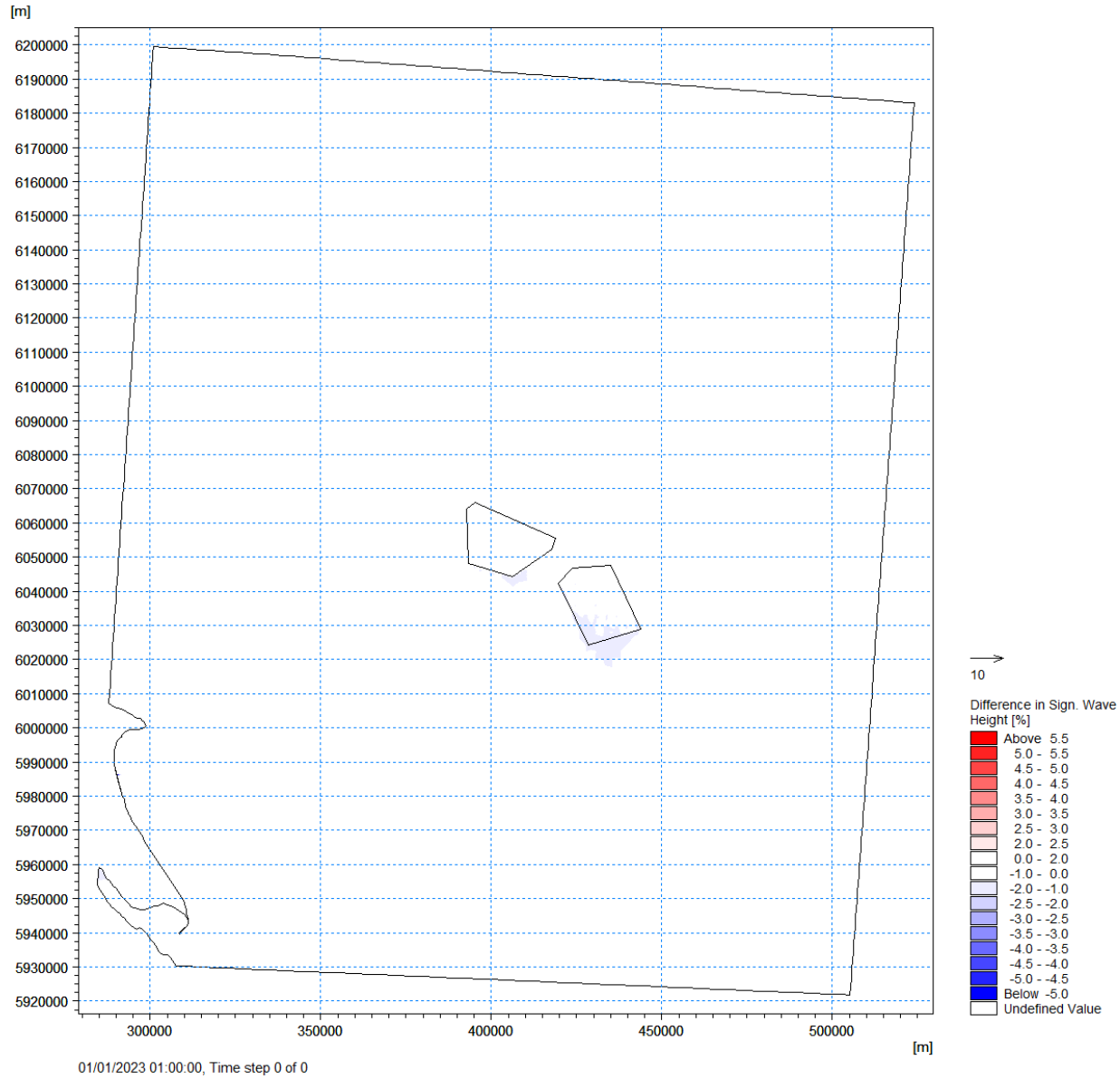

Figure B-21: Difference in Significant Wave Height in Percentage Between Baseline and Windfarm Option 1 for 1 in 1 Year Waves Coming From North

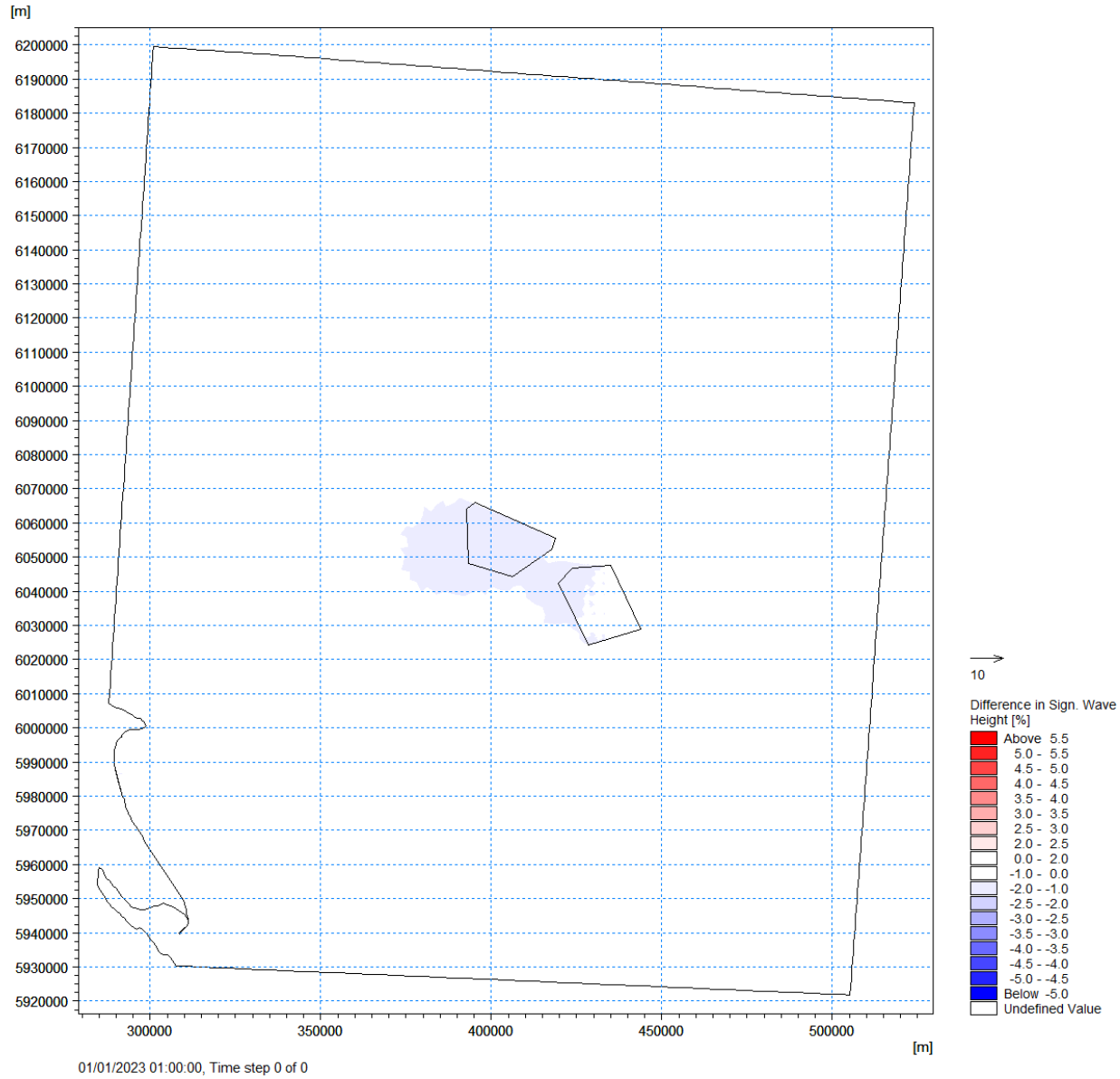

Figure B-22: Difference in Significant Wave Height in Percentage Between Baseline and Windfarm Option 1 for 1 in 1 Year Waves Coming From East

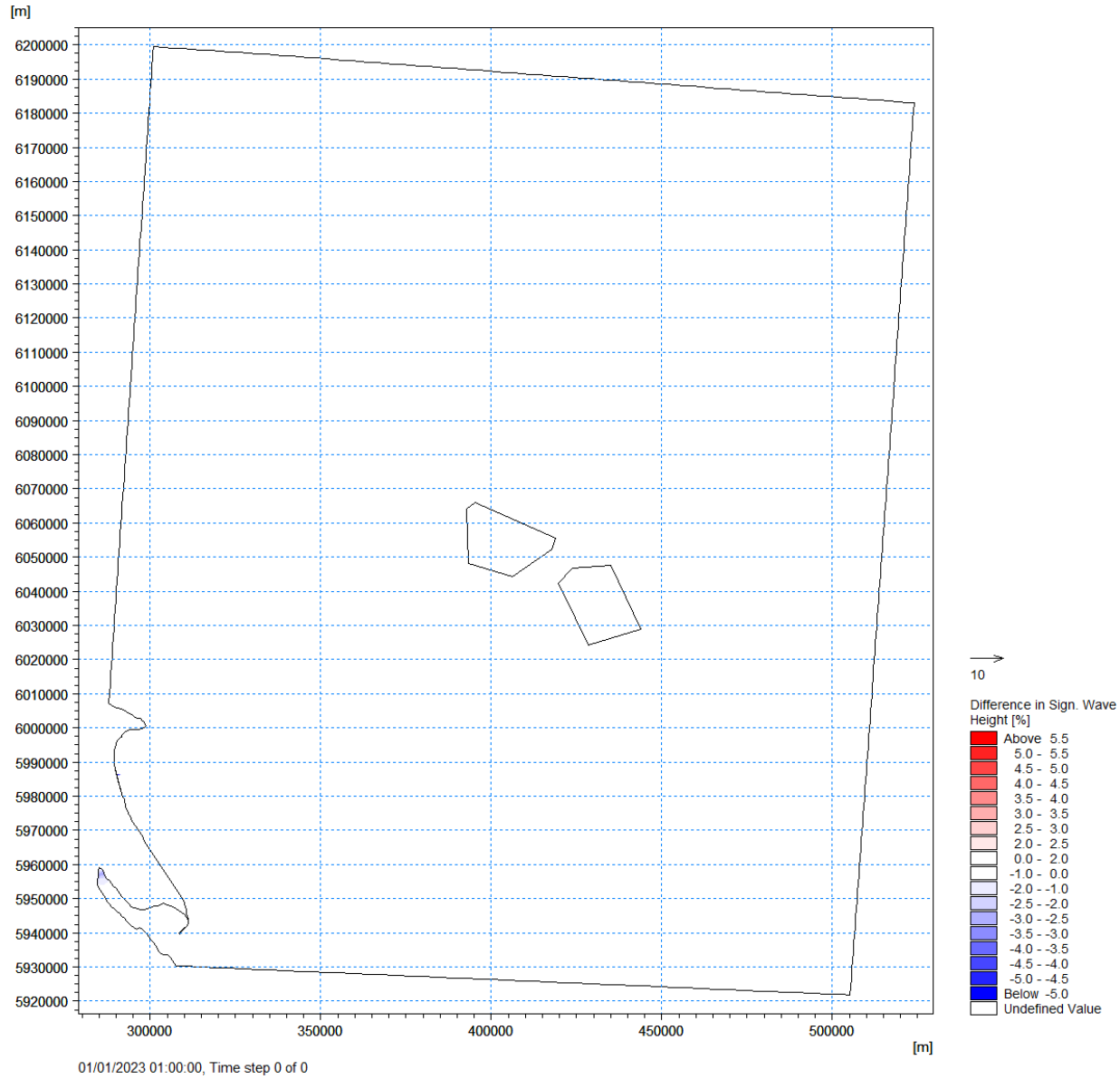

Figure B-23: Difference in Significant Wave Height in Percentage Between Baseline and Windfarm Option 1 for 1 In 100 Year Waves Coming From North

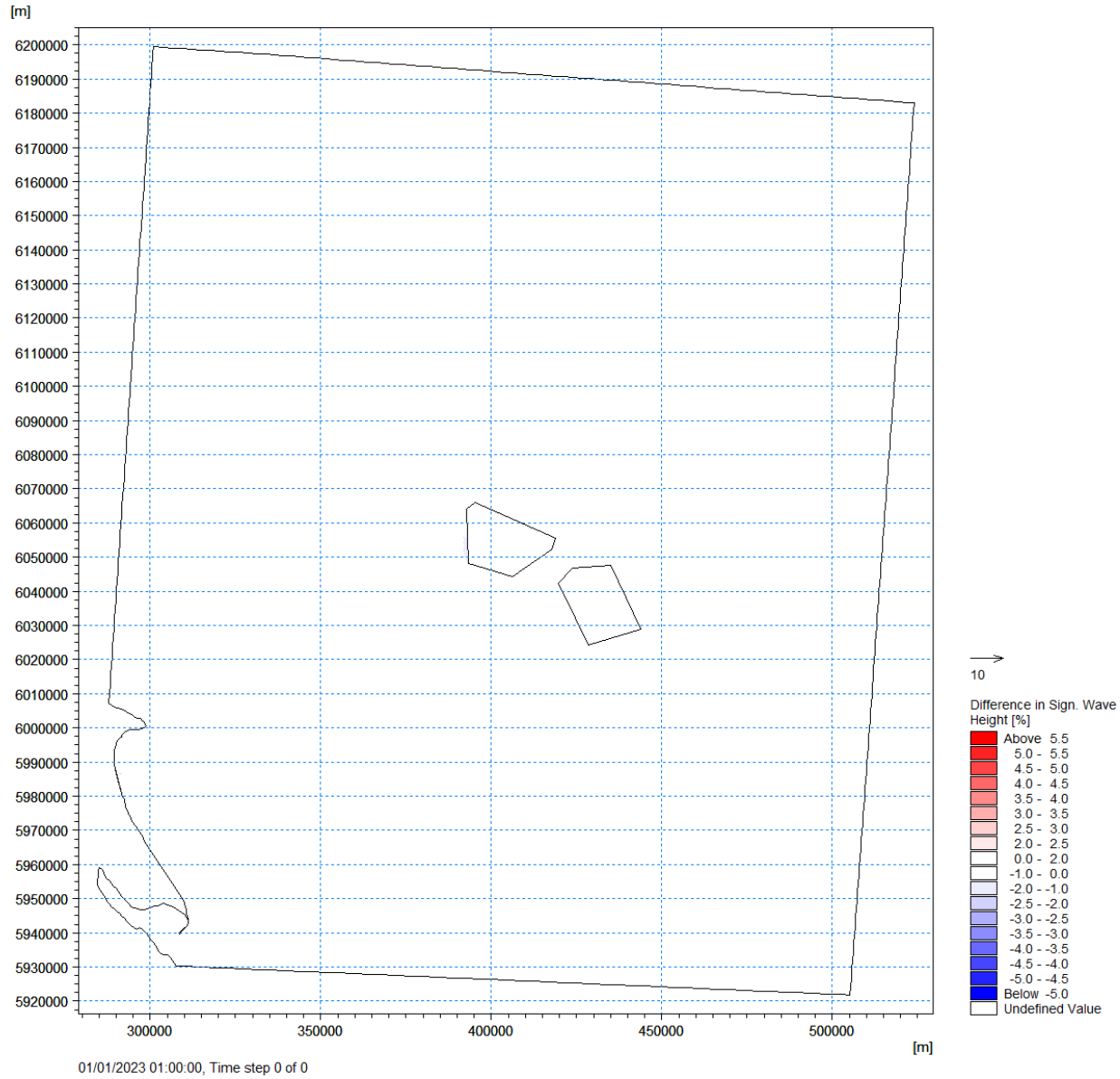

Figure B-24: Difference in Significant Wave Height in Percentage Between Baseline and Windfarm Option 1 for 1 in 100 Year Waves Coming From East

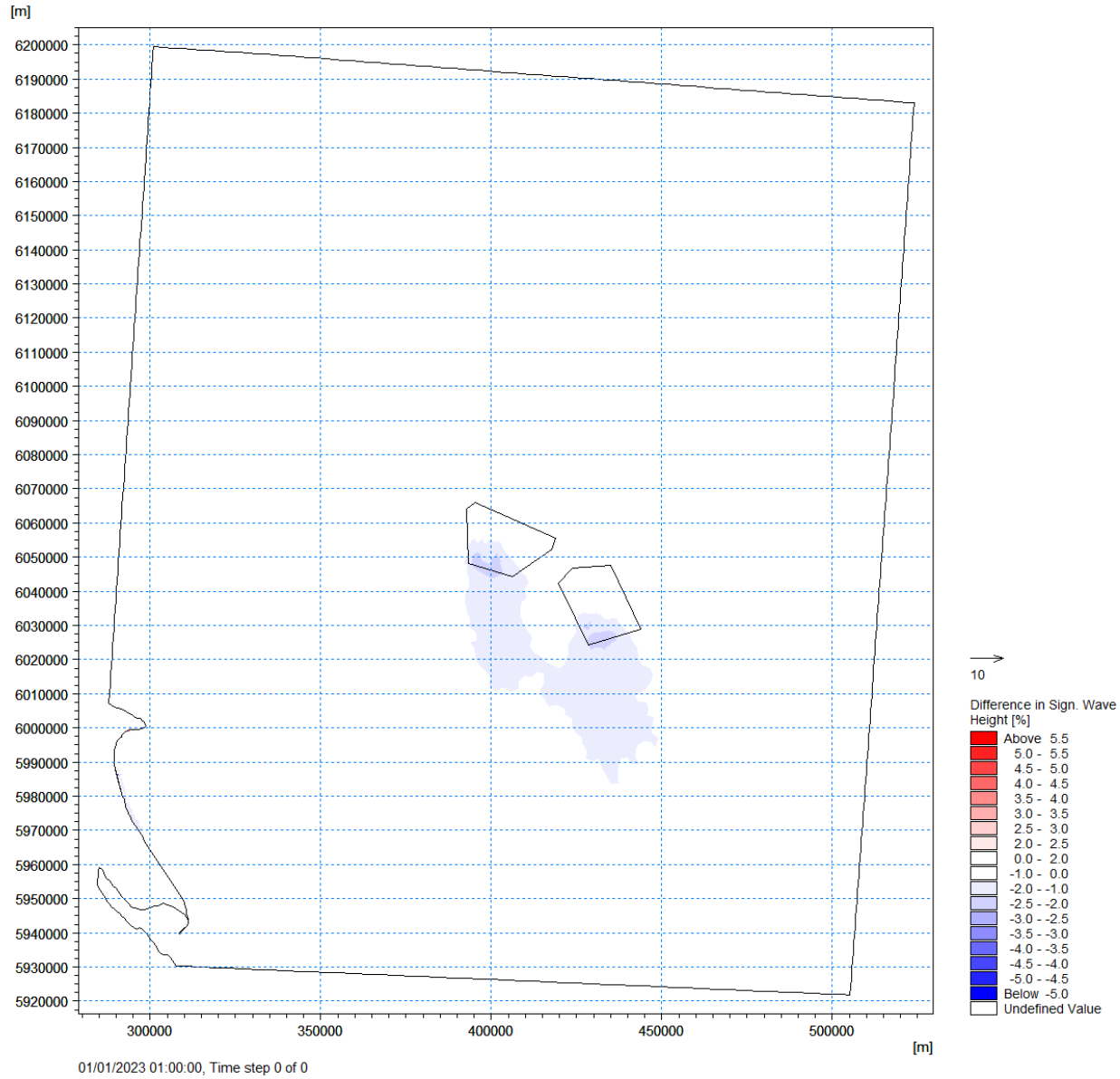

Figure B-25: Difference in Significant Wave Height in Percentage Between Baseline and Windfarm Option 2 for 50 Percentile Waves Coming From North

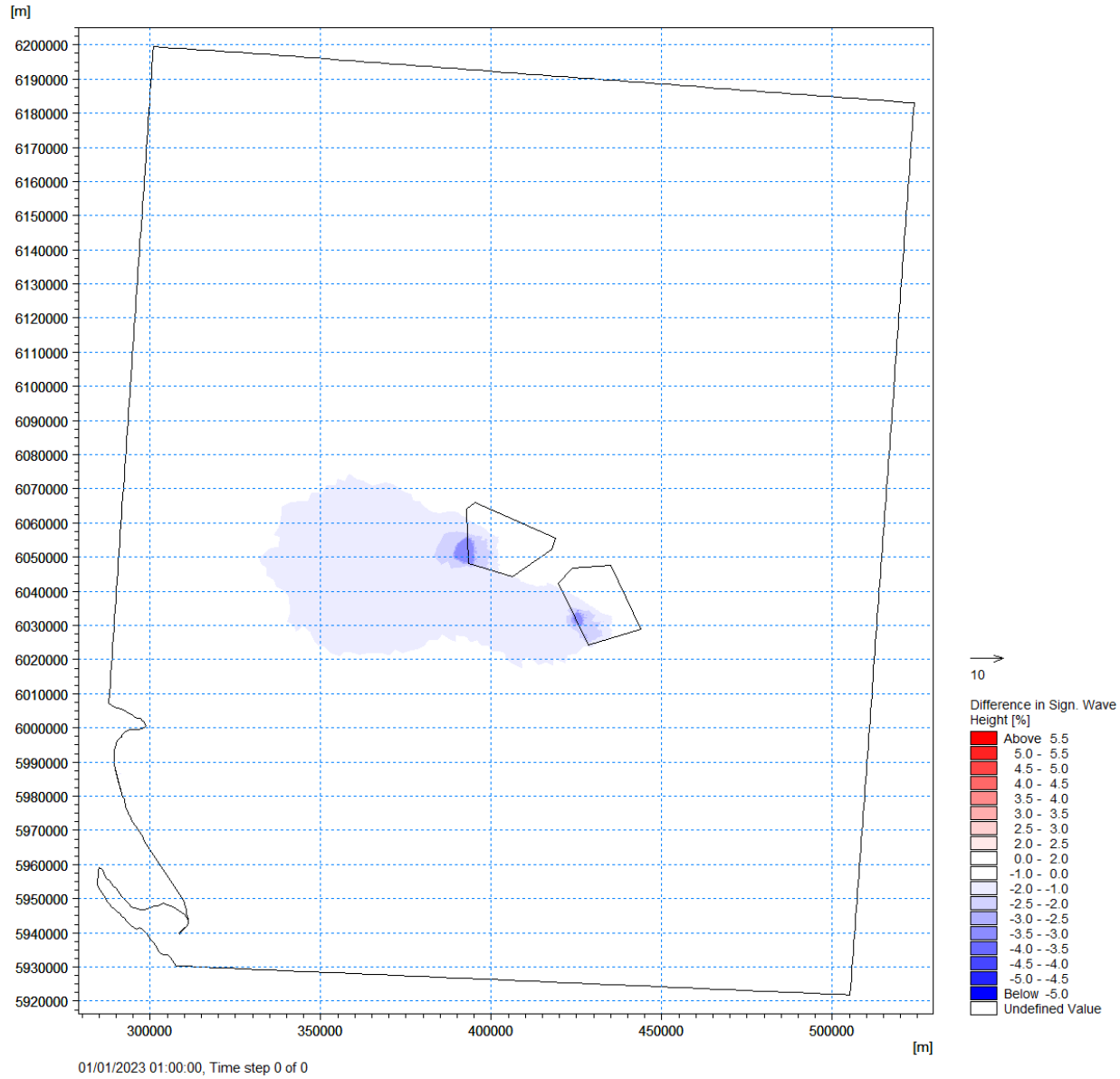

Figure B-26: Difference in Significant Wave Height in Percentage Between Baseline and Windfarm Option 2 for 50 percentile Waves Coming From East

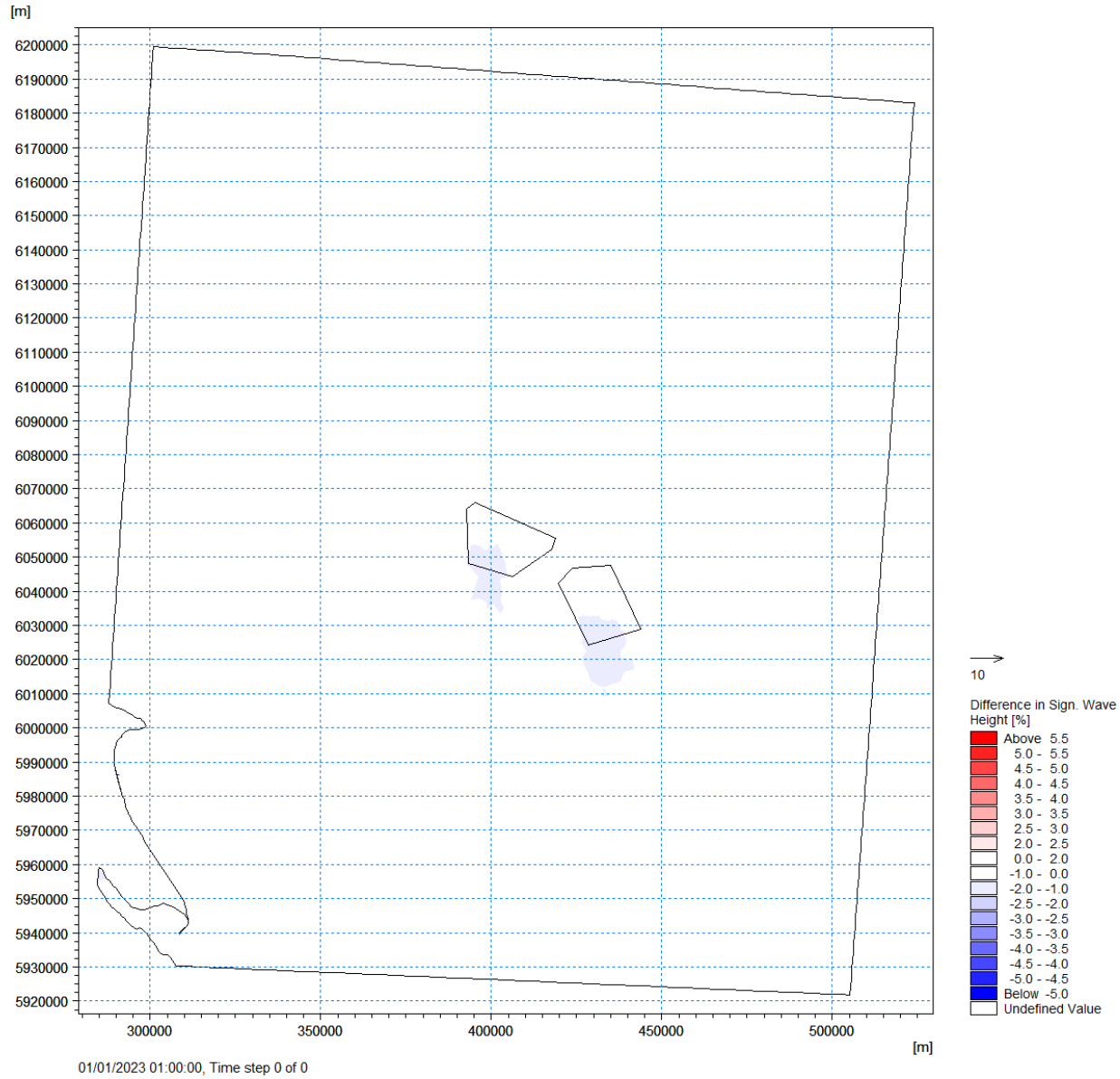

Figure B-27: Difference in Significant Wave Height in Percentage Between Baseline and Windfarm Option 2 for 1 in 1 Year Waves Coming From North

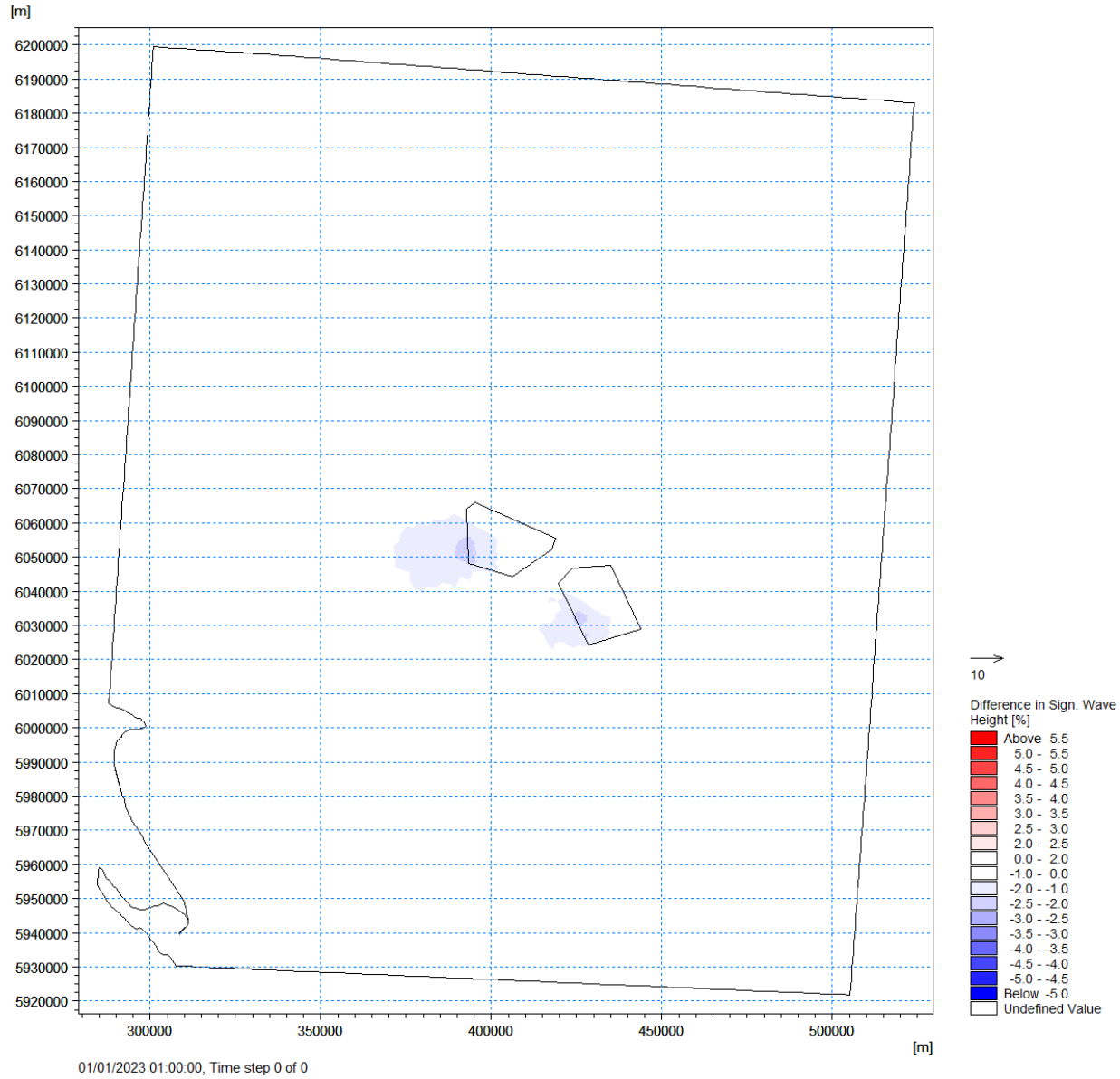

Figure B-28: Difference in Significant Wave Height in Percentage Between Baseline and Windfarm Option 2 for 1 in 1 Year Waves Coming From East

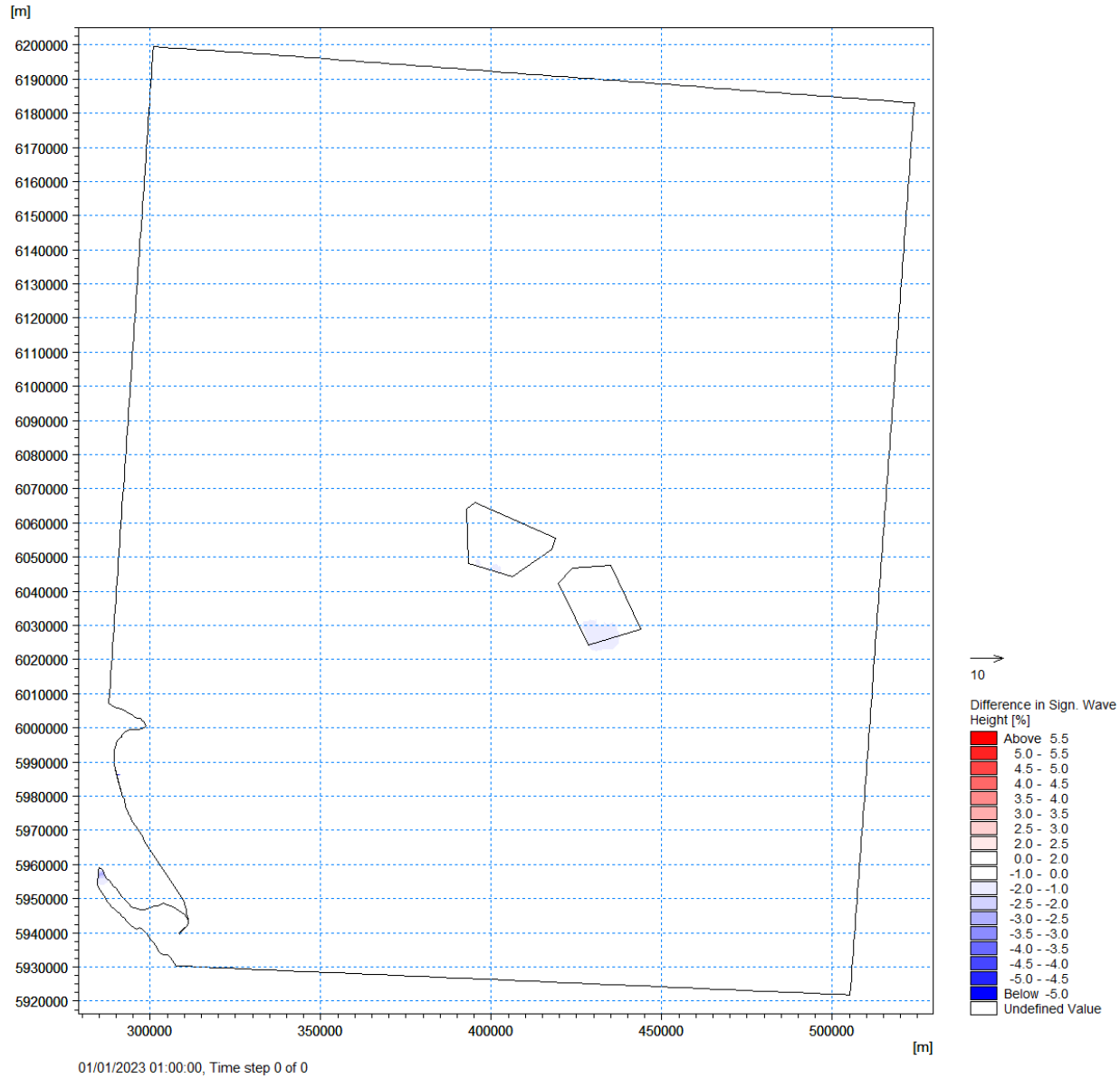

Figure B-29: Difference in Significant Wave Height in Percentage Between Baseline and Windfarm Option 2 for 1 in 100 Year Waves Coming From North

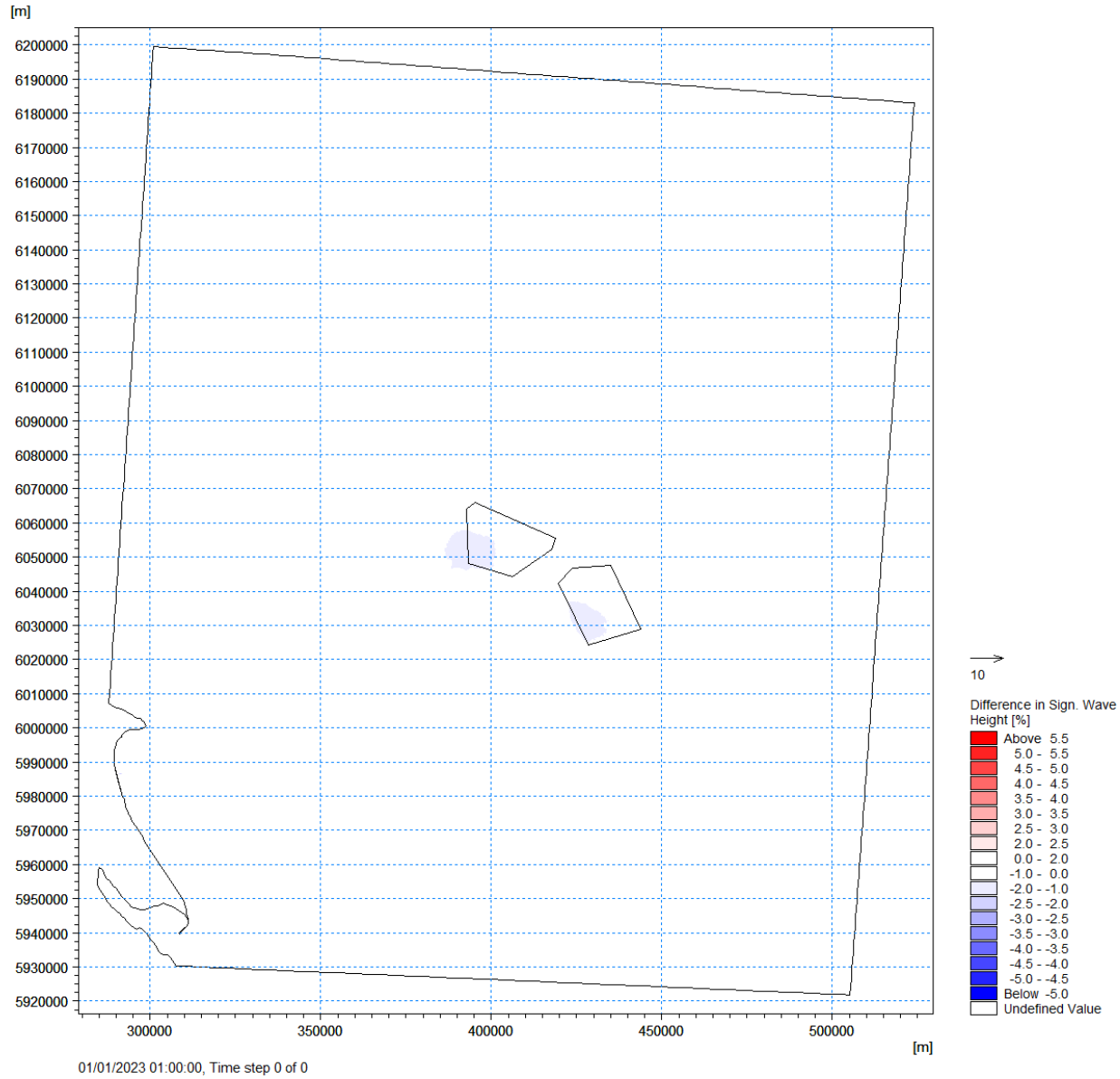

Figure B-30: Difference in Significant Wave Height in Percentage Between Baseline and Windfarm Option 2 for 1 in 100 Year Waves Coming From East

Annex C – Results of Hydrodynamic Model Assessment Runs

This section presents the model results from 30-day simulation of astronomical tides for Baseline, Option 1 and Option 2. The tidal level variation in the simulation period at the location of DBS East wave buoy (location is illustrated in Figure 8-3-3) is shown in Figure C-1.

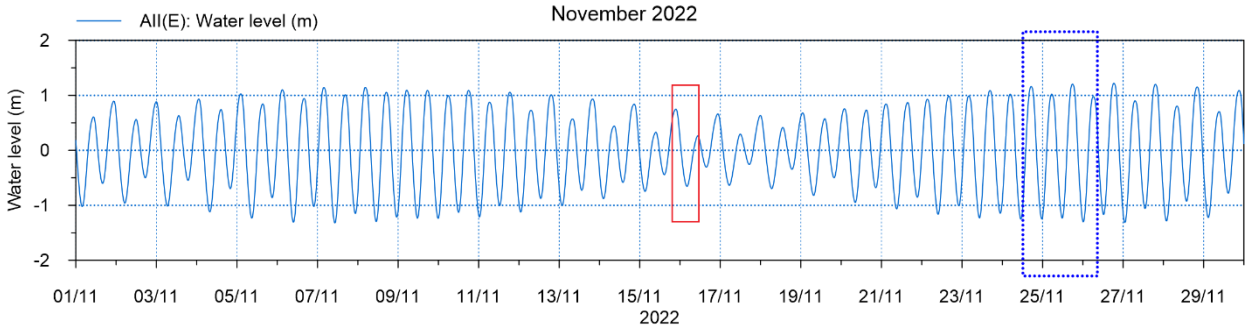

Figure C-1: Water Level Variation During 30-day Simulation Period at DBS East Wave Buoy (blue frame indicates spring tides and red frame indicates neap tide)

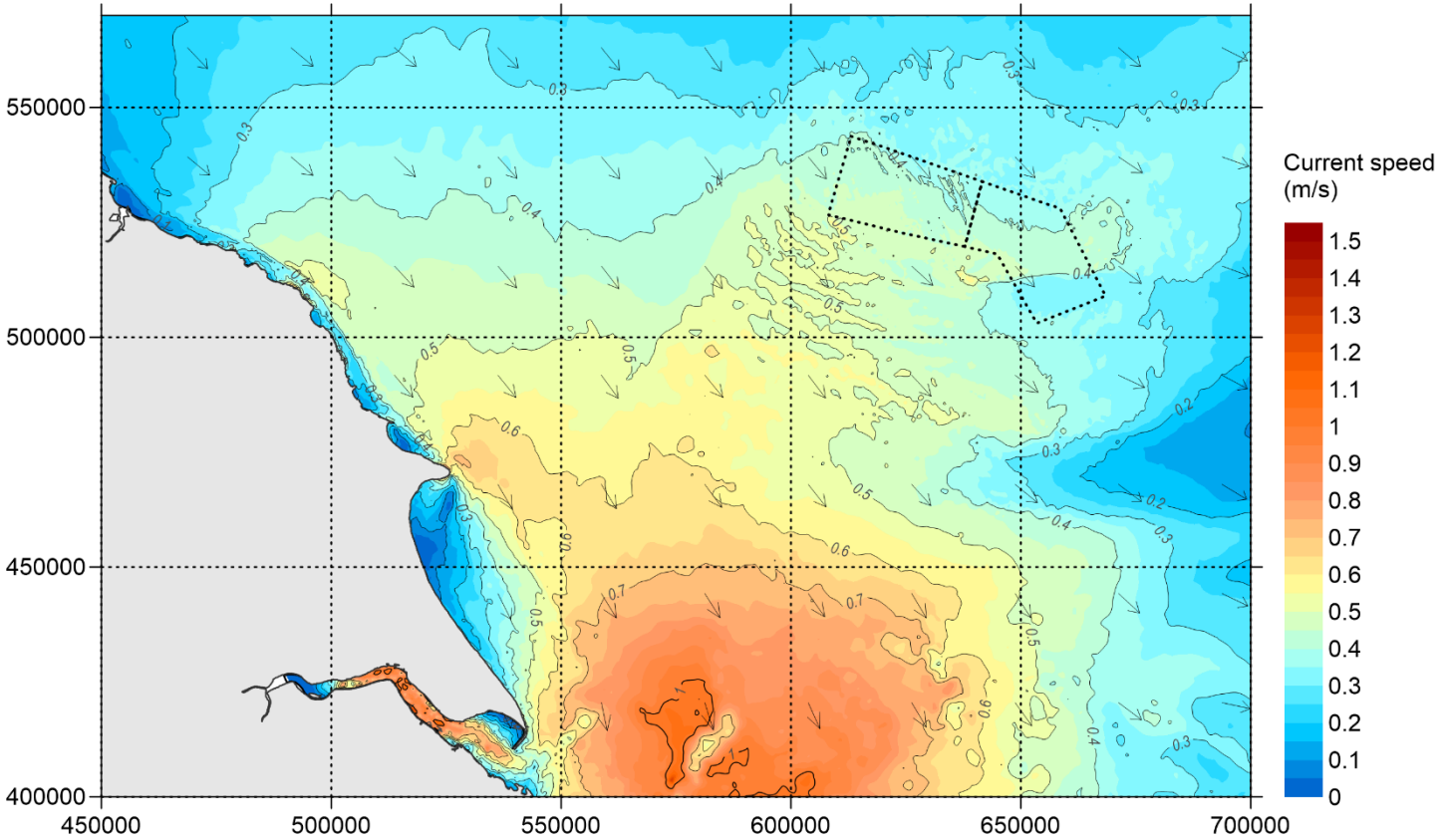

Figure C-2: Overview of Spatial Variation of Peak Southeast-Going Currents in a Spring Tide - Baseline

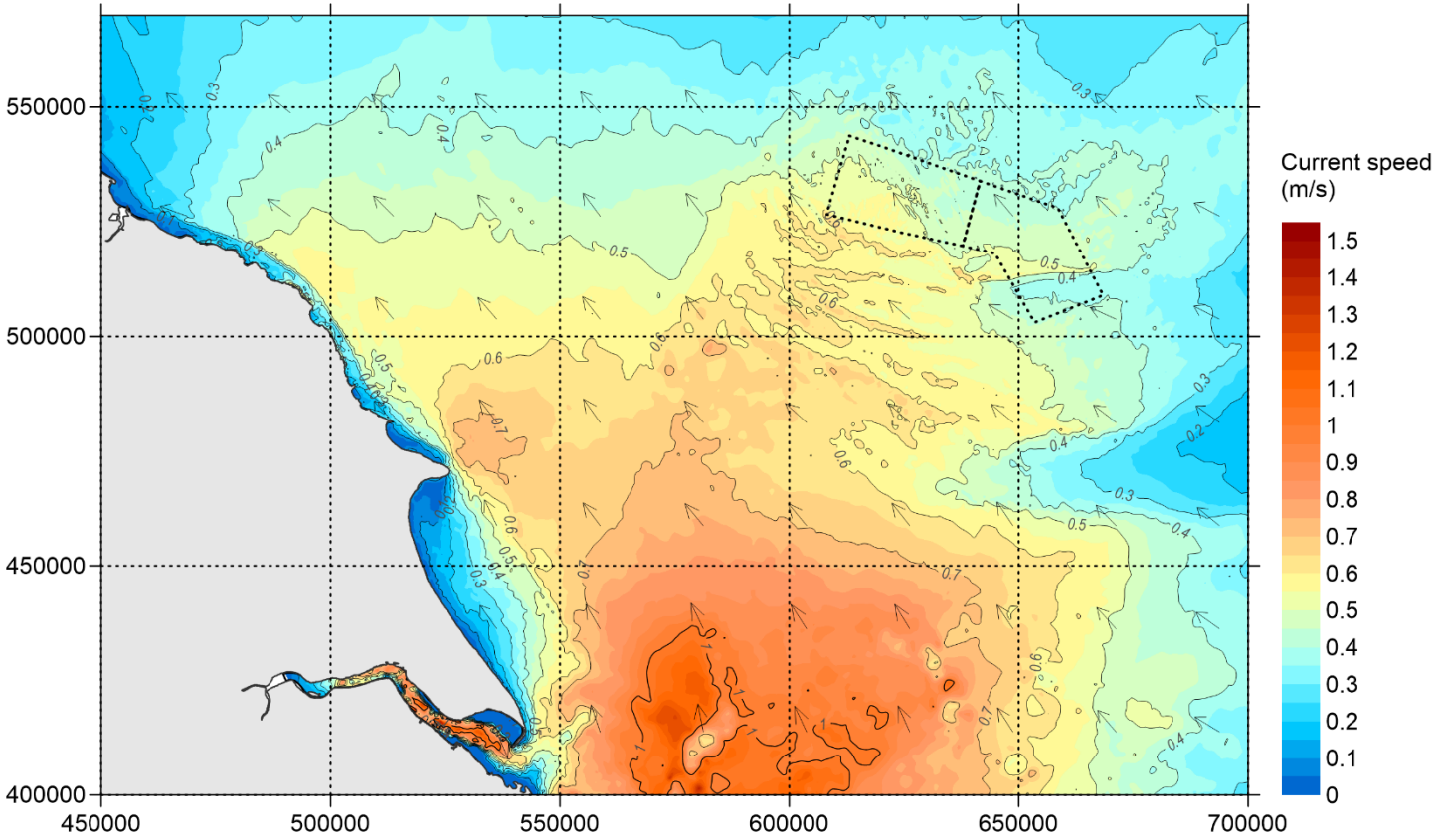

Figure C-3: Overview of Spatial Variation of Peak Northwest-Going Currents in a Spring Tide – Baseline

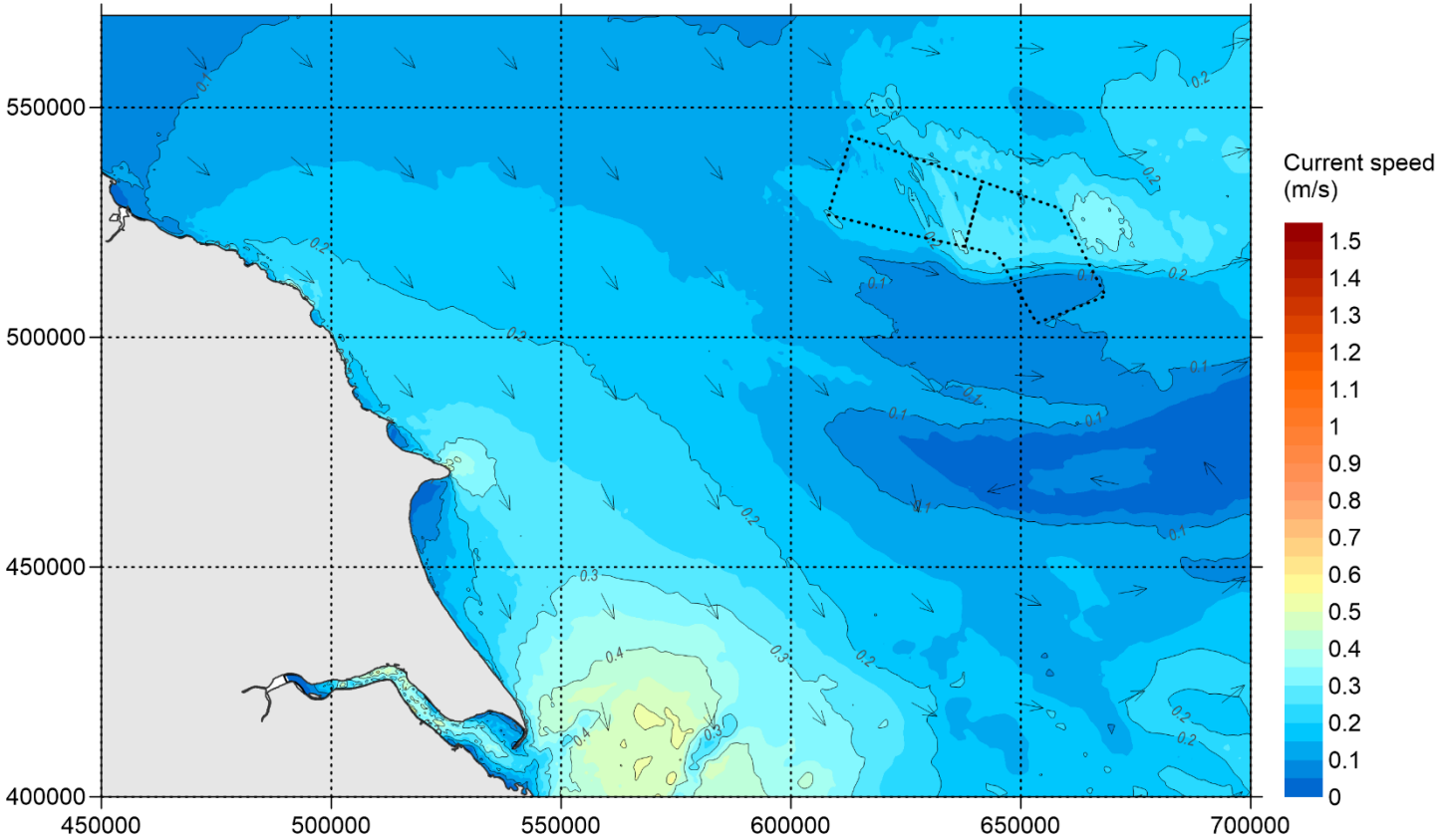

Figure C-4: Overview of Spatial Variation of Peak Southeast-Going Currents in a Neap Tide – Baseline

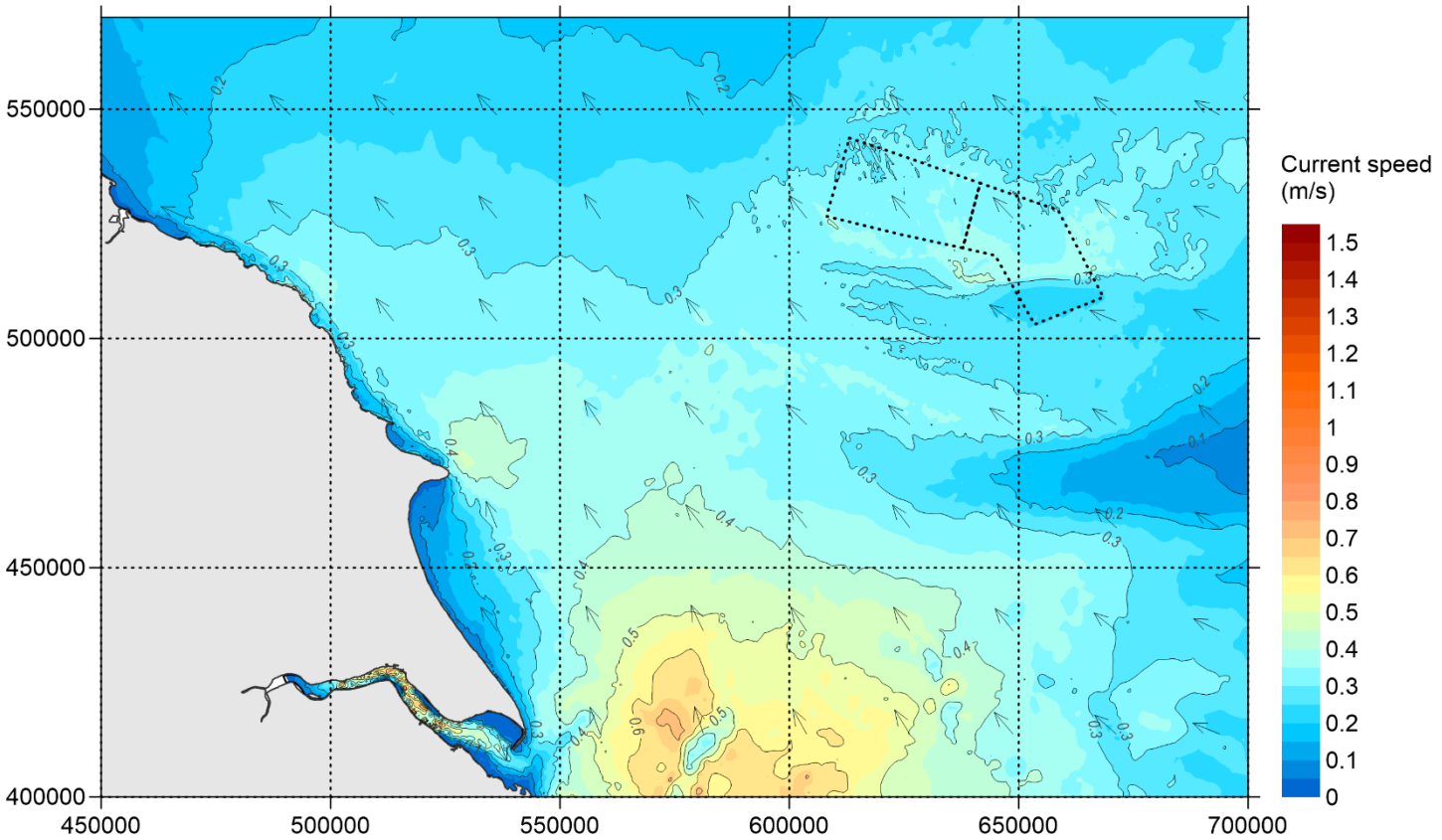

Figure C-5: Overview of Spatial Variation of Peak Northwest-Going Currents in a Neap Tide – Baseline

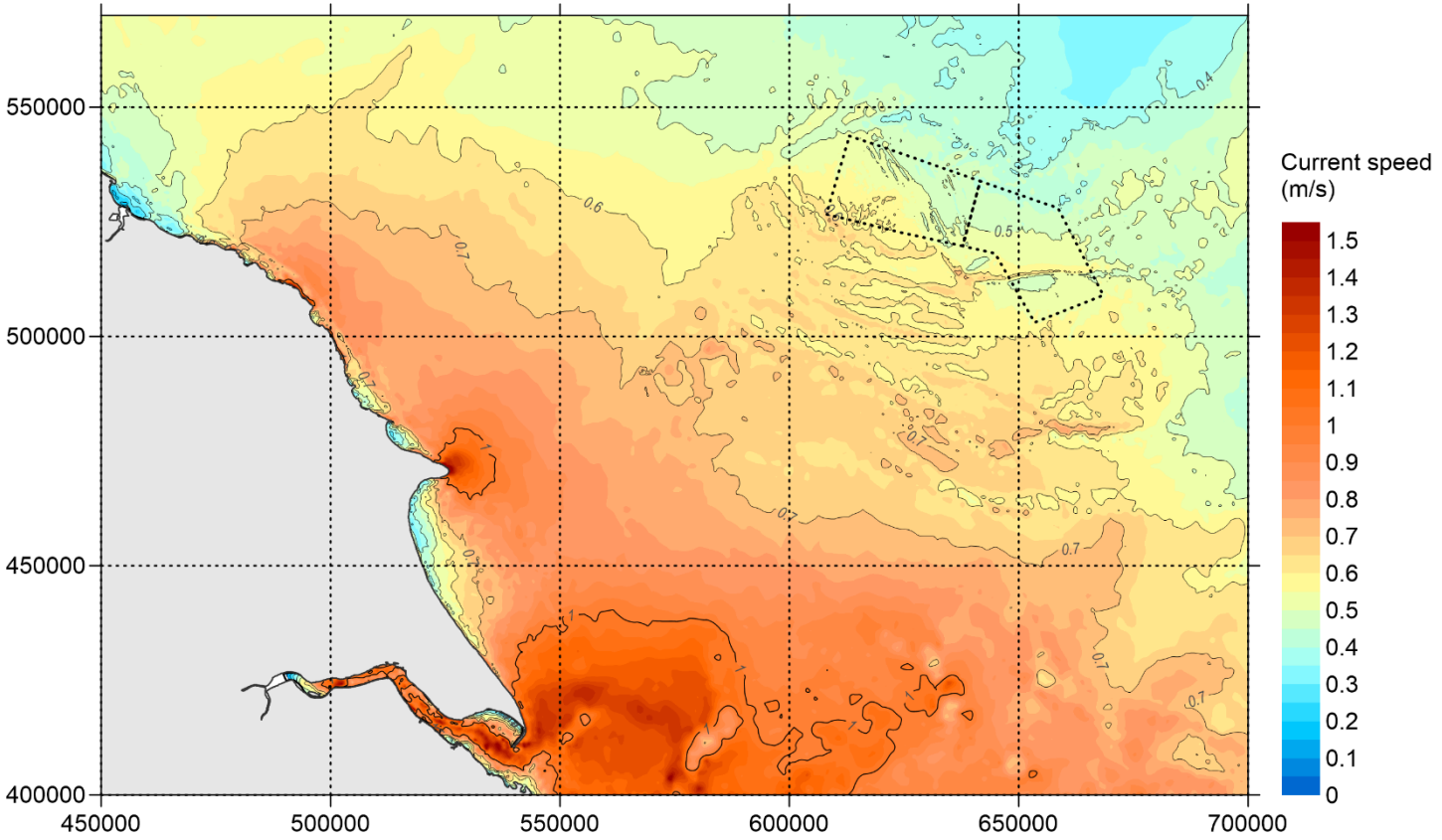

Figure C-6: Overview of Spatial Variation of Maximum Current Speed over 30 days- Baseline

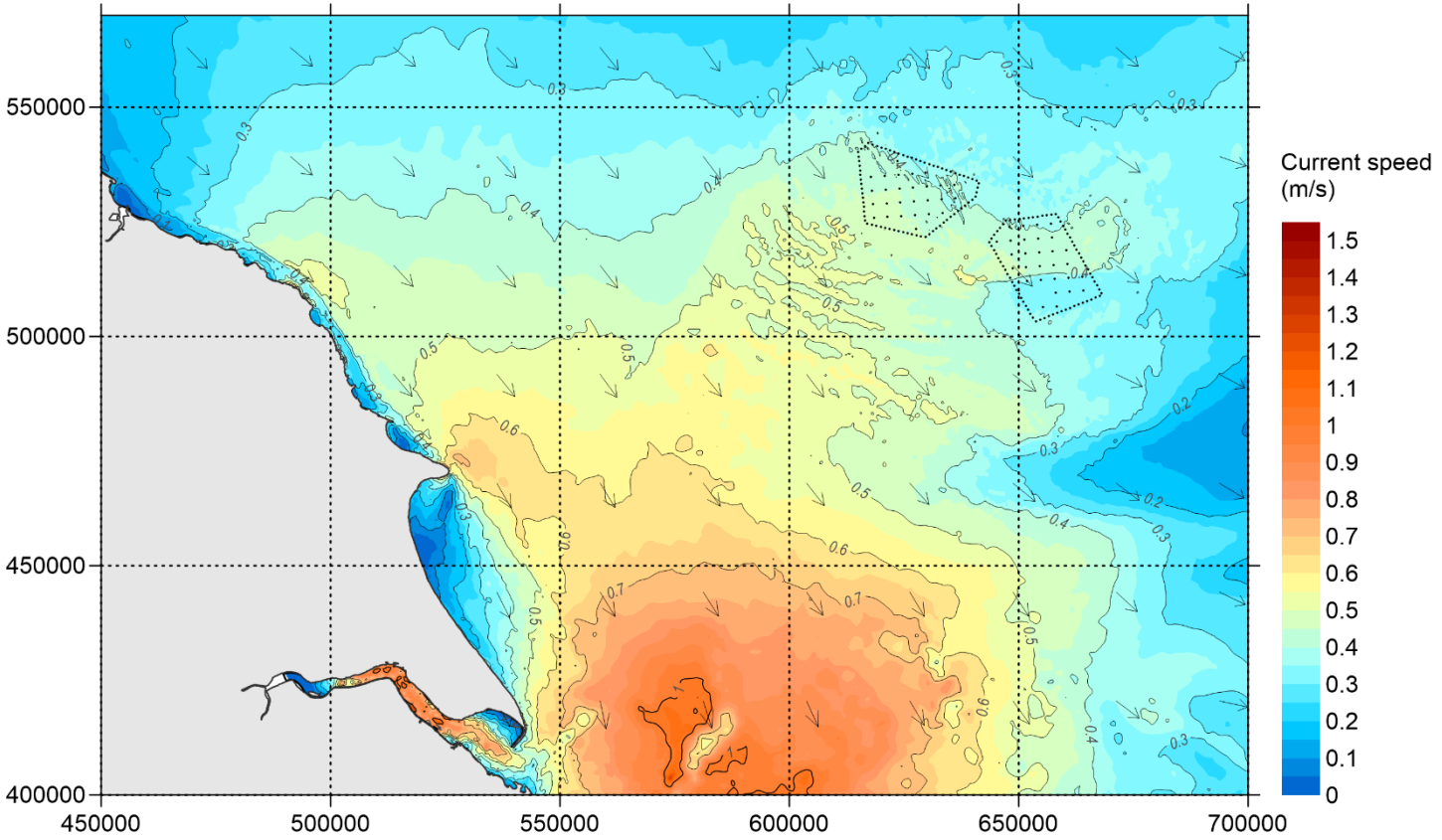

Figure C-7: Overview of Spatial Variation of Peak Southeast-Going Currents in a Spring Tide - Option 1

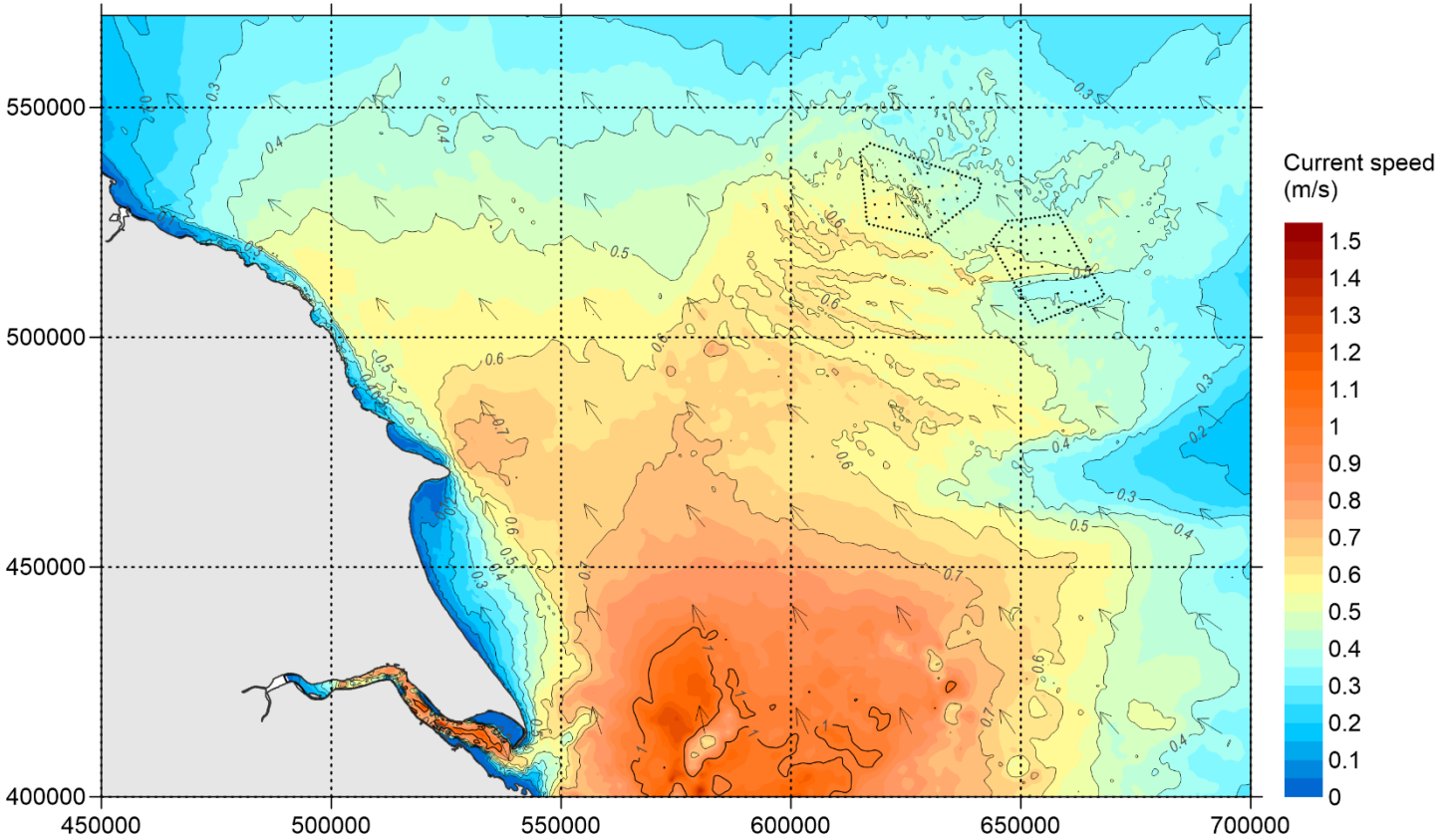

Figure C-8: Overview of Spatial Variation of ~~Northeast~~Northwest-Going Currents in a Spring Tide – Option 1

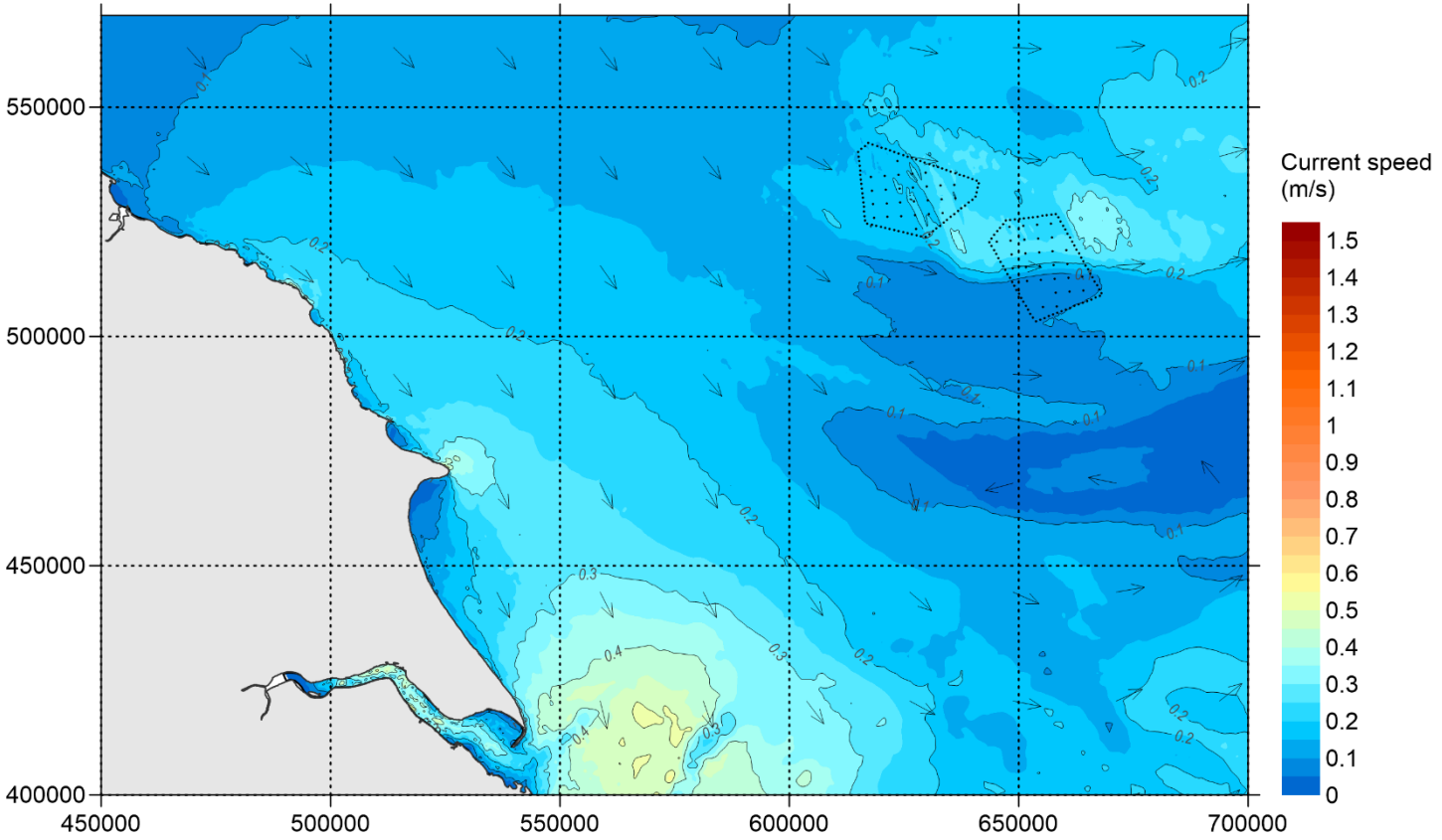

Figure C-9: Overview of Spatial Variation of Peak Southeast-Going Currents in a Neap Tide – Option 1

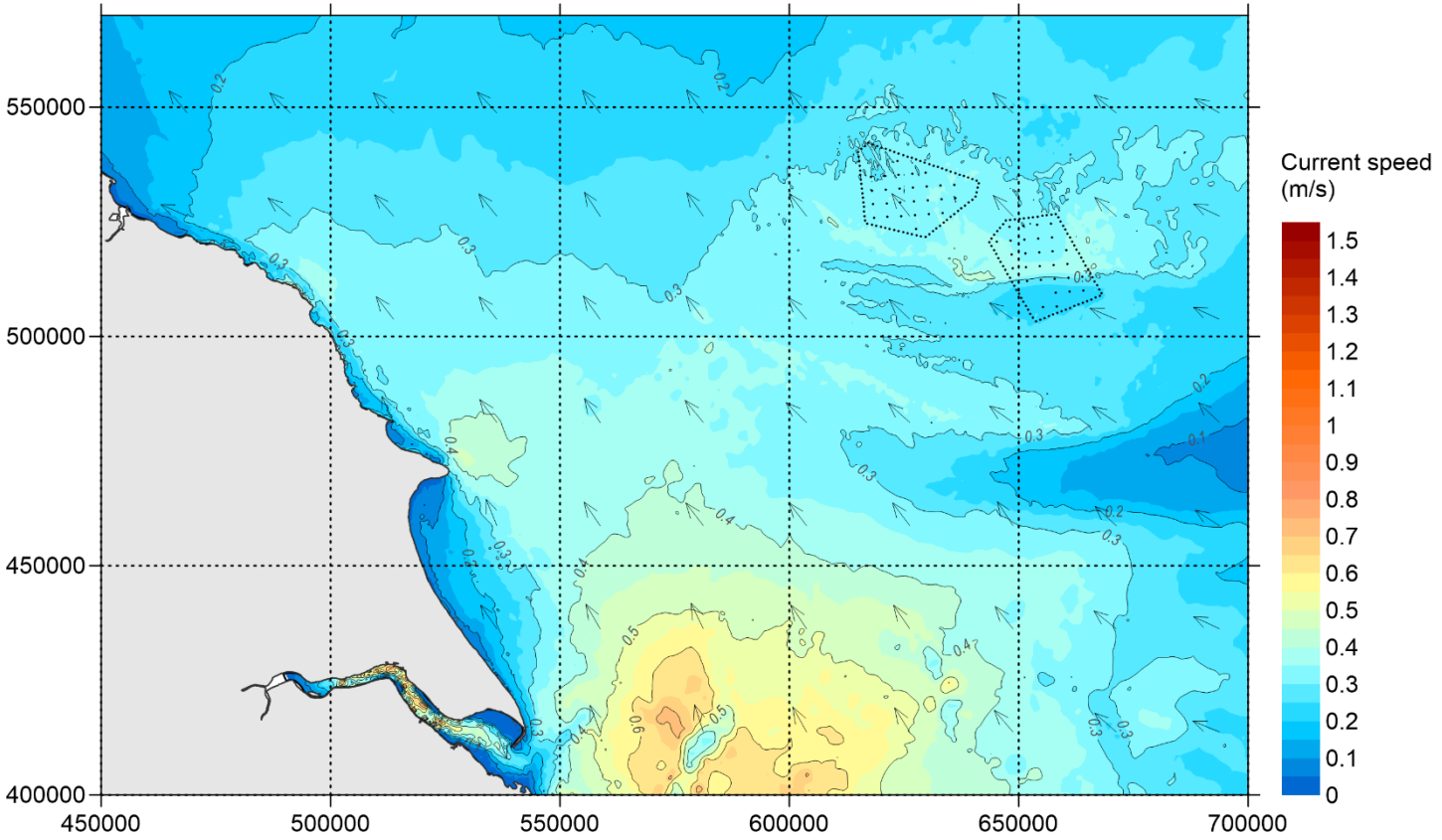

Figure C-10: Overview of Spatial Variation of Peak Northwest-Going Currents in a Neap Tide – Option 1

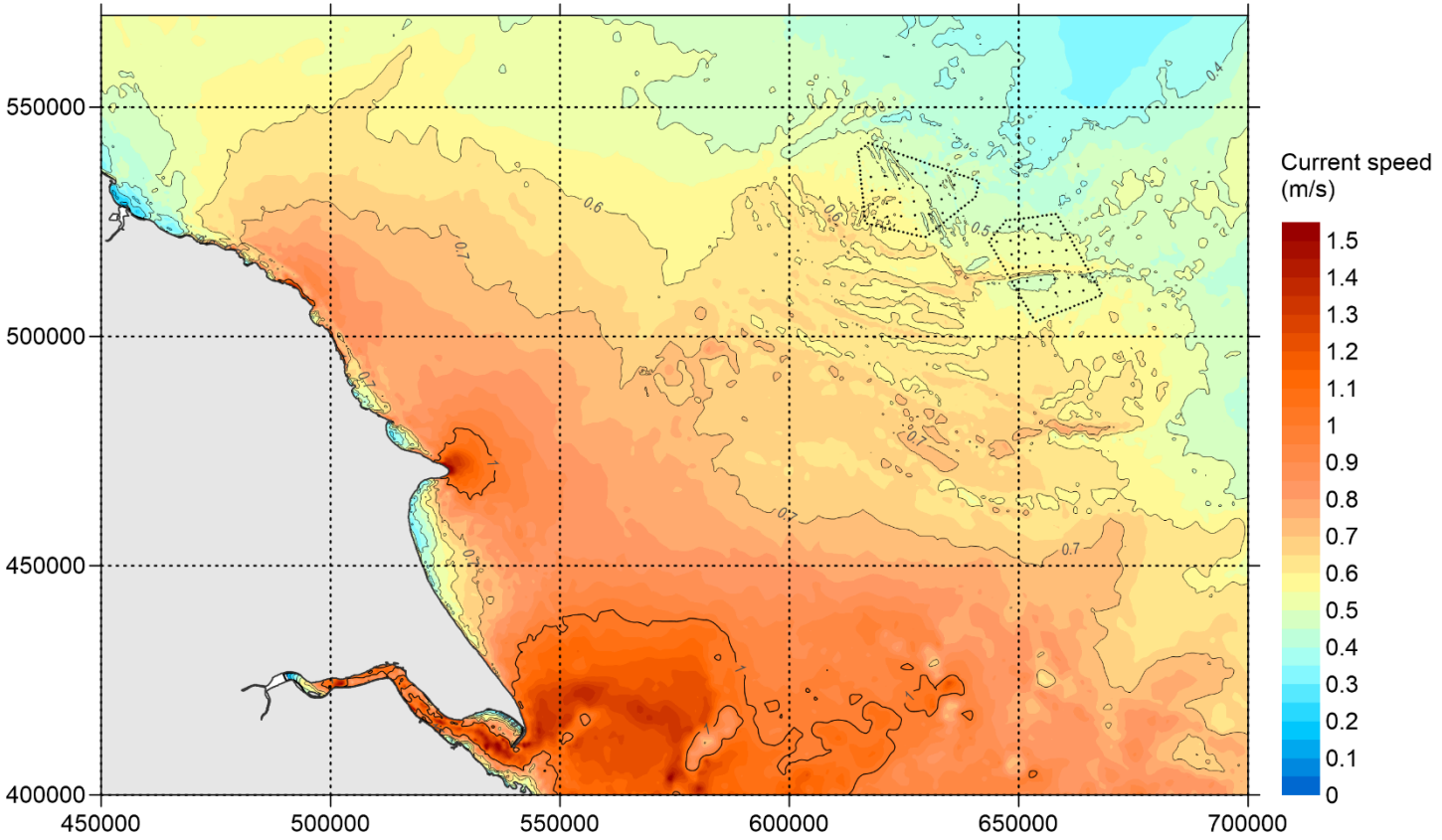

Figure C-11: Overview of Spatial Variation of Maximum Current Speed Over 30 days- Option 1

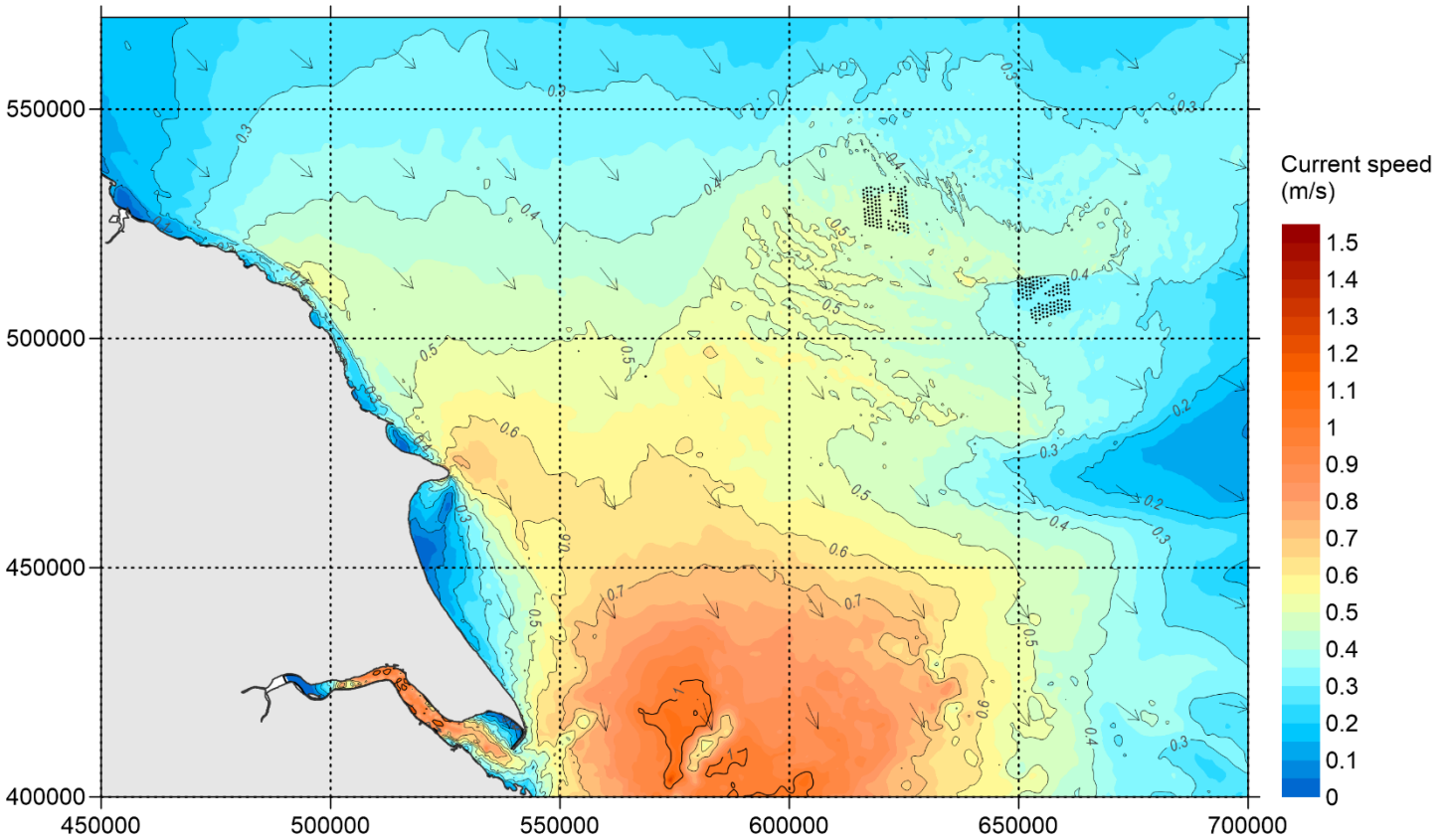

Figure C-12: Overview of Spatial Variation Of Peak Southeast-Going Currents in a Spring Tide - Option 2

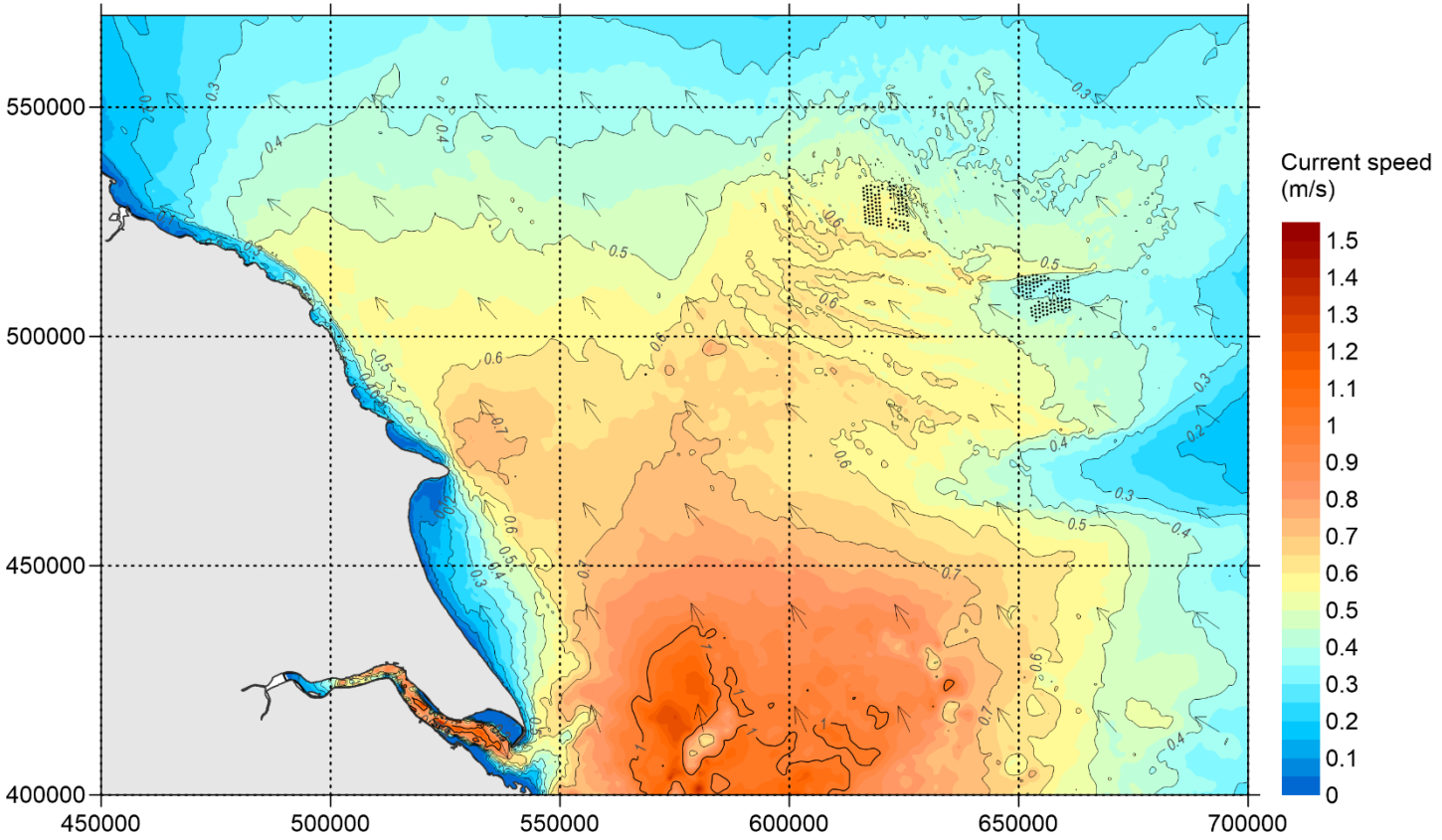

Figure C-13: Overview of Spatial Variation of Northwest-Going Currents in a Spring Tide - Option 2

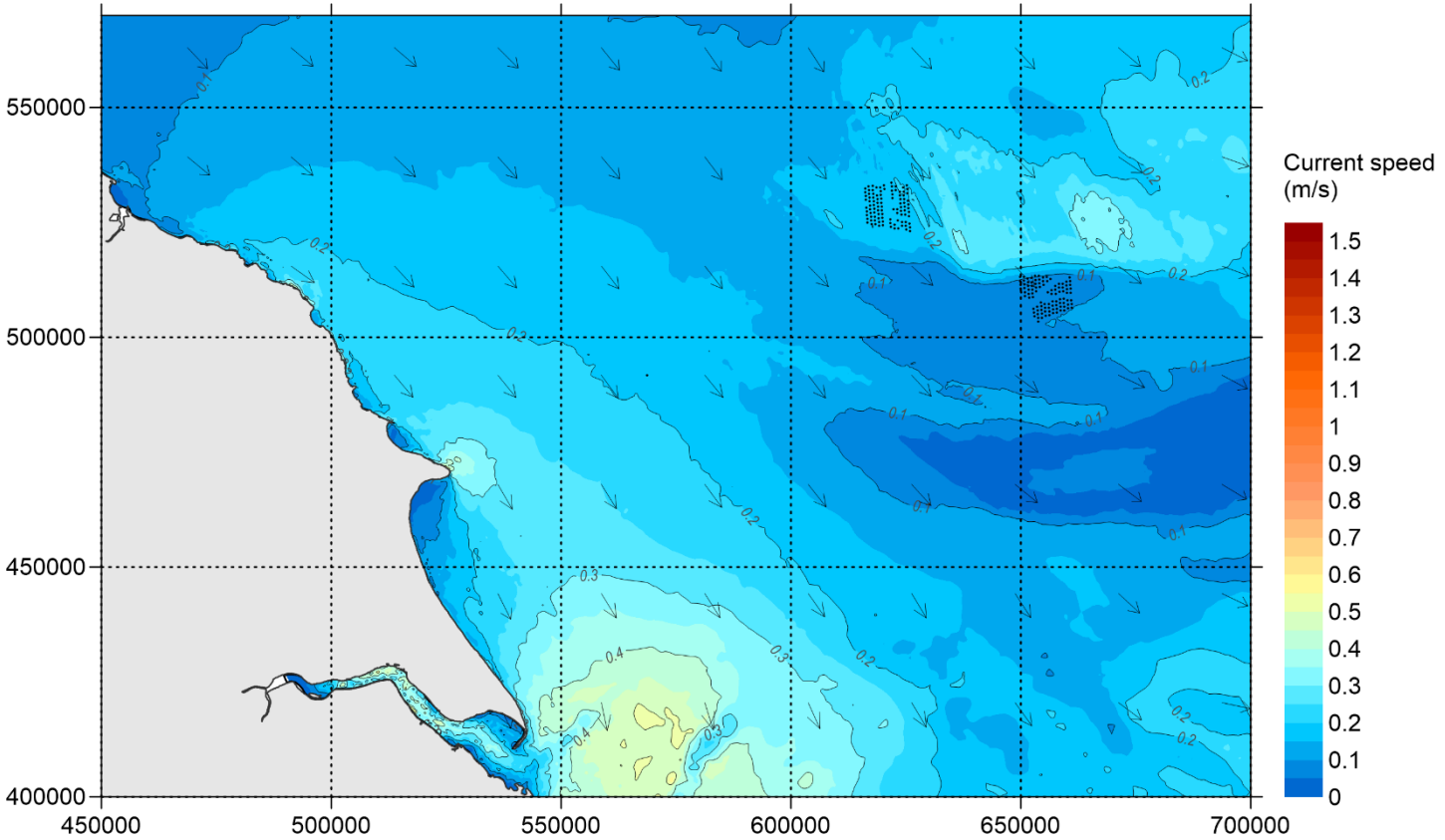

Figure C-14 Overview of Spatial Variation of Peak Southeast-Going Currents in a Neap Tide – Option 2

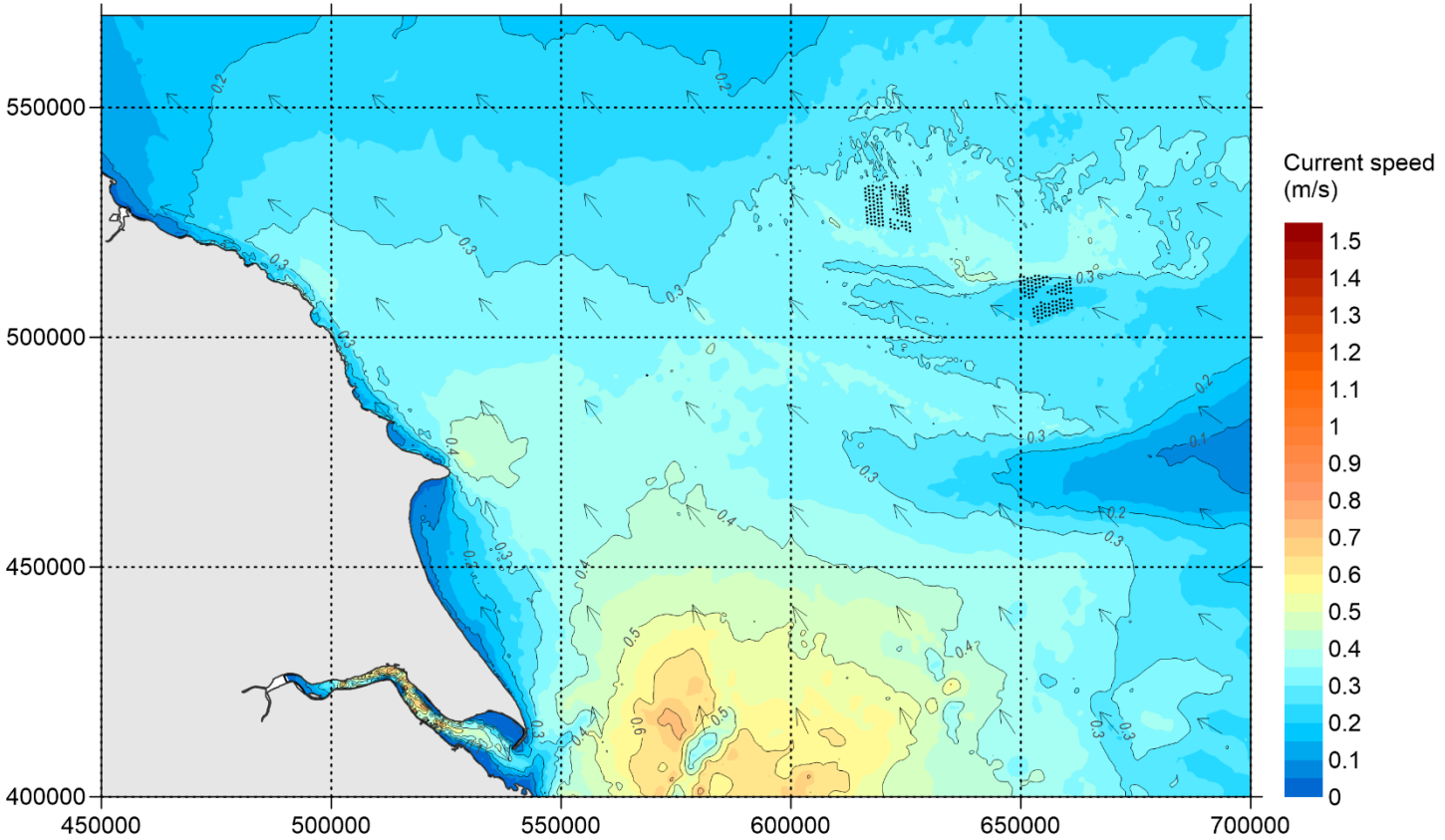

Figure C-15 Overview of Spatial Variation of Peak Northwest-Going Currents in a Neap Tide – Option 2

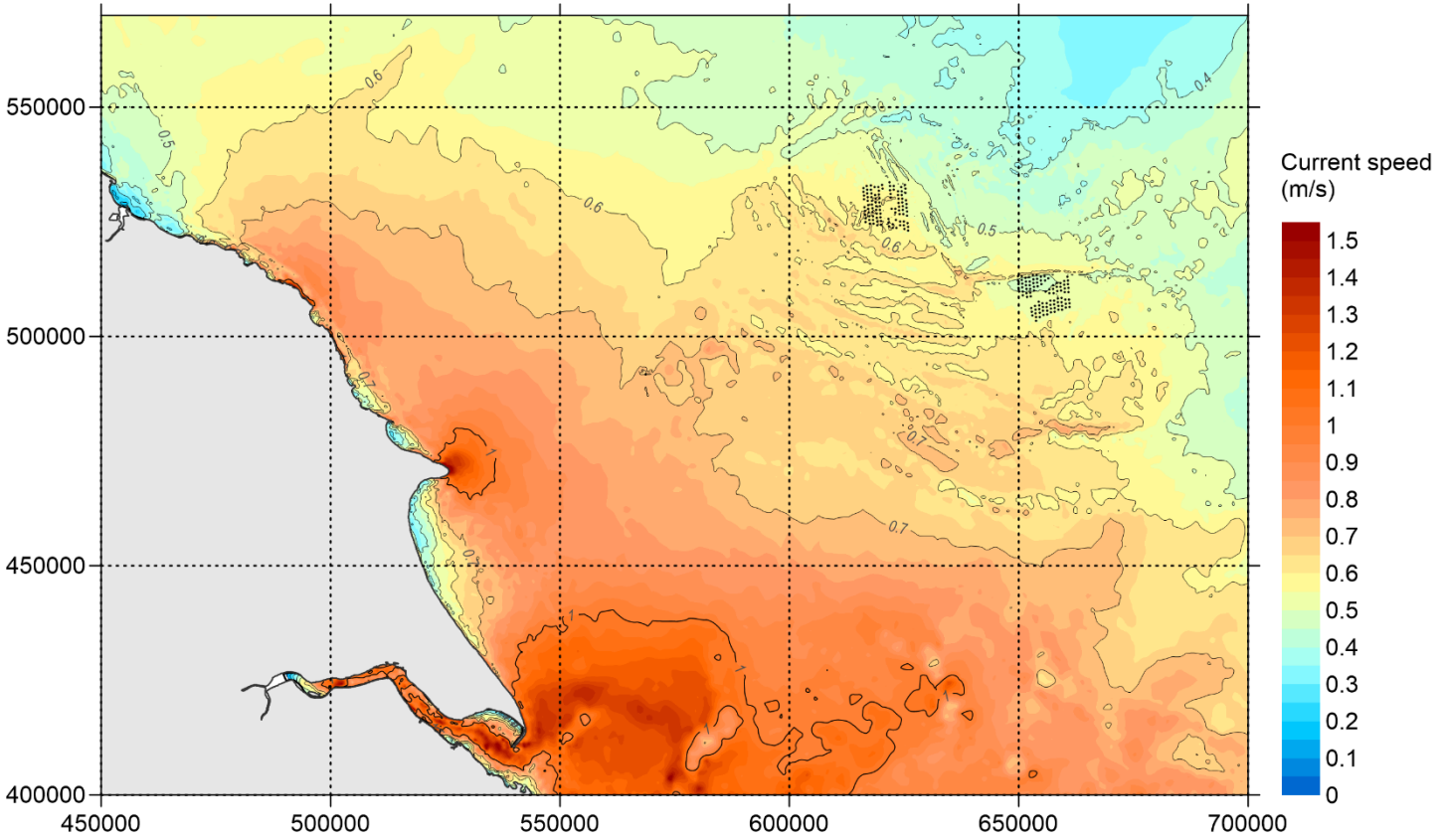

Figure C-16: Overview of Spatial Variation of Maximum Current Speed Over 30 Days- Option 2

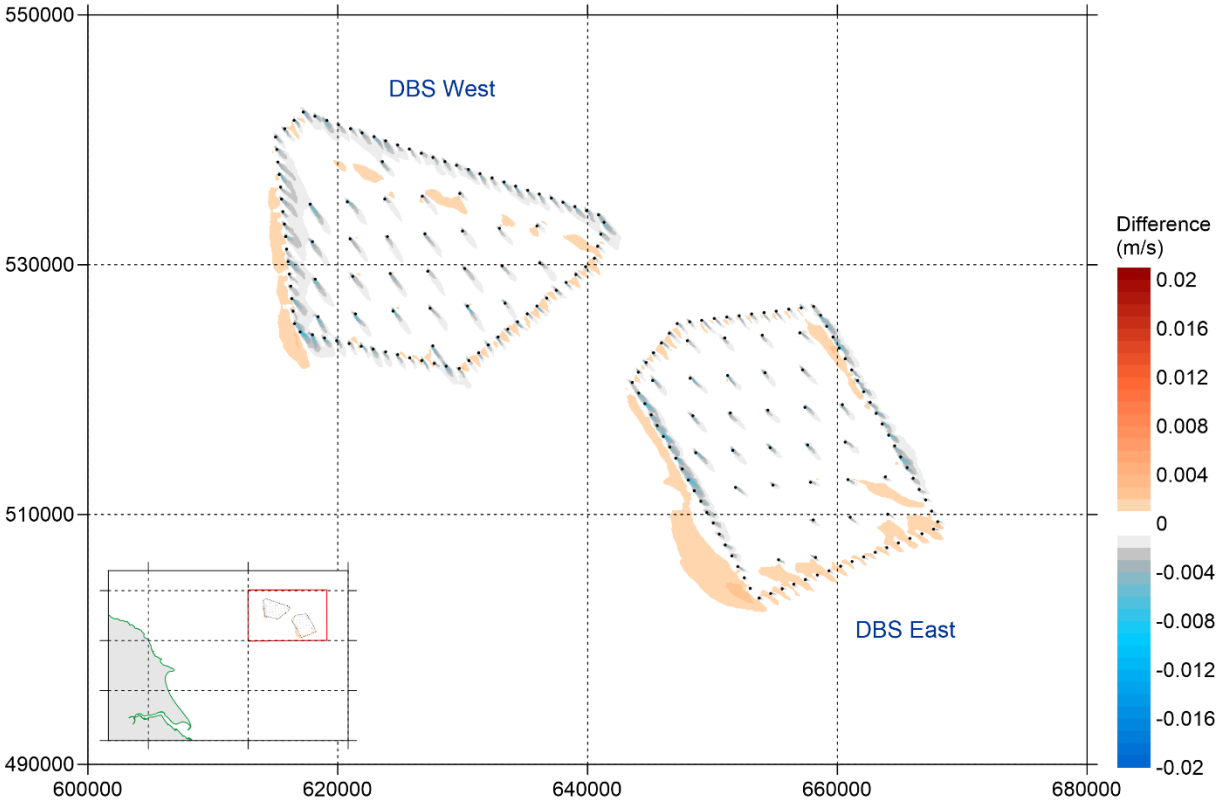

Figure C-17: Change of Speed of Peak Southeast-Going Currents in a Spring Tide – (Option 1 – Baseline)

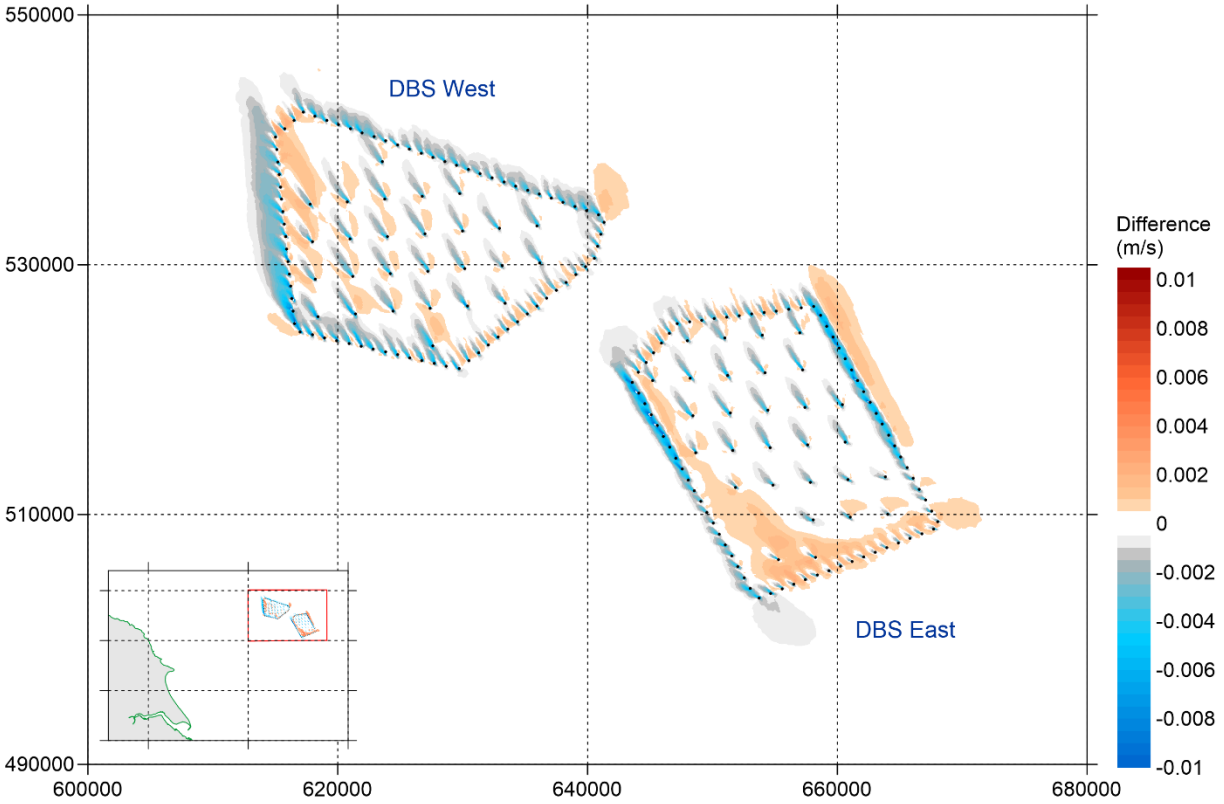

Figure C-18: Change of Speed of Peak Northwest-Going Currents in a Spring Tide – (Option 1 – Baseline)

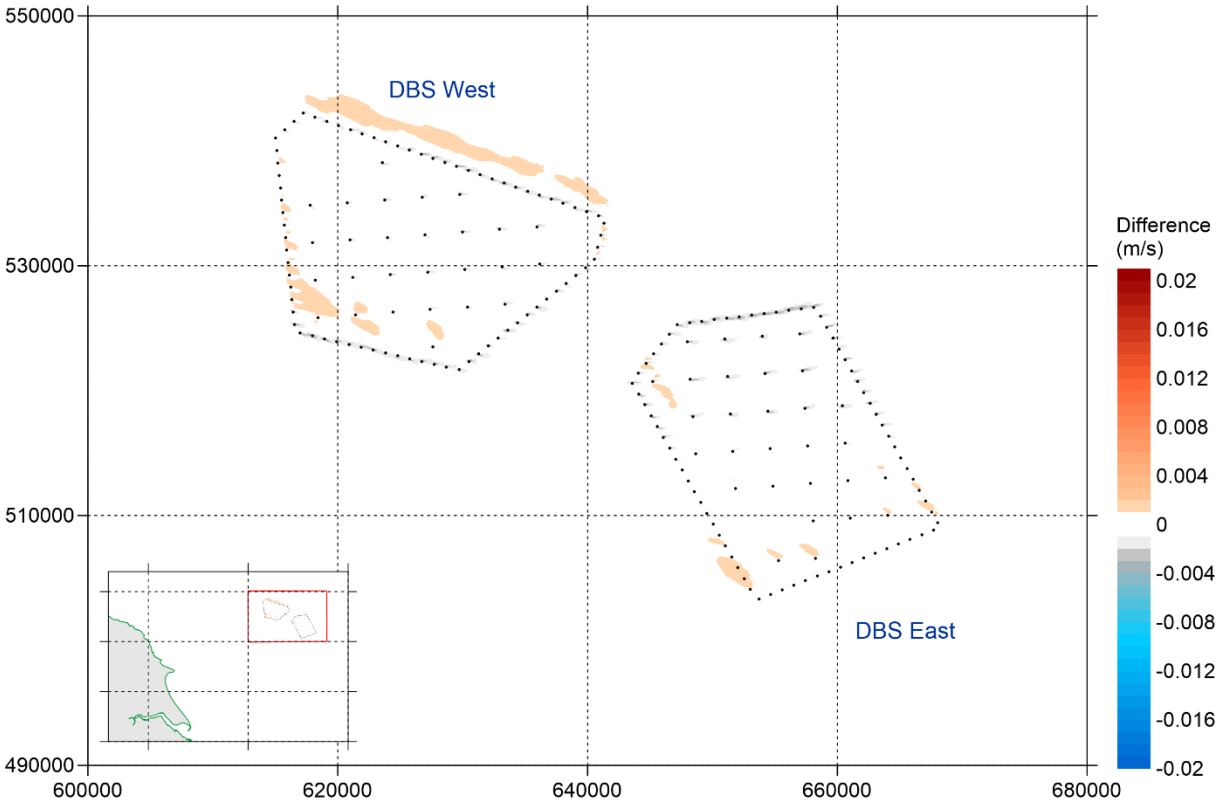

Figure C-19: Change of Speed of Peak Southeast-Going Currents in a Neap Tide – (Option 1 – Baseline)

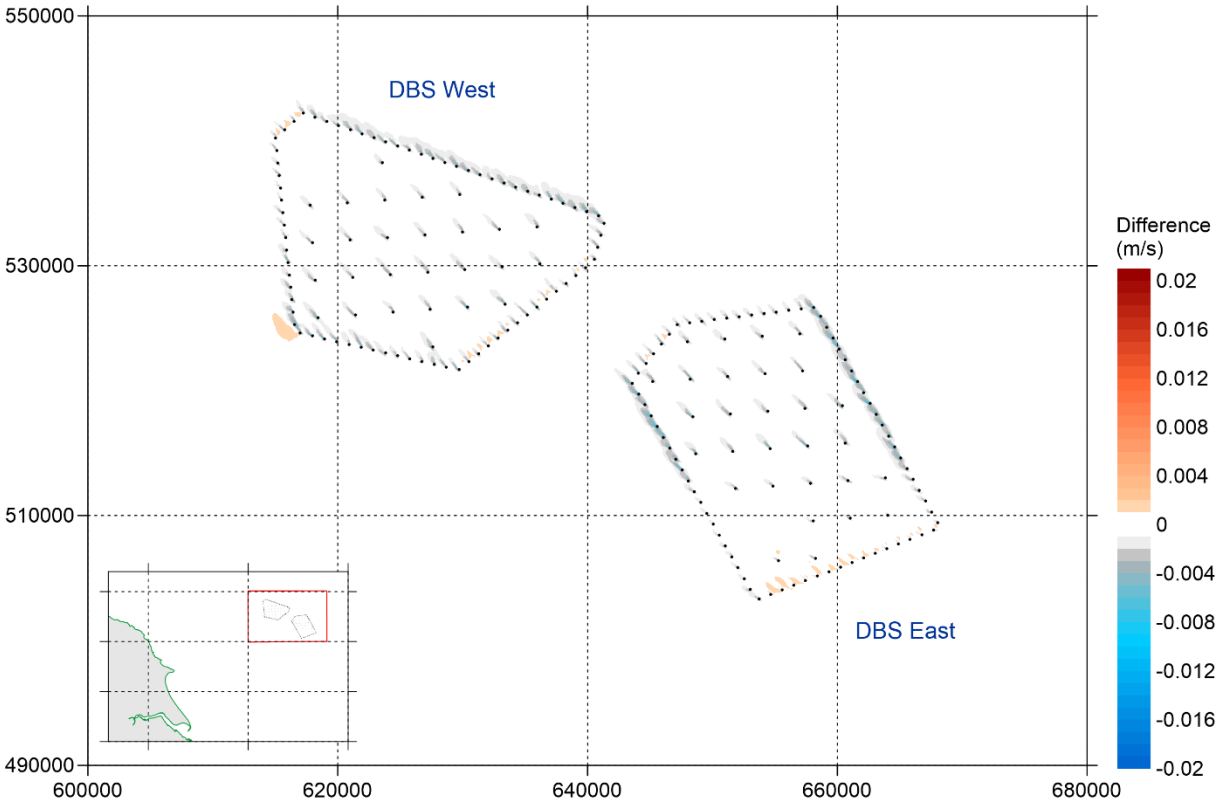

Figure C-20: Change of Speed of Peak Northwest-Going Currents in a Neap Tide – (Option 1 – Baseline)

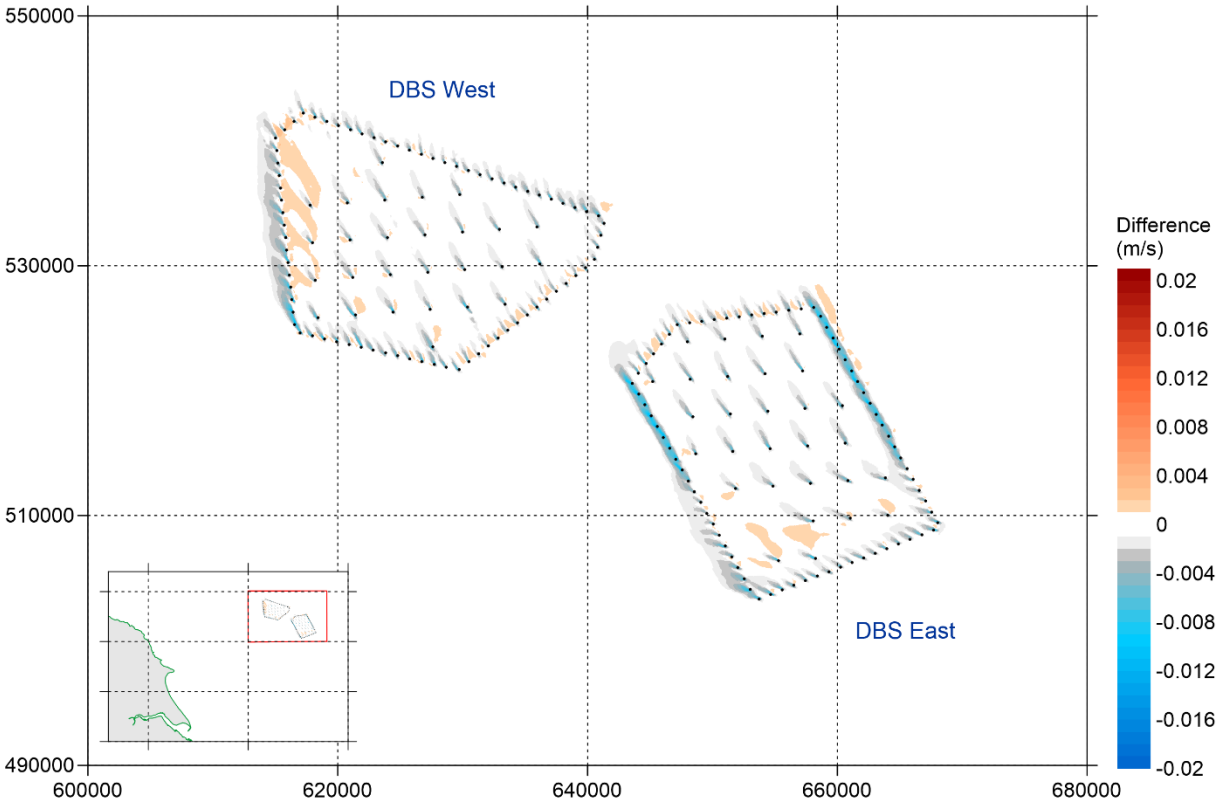

Figure C-21: Change of Maximum Current Speed over 30 Days – (Option 1 – Baseline)

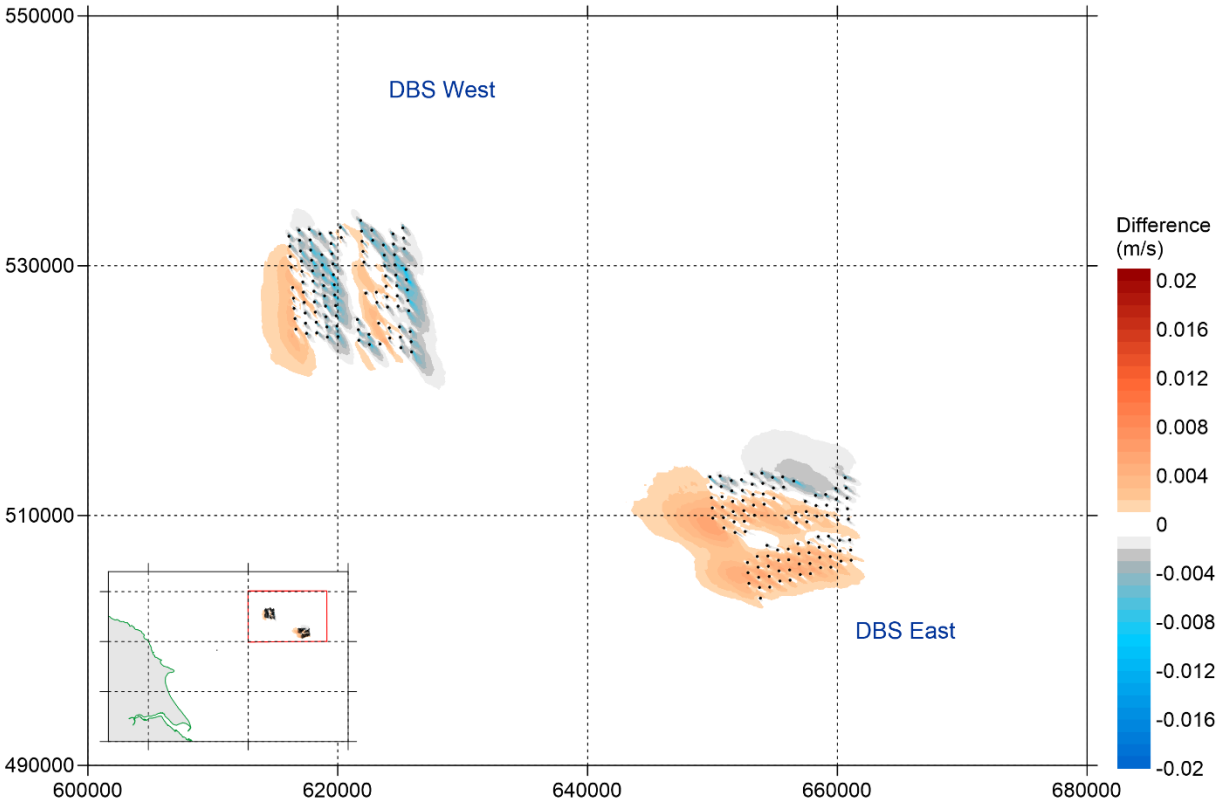

Figure C-22: Change of Speed of Peak Southeast-Going Currents in a Spring Tide – (Option 2 – Baseline)

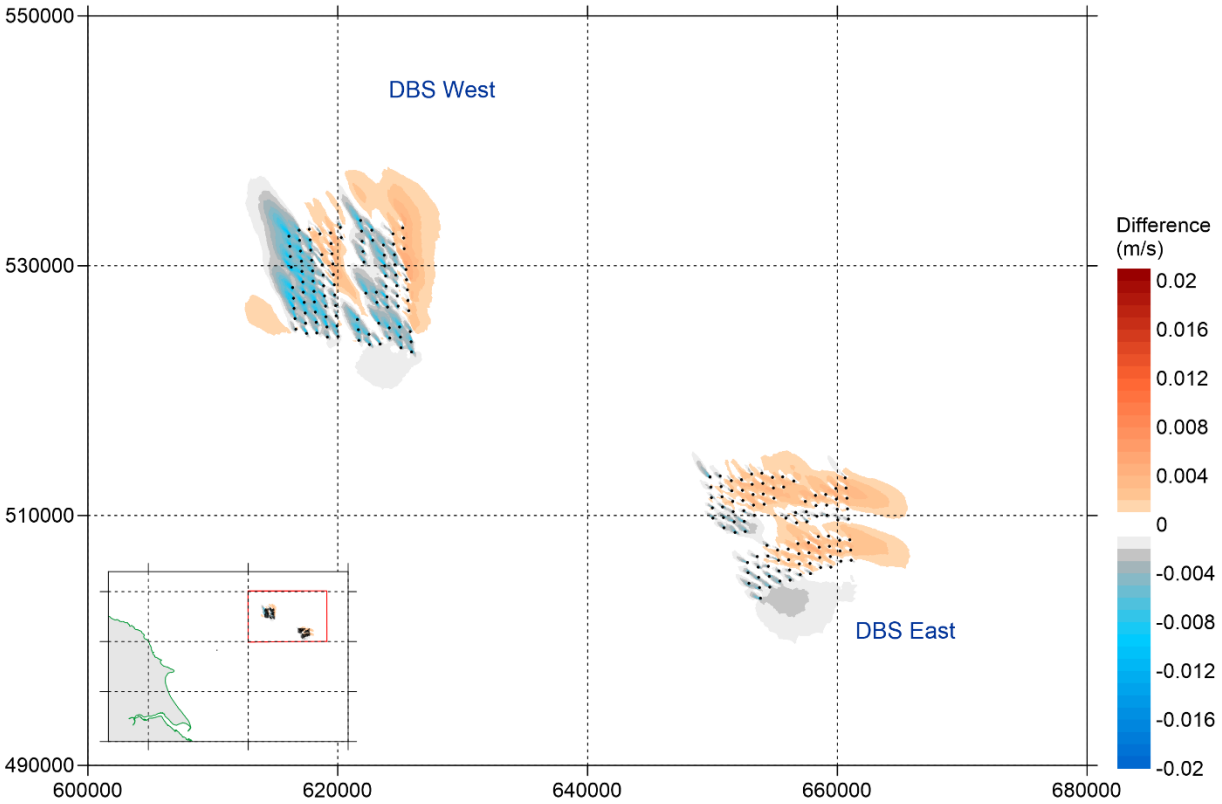

Figure C-23: Change of Speed of Peak Northwest-Going Currents in a Spring Tide – (Option 2 – Baseline)

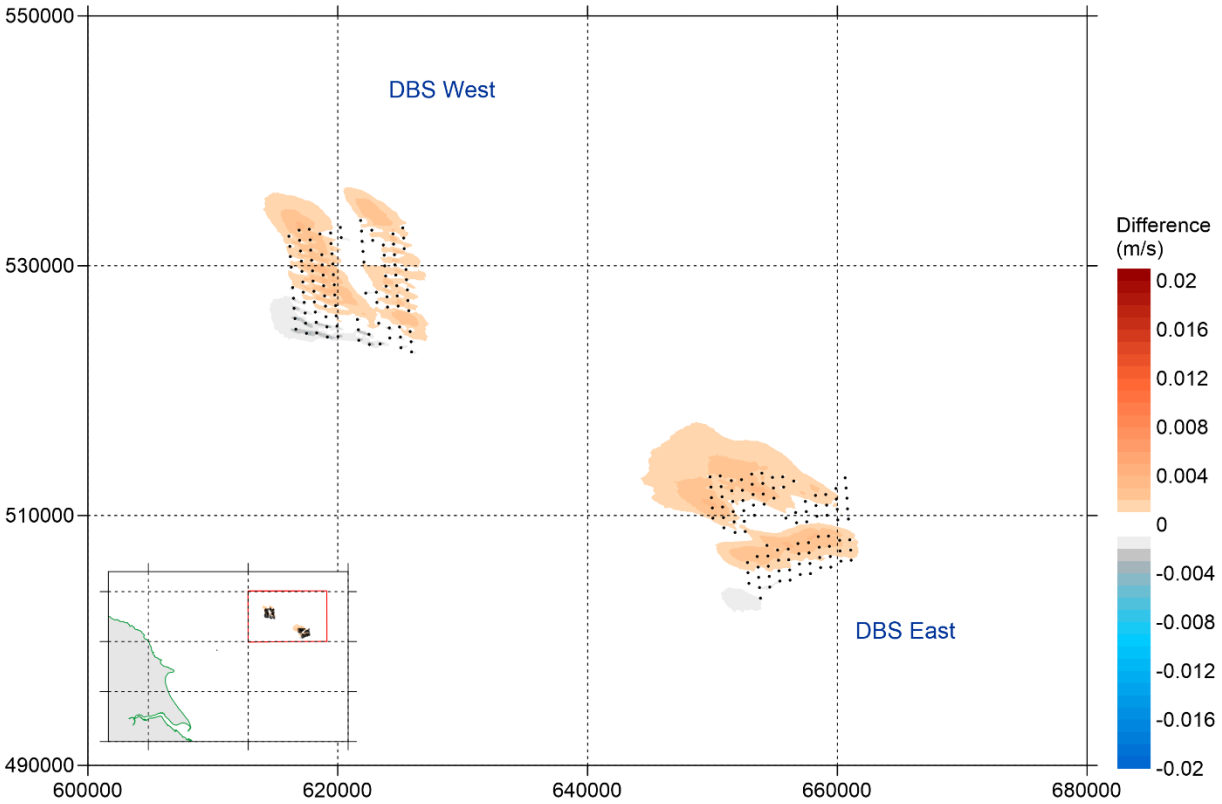

Figure C-24: Change of Speed of Peak Southeast-Going Currents in a Neap Tide – (Option 2 – Baseline)

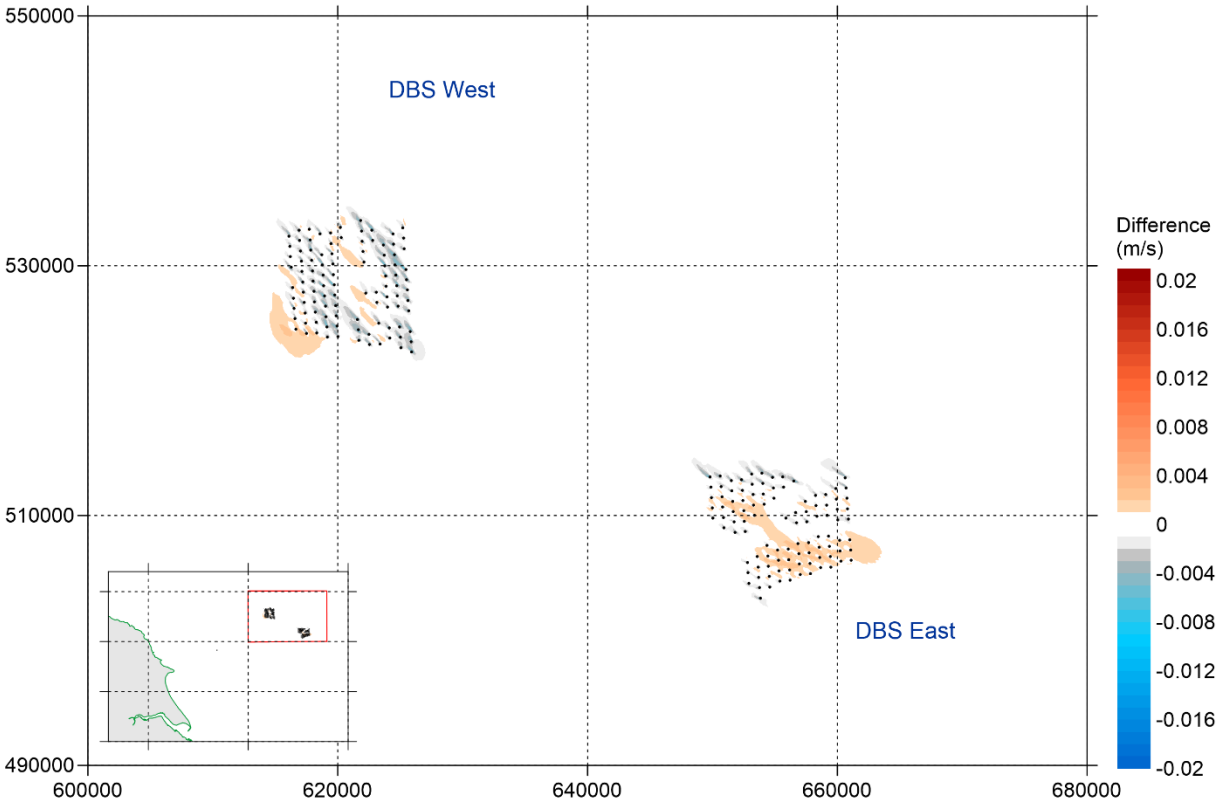

Figure C-25: Change of Speed of Peak Northwest-Going Currents in a Neap Tide – (Option 2 – Baseline)

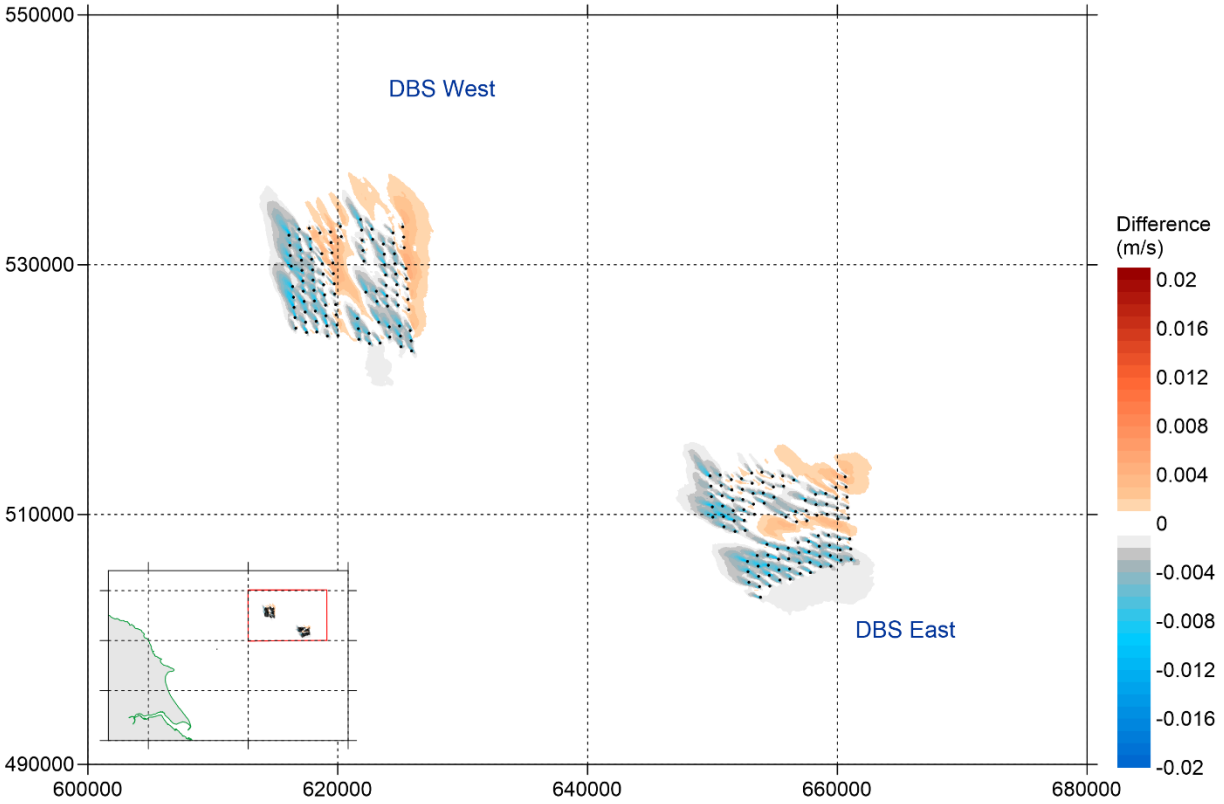

Figure C-26: Change of Maximum Current Speed Over 30 Days – (Option 2 – Baseline)

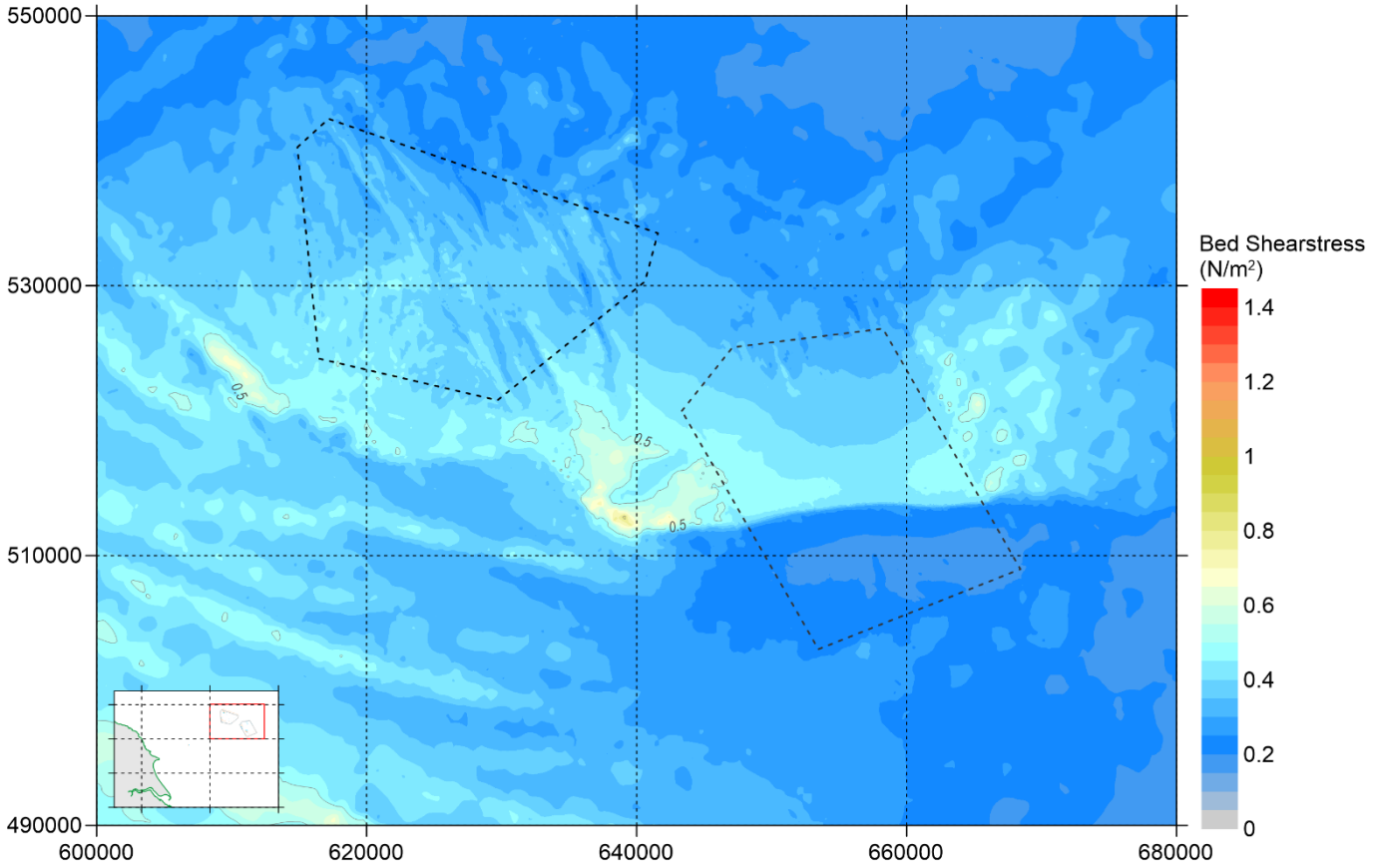

Figure C-27: Bed Shear Stress of Peak Southeast-Going Currents in a Spring Tide - Baseline

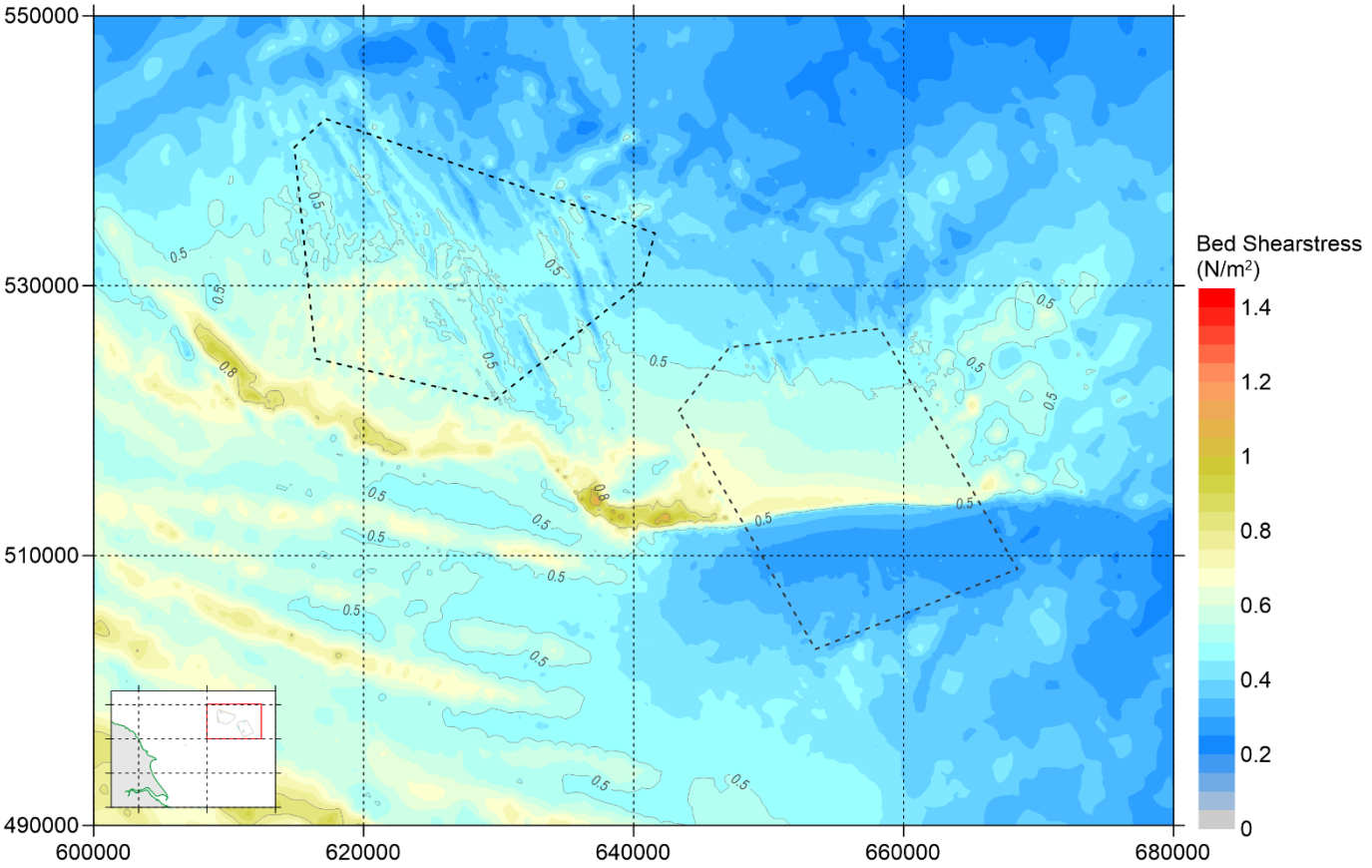

Figure C-28: Bed Shear Stress of Peak Northwest-Going Currents in a Spring Tide – Baseline

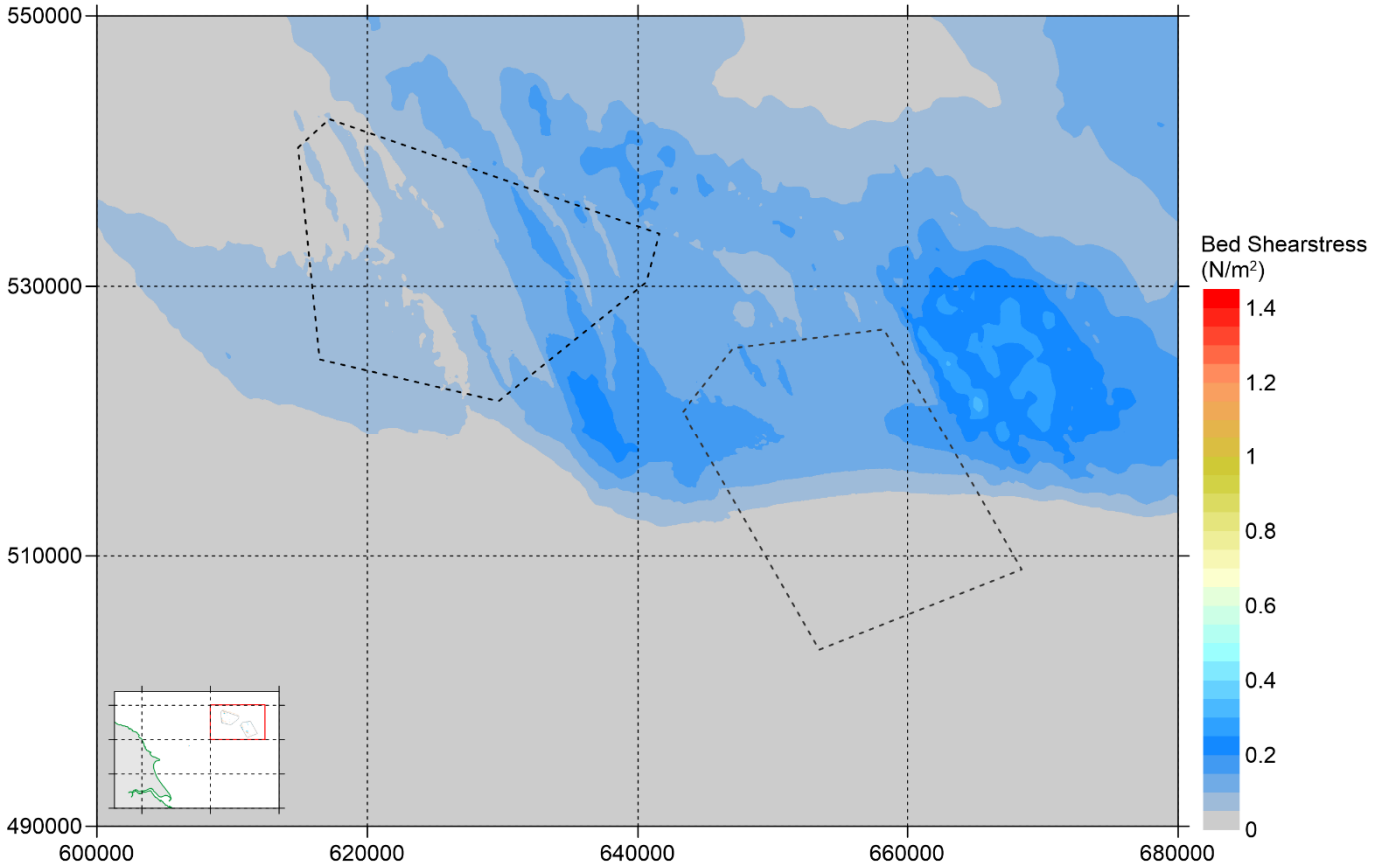

Figure C-29: Bed Shear Stress of Peak Southeast-Going Currents in a Neap Tide – Baseline

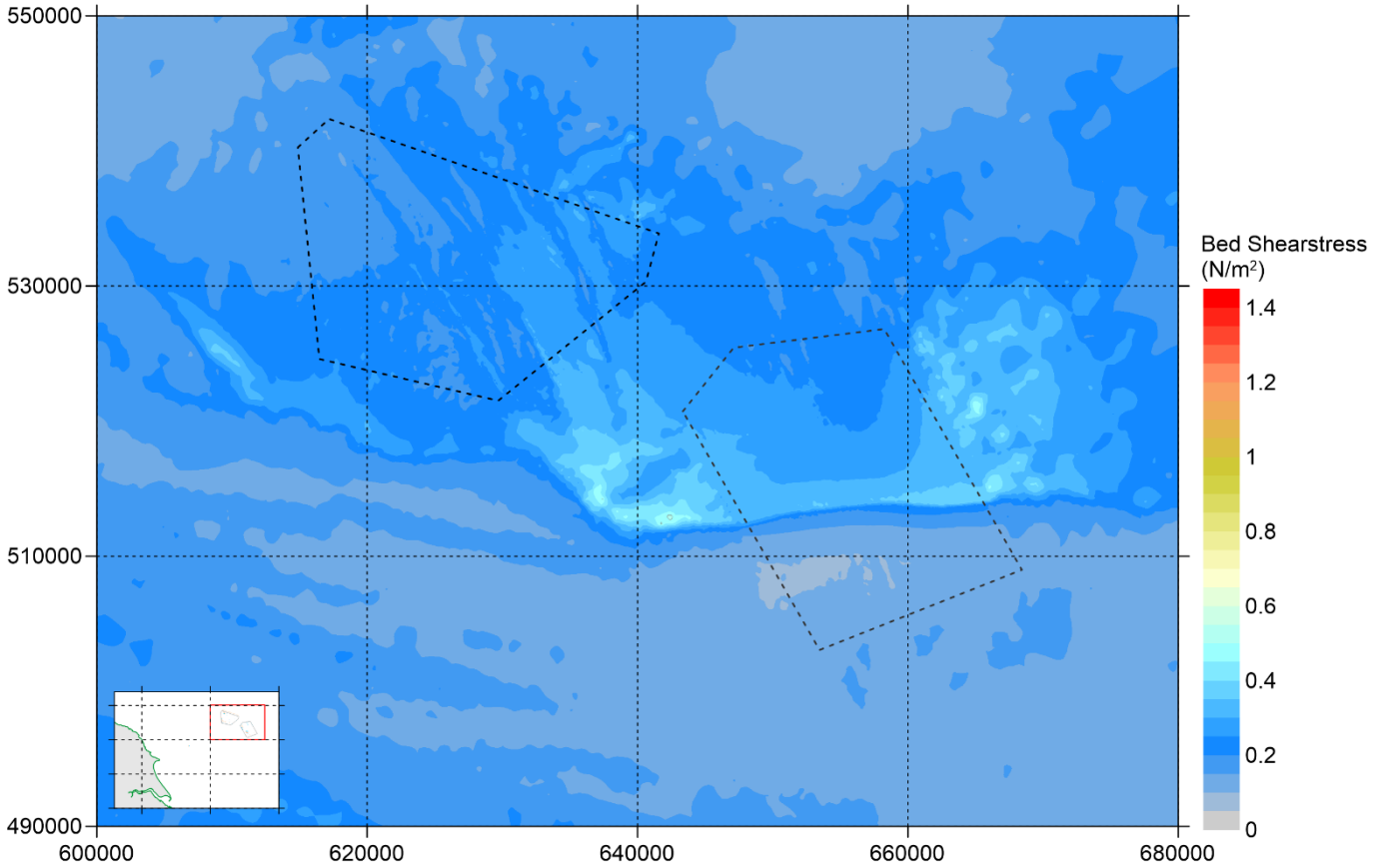

Figure C-30: Bed Shear Stress of Peak Northwest-Going Currents in a Neap Tide – Baseline

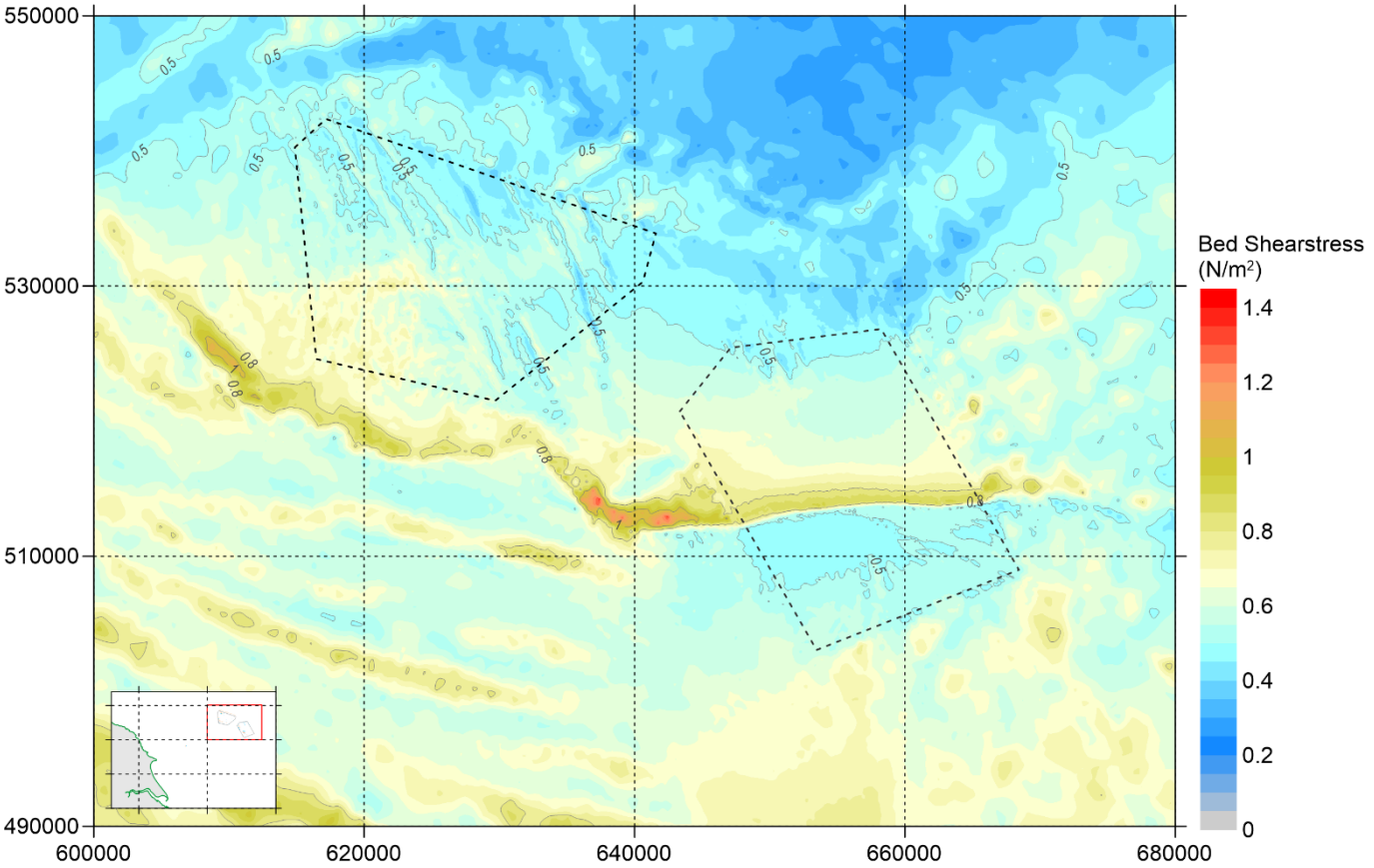

Figure C-31: Maximum Bed shear Stress Over 30 Days- Baseline

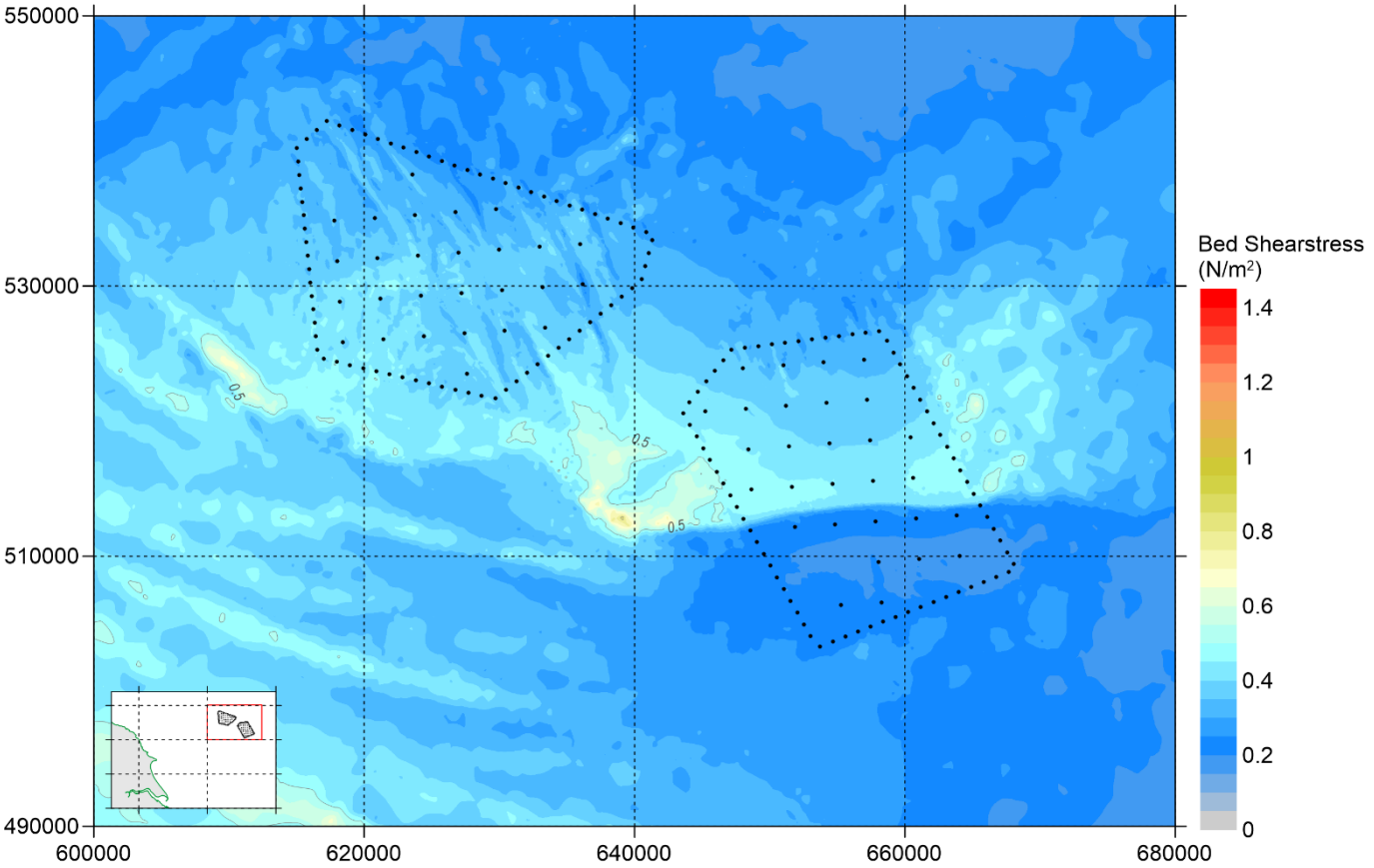

Figure C-32: Bed Shear Stress of Peak Southeast-Going Currents in a Spring Tide - Option 1

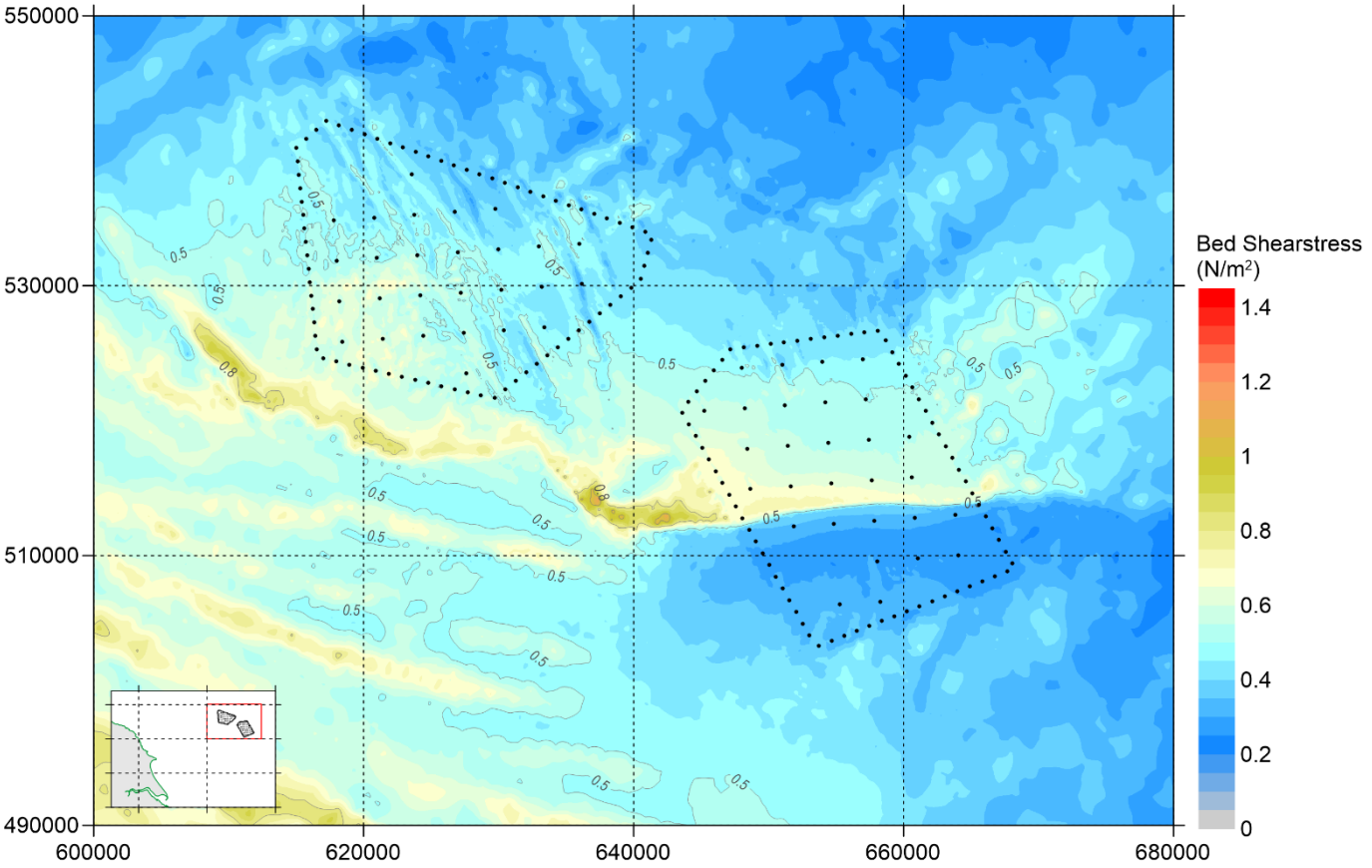

Figure C-33: Bed Shear Stress of Peak Northeast-Going Currents in a Spring Tide - Option 1

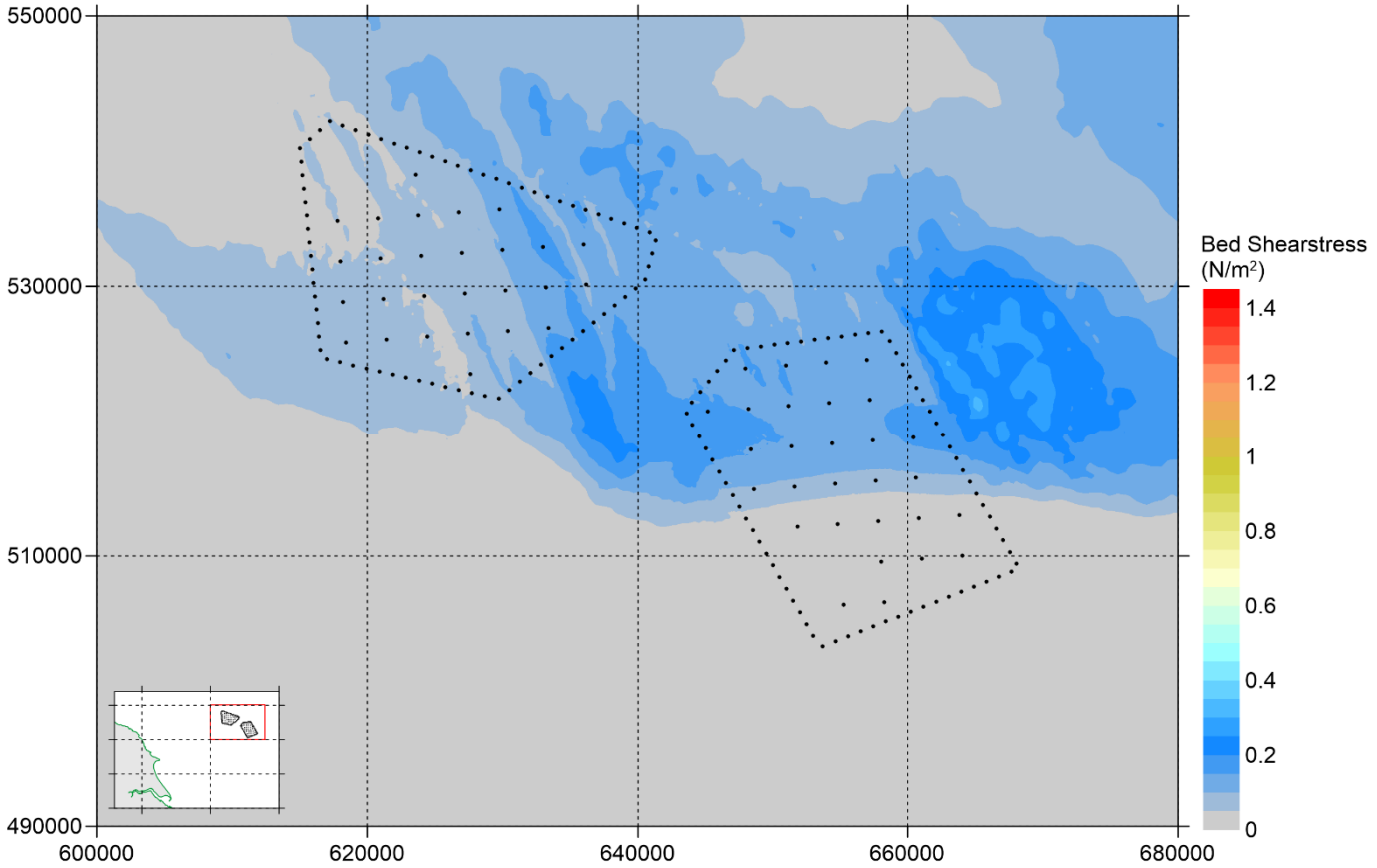

Figure C-34: Bed Shear Stress of Peak Southeast-Going Currents in a Neap Tide – Option 1

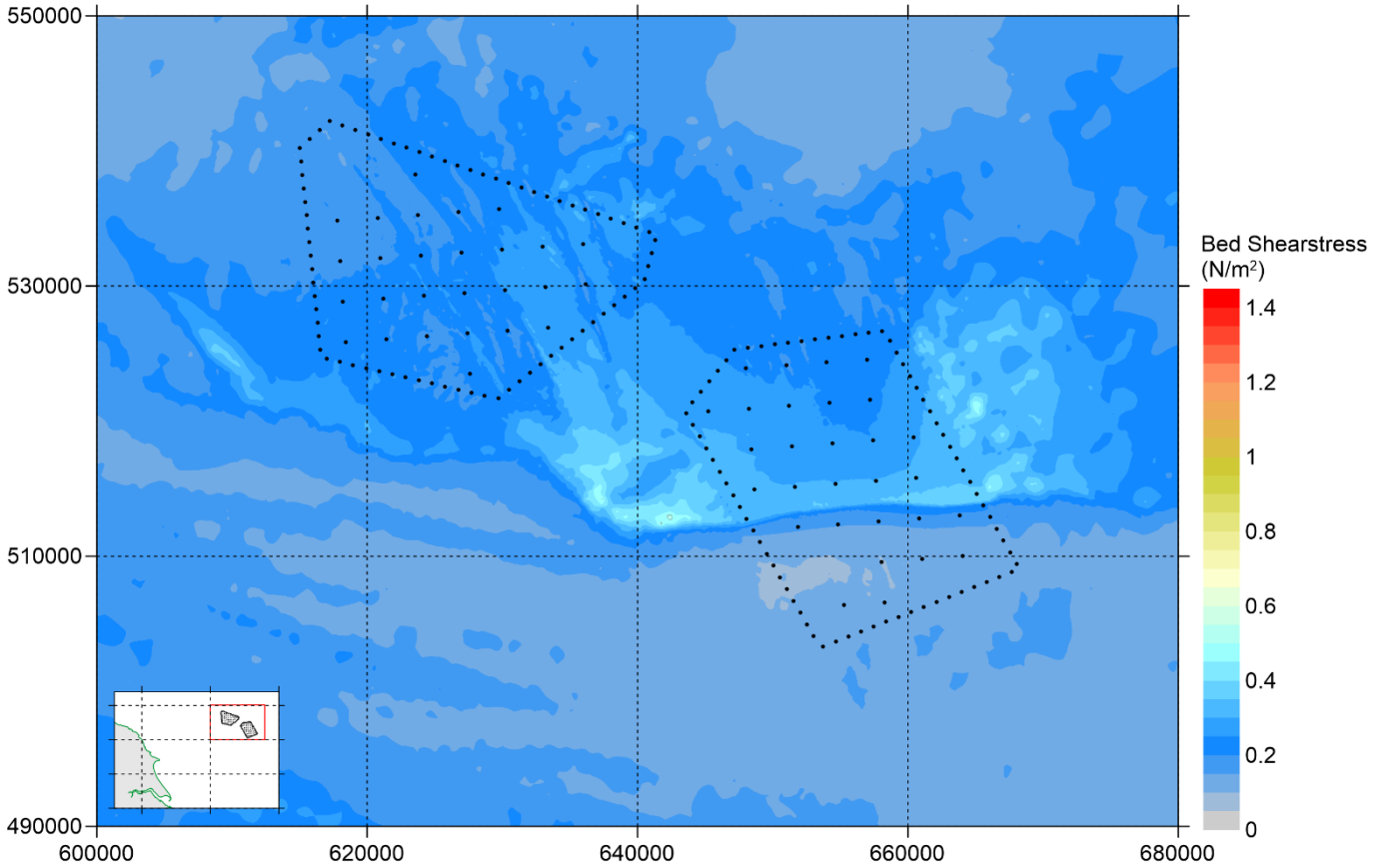

Figure C-35: Bed Shear Stress of Peak Northwest-Going Currents in a Neap Tide – Option 1

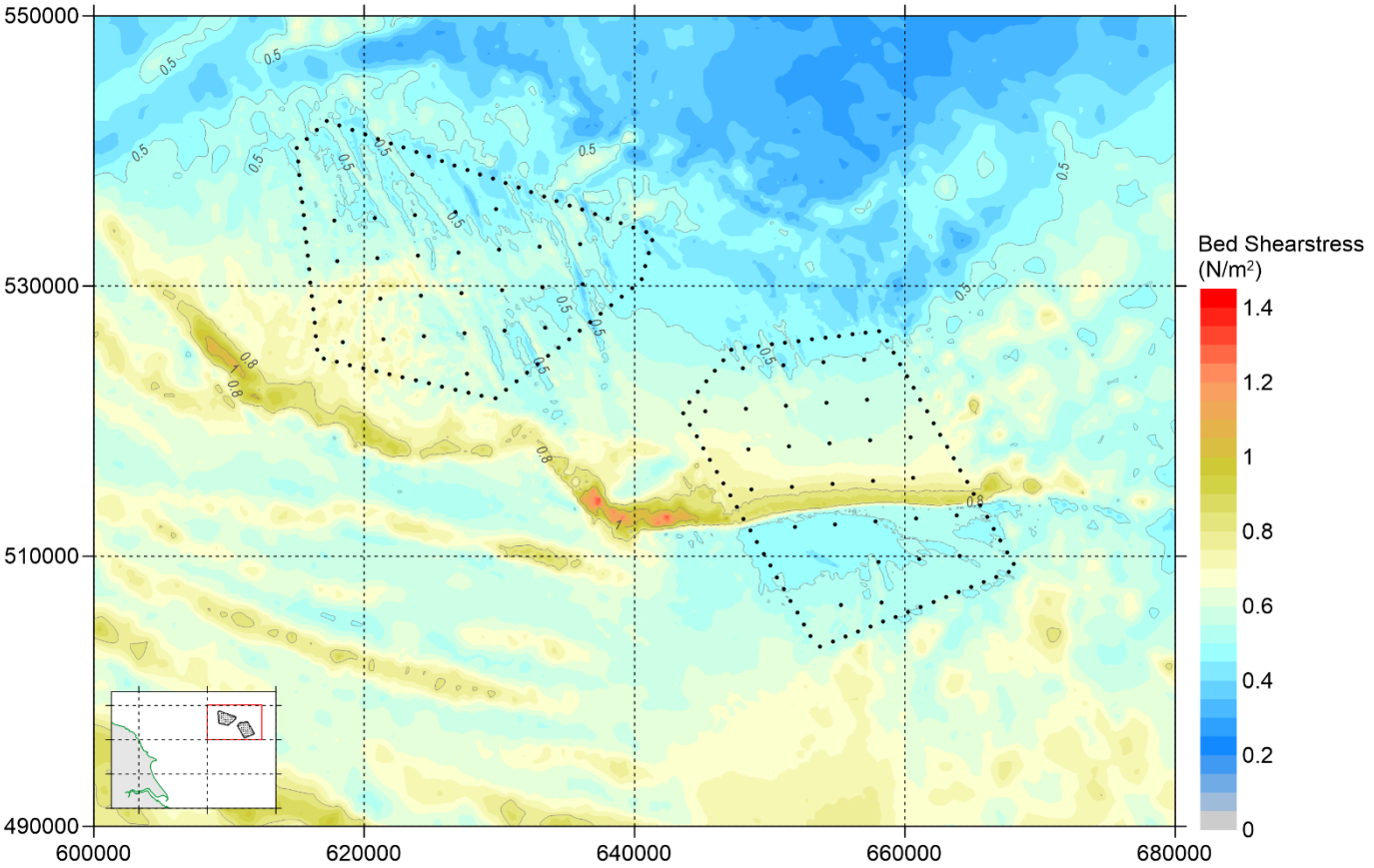

Figure C-36: Maximum Bed Shear Stress Over 30 days- Option 1

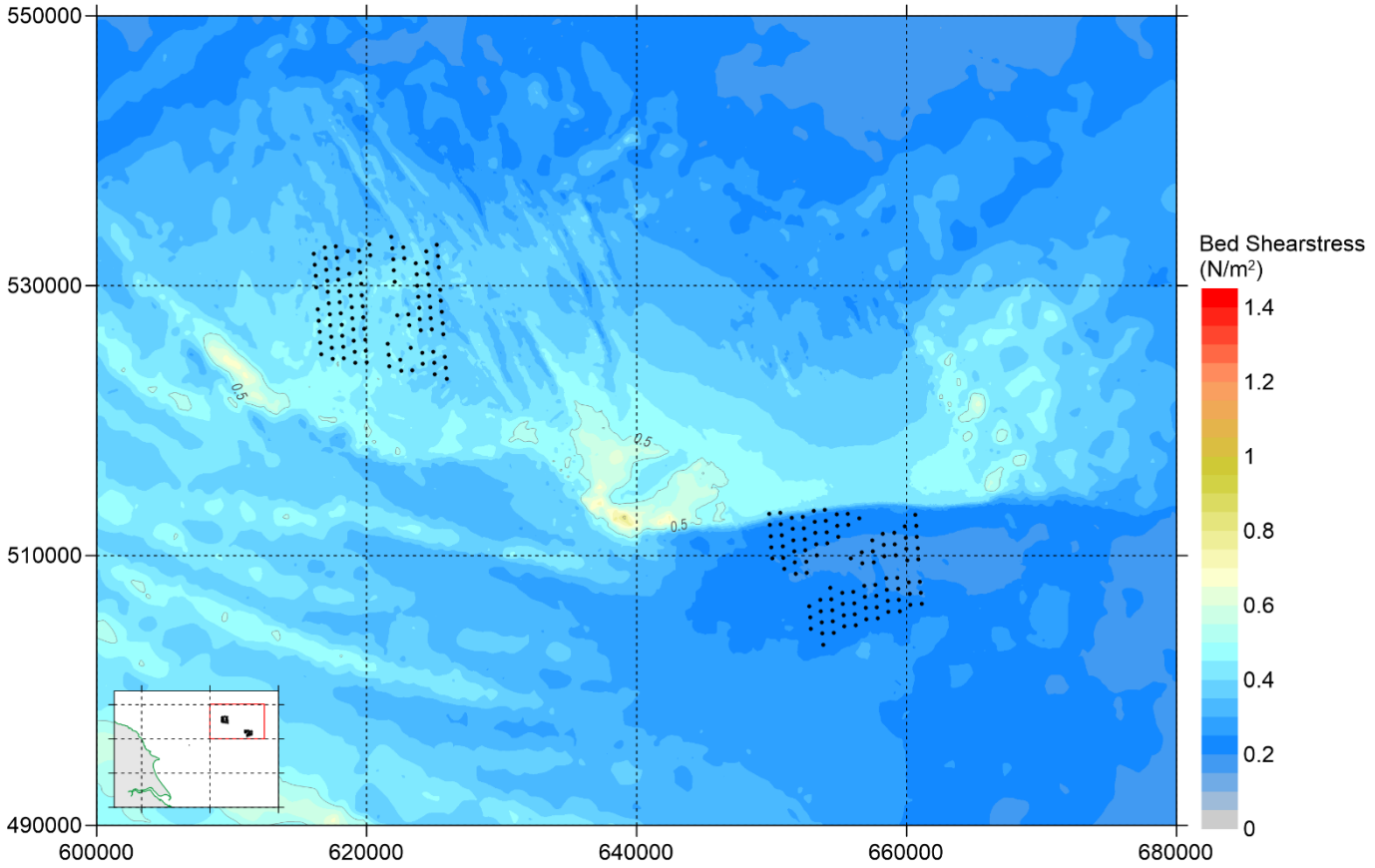

Figure C-37: Bed Shear Stress of Peak Southeast-Going Currents in a Spring Tide - Option 2

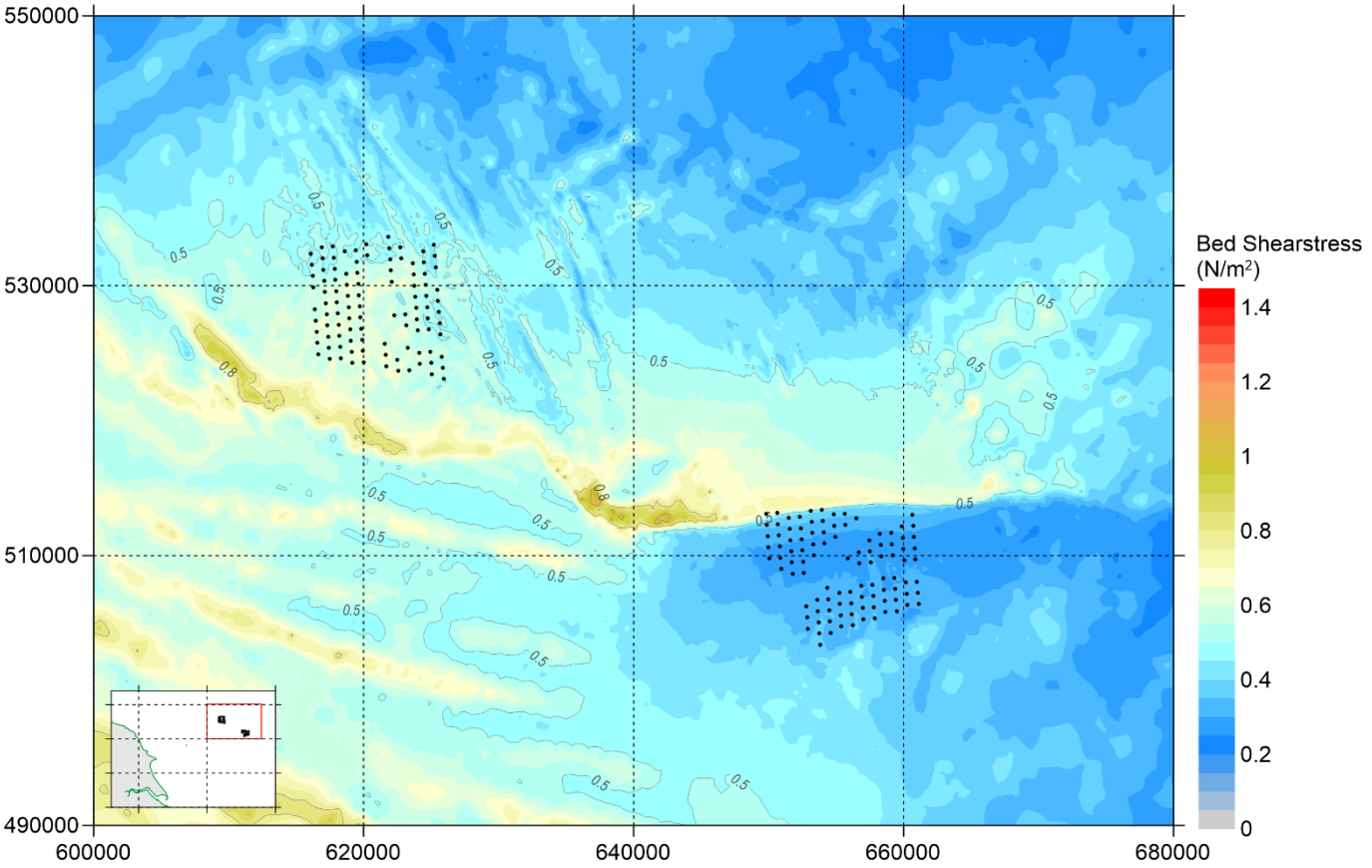

Figure C-38: Bed Shear Stress of Peak Northwest-Going Currents in a Spring Tide - Option 2

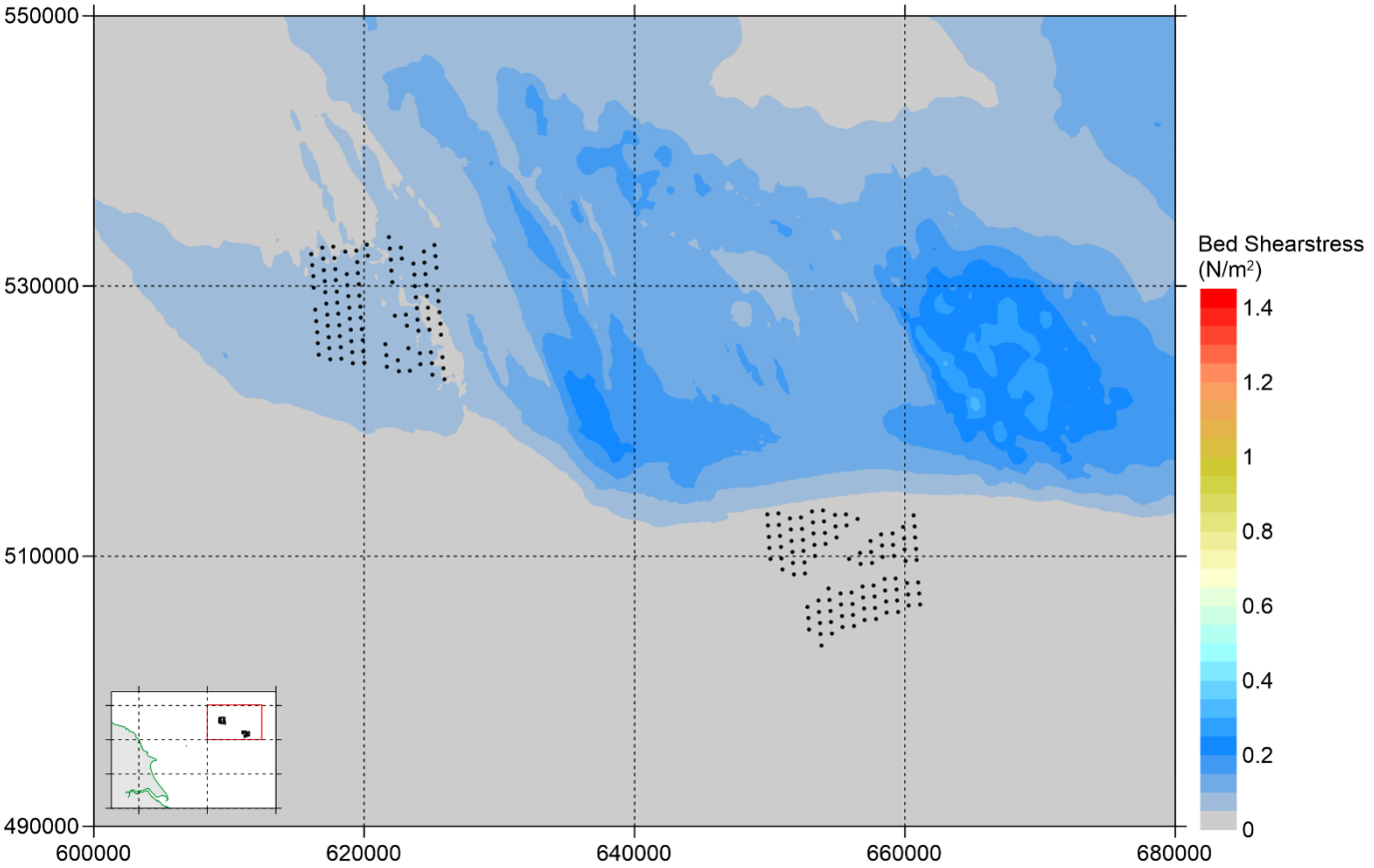

Figure C-39: Bed Shear Stress of Peak Southeast-Going Currents in a Neap Tide – Option 2

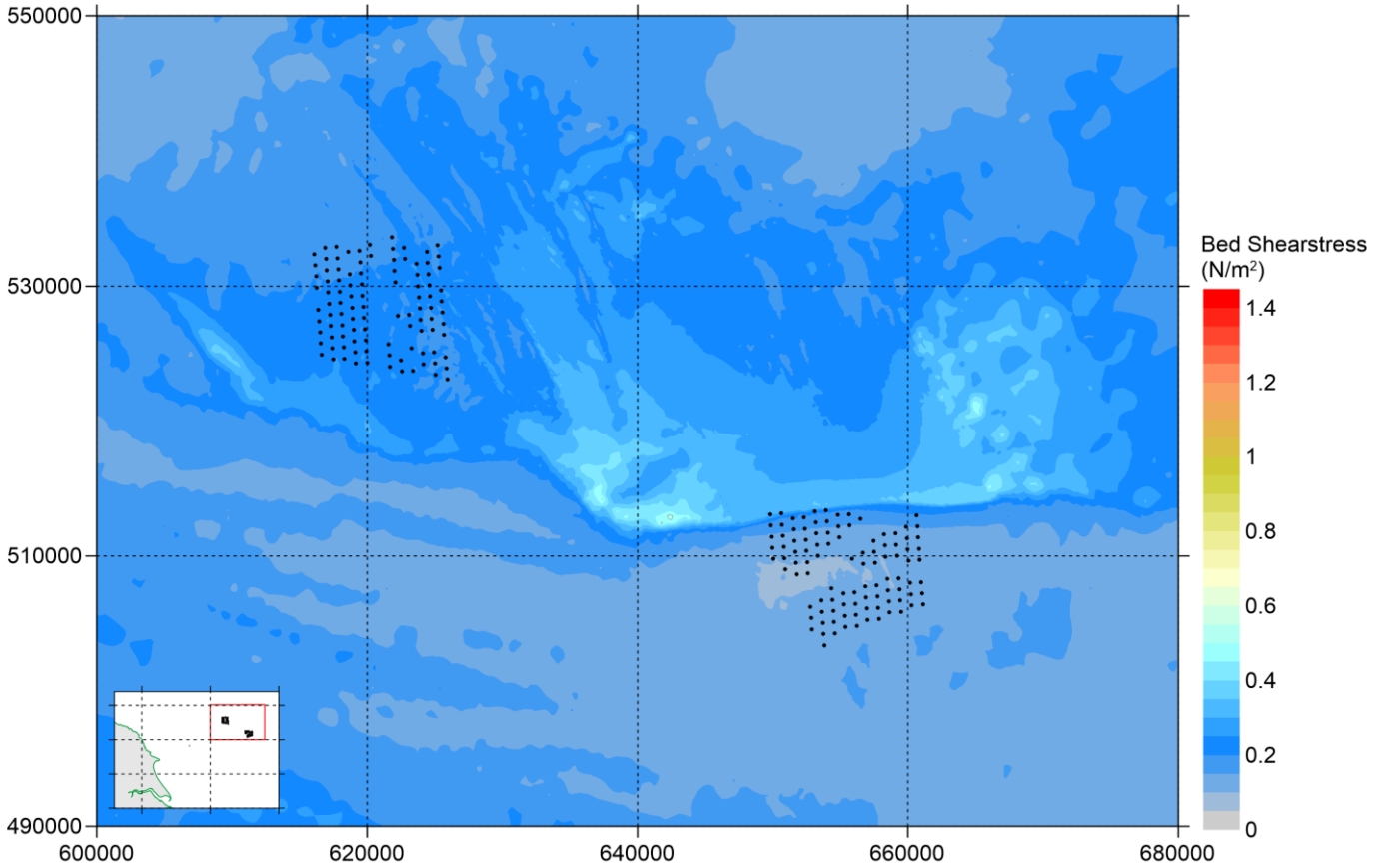

Figure C-40: Bed Shear Stress of Peak Northwest-Going Currents in a Neap Tide – Option 2

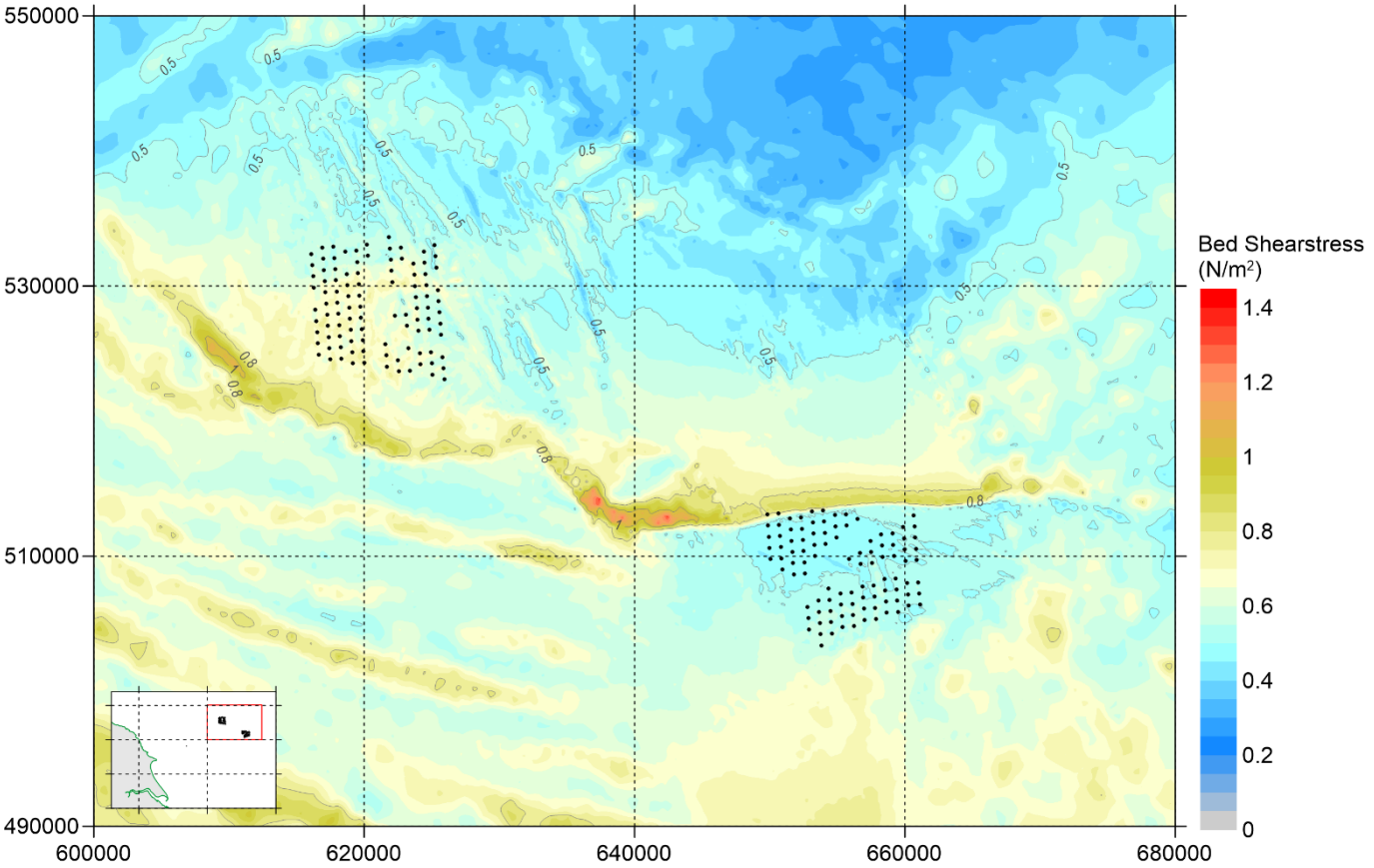

Figure C-41: Maximum Bed Shear Stress Over 30 days - Option 2

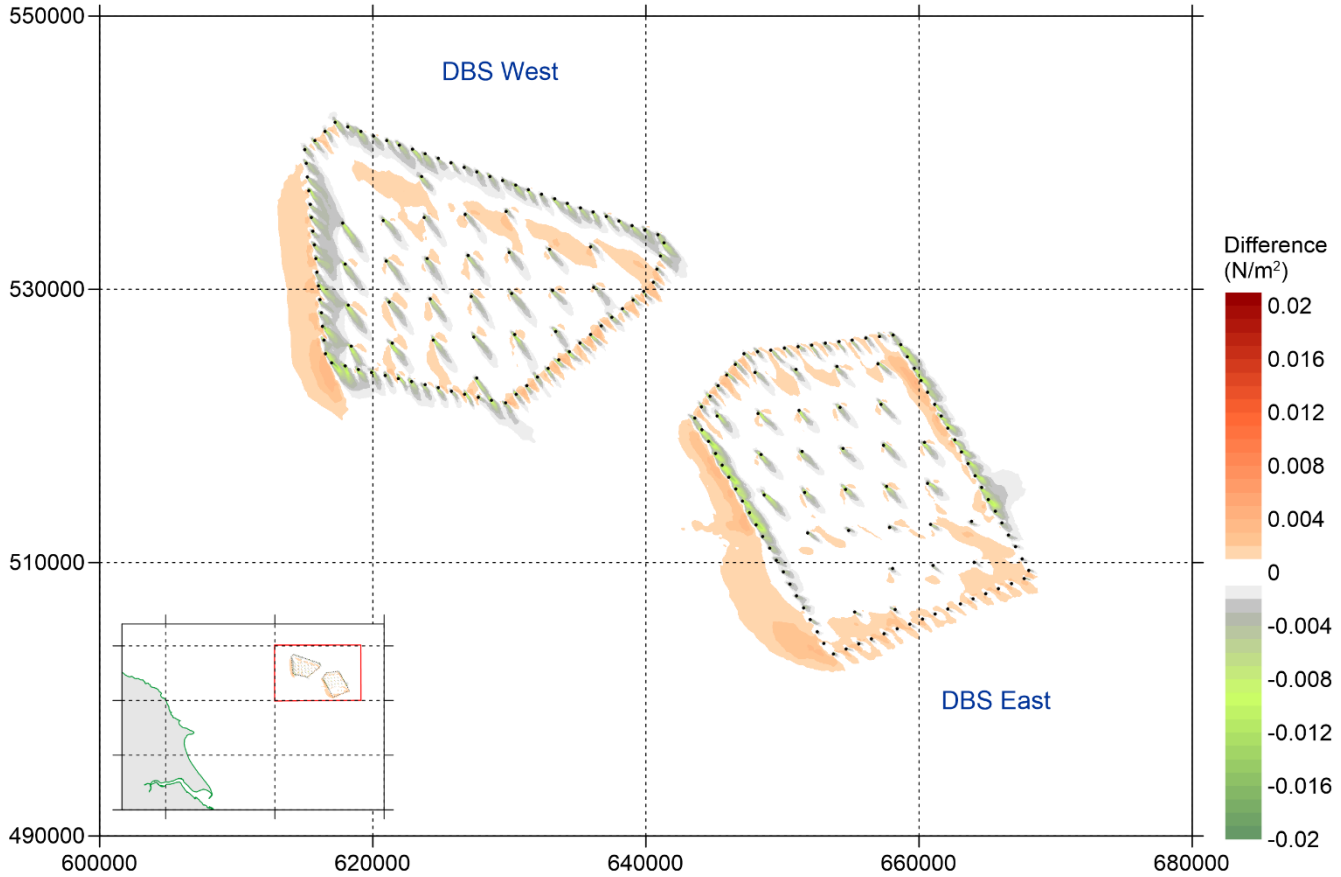

Figure C-42: Change of Bed Shear Stress of Peak Southeast-Going Currents in a Spring Tide – (Option 1 – Baseline)

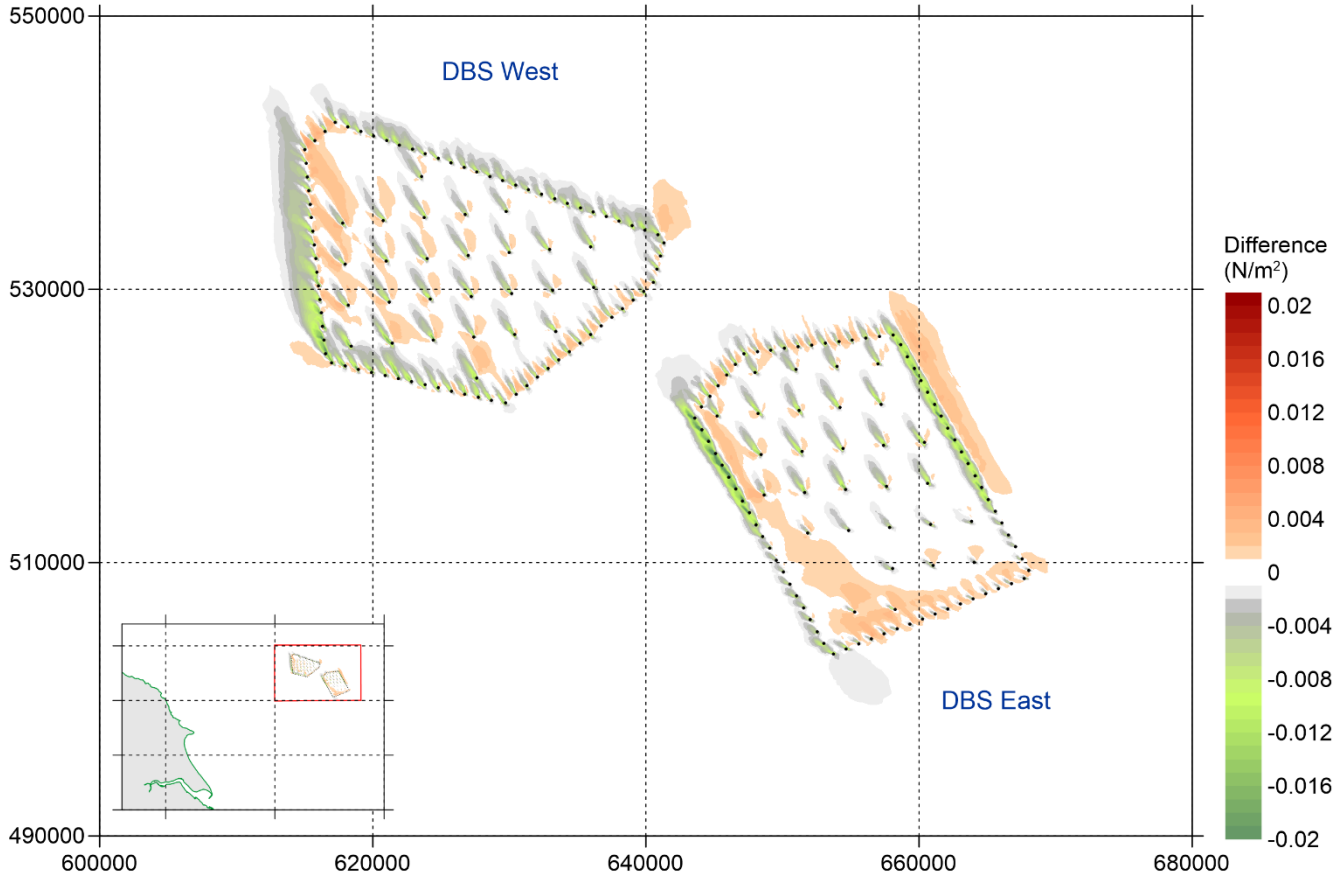

Figure C-43: Change of Bed Shear Stress of Peak Northwest-Going Currents in a Spring Tide – (Option 1 – Baseline)

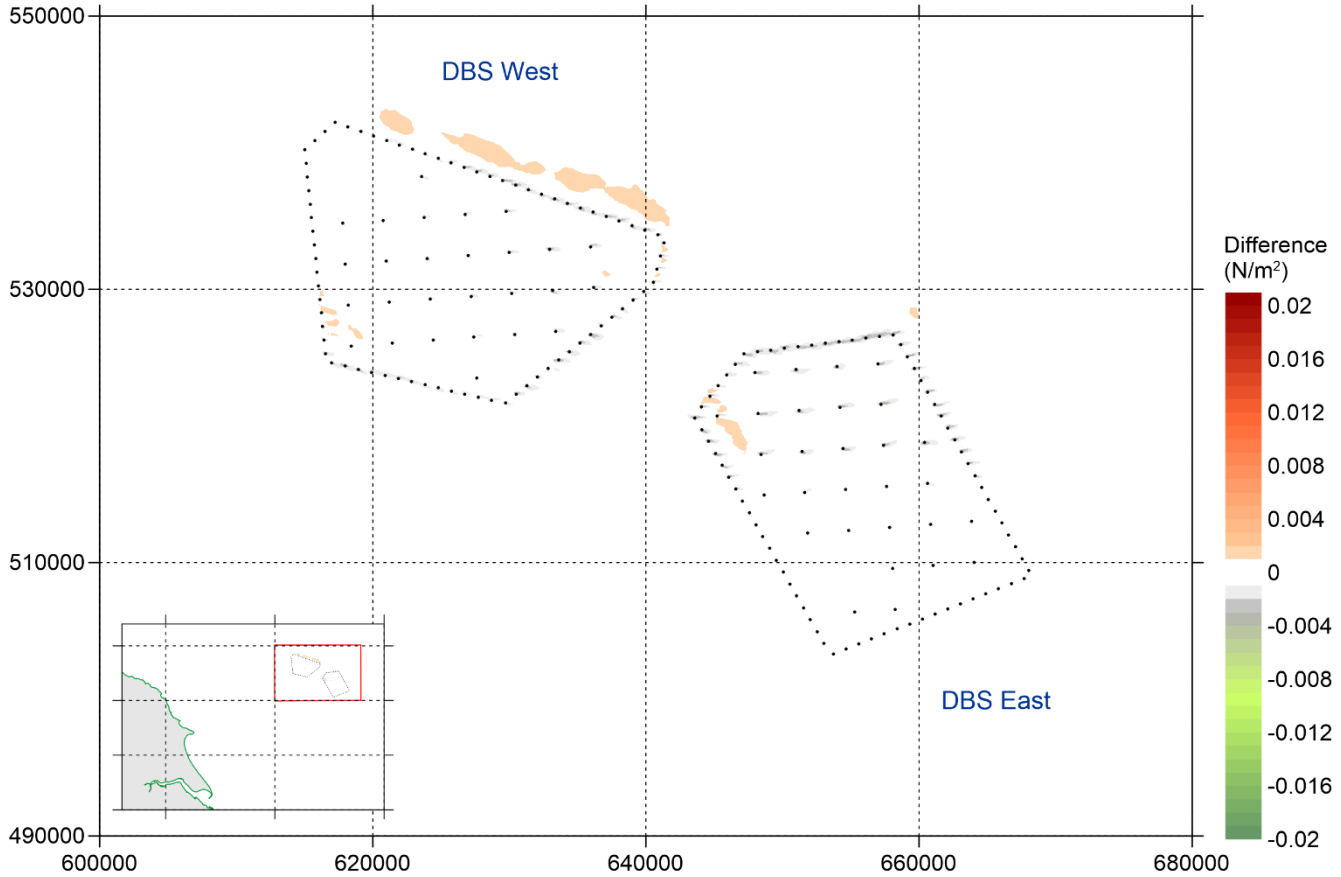

Figure C-44: Change of Bed Shear Stress of Peak Southeast-Going Currents in a Neap Tide – (Option 1 – Baseline)

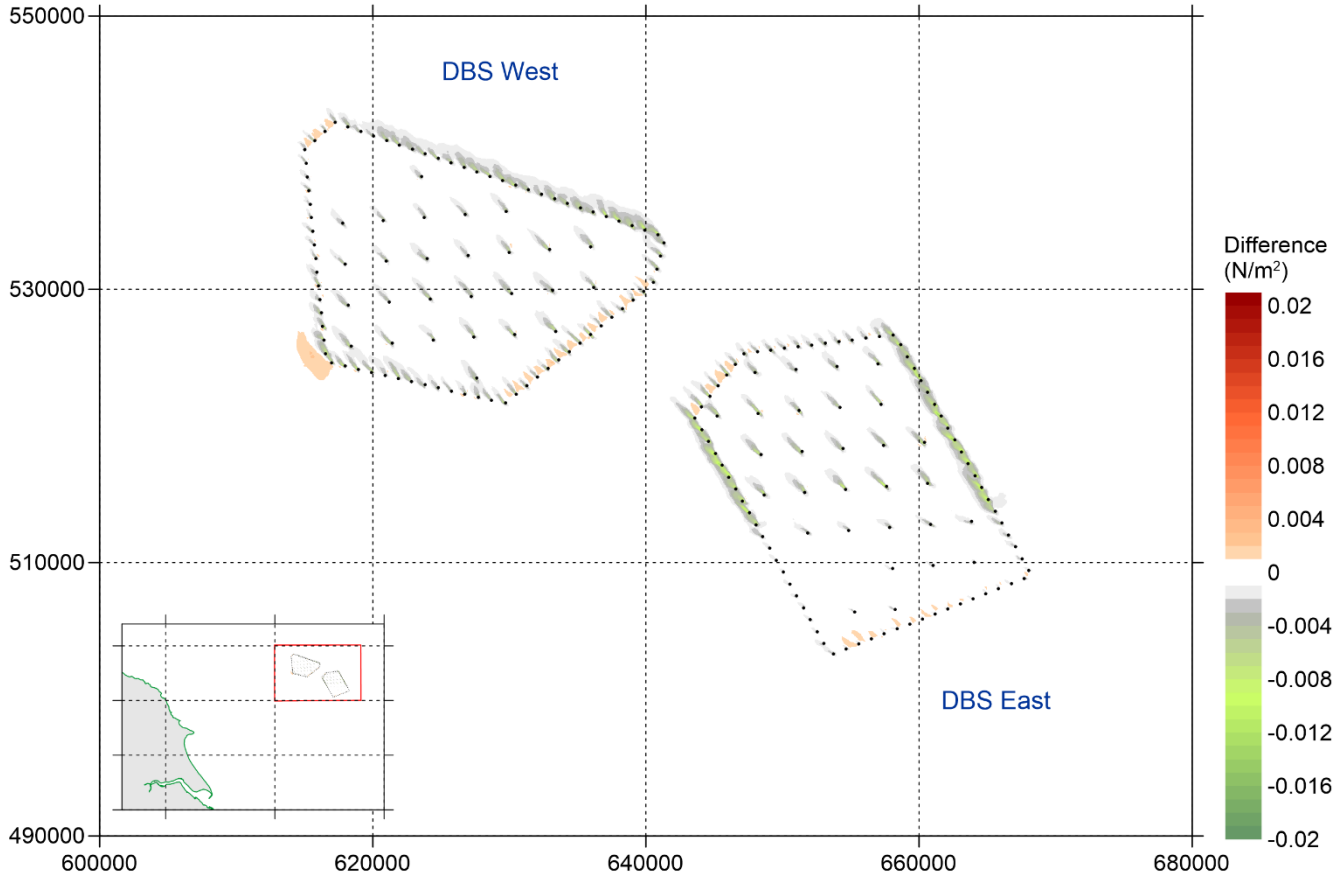

Figure C-45: Change of Bed Shear Stress of Peak Northwest-Going Currents in a Neap Tide – (Option 1 – Baseline)

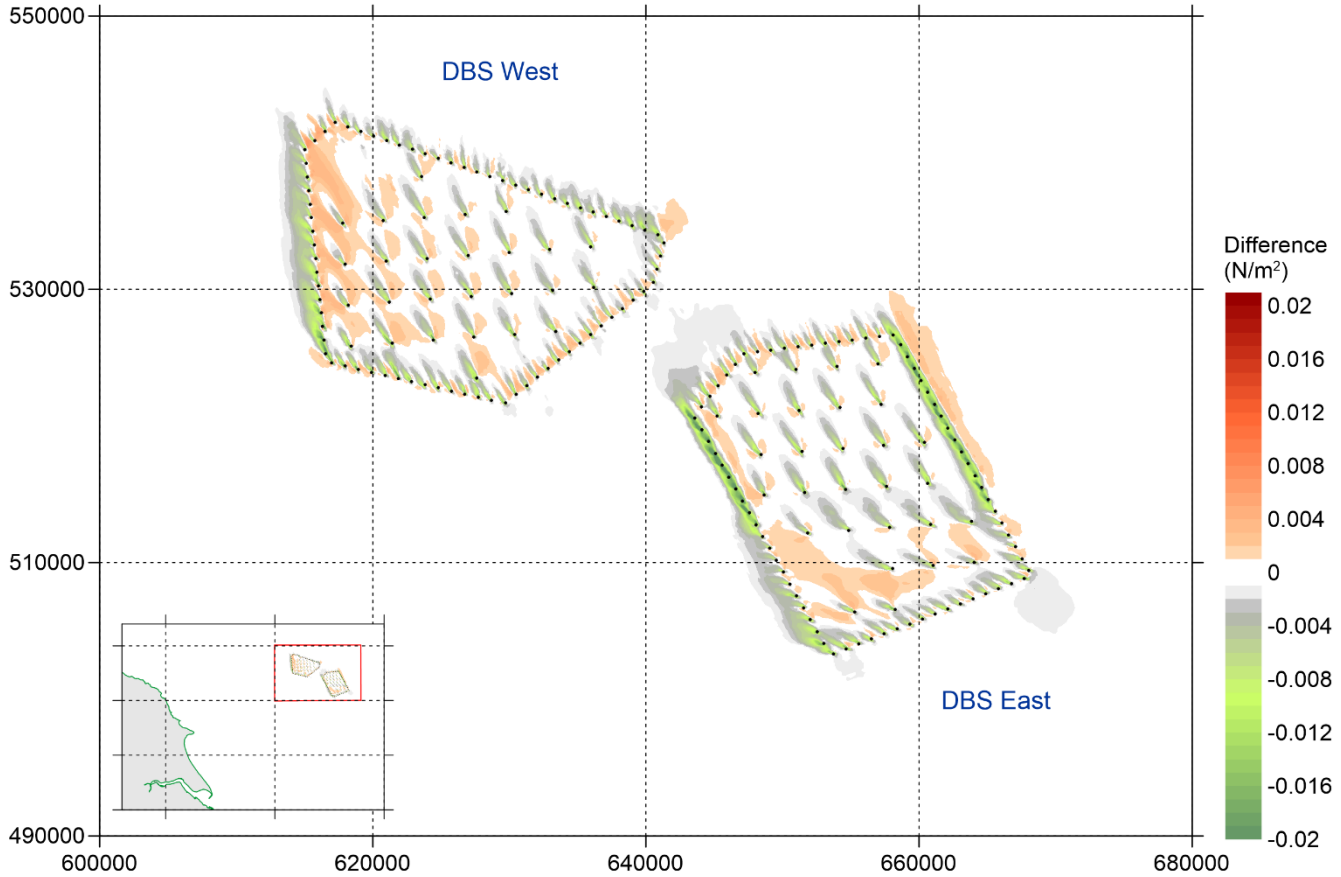

Figure C-46: Change of Maximum Bed Shear Stress Over 30 days – (Option 1 – Baseline)

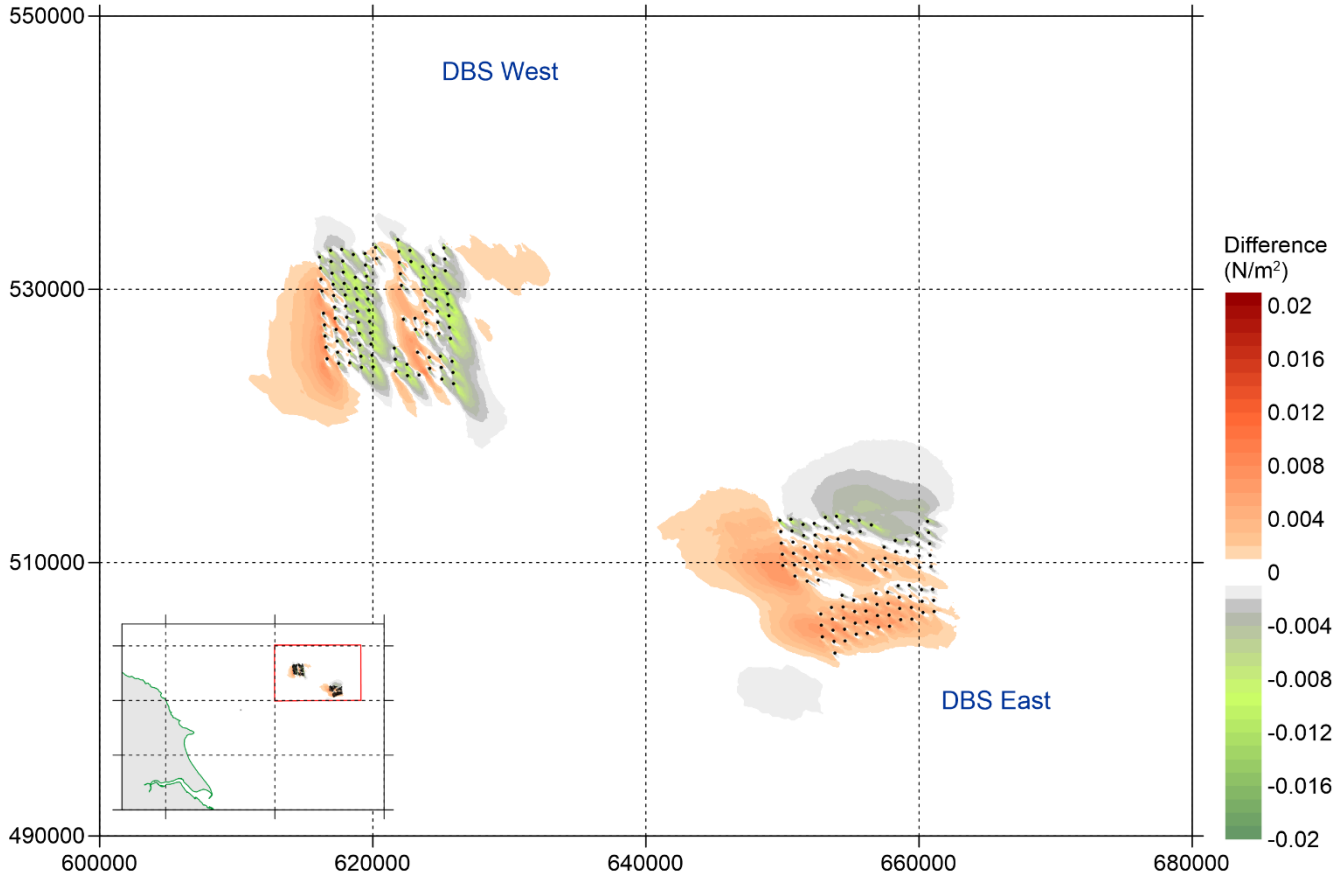

Figure C-47: Change of Bed Shear Stress of Peak Southeast-Going Currents in a Spring Tide – (Option 2 – Baseline)

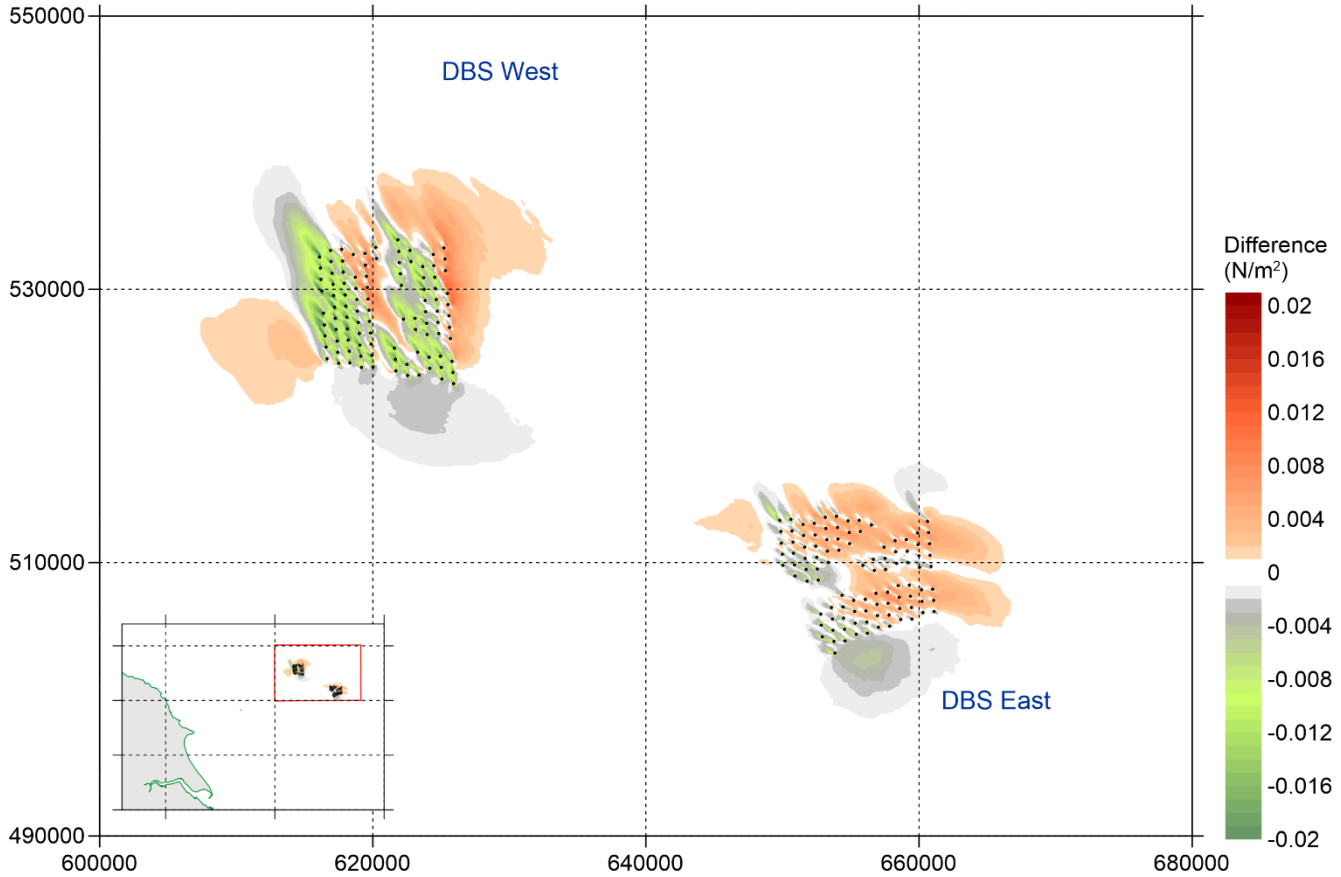

Figure C-48: Change of Bed Shear Stress of Peak Northwest-Going Currents in a Spring Tide – (Option 2 – Baseline)

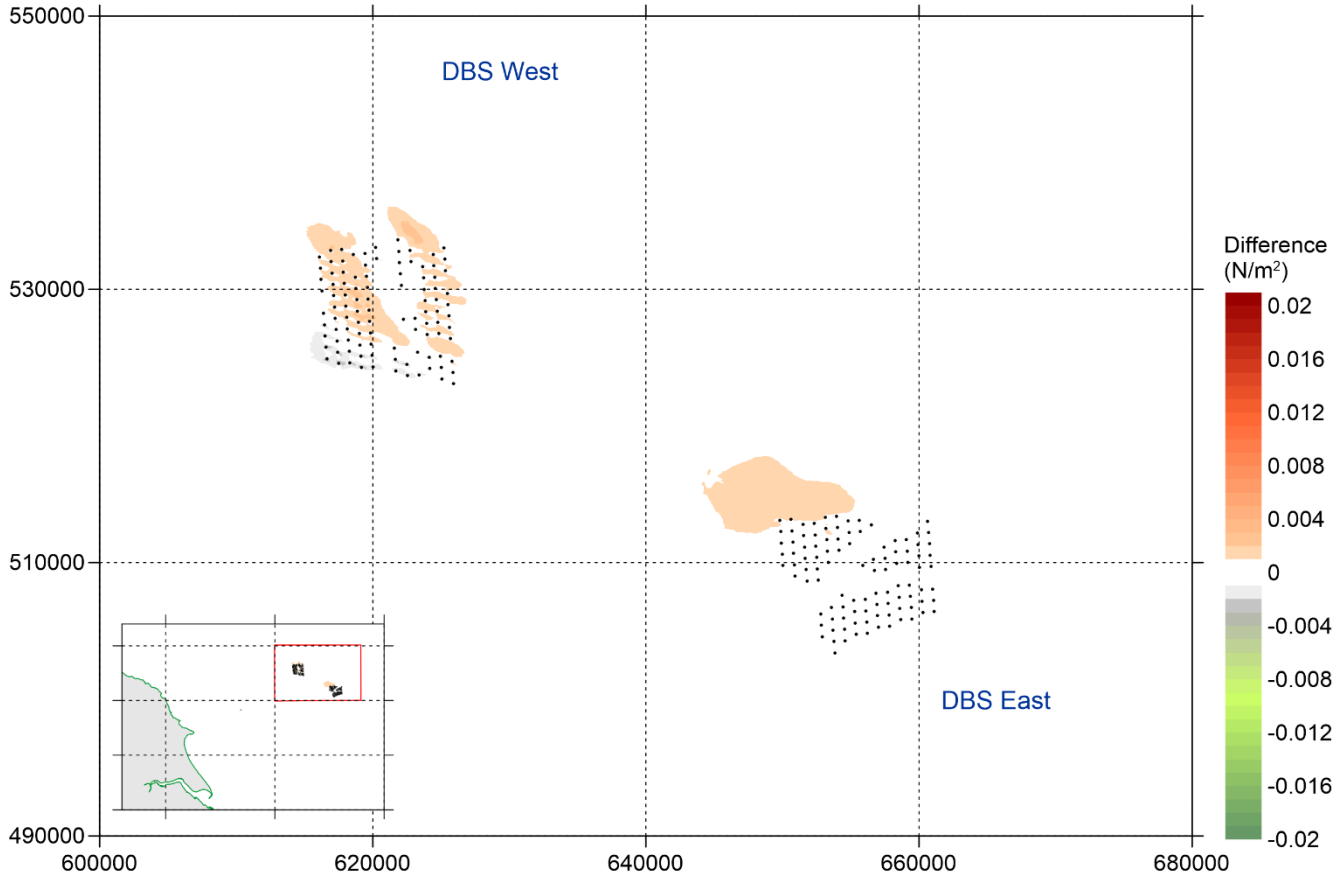

Figure C-49: Change of Bed Shear Stress of Peak Southeast-Going Currents in a Neap Tide – (Option 2 – Baseline)

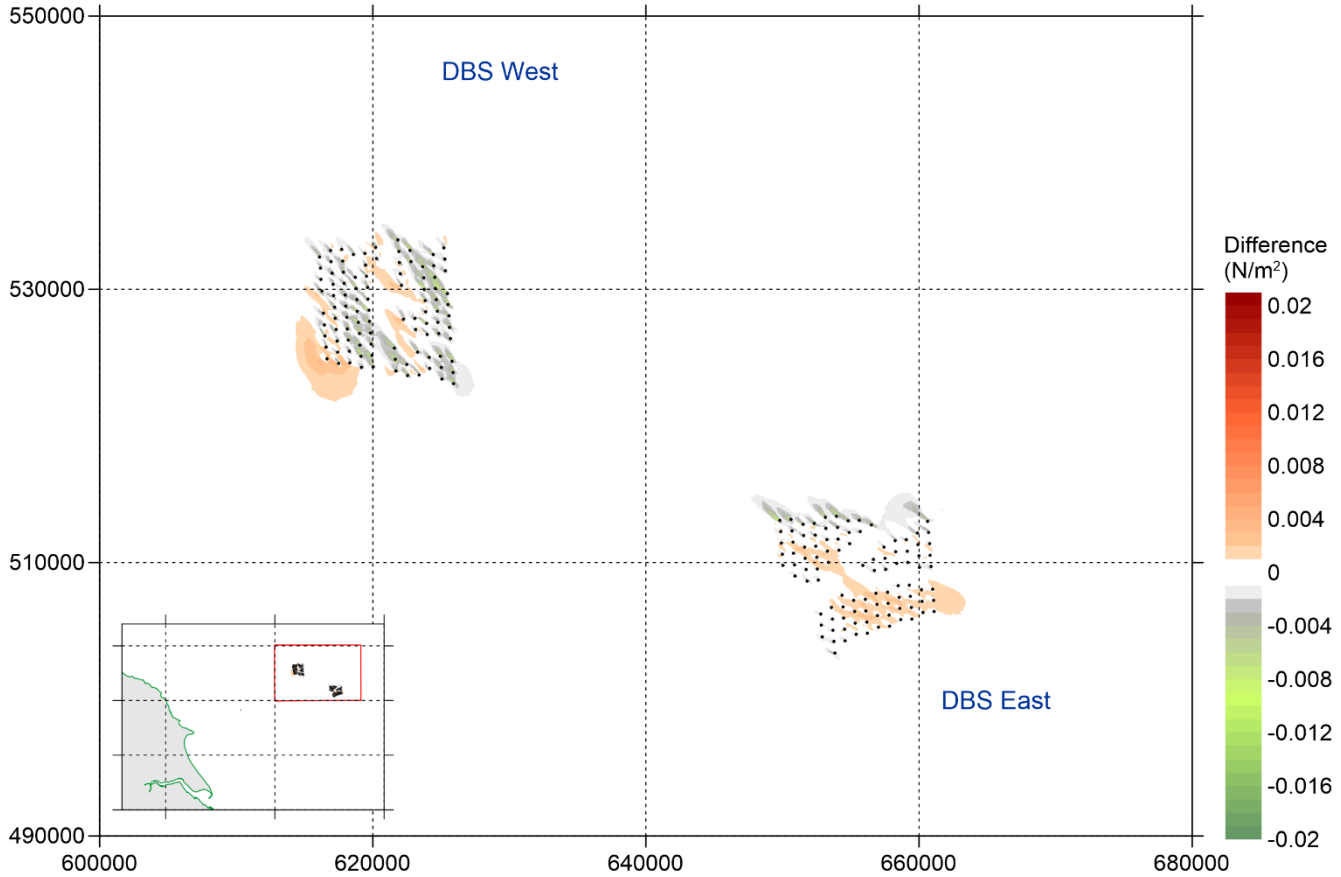

Figure C-50: Change of Bed Shear Stress of Peak Northwest-Going Currents in a Neap Tide – (Option 2 – Baseline)

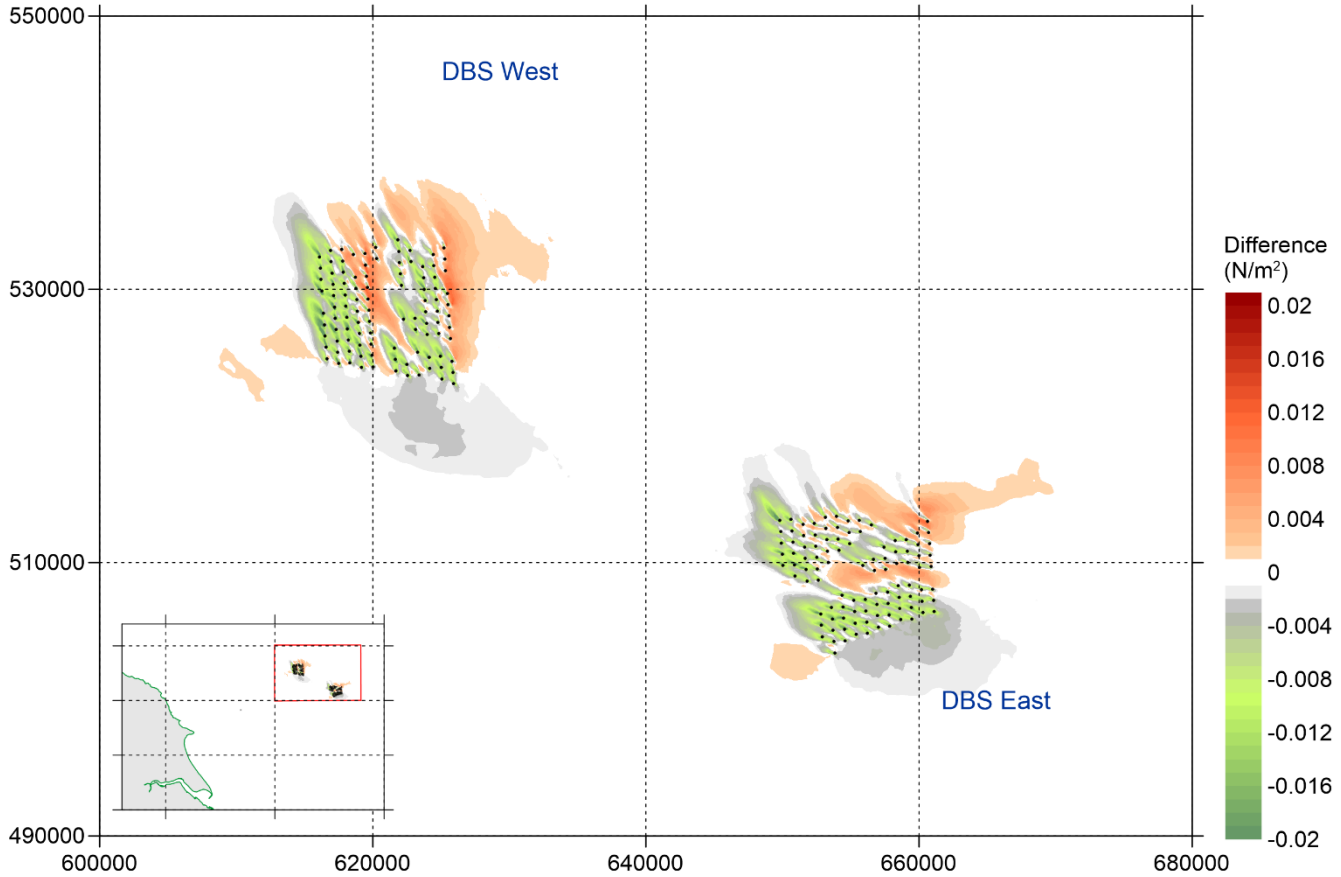

Figure C-51: Change of Maximum Bed Shear Stress Over 30 days – (Option 2 – Baseline)

Annex D – Results of Dispersion Model Assessment Runs

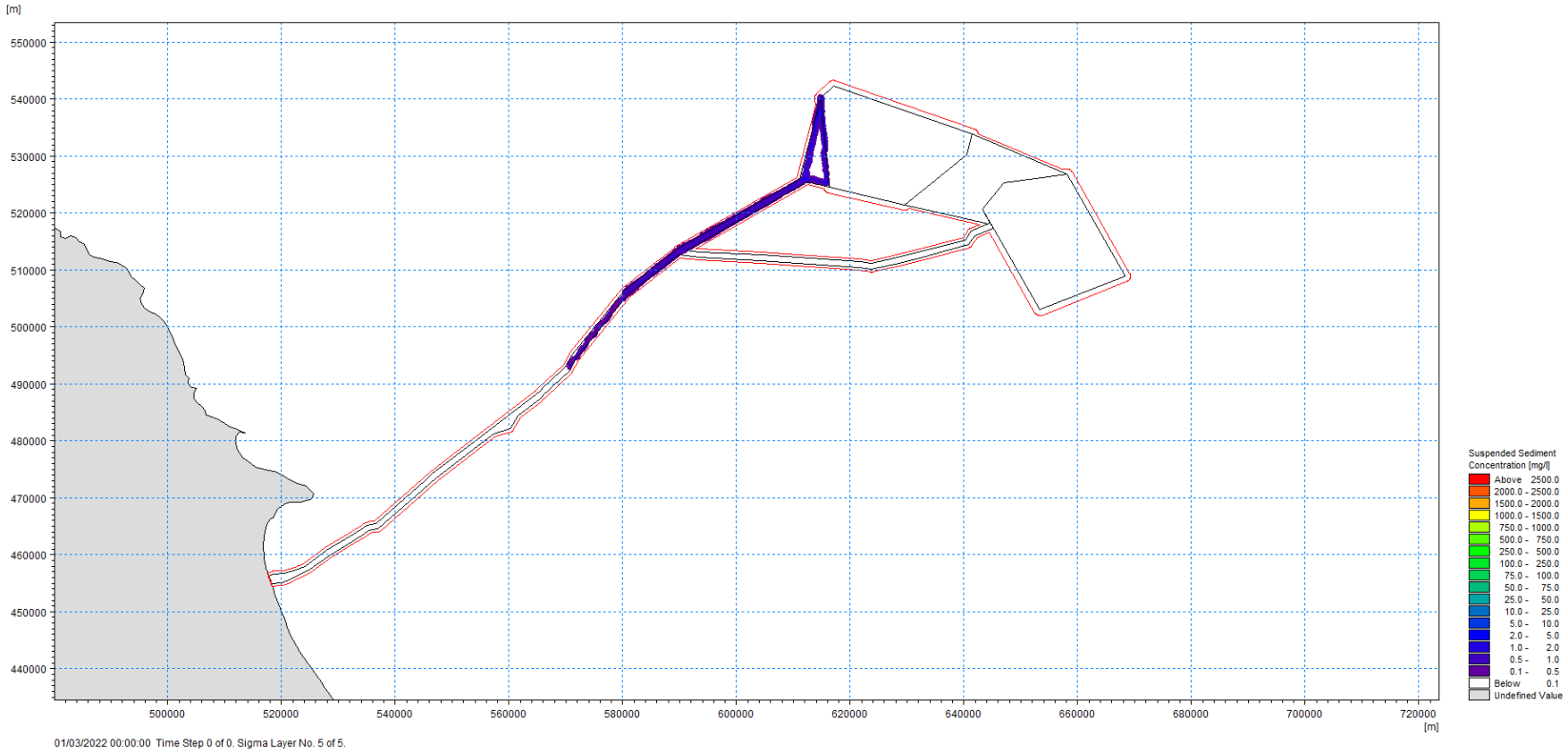

Figure D-1: Maximum Suspended Sediment Concentration (surface layer) – Export Cable Route to DBS West – Levelling

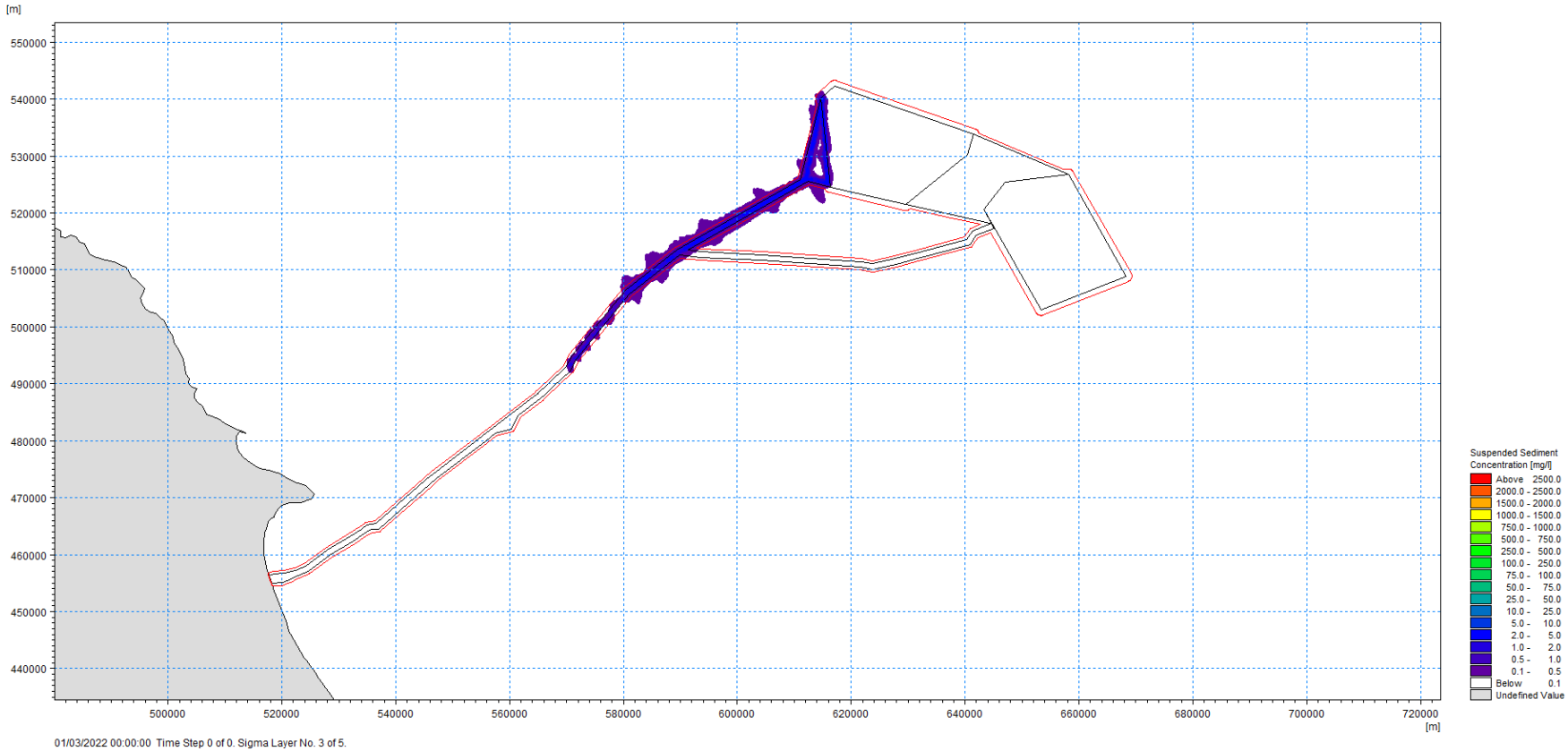

Figure D-2: Maximum Suspended Sediment Concentration (middle layer) – Export Cable Route to DBS West – Levelling

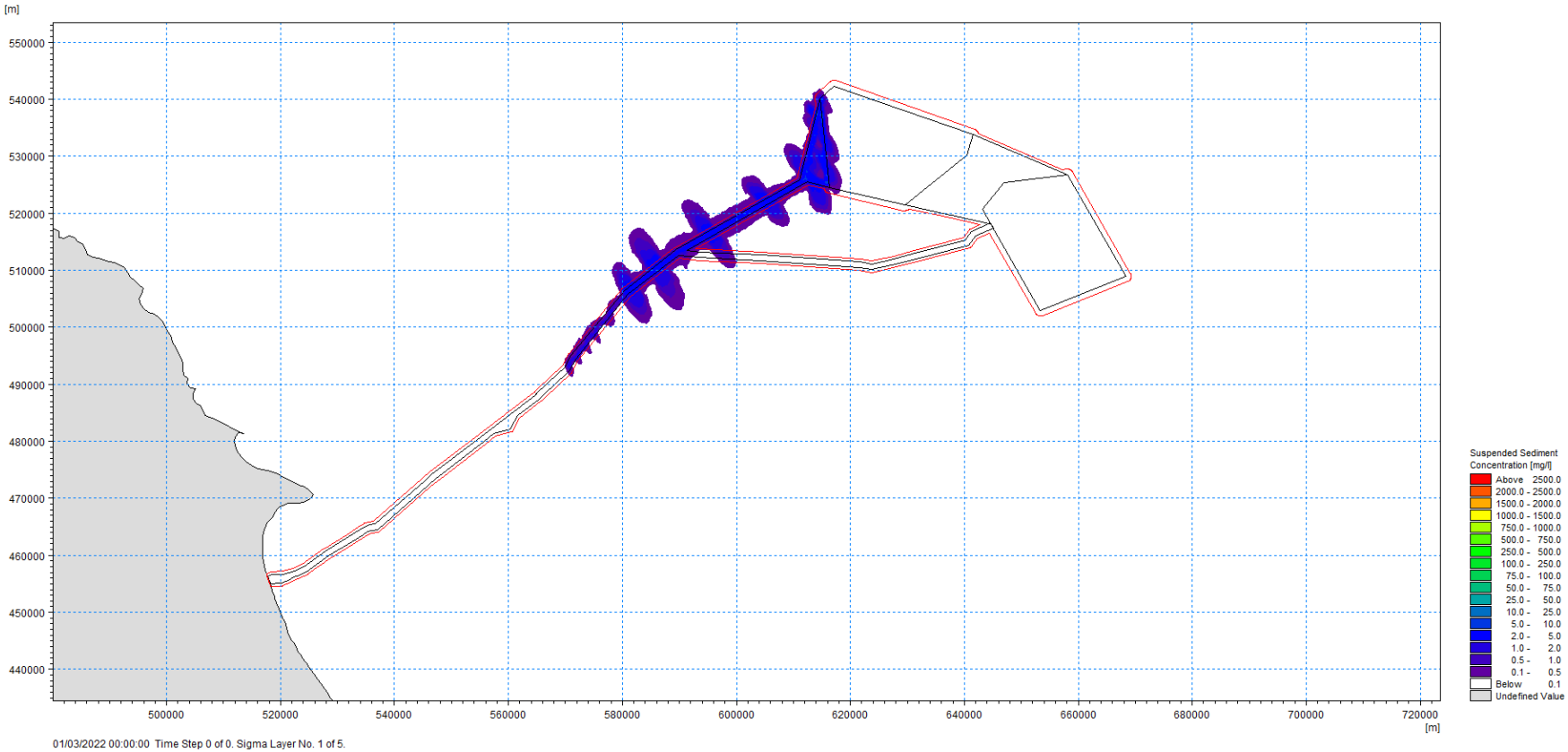

Figure D-3: Maximum Suspended Sediment Concentration (bottom layer) – Export Cable Route to DBS West – Levelling

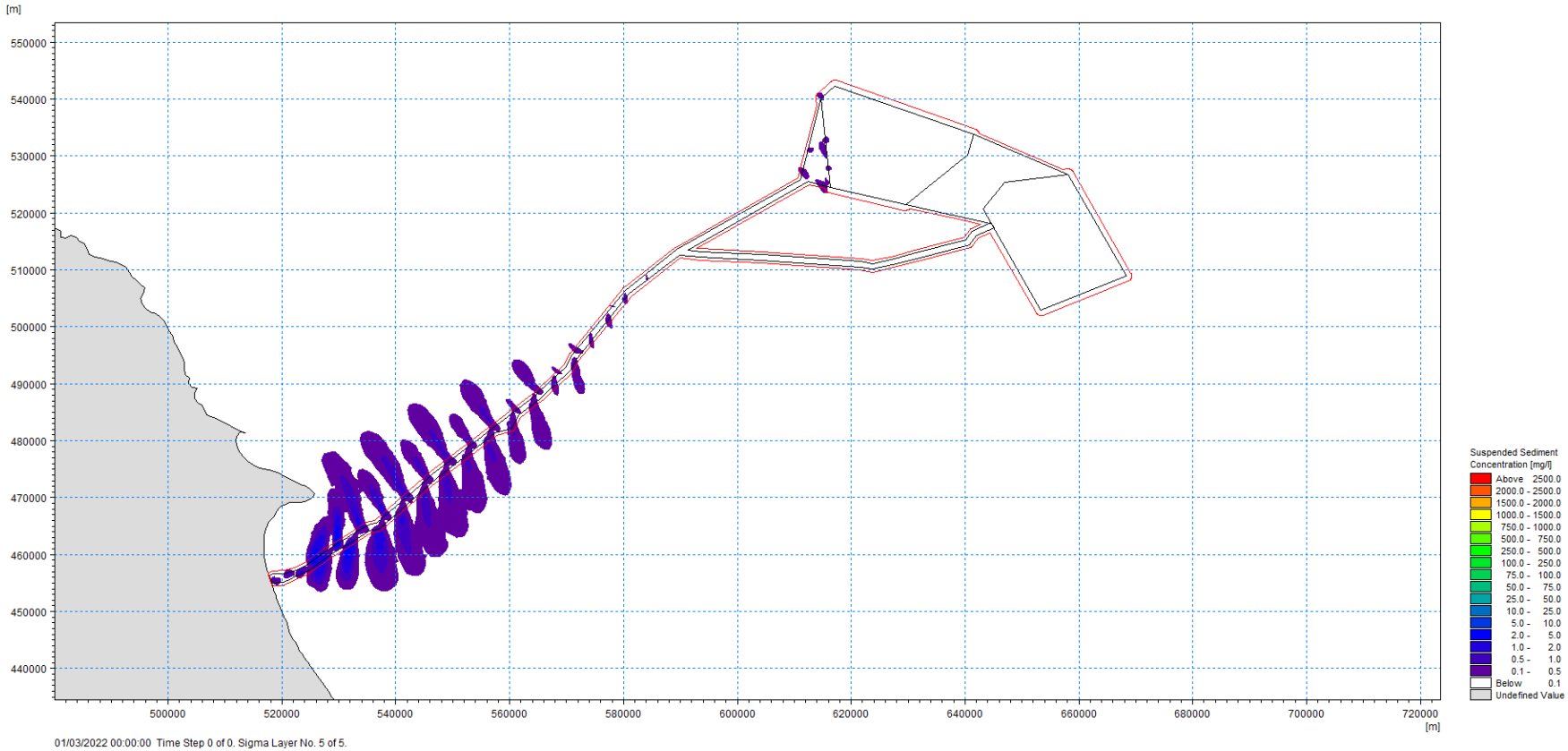

Figure D-4: Maximum Suspended Sediment Concentration (surface layer) – Export Cable Route to DBS West – Trenching

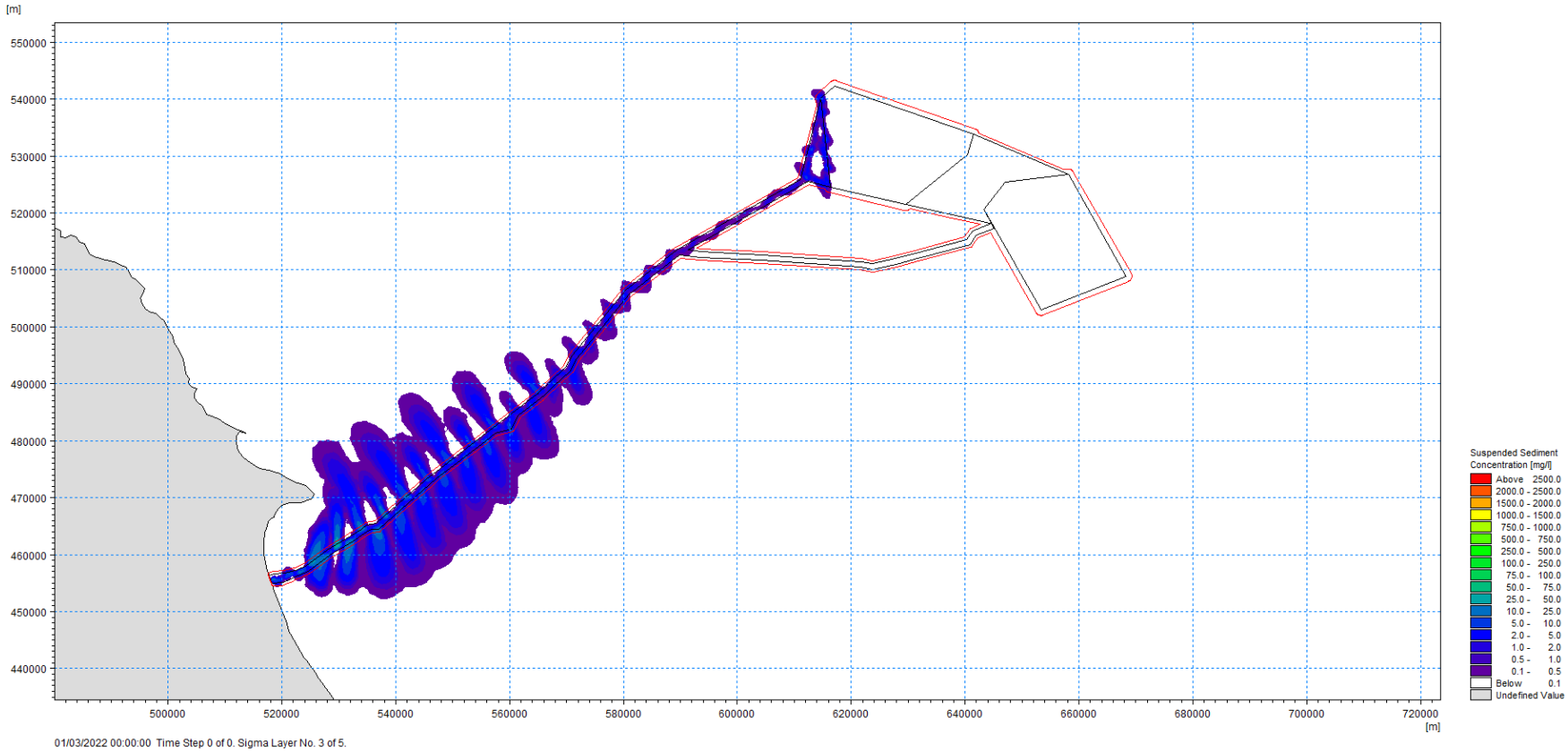

Figure D-5: Maximum Suspended Sediment Concentration (middle layer) – Export Cable Route to DBS West – Trenching

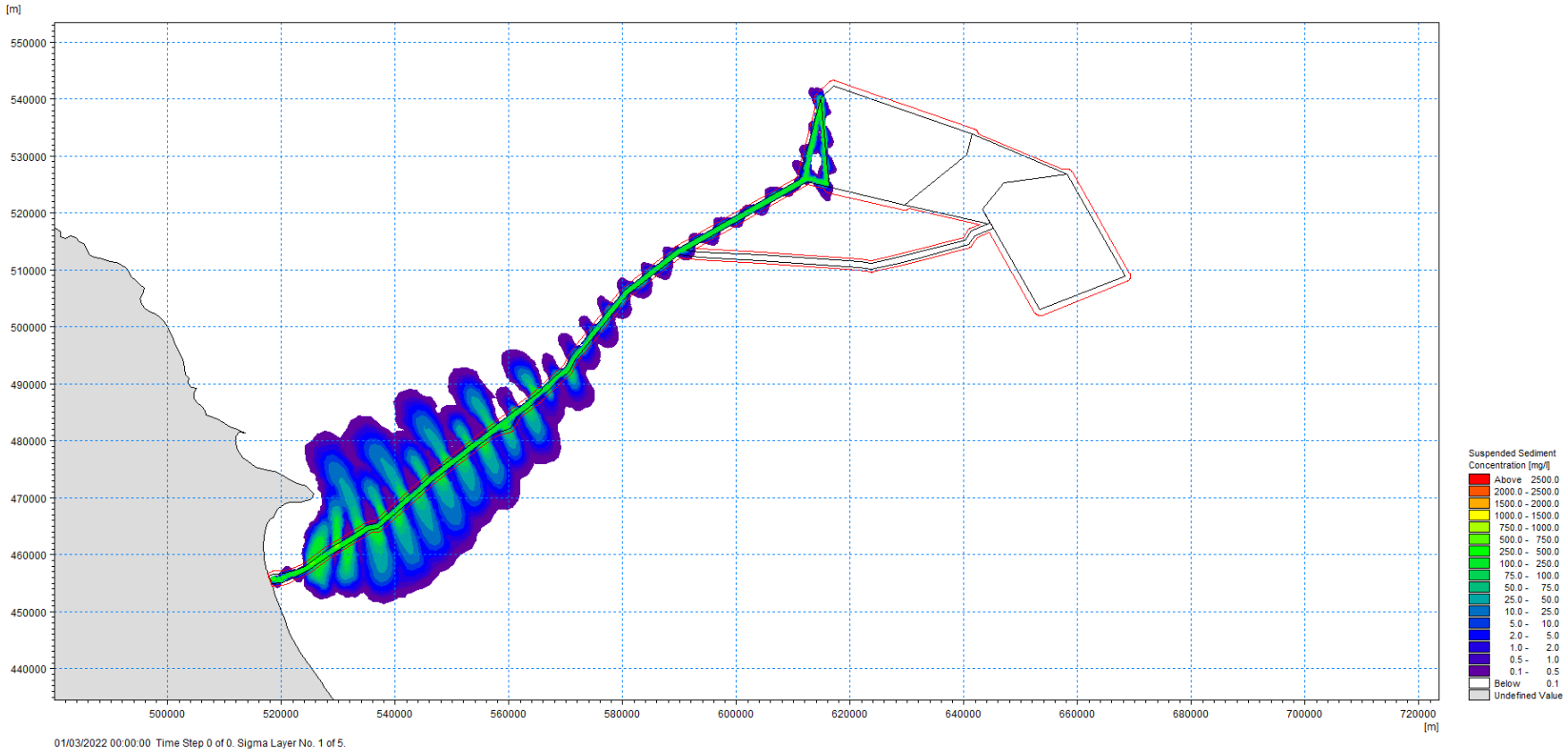

Figure D-6: Maximum Suspended Sediment Concentration (bottom layer) – Export Cable Route to DBS West – Trenching

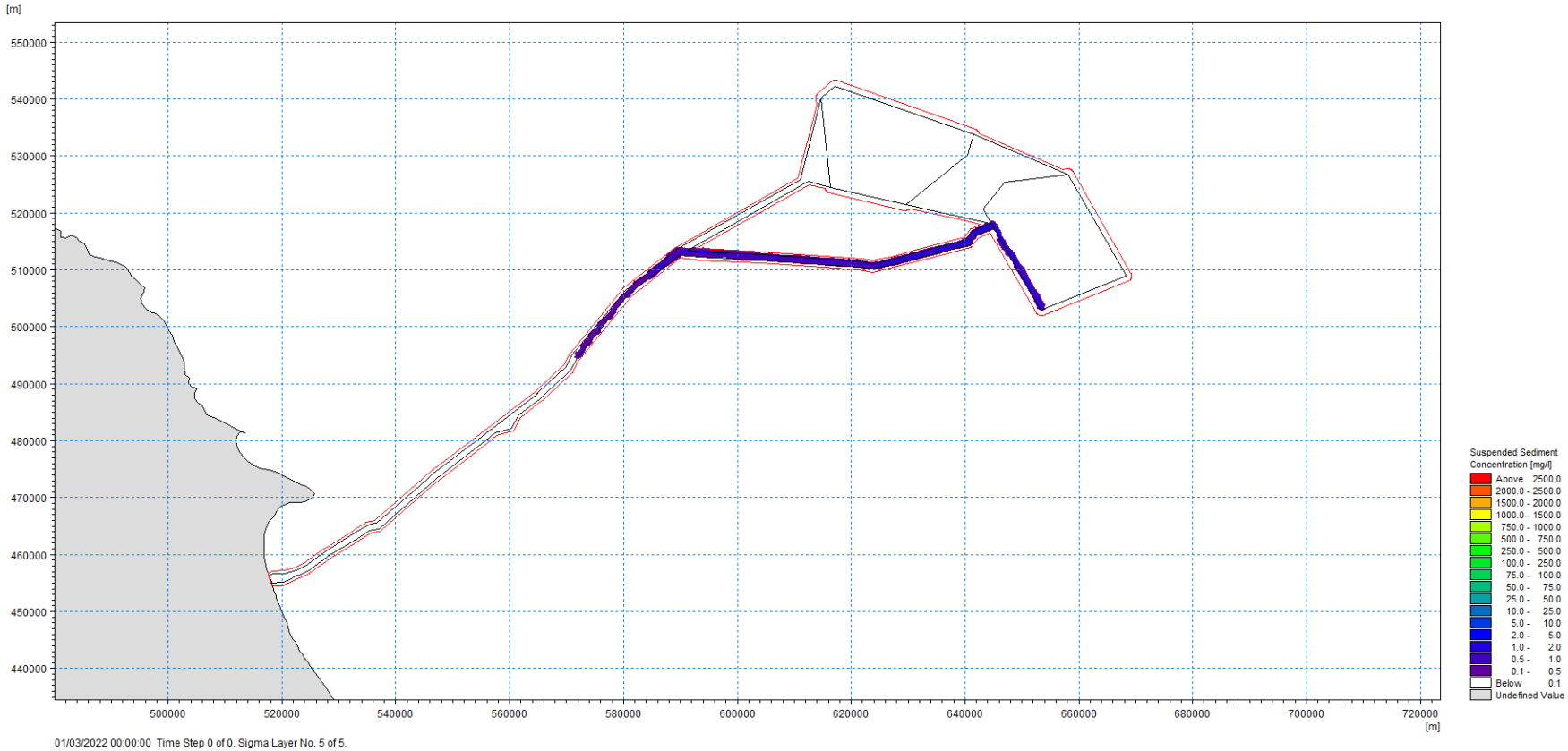

Figure D-7: Maximum Suspended Sediment Concentration (surface layer) – Export Cable Route to DBS East – Levelling

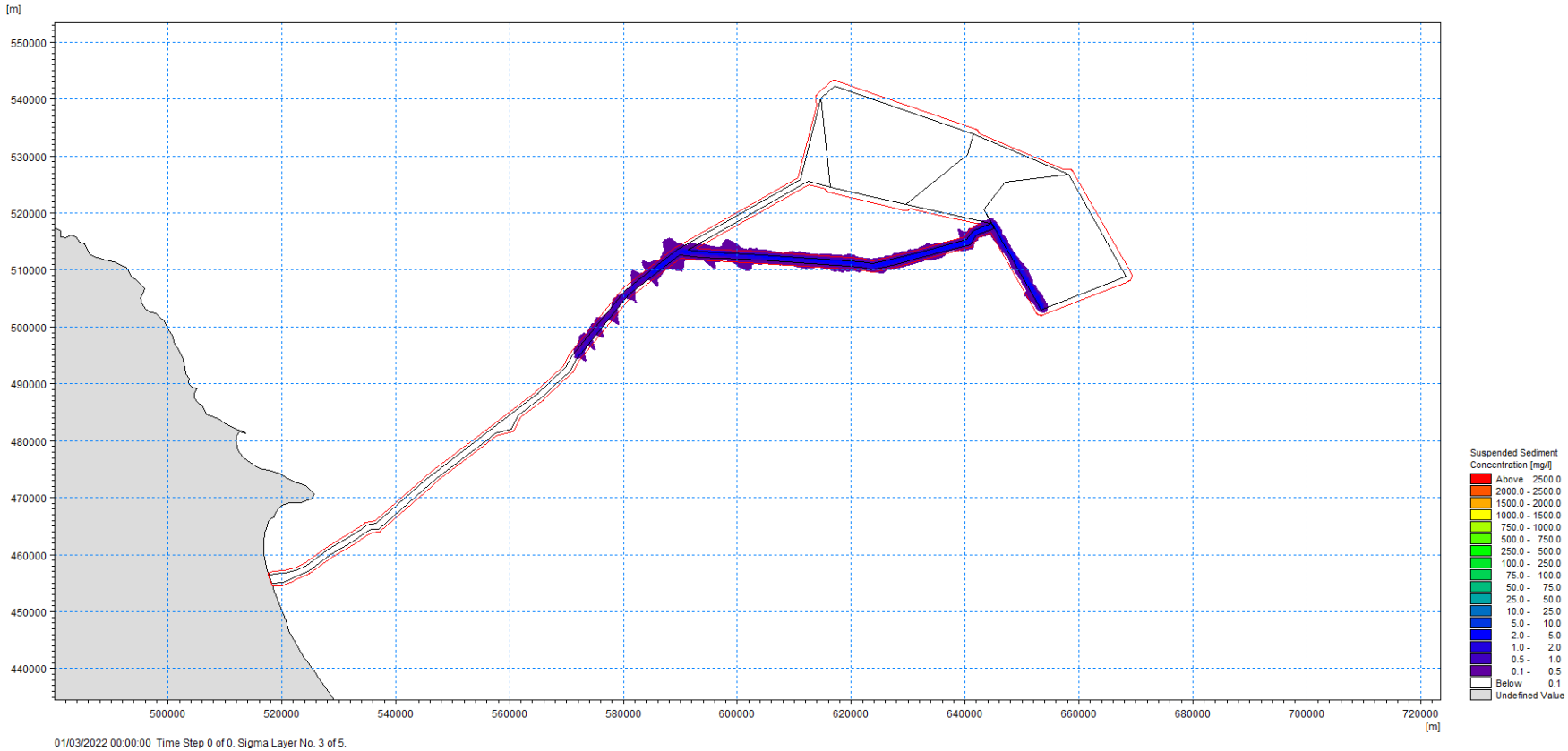

Figure D-8: Maximum Suspended Sediment Concentration (middle layer) – Export Cable Route to DBS East – Levelling

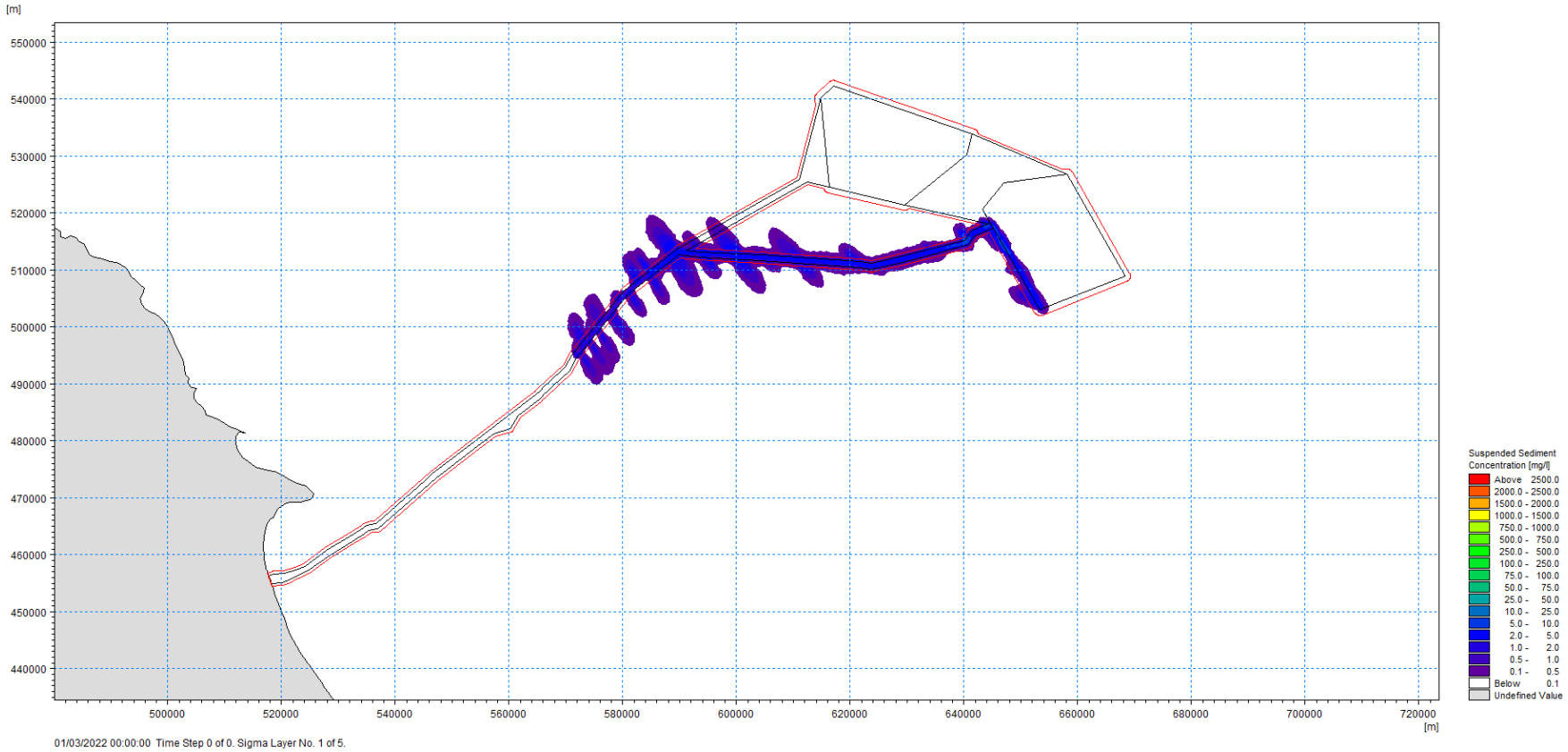

Figure D-9: Maximum Suspended Sediment Concentration (bottom layer) – Export Cable Route to DBS East – Levelling

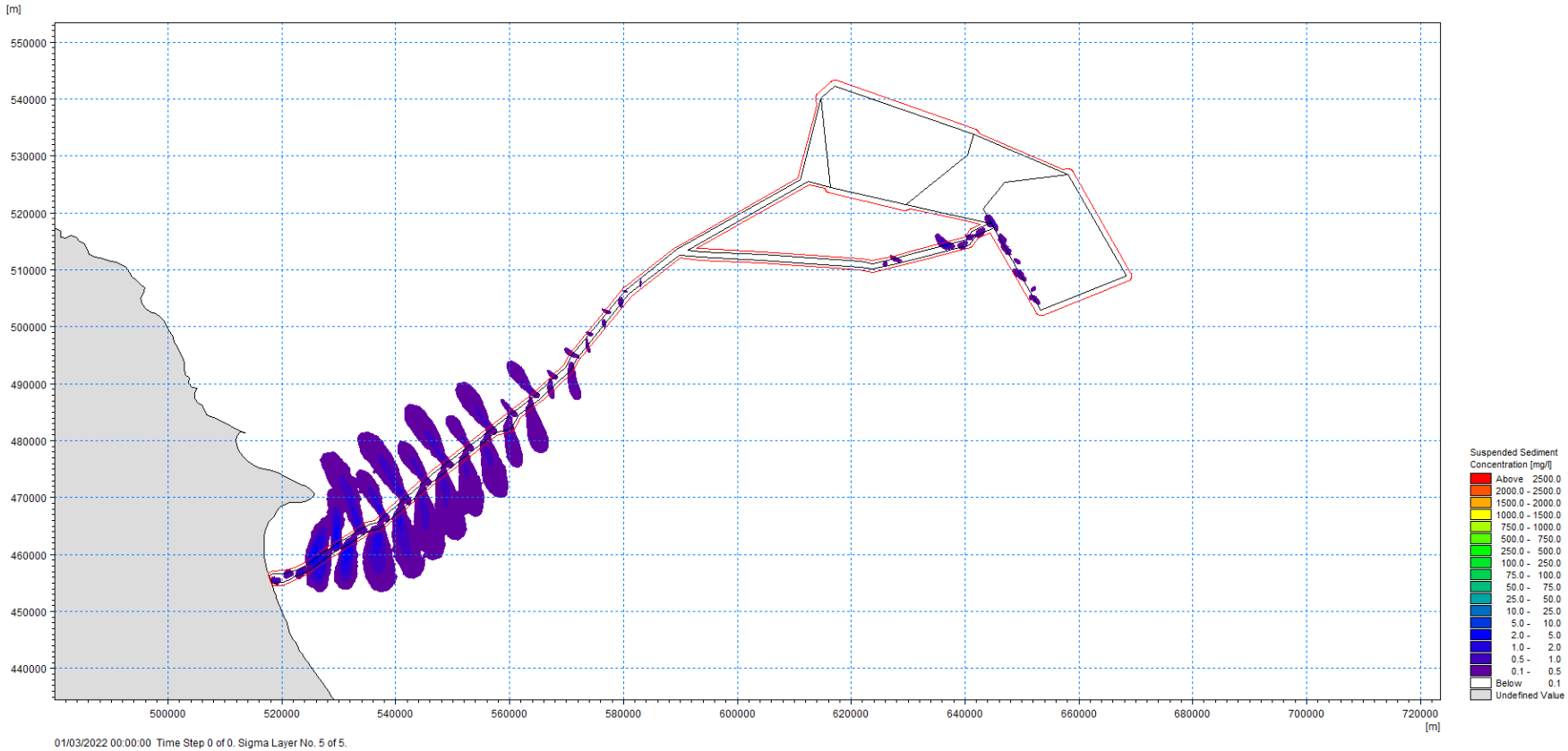

Figure D-10: Maximum Suspended Sediment Concentration (surface layer) – Export Cable Route to DBS East – Trenching

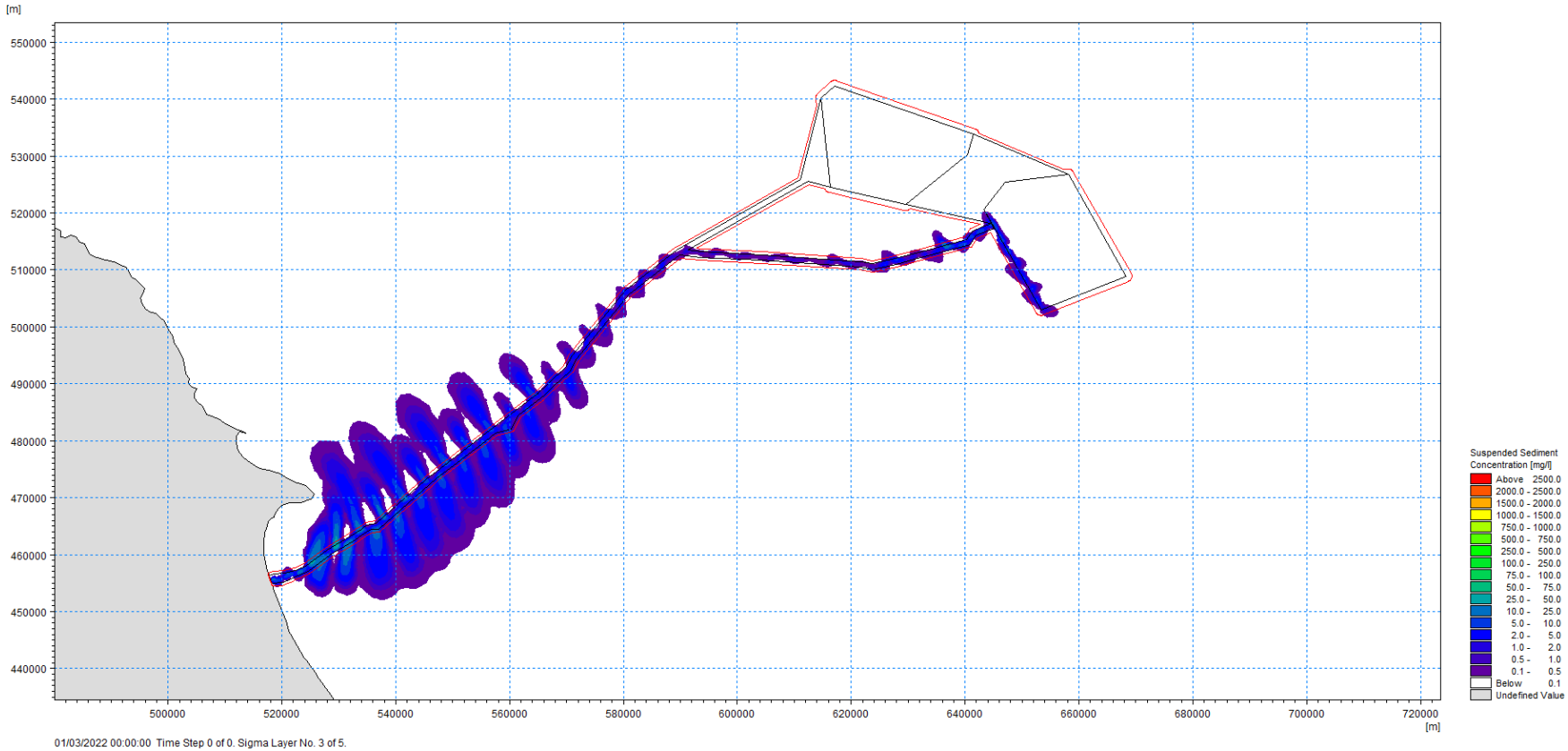

Figure D-11: Maximum Suspended Sediment Concentration (middle layer) – Export Cable Route to DBS East – Trenching

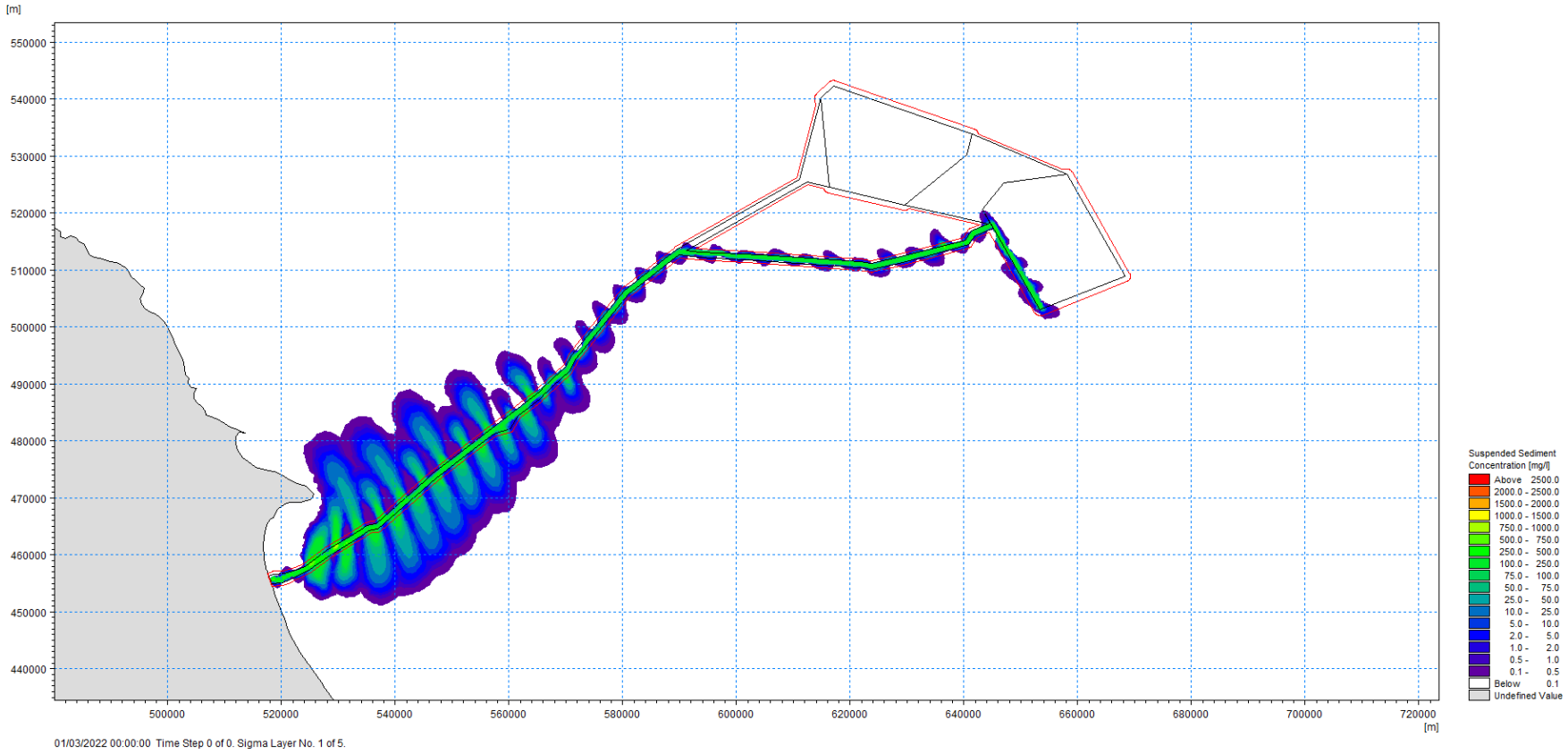

Figure D-12: Maximum Suspended Sediment Concentration (bottom layer) – Export Cable Route to DBS East – Trenching

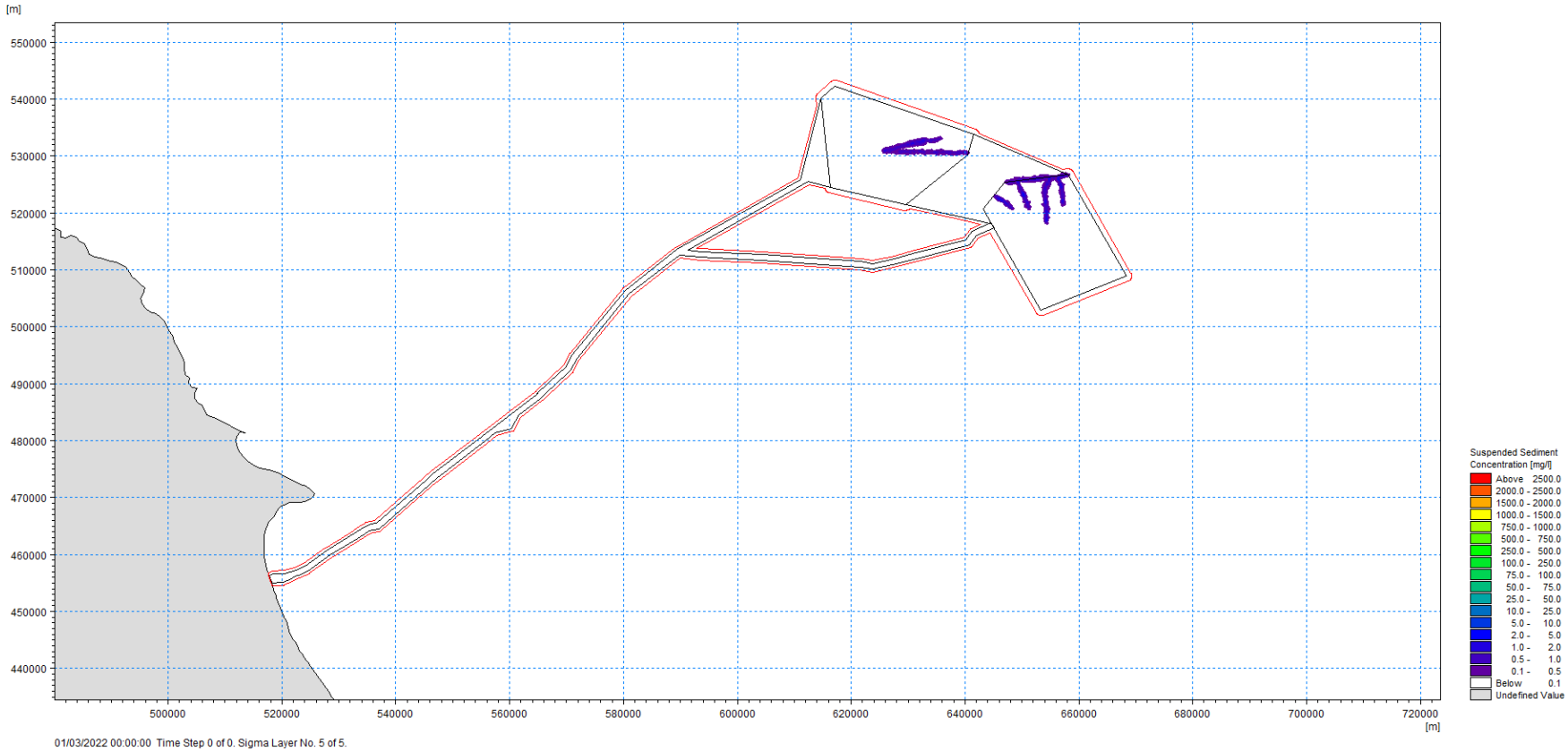

Figure D-13: Maximum Suspended Sediment Concentration (surface layer) – Array Cable – Levelling

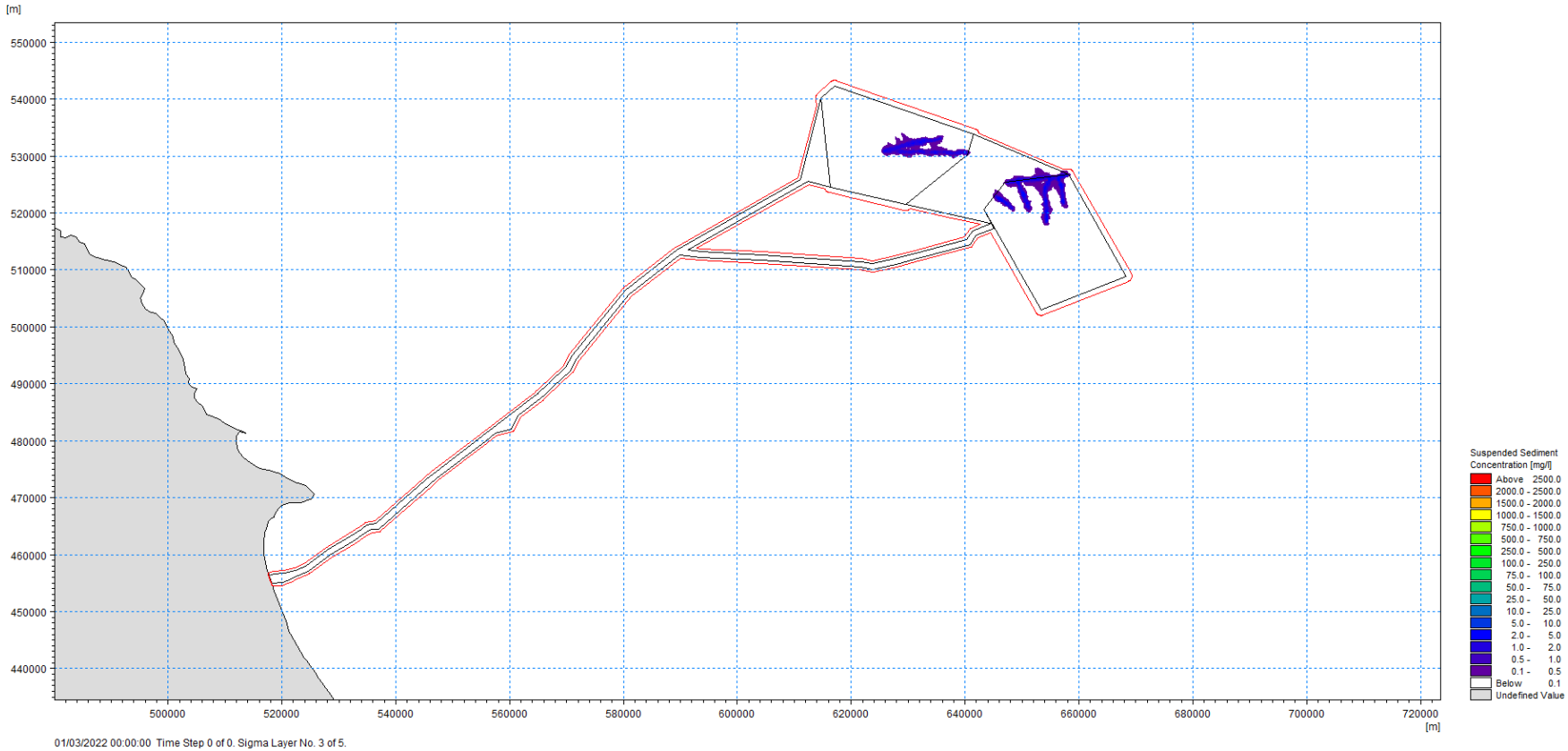

Figure D-14: Maximum Suspended Sediment Concentration (middle layer) – Array Cable – Levelling

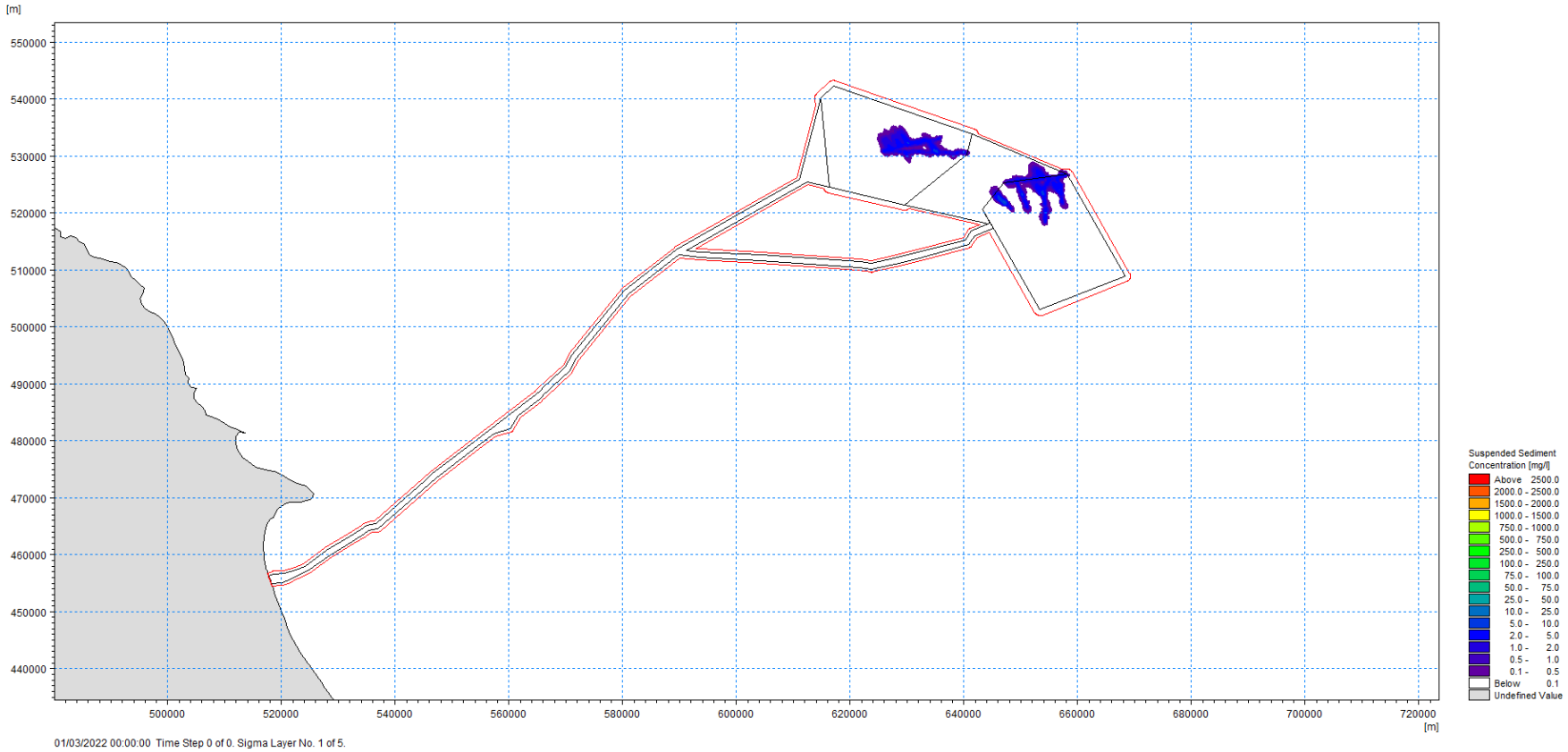

Figure D-15: Maximum Suspended Sediment Concentration (bottom layer) – Array Cable – Levelling

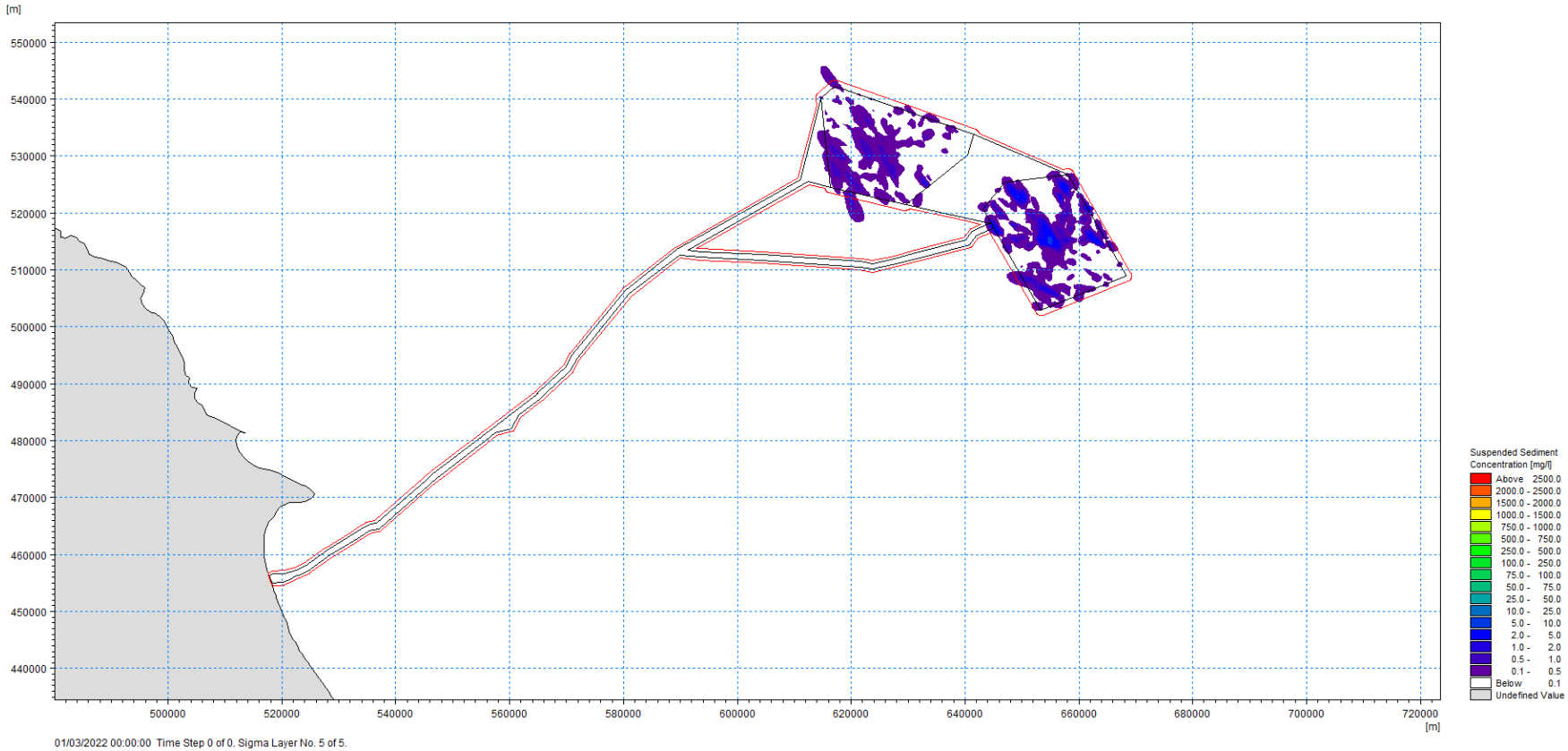

Figure D-16: Maximum Suspended Sediment Concentration (surface layer) – Array Cable – Trenching

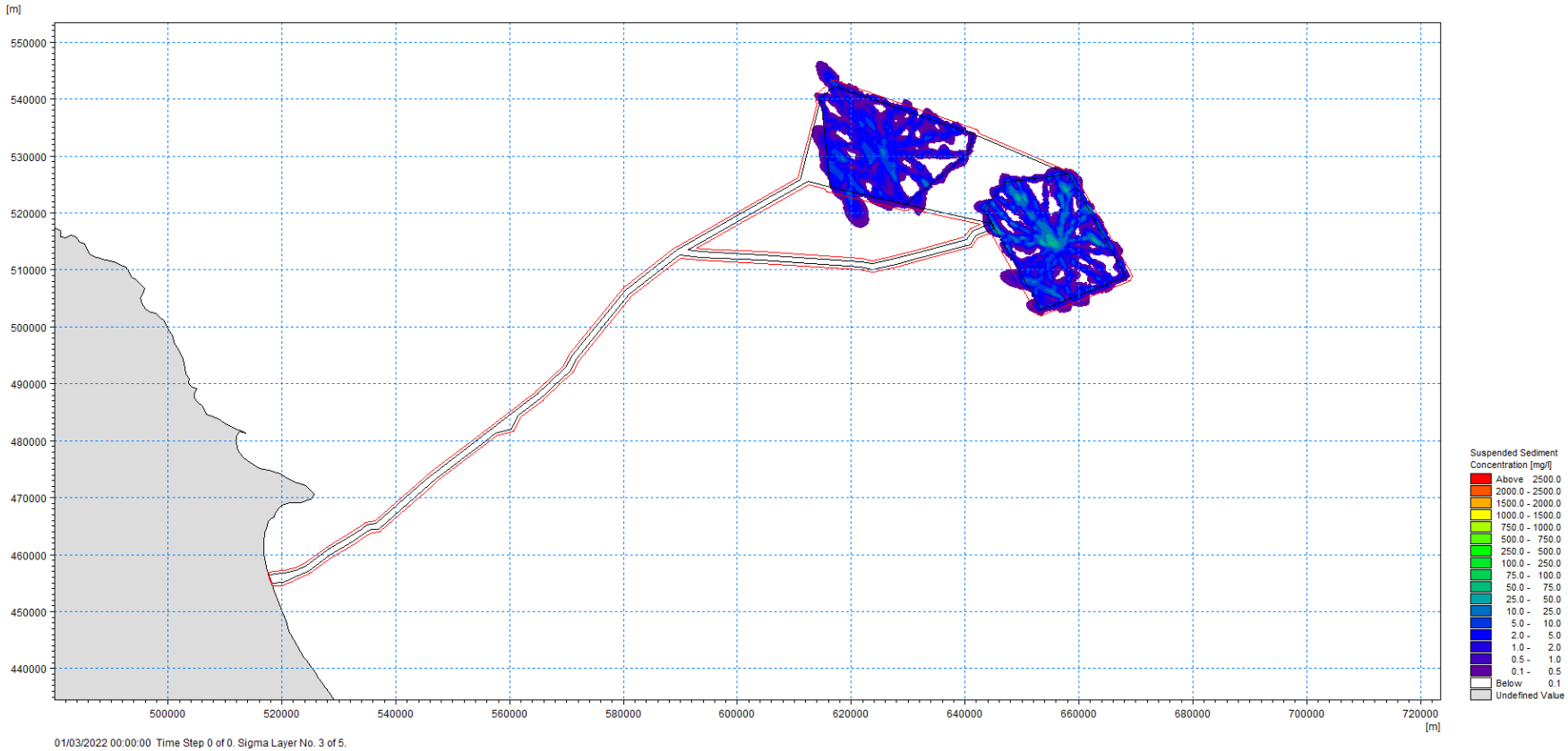

Figure D-17: Maximum Suspended Sediment Concentration (middle layer) – Array Cable – Trenching

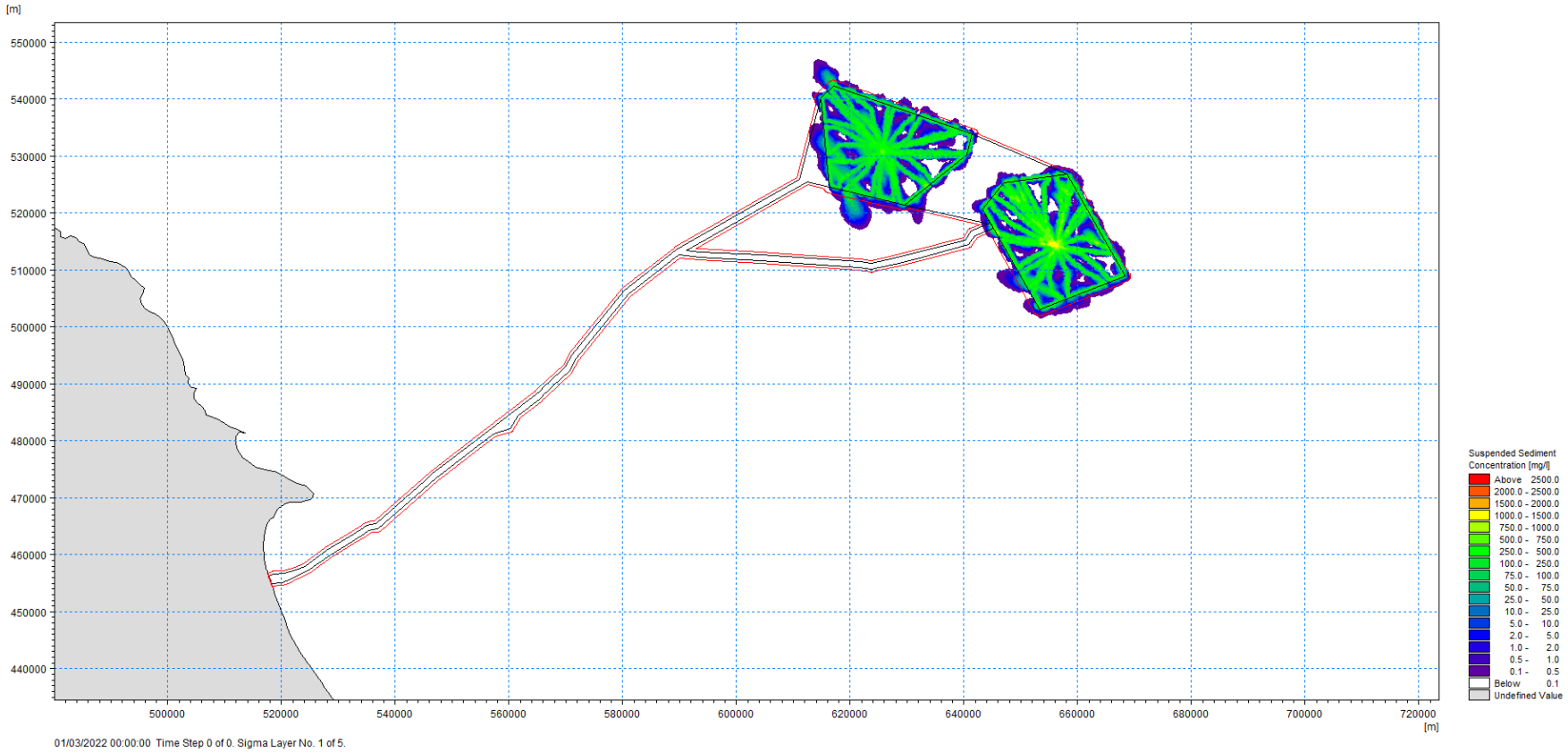

Figure D-18: Maximum Suspended Sediment Concentration (bottom layer) – Array Cable – Trenching

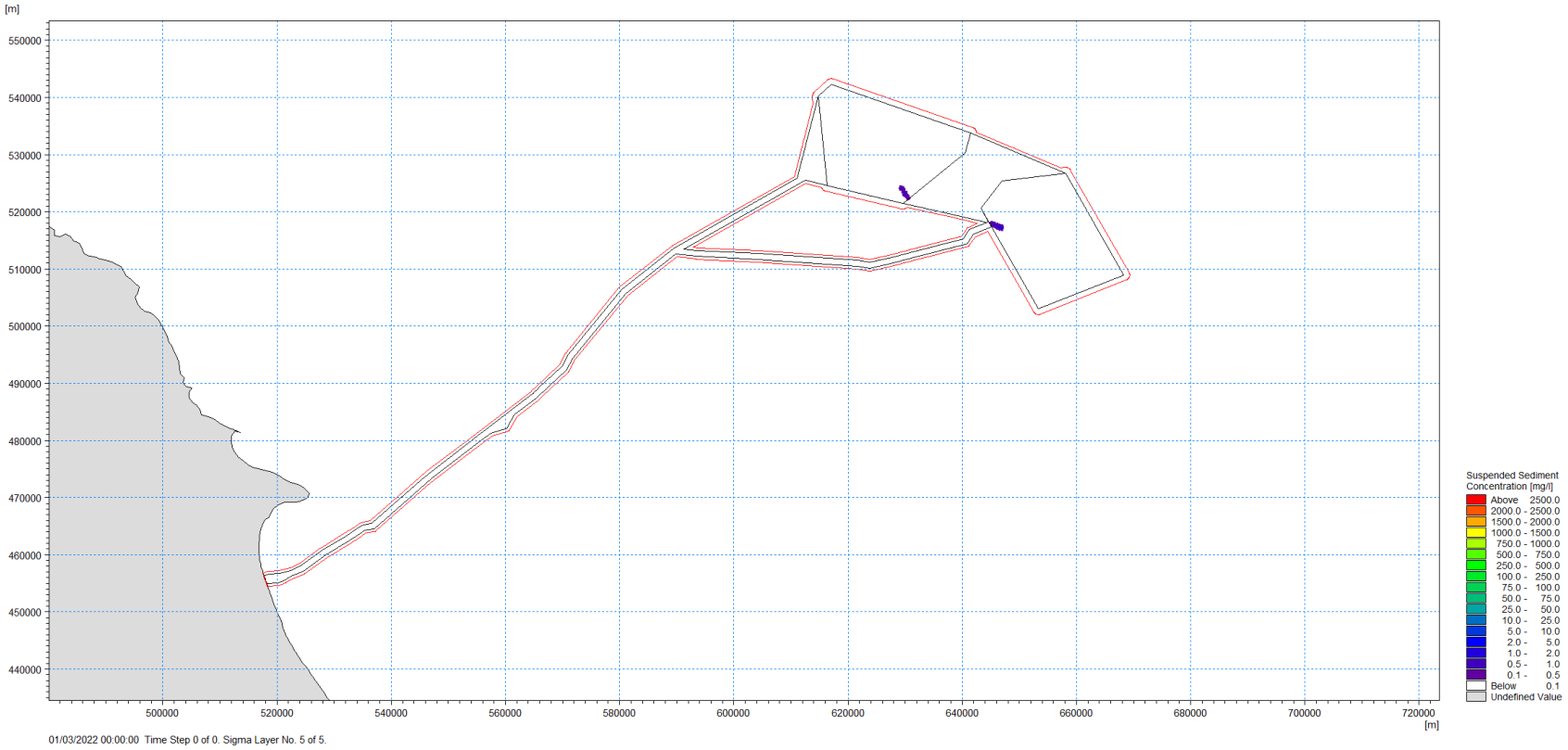

Figure D-19: Maximum Suspended Sediment Concentration (surface layer) – Inter-platform Cable (West and East) – Levelling

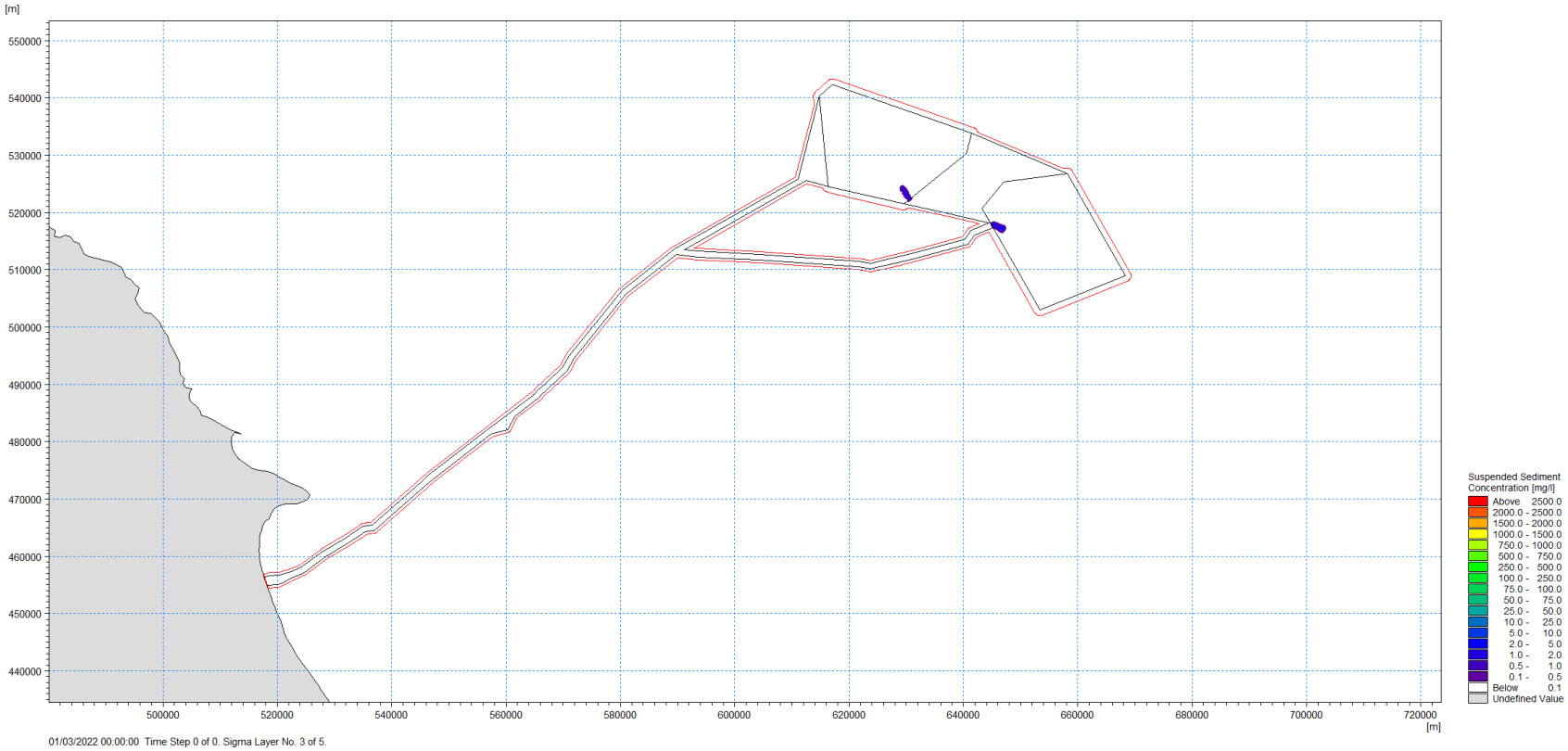

Figure D-20: Maximum Suspended Sediment Concentration (middle layer) – Inter-platform Cable (West and East) – Levelling

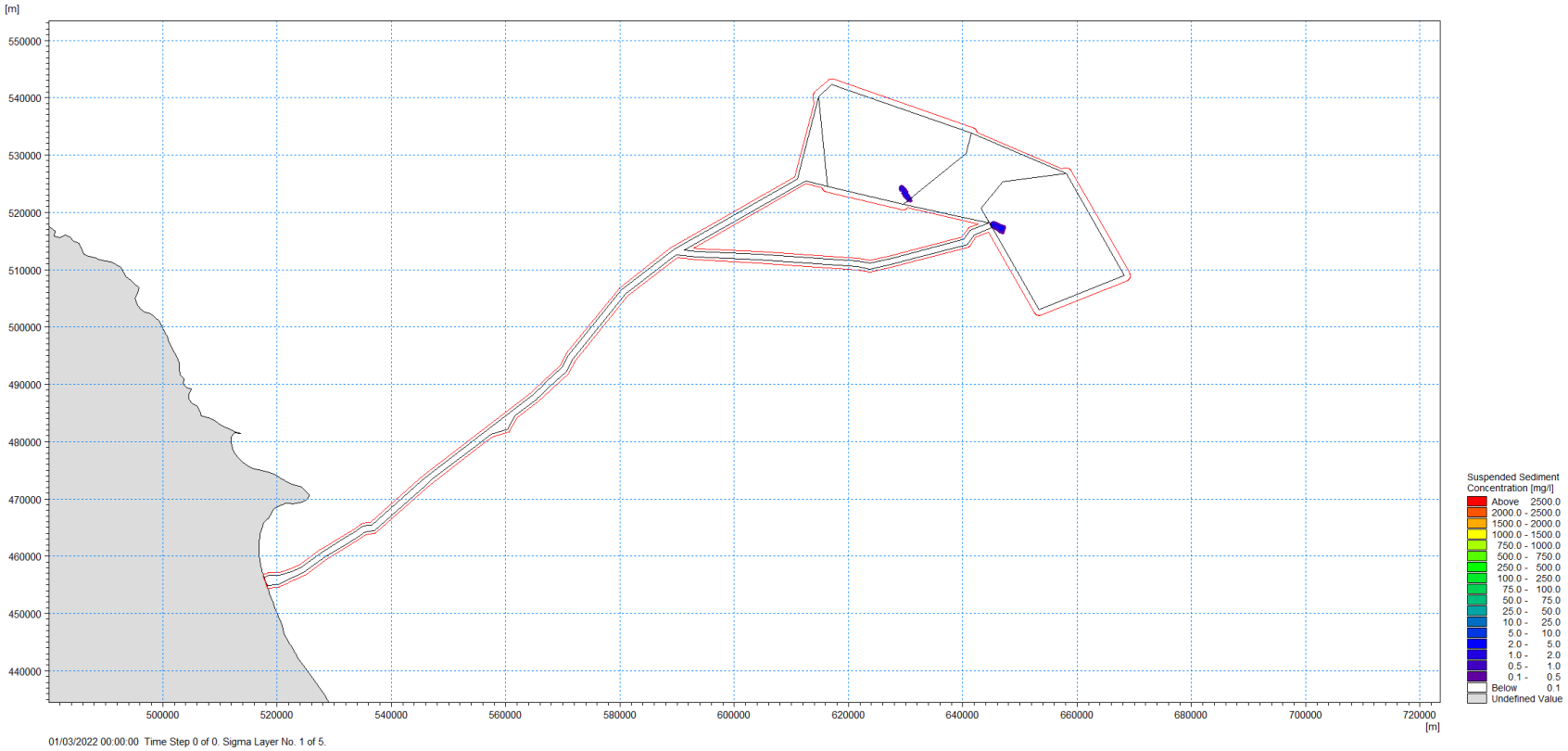

Figure D-21: Maximum Suspended Sediment Concentration (bottom layer) – Inter-platform Cable (West and East) – Levelling

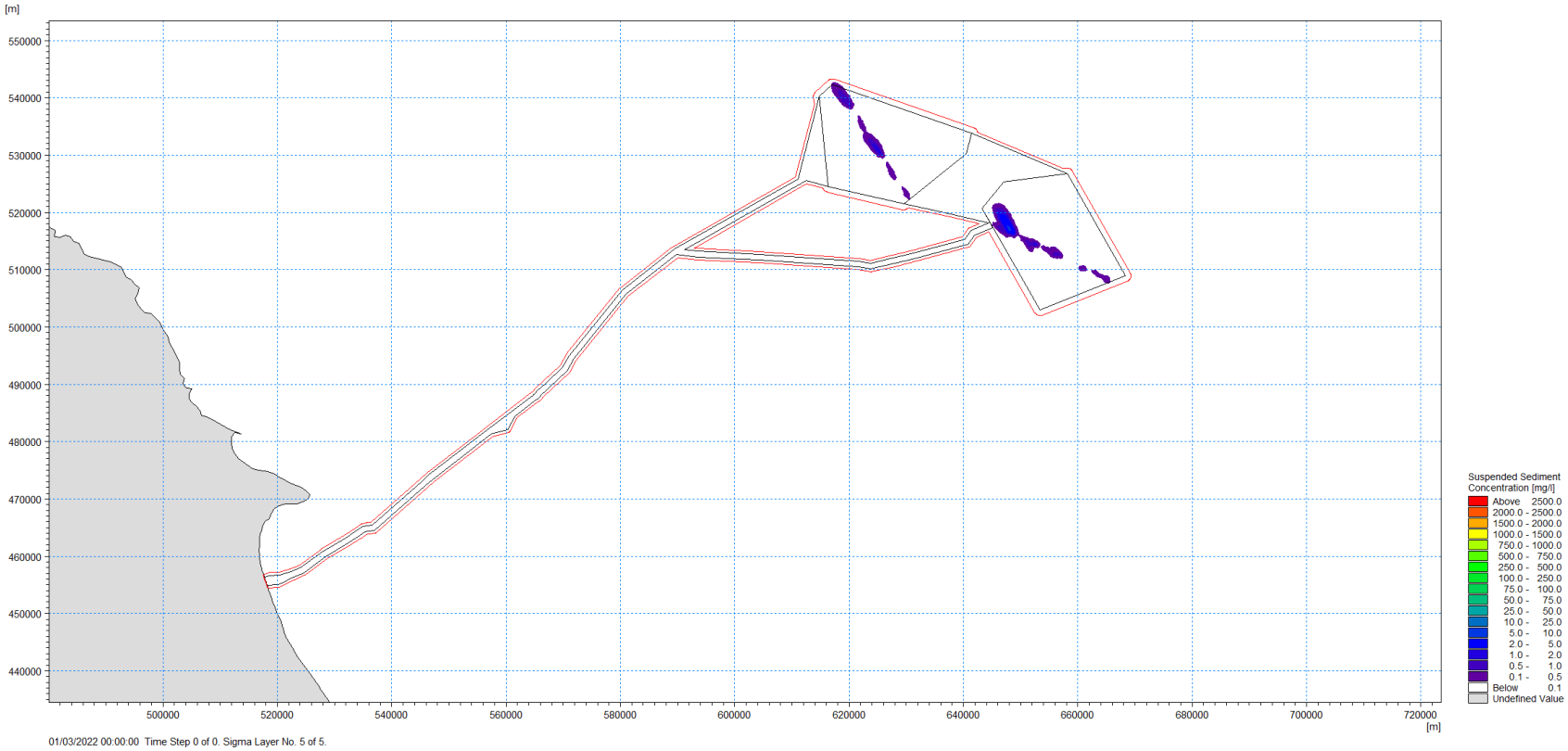

Figure D-22: Maximum Suspended Sediment Concentration (surface layer) – Inter-platform Cable (West and East) – Trenching

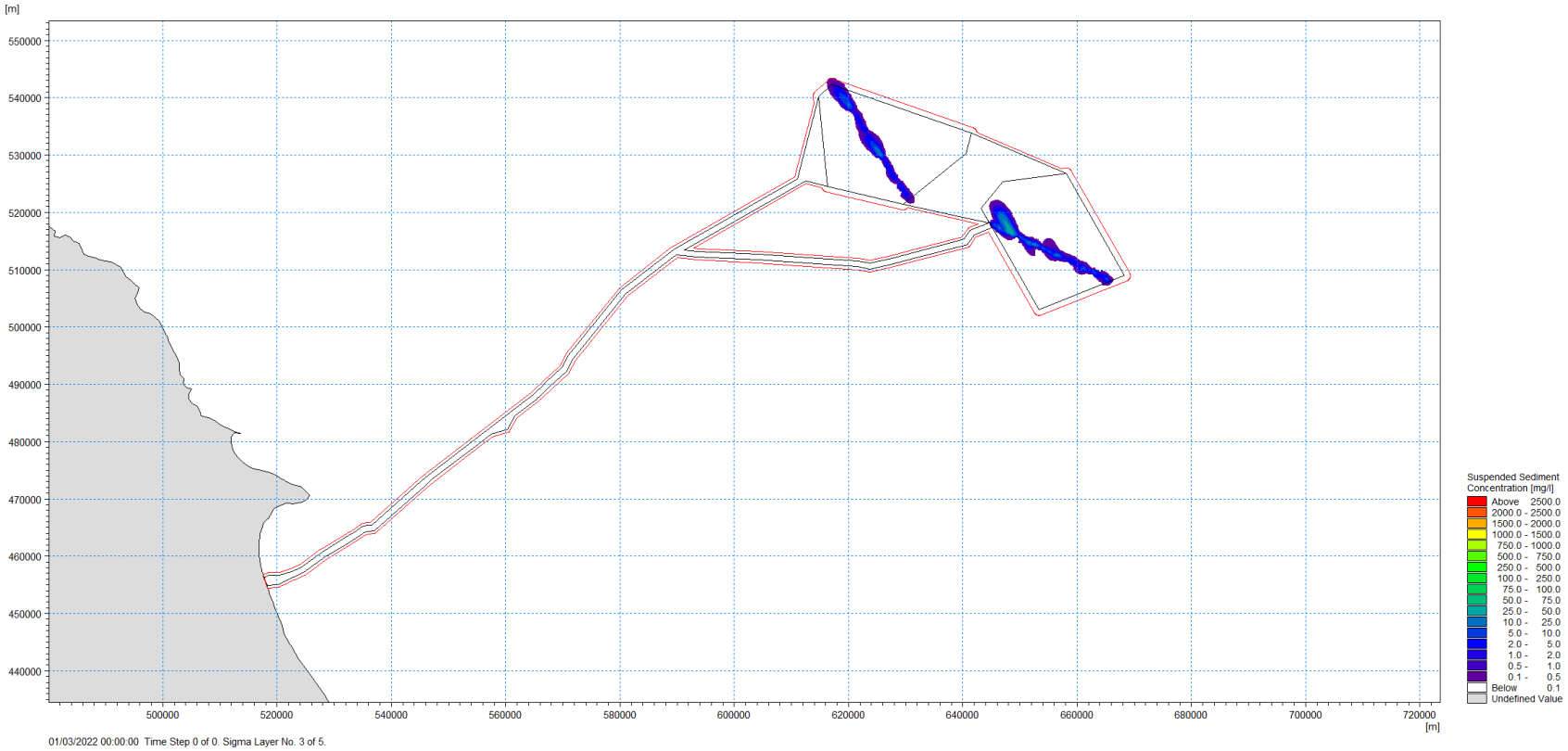

Figure D-23: Maximum Suspended Sediment Concentration (middle layer) – Inter-platform Cable (West and East) – Trenching

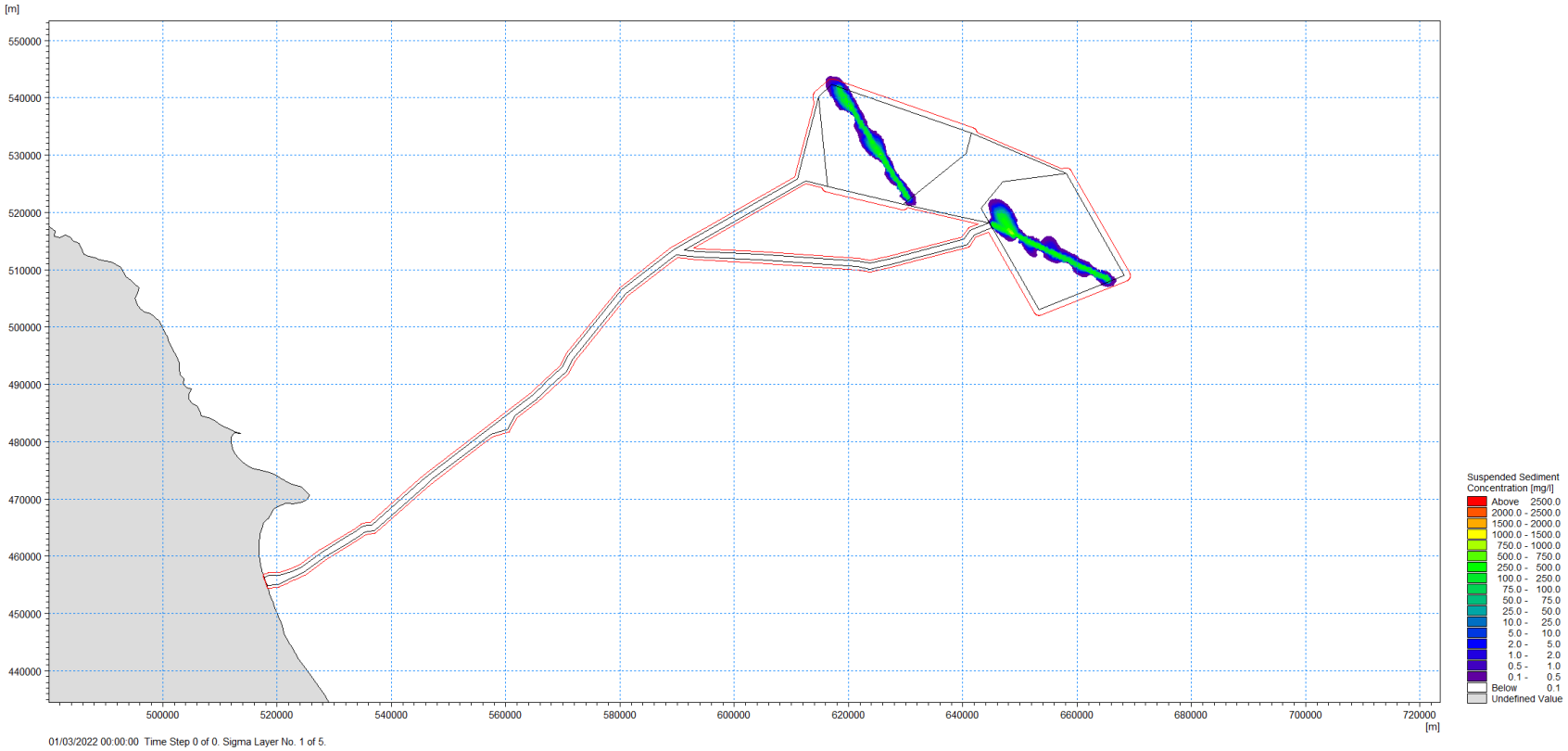

Figure D-24: Maximum Suspended Sediment Concentration (bottom layer) – Inter-platform Cable (West and East) – Trenching

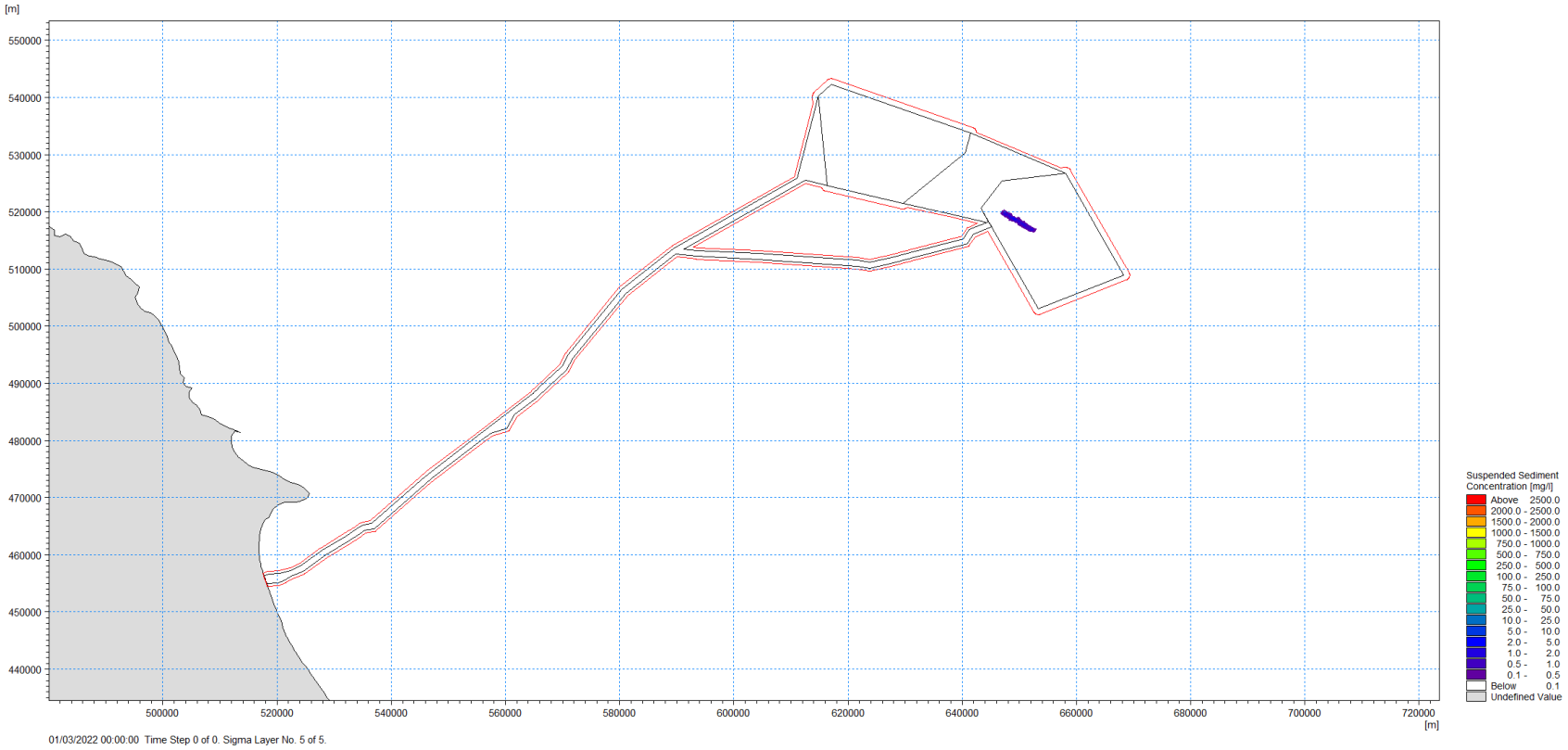

Figure D-25: Maximum Suspended Sediment Concentration (Surface Layer) – Inter-Platform Cable ("West and East") – Levelling

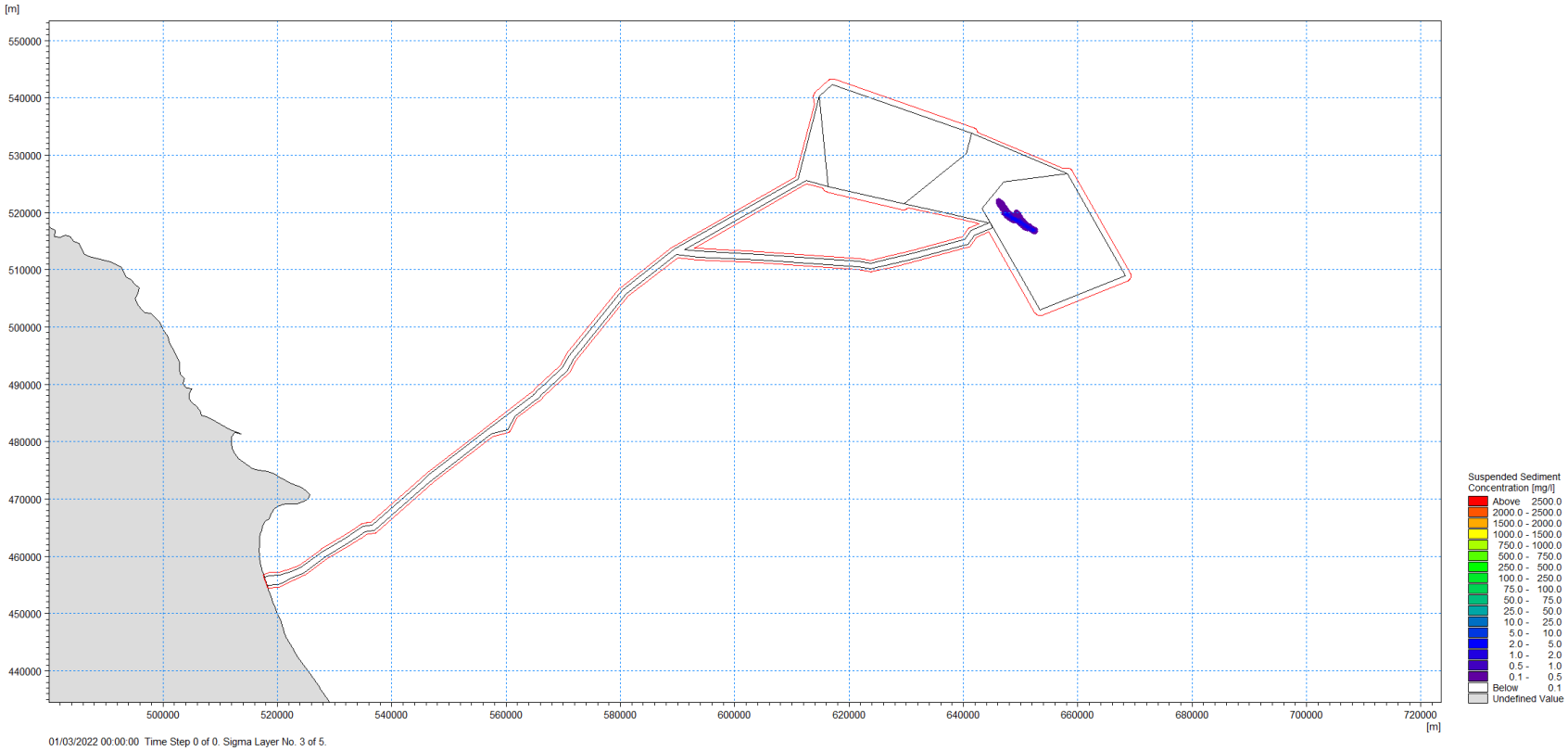

Figure D-26: Maximum Suspended Sediment Concentration (middle layer) – Inter-platform Cable ("West+East") – Levelling

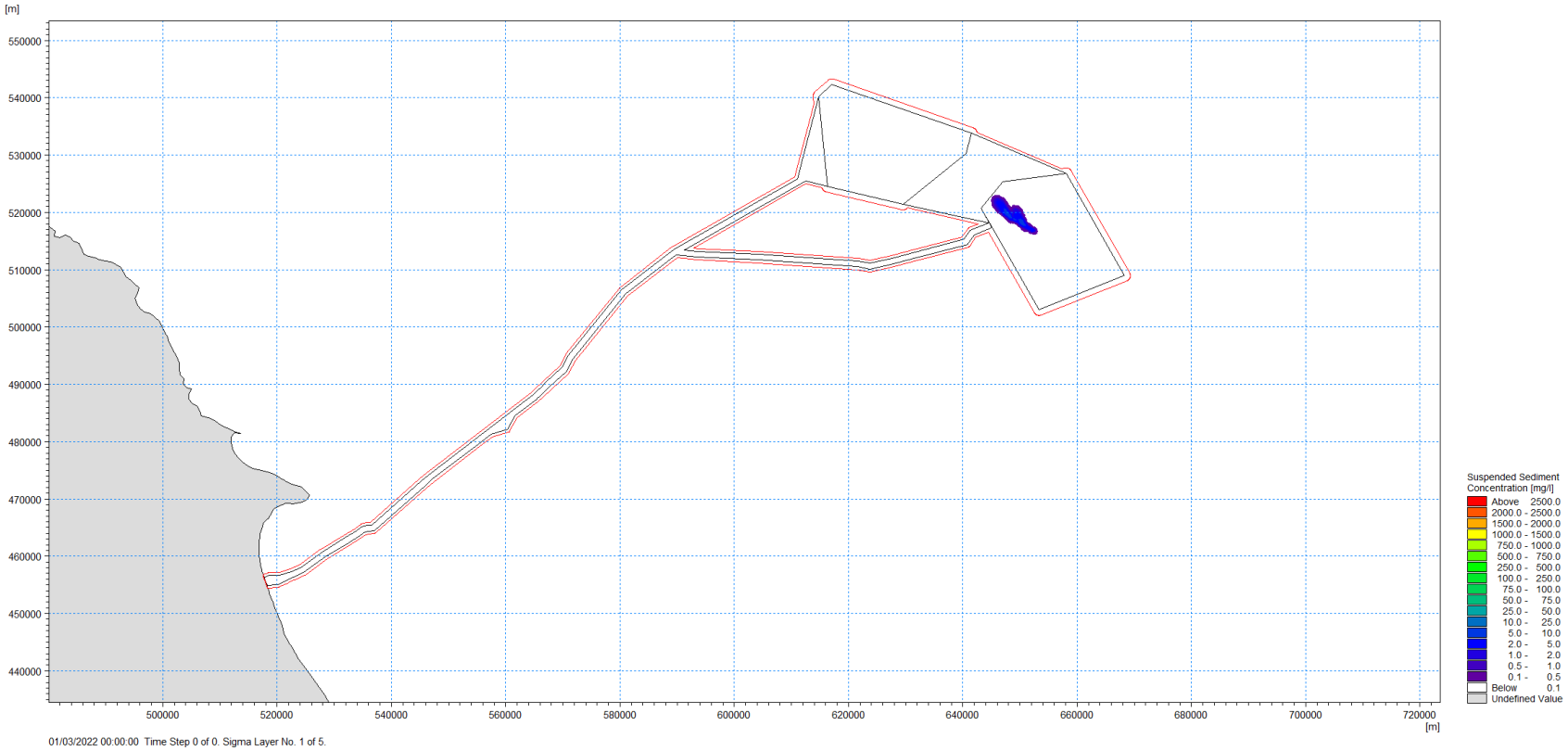

Figure D-27: Maximum Suspended Sediment Concentration (bottom layer) – Inter-platform Cable ("West+East") – Levelling

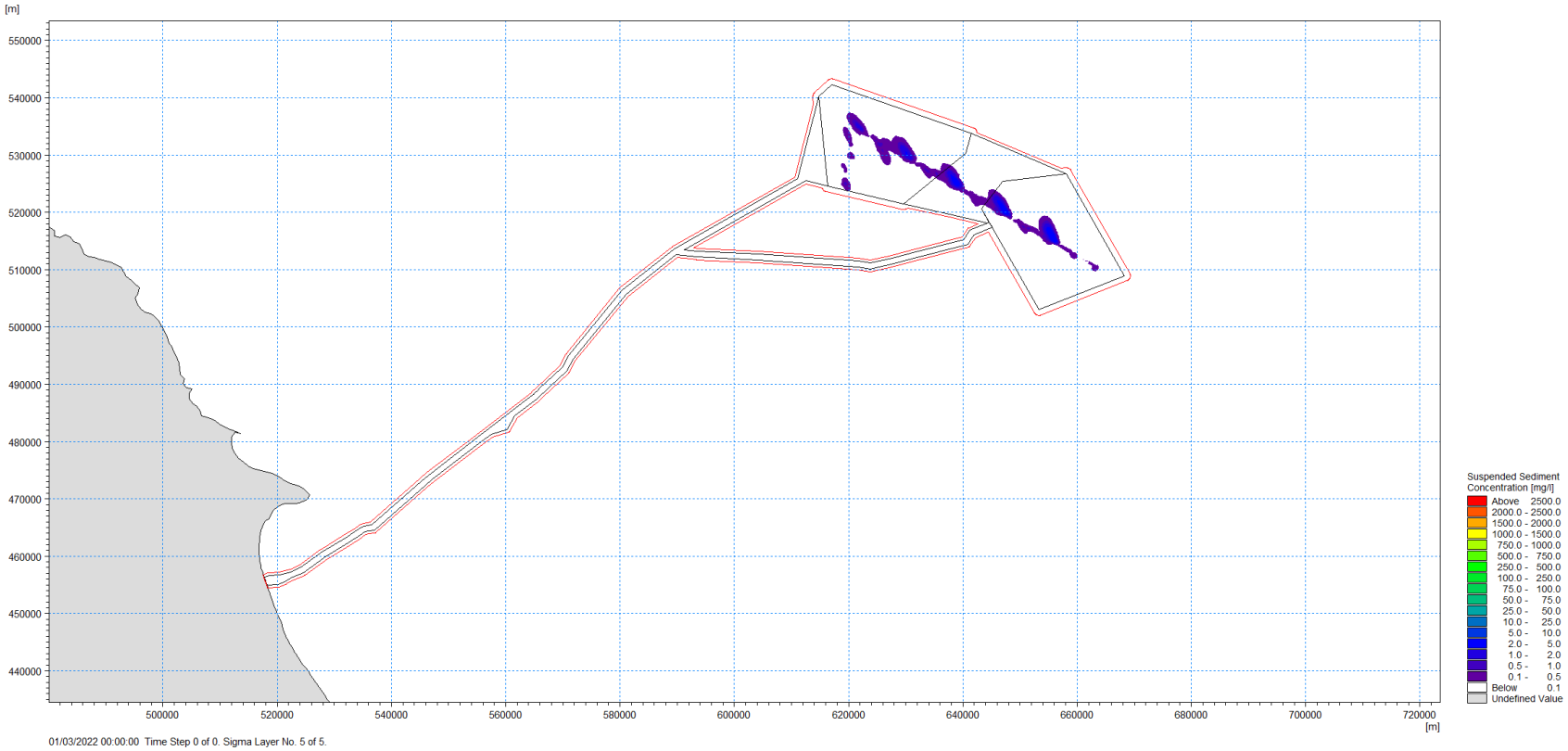

Figure D-28: Maximum Suspended Sediment Concentration (surface layer) – Inter-platform Cable ("West+East") – Trenching

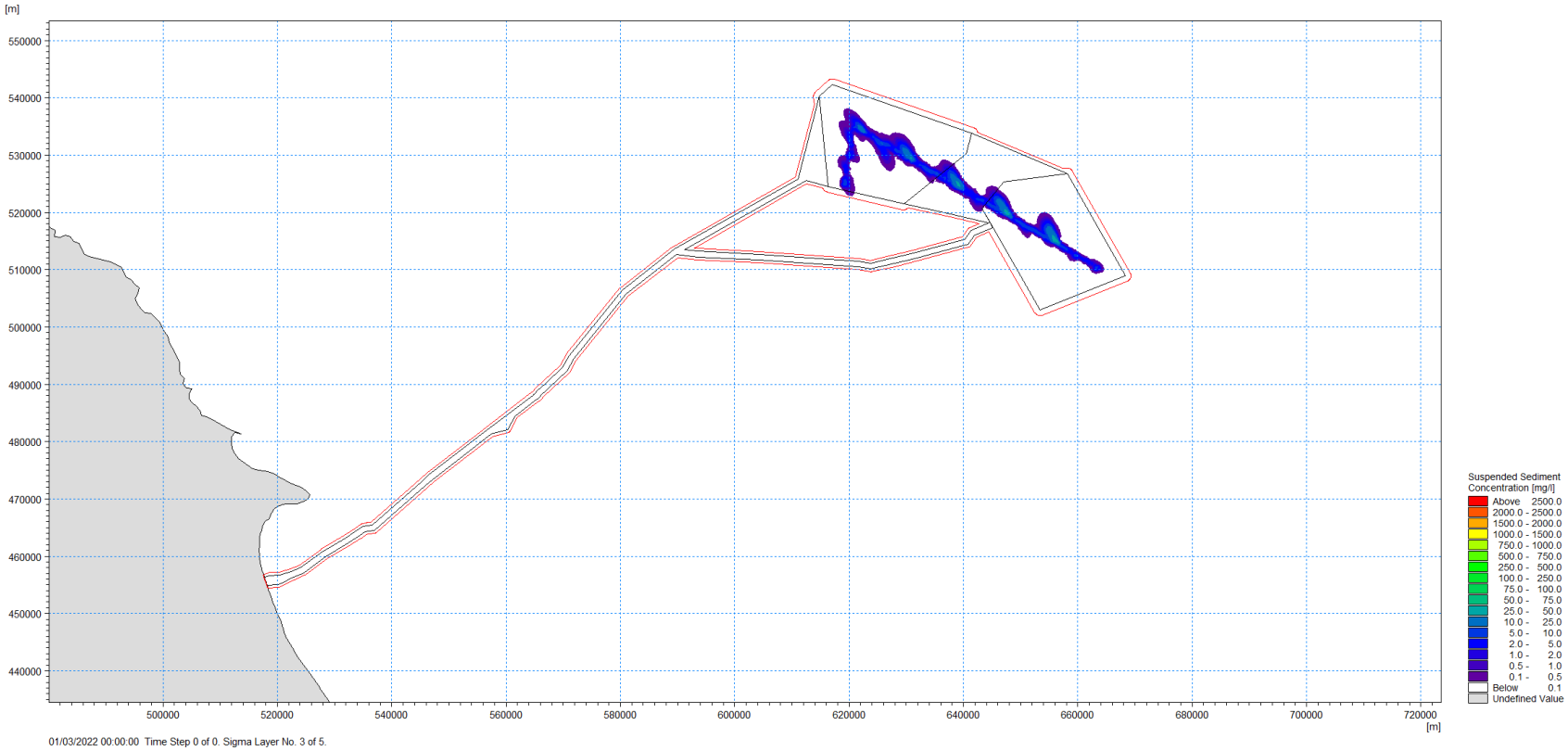

Figure D-29: Maximum Suspended Sediment Concentration (middle layer) – Inter-platform Cable ("West+East") – Trenching

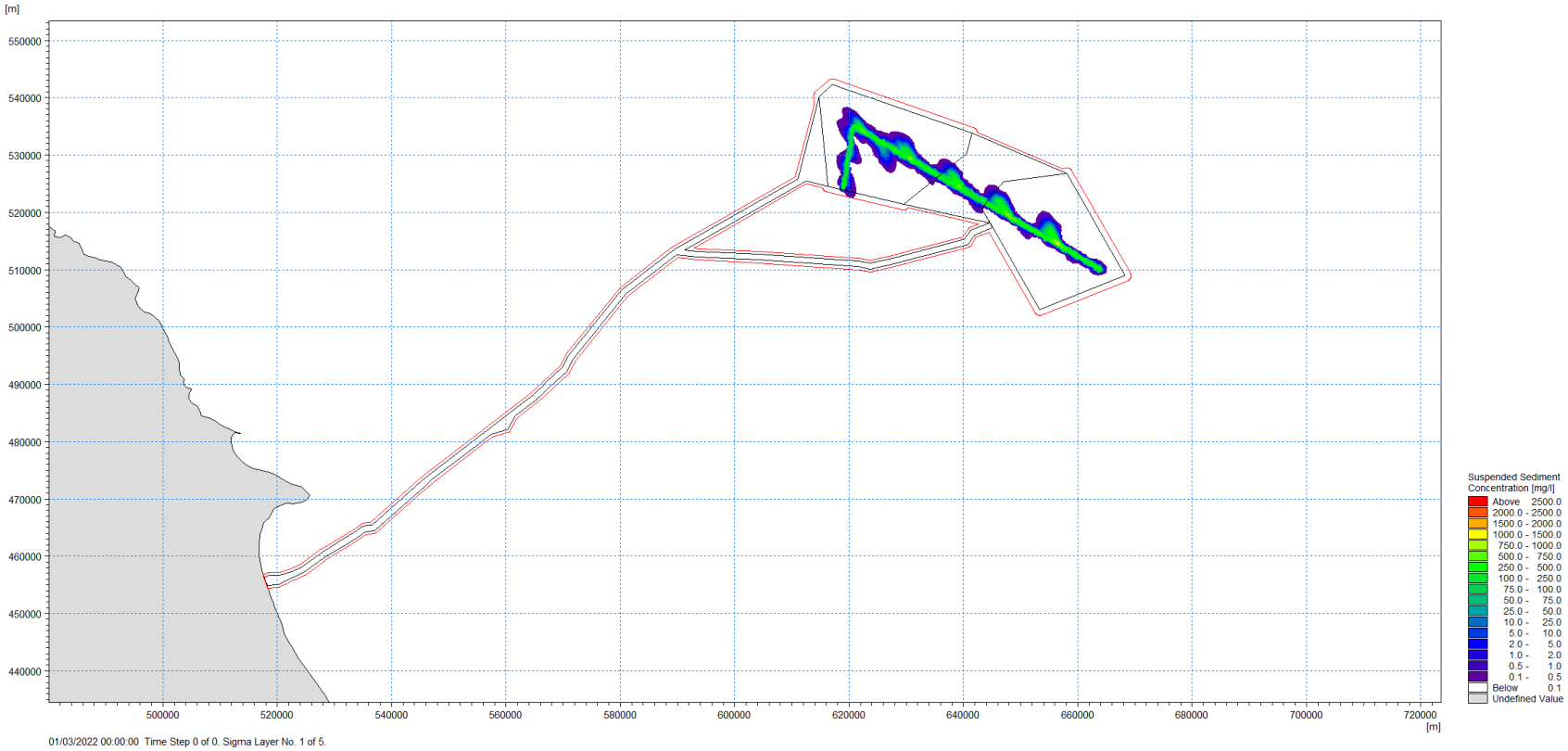

Figure D-30: Maximum Suspended Sediment Concentration (bottom layer) – Inter-platform Cable ("West+East") – Trenching

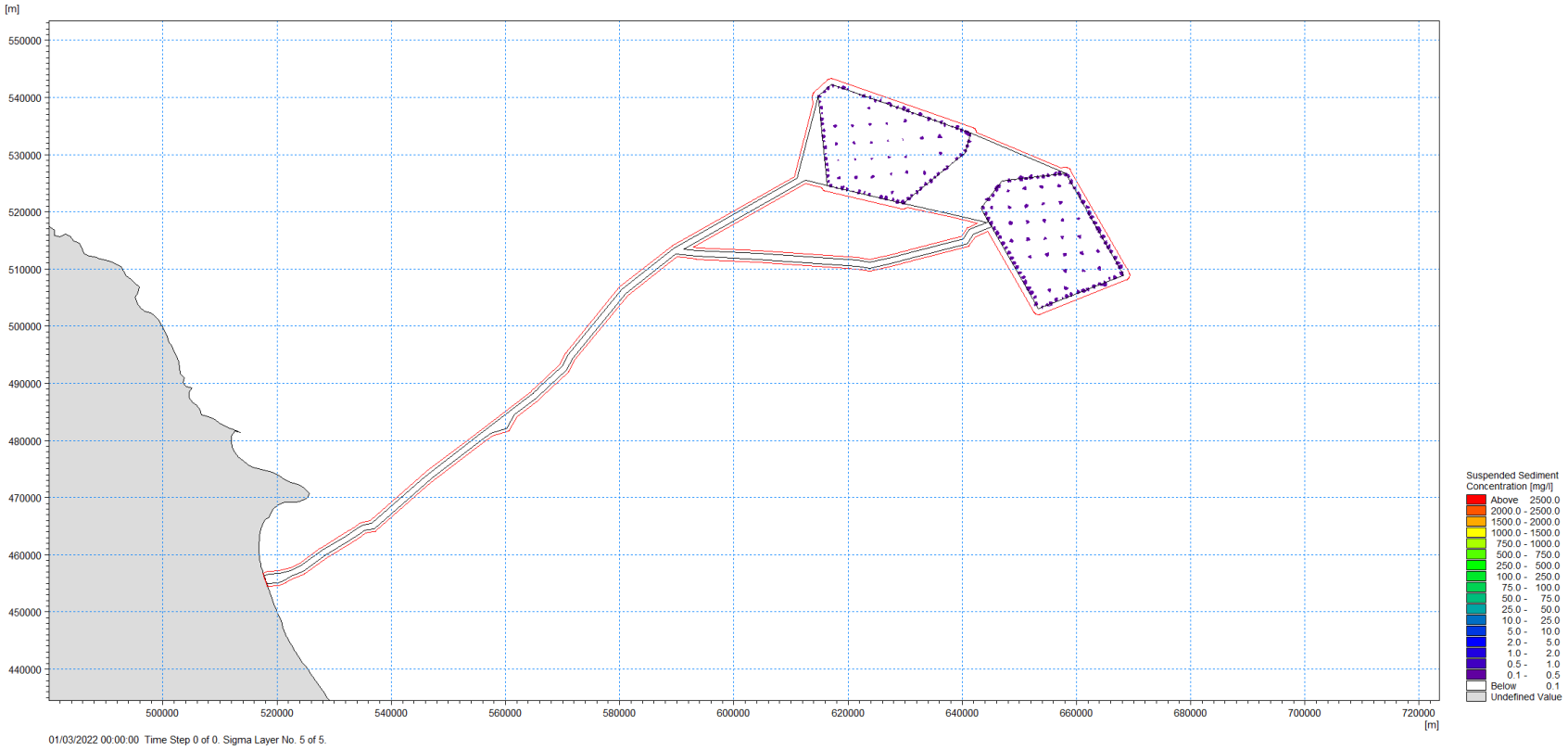

Figure D-31: Maximum Suspended Sediment Concentration (surface layer) – Turbine and Platform Foundations – Drill Arising

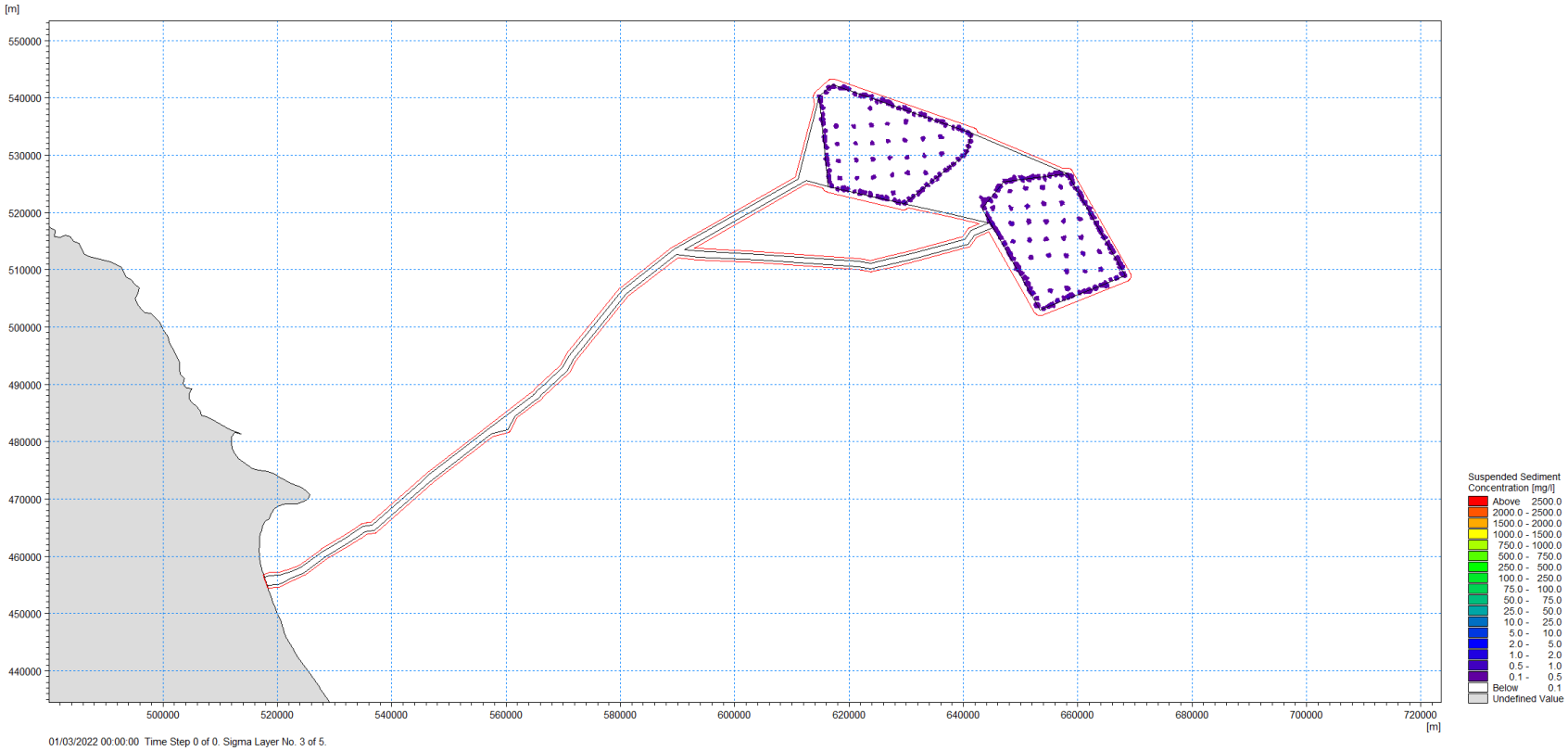

Figure D-32: Maximum Suspended Sediment Concentration (middle layer) – Turbine and Platform Foundations – Drill Arising

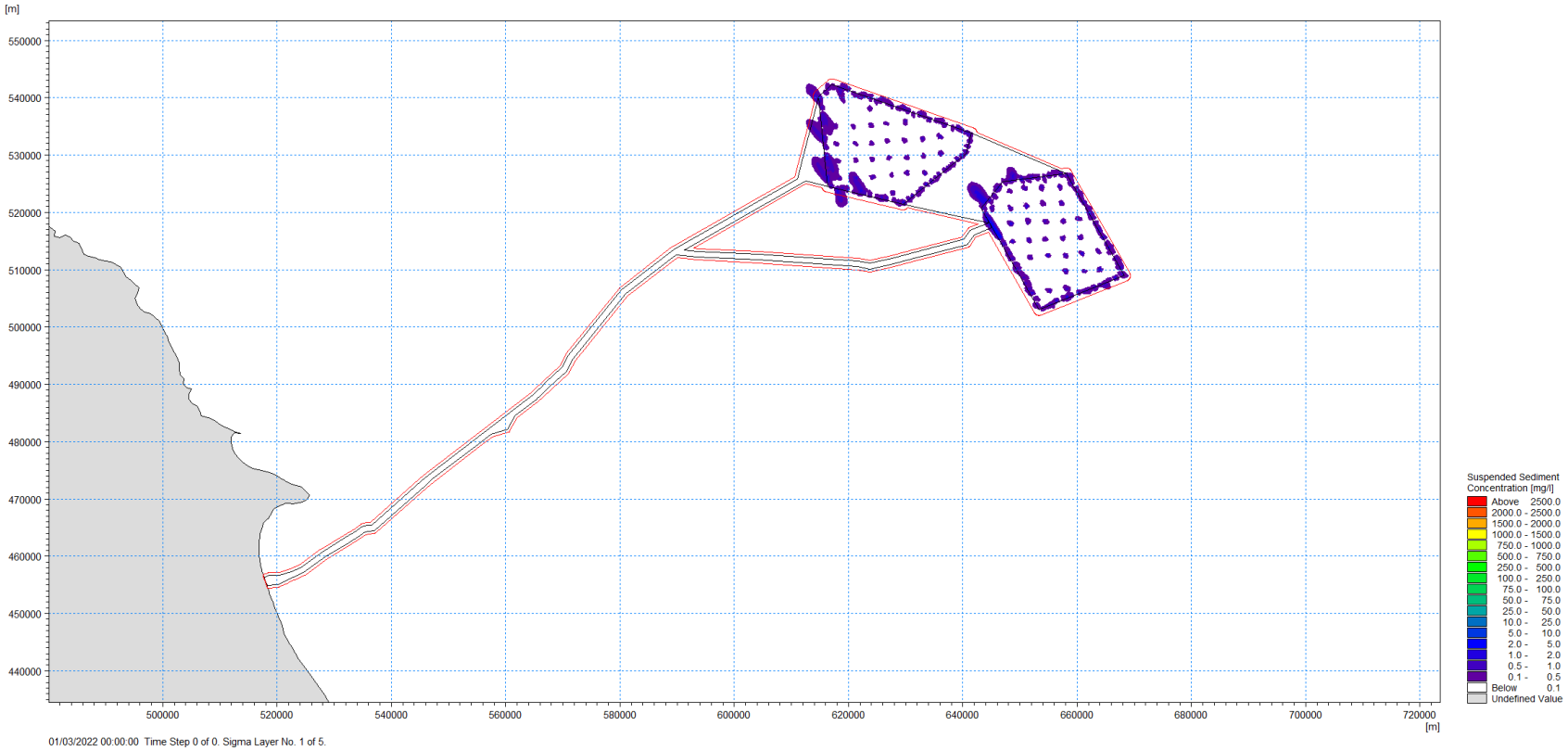

Figure D-33: Maximum Suspended Sediment Concentration (bottom layer) – Turbine and Platform Foundations – Drill Arising

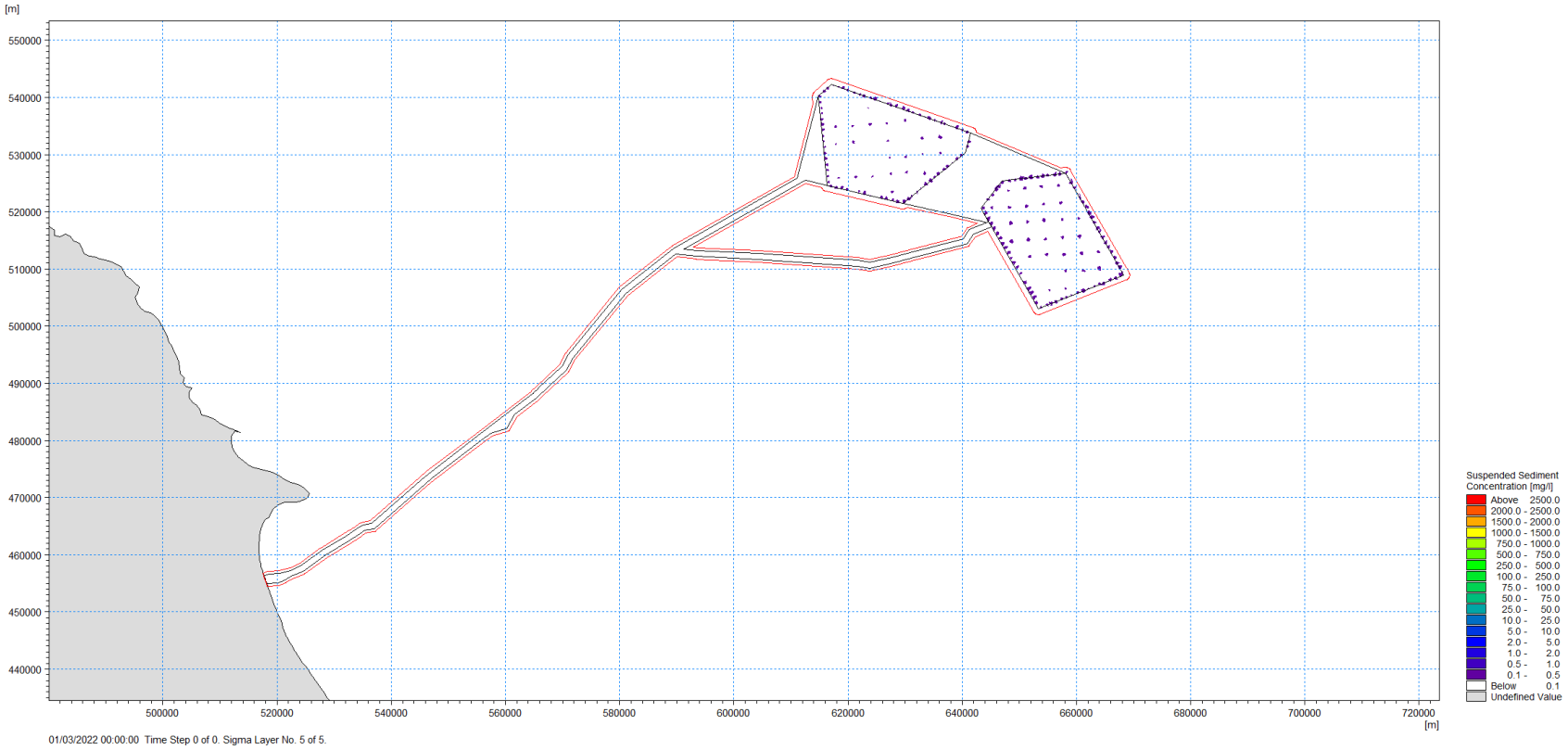

Figure D-34: Maximum Suspended Sediment Concentration (surface layer) – Turbine and Platform Foundations – Bed Preparation

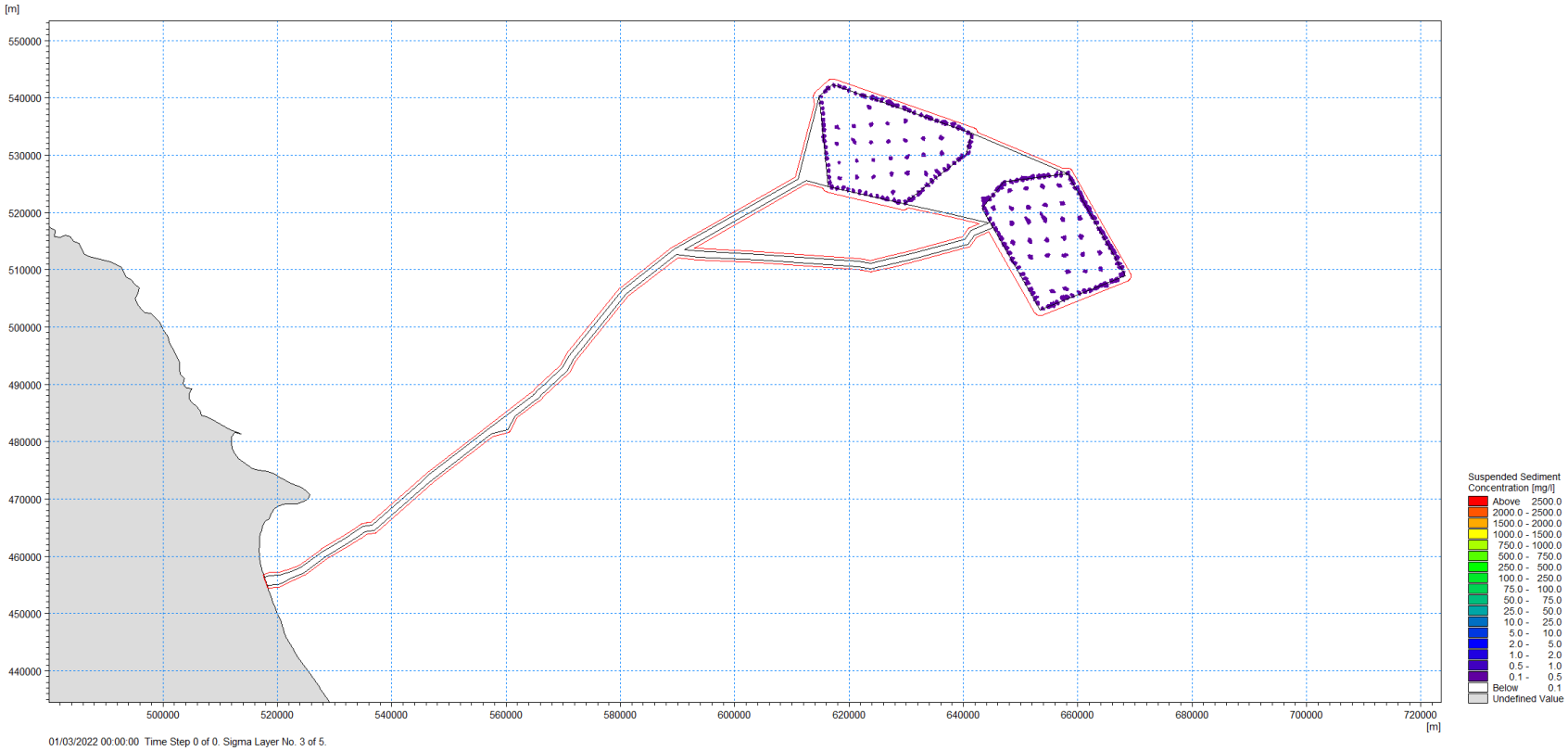

Figure D-35: Maximum Suspended Sediment Concentration (middle layer) – Turbine and Platform Foundations – Bed Preparation

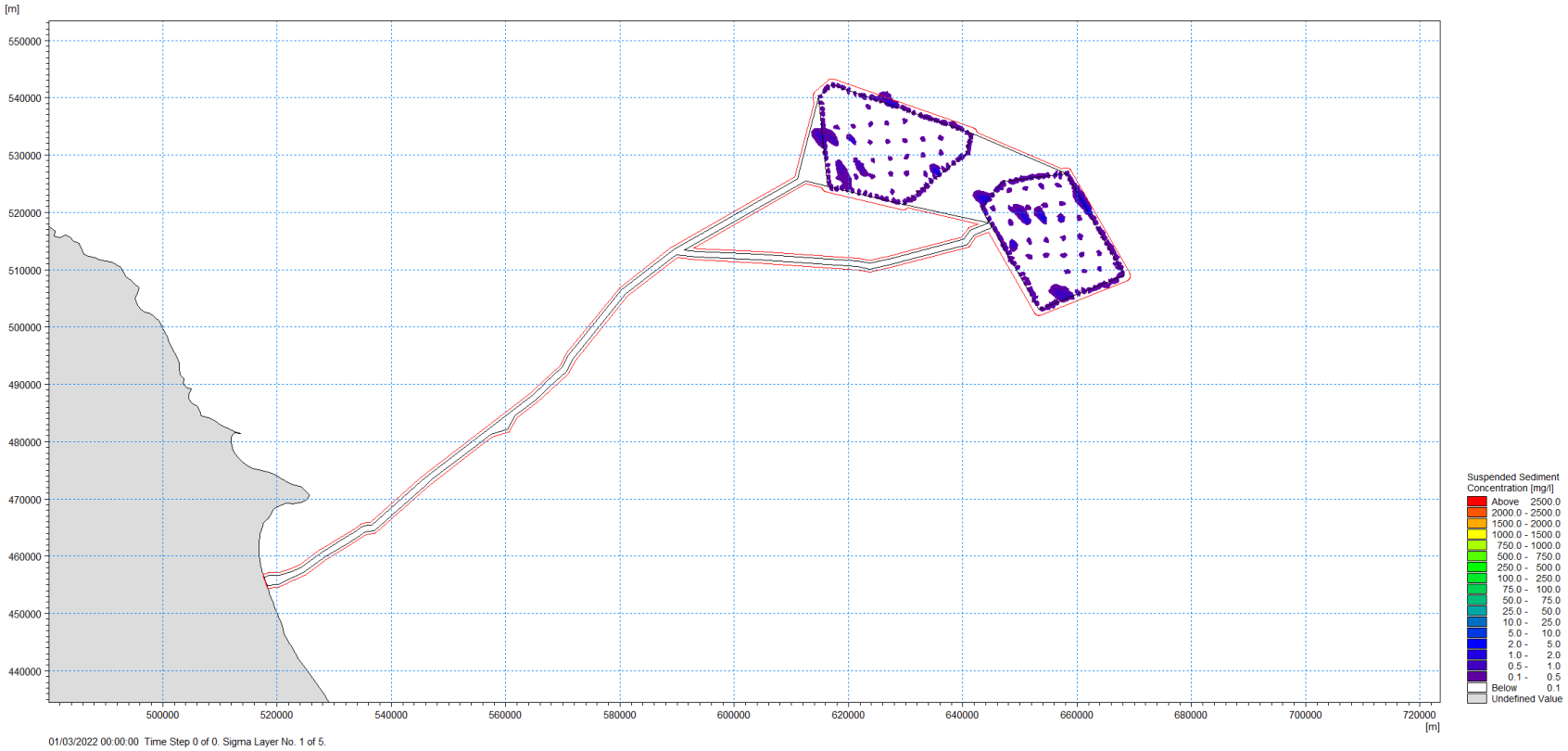

Figure D-36: Maximum Suspended Sediment Concentration (bottom layer) – Turbine and Platform Foundations – Bed Preparation

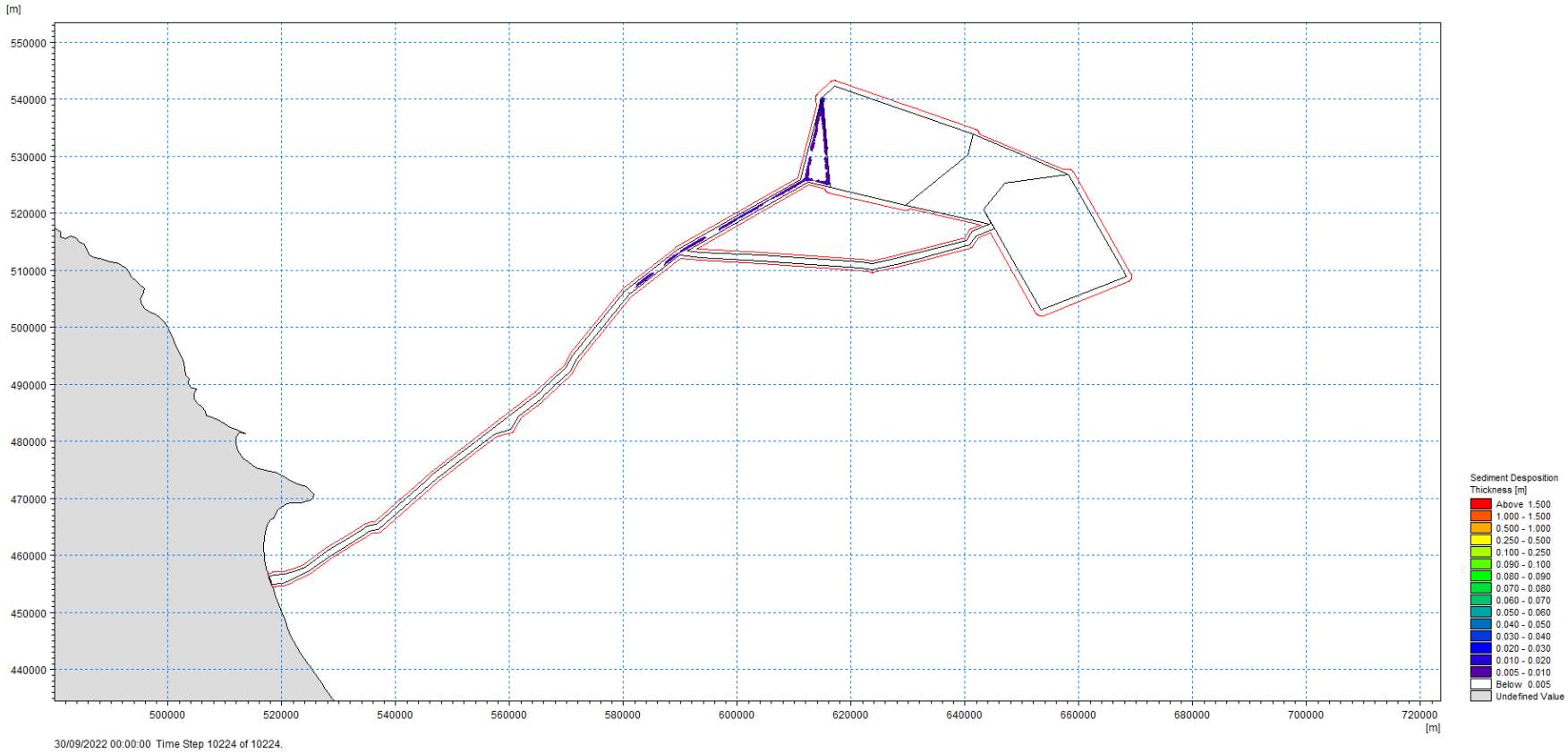

Figure D-37: Total Sediment Deposition Thickness – Export Cable Route to DBS West – Levelling

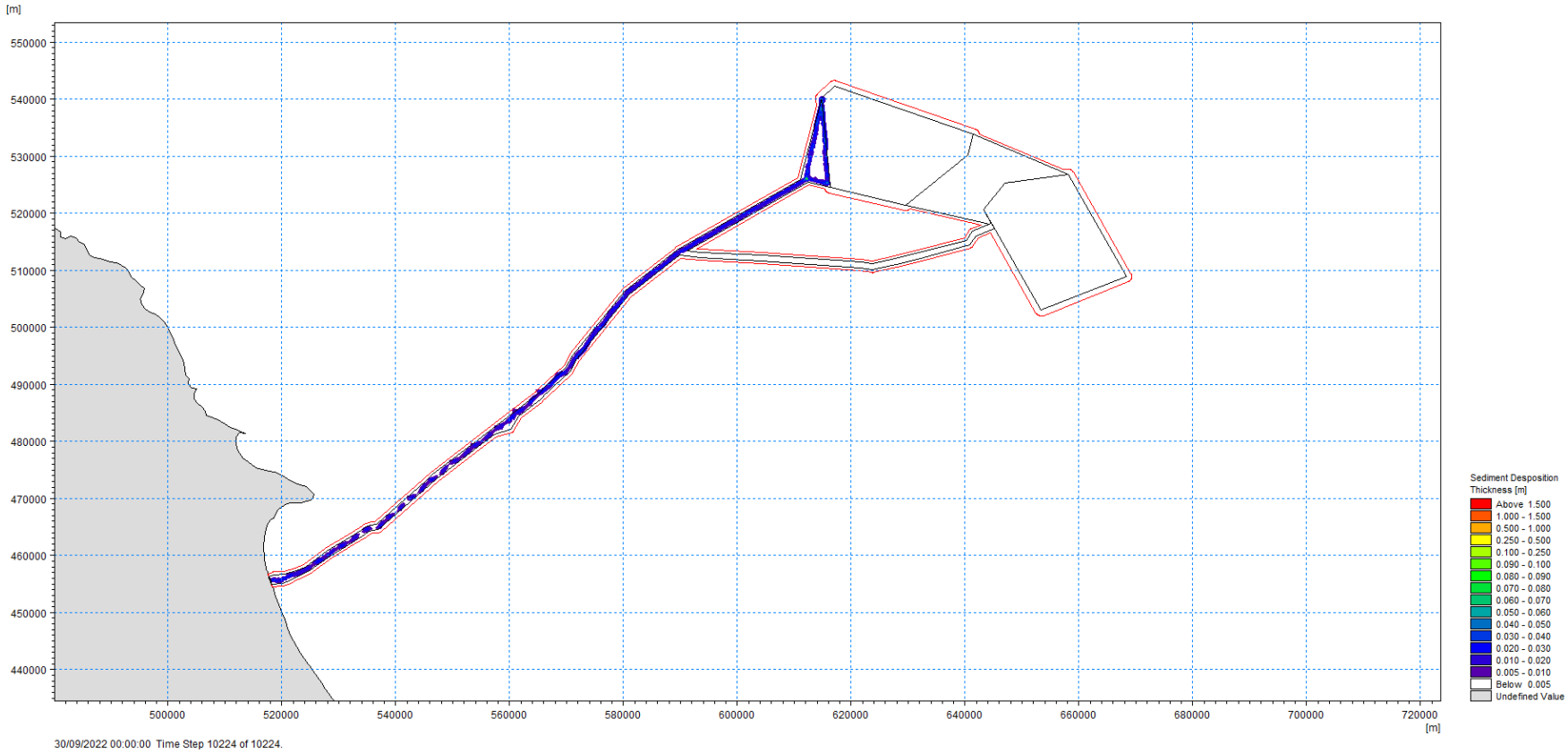

Figure D-38: Total Sediment Deposition Thickness – Export Cable Route to DBS West – Trenching

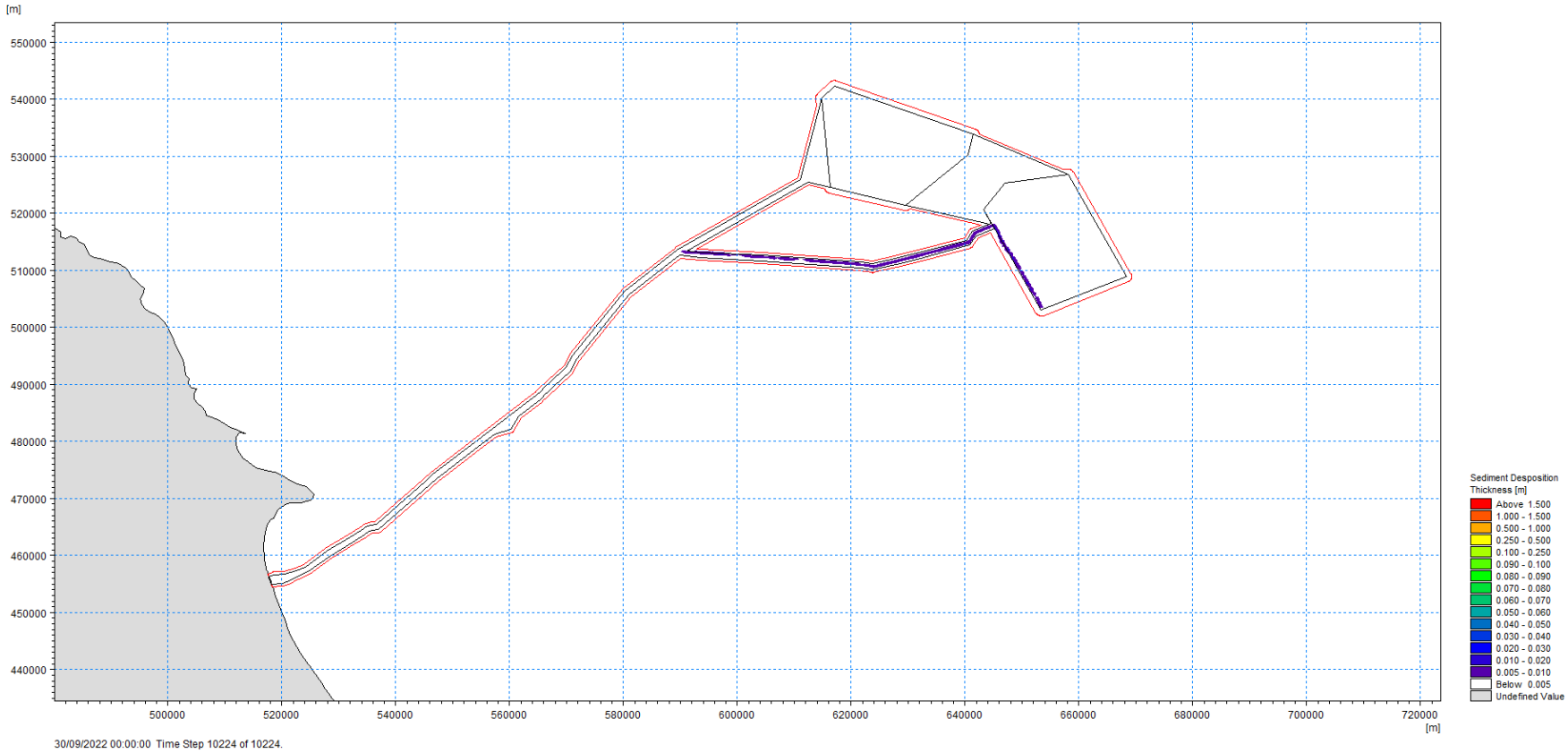

Figure D-39: Total Sediment Deposition Thickness – Export Cable Route to DBS East – Levelling

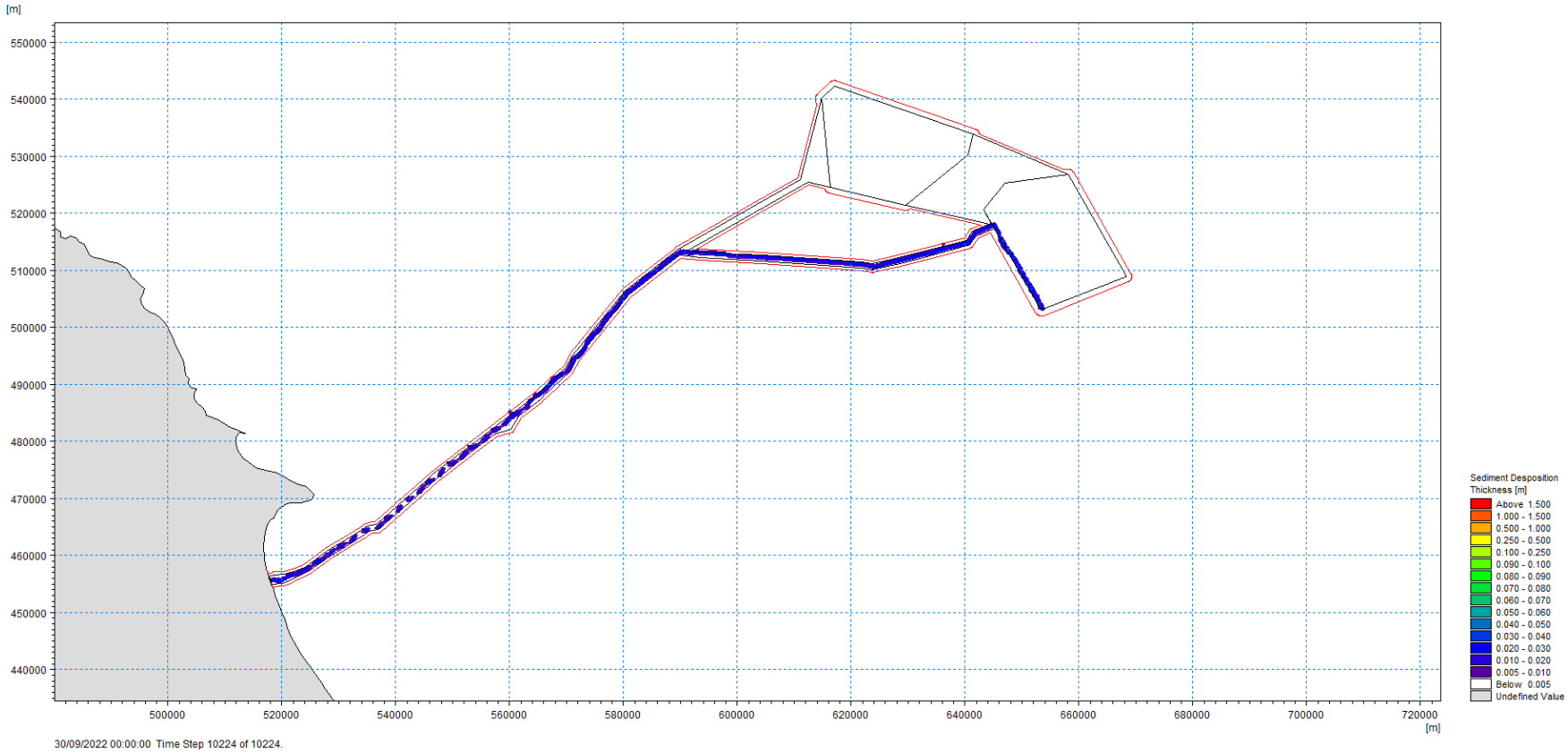

Figure D-40: Total Sediment Deposition Thickness – Export Cable Route to DBS East – Trenching

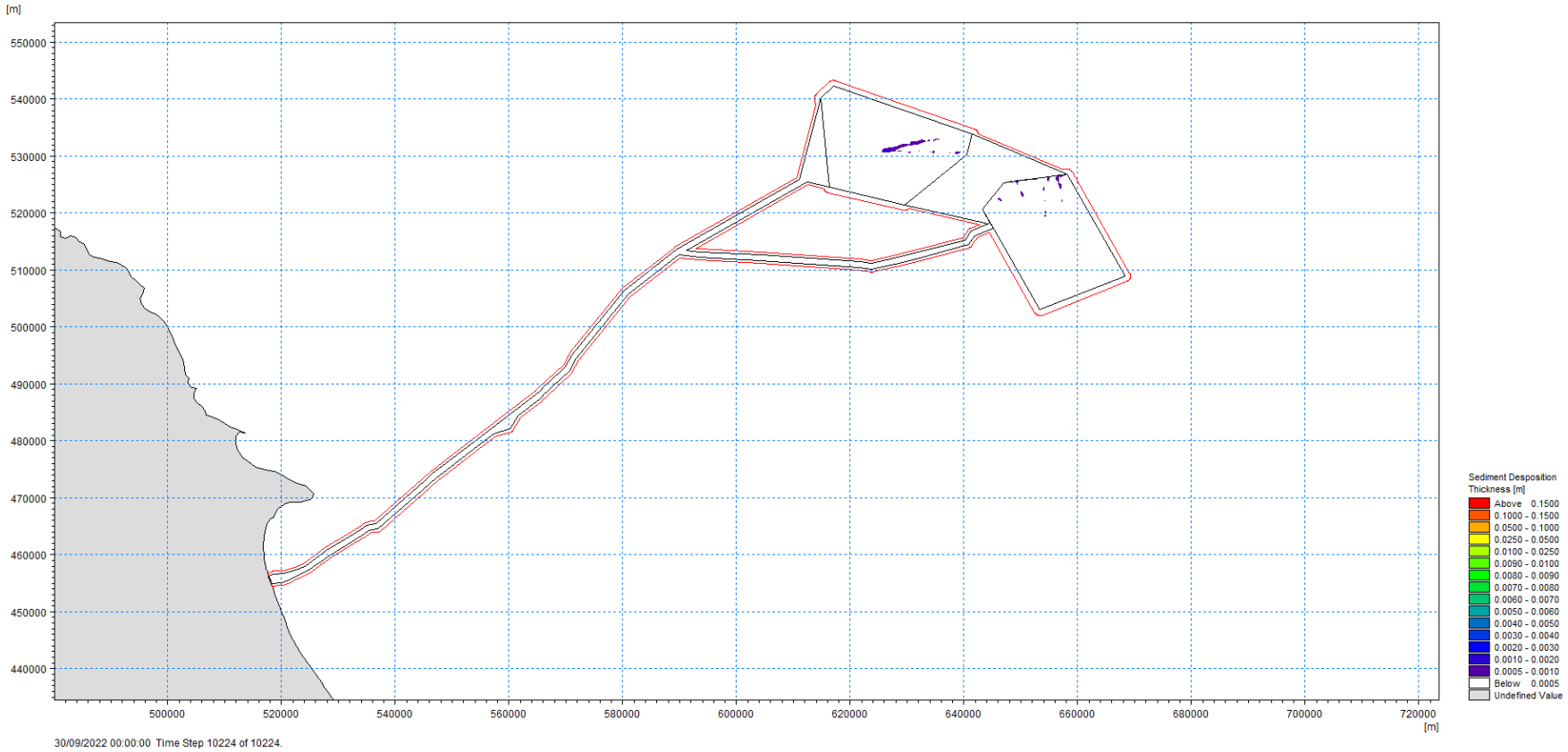

Figure D-41: Total Sediment Deposition Thickness – Array Cable – Levelling

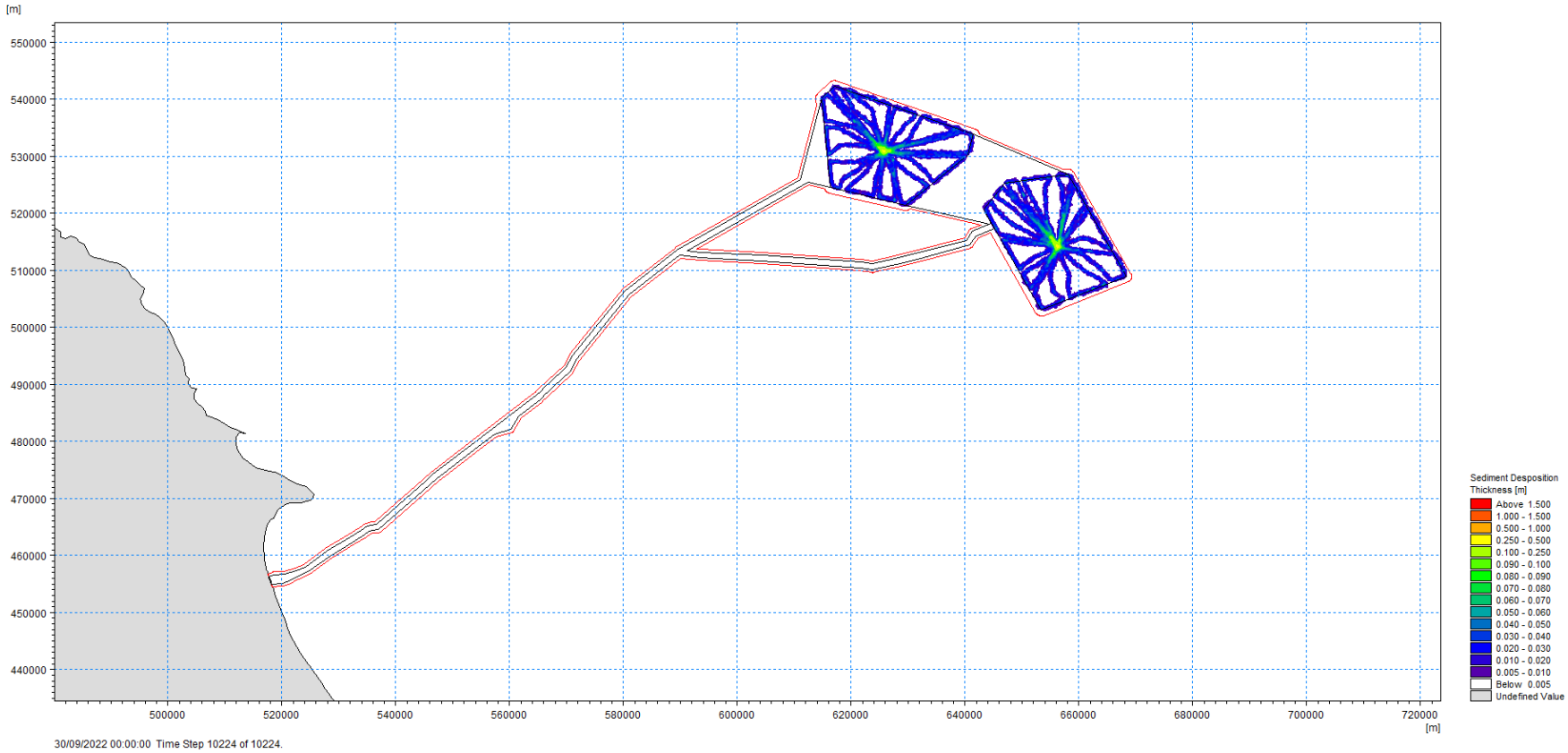

Figure D-42: Total Sediment Deposition Thickness – Array Cable – Trenching

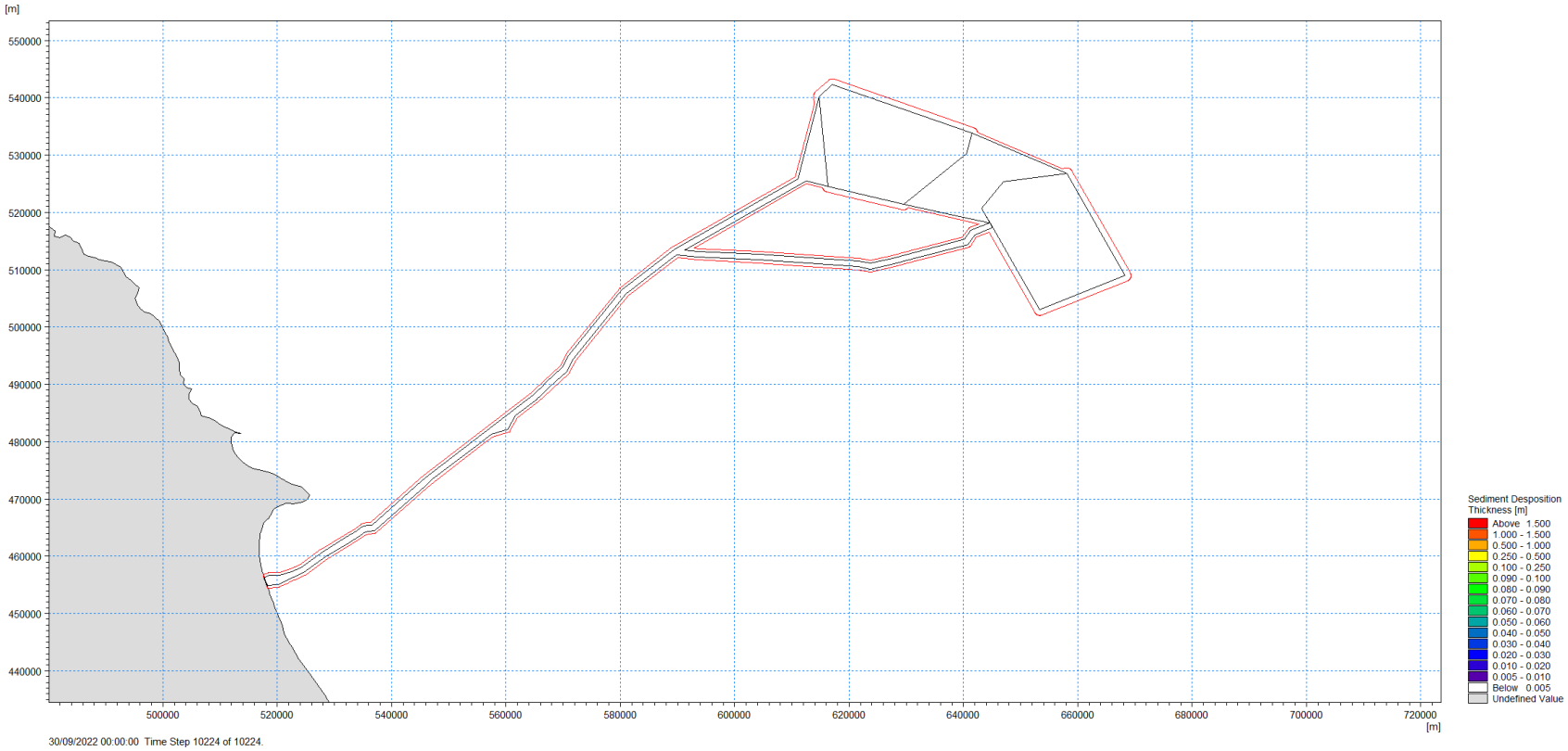

Figure D-43: Total Sediment Deposition Thickness – Inter-platform Cable (West and East) – Levelling

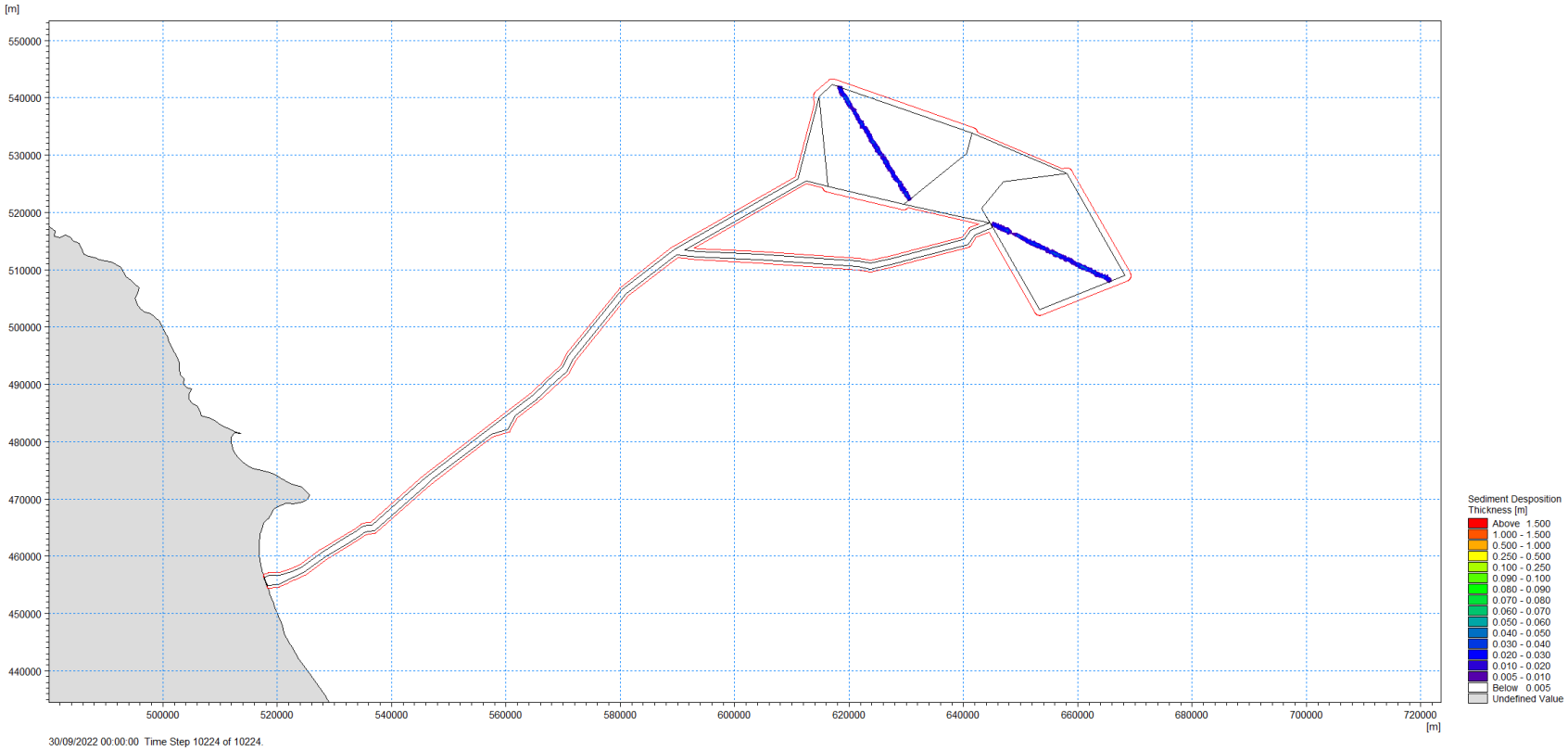

Figure D-44: Total Sediment Deposition Thickness – Inter-platform Cable (West and East) – Trenching

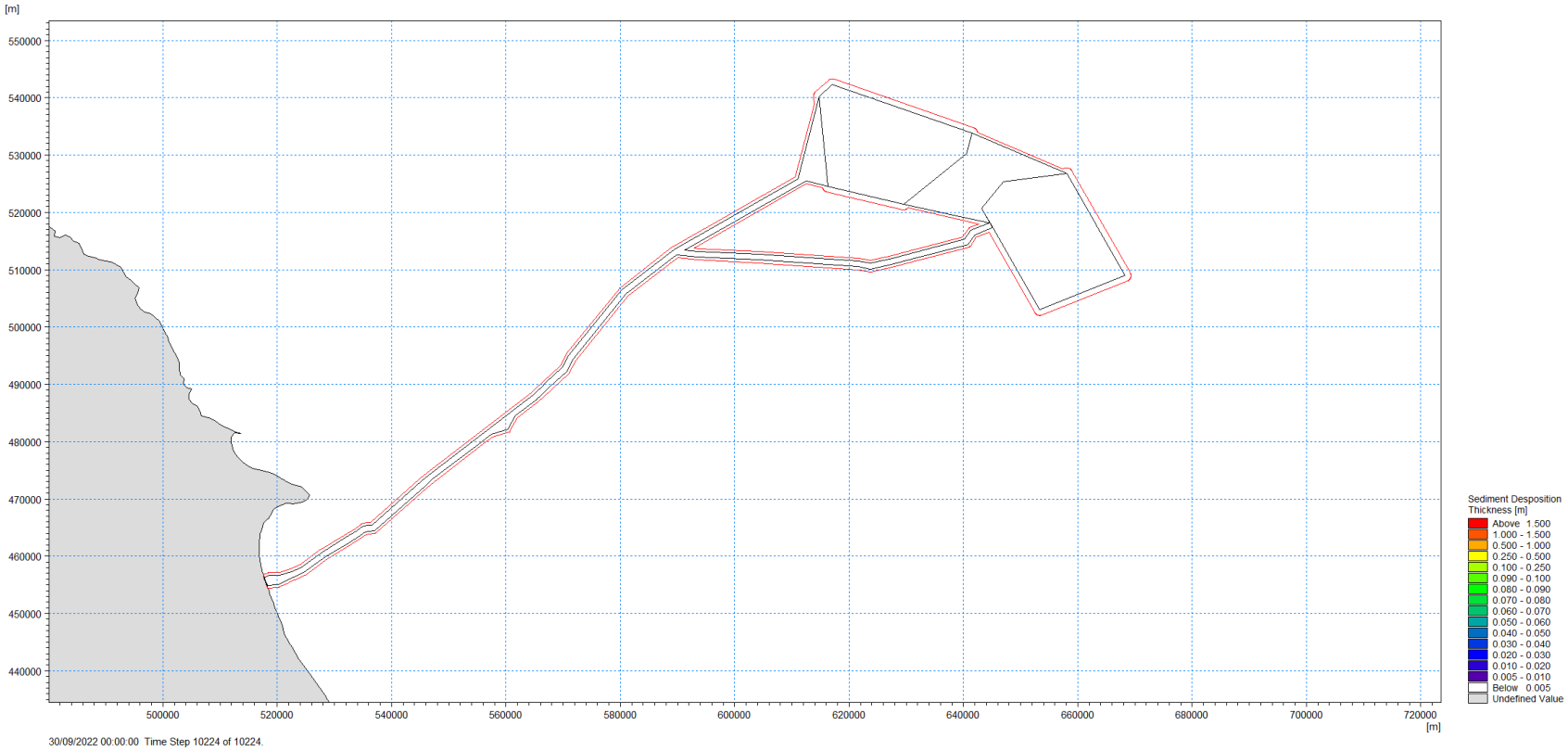

Figure D-45: Total Sediment Deposition Thickness – Inter-platform Cable ("West+East") – Levelling

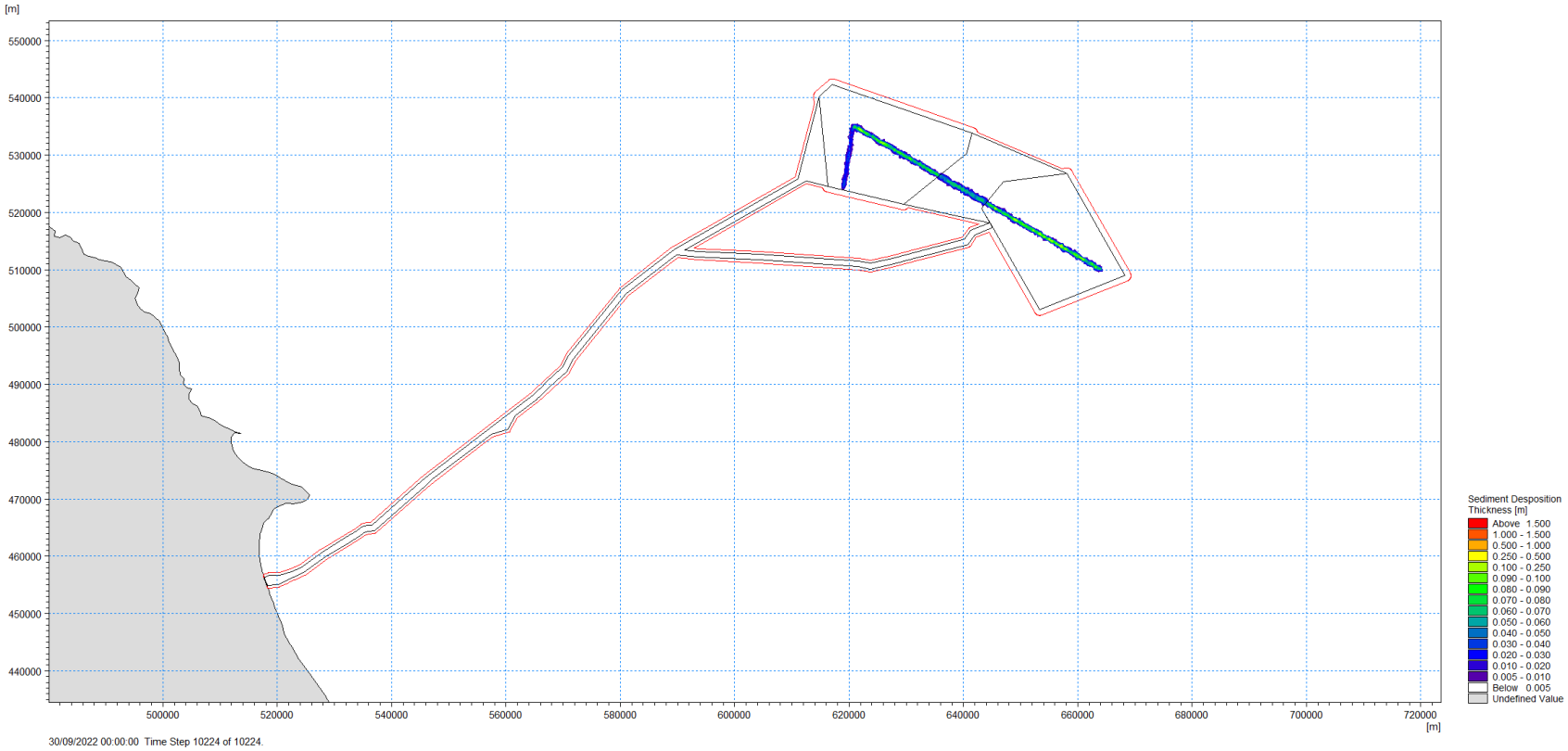

Figure D-46: Total Sediment Deposition Thickness – Inter-platform Cable ("West+East") – Trenching

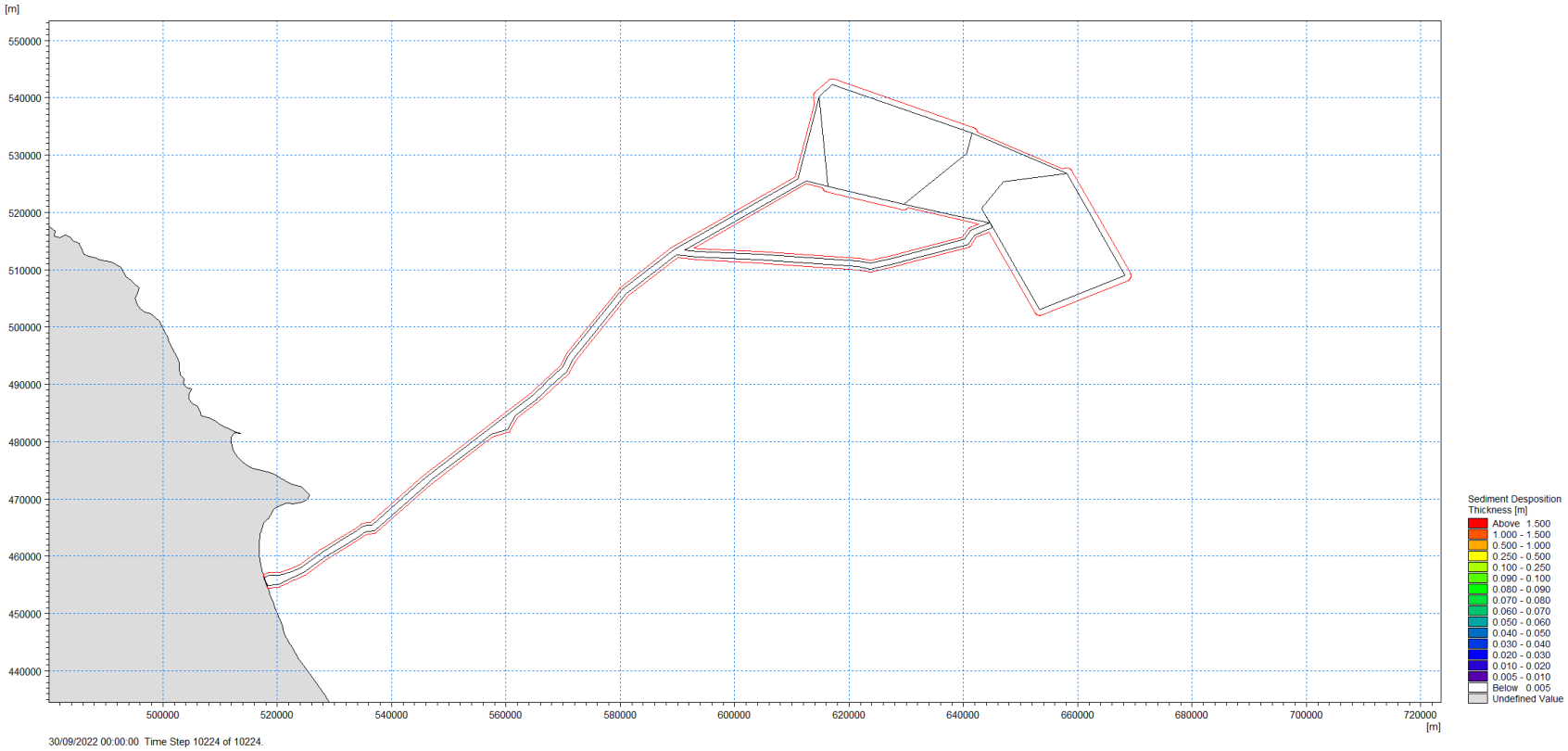

Figure D-47: Total Sediment Deposition Thickness – Turbine and Platform Foundations – Drill Arising

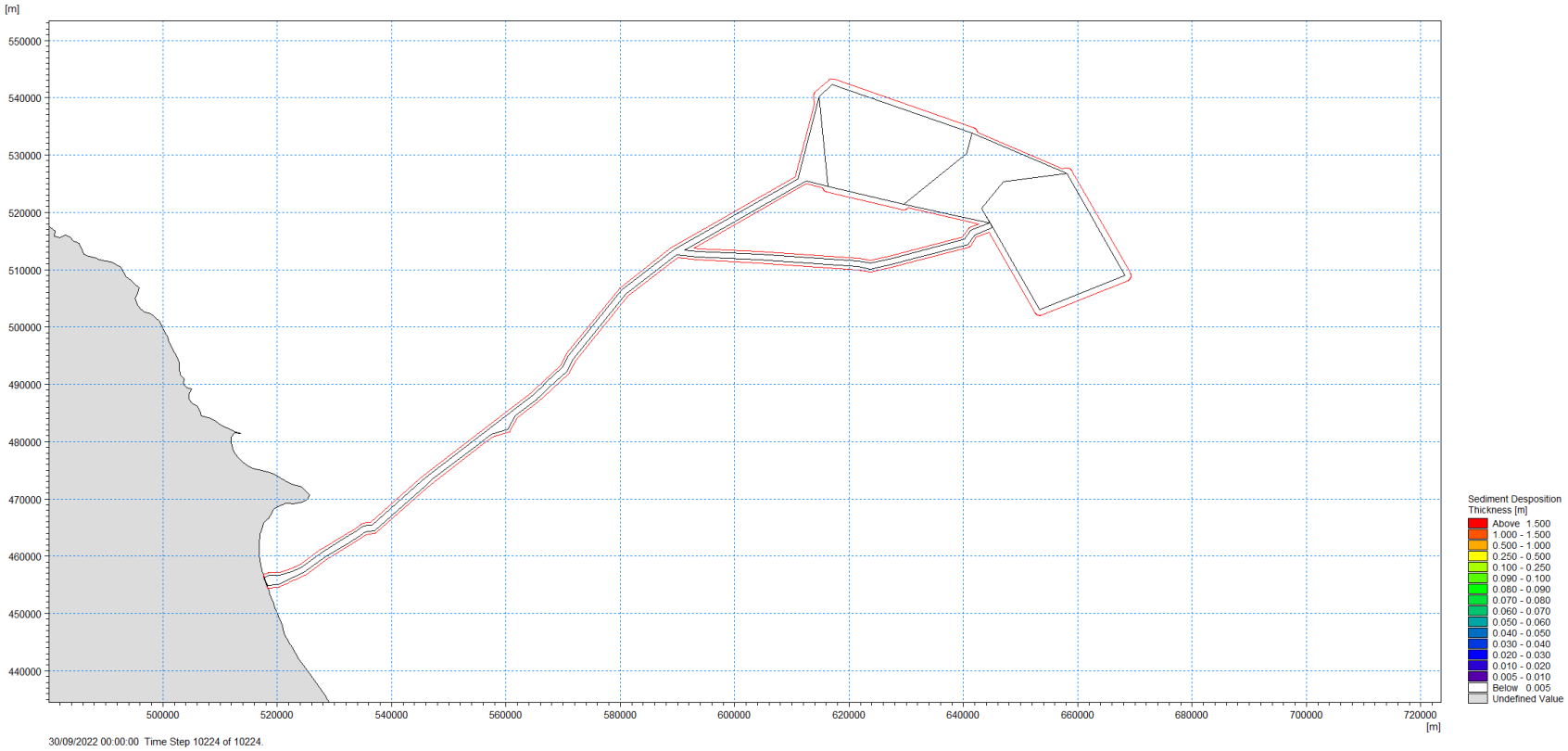

Figure D-48: Total Sediment Deposition Thickness – Turbine and Platform Foundations – Bed Preparation